Mémoires de Géologie (Lausanne) No. 41, 2003

# New stratigraphic, structural and geochemical data from the Val Formazza – Binntal area (Central Alps)

Elisabeth Carrupt

IMPRIMERIE CHABLOZ S.A., LAUSANNE

ISSN 1015-3578

# 41

# Mémoires de Géologie (Lausanne)

*Section des Sciences de la Terre*
*Université de Lausanne*
BFSH-2, 1015 Lausanne, Suisse

# Mémoires de Géologie (Lausanne)



Mémoires de Géologie (Lausanne)
Section des Sciences de la Terre
Institut de Géologie et Paléontologie
Université de Lausanne
BFSH-2, CH-1015 Lausanne

CARRUPT Elisabeth
Titre: New stratigraphic, structural and geochemical data from the Val Formazza – Binntal area (Central Alps)
Mém. Géol. (Lausanne), n° 41, 2003, 116 pp., 46 text-figs, 3 Pl.
ISSN: 1015-3578

Imprimeur: Chabloz S.A., Tolochenaz

Page de couverture: Punta Lebendun et Hohsandhorn vus de l'est.

# New stratigraphic, structural and geochemical data from the Val Formazza – Binntal area (Central Alps)

Elisabeth Carrupt

Mémoire de Géologie (Lausanne) No. 41, 2003

A Christian et Jean-François

# Remerciements

Au terme de ce travail, qui est la prolongation de ma thèse de doctorat, je tiens à remercier plusieurs personnes qui ont participé à son élaboration.

Premièrement je tiens à remercier le professeur Henri Masson pour m'avoir offert la possibilité de faire une thèse, fiancée par l'Université de Lausanne. Je le remercie également, ainsi que le professeur Albrecht Steck, pour m'avoir appris à cartographier avec rigueur dans des terrains alpins difficiles. Enfin je remercie tous les membres de mon jury de thèse, le président M. Oscar Karl Burlet, les professeurs Henri Masson, Albrecht Steck et Giorgio Martinott ainsi que le docteur Yves Gouffon pour m'avoir accompagnée sur le terrain et/ou avoir consacré du temps à ma thèse.

Christian, David, Franco et Matthieu ont eu la gentillesse de venir me voir sur le terrain, et pour deux d'entre eux, de m'accompagner, crampons au pied, dans les endroits les plus difficiles d'accès du terrain. Christian a aussi eu le courage de m'accompagner pendant plus d'une semaine lorsque j'ai cartographié la région de l'Alpe Giove et des lacs Busin (alpage et lacs qui portent bien leurs noms); il a porté plusieurs dizaines d'échantillons pendant de longues heures pour rejoindre la première route.

J'ai toujours eu de très bons contacts avec les personnes responsables d'un laboratoire, à savoir le privat docent François Bussy, le professeur Jan Kramers, Jean-Claude Lavanchy et Laurent Nicod.

Je remercie les fondations et associations qui m'ont apporté leur soutien financier, logistique ou autre: la Commission des thèses de la faculté des Sciences de lausanne, la Fondation du 450ème anniversaire de l'Université de Lausanne, la Société Académique Vaudoise, und die Stiftung de Giacomi.

Mes parents sont souvent venus me rendre visite: leur continuelle bonne humeur, leur enthousiasme, ainsi que leur intérêt géologique marqué m'ont beaucoup aidée.

Je remercie ici cordialement Christian et Jackie pour le temps passer à améliorer ce manuscrit.

Je dois aussi ici remercier Michel (mieux connu sous le nom de Popoff), Jean-Frédéric, Loulou, Annett, et François pour la bonne humeur et la bonne entente qui a toujours régné dans le bureau 4168.

Nicolas, Jérôme, Raphaël, Markus, Grégoire, Gilles, Olivier, François, Marc et Colin (j'espère n'oublier personne) sont les assistants, avec qui j'ai pu "torturer", dans la joie et la bonne humeur les étudiants lors des séances de travaux pratiques et des camps de terrain.

Nicolas Gilardi a toujours été d'une grande disponibilité pour régler mes problèmes informatiques.

Le refuge Cesare Mores possède un charme unique; la famille Valci le rend très chaleureux et accueillant. N'hésitez pas à y aller!

Enfin je remercie toutes les personnes que j'aurais malencontreusement oubliées ainsi que tous les assistants et étudiants des Sciences de la Terre de Lausanne pour la bonne humeur ambiante.

# Abstract

The Penninic domain represents a complex suture zone between the European foreland and the overriding Austro- and South- alpine realm. This domain is made of pre-Triassic basements, of Mesozoic to Tertiary cover series (often detached from their basement), and of ophiolites, in which polyphase penetrative deformations and an intense metamorphism erase the primary structural and sedimentological relations. This PhD work reports results (stratigraphic, tectonics, geochemical and metamorphic) obtained from during the investigations of parts of the lower Penninic units outcropping in the Lepontine Alps.

An area covering principally the High Val Formazza in Italy and the upper part of the Binntal in Switzerland has been mapped in detail. These valleys show natural cross sections, differently oriented, of six nappes belonging to the lower Penninic: the Camosci (newly defined here), Antigorio, Lebendun, Monte Leone, and Pizzo del Vallone (newly defined here) nappes and the Rosswald series. The stratigraphy, tectonic history and metamorphic grade of the various nappes were investigated in details

The stratigraphic study of the Mesozoic cover series shows strong analogies as well as obvious differences. However the stratigraphic section put in a paleogeographic order show the image of a structured passive margin, now severely deformed. The T-MORB like signature of the basalts present in the Pizzo del Vallone nappe reinforces this conclusion.

The Pizzo del Vallone, Monte Leone and Lebendun nappes show obvious similarities with the prépiémontais and ultrabriançonnais series, favouring a paleogeographic position on the northern margin of the Alpine Tethys. The Antigorio nappe was the shoulder, and the Camosci nappe, situated north of the shoulder, marked the beginning of the southern part of the Helvetic s.l. basin.

The superposed folds and the different schistosities highlight seven successive deformations. The deduced regional structural model shows that the deformation D3 (dominant schistosity) and the deformation D4 (crenulative schistosity) are the dominant structures. They follow the initial thrusting of the various nappes and mark the end of the prochariage. The backfolding D5, characterised by open folds, precedes a dextral shear movement D6. The latter obliterates most of the structural relations with the Eastern Alps because it strongly reorients the structures between the Morasco and Busin lakes. Finally the D7 folds, characterised by horizontal axial surfaces, are probably coeval to the late vertical strain related to the late exhumation of the Lepontine Alps.

The culmination of the amphibolitic Lepontine metamorphism was reach at the end of the procharriage (D4). The metamorphic conditions were first identified by studying the mineralogical assemblages and were then estimated using the software THERMOCALC (~580°C, ~9.6 kbar). An approximation of the metamorphic history is based upon the zoned garnets.

# Résumé

Les Alpes sont le résultat de la collision et de l'empilement de plusieurs domaines paléogéographiques. Parmi ceux-ci, le domaine Pennique inférieur, dont fait partie la zone étudiée, est constitué de nappes de socle, de couverture Mésozoïque à Tertiaire, et de roches basiques.

Une cartographie au 1:10'000 et l'étude détaillée des métasédiments Mésozoïques à Tertiaire montrent que six unités tectoniques appartenant au Pennique inférieur affleurent entre le Val Formazza (Italie) et le Binntal (Suisse). Ce sont les nappes de Camosci (nouvellement définie), d'Antigorio, du Lebendun, du Monte Leone et de Pizzo del Vallone (nouvellement définie), et la série de Rosswald.

L'étude stratigraphique des diverses couvertures mésozoïques montre que ces nappes, bien que clairement différentiables, possèdent des analogies frappantes. L'organisation des colonnes stratigraphiques des nappes étudiées selon leur succession paléogéographique relative permet de reconstruire un paléoenvironnement évoluant, dès le Lias inférieur, d'un rift vers une marge passive structurée. Ce résultat concorde avec la mise en place en milieu continental des roches vertes contenues dans la nappe de Pizzo del Vallone, ainsi qu'avec leur signature géochimique. Celle-ci indique des tholéiites de type T-MORB, variablement enrichies en LREE.

Une étude stratigraphique comparative avec des séries Prépiémontaises à Ultrabriançonnaises permet de déduire que les nappes de Pizzo del Vallone, du Monte Leone et du Lebendun représentaient une partie de la marge passive distale nord piémontaise. La nappe d'Antigorio formaient l'épaulement de la Téthys Alpine, et la nappe de Camosci, située au Nord de cet épaulement, constituaient la partie la plus interne du bassin frangeant Helvétique s.l.

Sept phases alpines de déformation ductile ont été mises en évidence par l'étude des figures d'interférence et des relations entre les différentes schistosités. Elles ont permis de présenter un modèle structural régional dans lequel le plissement principal D3 (structure dominante dans la région) et la phase crénulative D4 suivent la mise en place initiale des différentes unités. Après le rétroplissement D5, qui crée des plis ouverts caractéristiques, une phase de cisaillement dextre D6 réoriente fortement les structures. Cette phase représente une complication importante dans l'étude des relations avec les Alpes Orientales. Enfin des plis à surface axiale horizontale D7 indiquent un épisode tardif de compression verticale qui pourrait correspondre à l'exhumation tardive des Alpes Lepontines.

L'ensemble des roches étudiées a subi un métamorphisme de faciès amphibolite. Les relations texturales, les assemblages minéralogiques et la thermométrie montrent que le pic du métamorphisme est associé à la fin du procharriage D4 avec des conditions P-T estimées à ~580°C, ~9.6 kbar. D'autre part une étude détaillée de la zonation chimique des grenats a permis de proposer une histoire métamorphique pour l'ensemble de la région concernée à partir d'une modélisation semi-quantitative.

# Riassunto

Le Alpi risultano dalla collisione e superposizione di numerosi domini paleogeografici, il Pennidico fra questi è il più difficilmente interpretabile. E costituito da falde appartenenti al basamento e alla copertura Mesozoica, e di ofioliti nelle quali il forte grado di metamorfismo ha sovente cancellato le strutture e le relazioni sedimentarie.

Questo lavoro esplicita i risultati ottenuti grazie ad un lavoro dettagliato di cartografia su un settore situato principalmente in Alta Val Formazza (IT), ma con qualche passaggio nel Binntal (Svizzera). Sei unità tettoniche appartenenti al dominio Pennidico inferiore affiorano in queste regioni. Si tratta delle falde dei Camosci, d'Antigorio, del Lebendun, del Monte Leone e del Pizzo del Vallone; a queste si aggiunge la serie del Rosswald. Un attenzione particolare è stata prestata alla stratigrafia di queste falde, alla tettonica e al grado di metamorfismo da loro raggiunto durante la fase detta "Lepontina".

La ricostruzione stratigrafica dettagliata delle coperture mesozoiche mostra delle forti similitudini, malgrado le differenze che sembrano scaturire da un esame poco approfondito. Mostrano pure una struttura coerente e compatibile con una situazione paleotettonica del tipo margine passivo.
I basalti contenuti nella falda del Pizzo del Vallone mostrano dei profili geochimici del tipo T-MORB, dunque compatibili con una tale situazione.

Il confronto con le serie prepiemontesi e le ultrabrianzonesi mostra delle similitudini evidenti, che permettono di concludere che le falde del Pizzo del Vallone, del Monte Leone e del Lebendun hanno costituito una parte del margine passivo nord piemontese. La falda di Antigorio ha costituito dunque la spalla geomorphologia e la falda dei Camosci, situata a nord della spalla, la parte interna del bacino Elvetico s.l.

Sette fasi di deformazione duttile alpina sono state messe in evidenza dallo studio delle figure d'interferenza e dalle relazioni fra le scistosità. Hanno permesso di presentare un modello strutturale a scala regionale nel quale la fase di piegamento principale D3 (struttura dominante nella regione) e la fase di crenulazione D4 seguono la messa in posto delle differenti unità. Dopo la fase plicativa retrograda D5, che genera delle pieghe aperte caratteristiche, una faglia a scorrimento orizzontale destra D6 cambia fortemente le orientazioni delle strutture fra Morasco e Busin. La descrizione di questa fase è importante per stabilire una relazione con le unità appartenenti alle Alpi orientali. Per finire delle pieghe con superficie assiale orizzontale D7 sottolineano un episodio tardivo di compressione verticale (collasso) che potrebbe essere associato all'esumazione tardiva delle Alpi Lepontine.

L'episodio metamorfico Lepontino, caratterizzato da un facies anfibolitico, ha influenzato la regione a partire dalla fine della fase di somascorrimento prograd (D4). Le condizioni di pressione e temperatura sono dapprima state stimate grazie allo studio delle caratteristiche chimiche delle fasi e degli assemblaggi mineralogici, e in seguito stabilite con precisione grazie ad uno studio termobarometrico (580°C, 9.6kbar). La zonatura chimica dei granati ha permesso di proporre una storia metamorfica (risultati semiquantitativi) della regione.

# Zusammenfassung

Die Alpen sind das Ergebnis der Kollision und Stapelung mehrerer paläogeographischer Einheiten. Die komplexeste dieser Einheiten, das Penninikum, besteht aus überfalteten Decken des Grundgebirges, mesozoischen Sedimenten und Ophioliten, deren primäre Strukturen oftmals durch den hohen Metamorphosegrad unkenntlich gemacht wurden.

Die vorliegende Arbeit ist das Ergebnis detaillierter geologischer Kartierungen im Bereich des oberen Val Formazza (Italien) und des angrenzenden Binntals (Schweiz). Im oberen Val Formazza sind sechs tektonische Einheiten des unteren Penninikums aufgeschlossen. Es sind dies die Camosci-, Antigorio-, Lebendun, Monte Leone- und Pizzo del Vallone-Decken sowie die Rosswald Serie. Besondere Aufmerksamkeit wurde der Internstratigraphie dieser Decken und ihrer tektonischen und metamorphen Entwicklung während der Bildung des Lepontins gewidmet.

Detaillierte stratigraphische Untersuchungen der verschiedenen mesozoischen, metasedimentären Einheiten zeigen, dass diese eindeutig unterscheidbar sind, jedoch bemerkenswerte Analogien aufweisen. Der kohärente Aufbau dieser Einheiten erlaubt weiterhin eine paläotektonische Rekonstruktion, in der diese Einheiten das Ergebnis der Deformation und Metamorphose eines liassischen, passiven Kontinentalrandes darstellen. Die chemische Signatur der intrusiven und extrusiven Basalte der Pizzo del Vallone -Decke (T-MORB) unterstützt eine solche Rekonstruktion

Vergleiche mit den Einheiten des „Prépiémont“ und des Ultrabriançonnais zeigen deutliche Gemeinsamkeiten, welche den Schluss zulassen, dass die Pizzo del Vallone -, Monte Leone- und Lebendun-Decken einen Teil des nord-piémontesischen passiven Kontinentalrands darstellen. Die Antigorio-Decke stellt ein topographisches Hoch dar, während die Camosci-Decke, im Norden der Antigorio-Decke, als Internbereich des helvetischen Beckens s.l. interpretiert wird.

Im Zuge der vorliegenden Arbeit wurden sieben Phasen alpiner, duktiler Verformung aufgrund ihrer Interferenzstrukturen und unterschiedlicher Foliationsbeziehungen festgestellt. Mit Hilfe dieser Deformationsphasen gelang es, ein grossräumiges strukturelles Modell zu erstellen, in welchem die Hauptphase der Faltung D3 (welche die dominante Struktur der Region darstellt) und die darauffolgende Ausbildung einer crenulierten Foliation D4 sich der Deckenplatznahme anschliessen. Nach der Rückfaltungsphase D5, welche sich in typischerweise offenen Falten zeigt, wurden die Strukturen im Bereich zwischen Morasco und Busin im Zuge einer dextralen Scherung D6 stark überprägt. Diese Deformationsphase erschwert die tektonische Korrelation zwischen den Zentral- und Westalpen. Die jüngsten Strukturen sind Falten mit horizontaler Achsenebene (D7), welche eine späte Phase vertikaler Kompression (Kollaps), die mit der Hebung und Ausbildung des Lepontischen Doms in Zusammenhang gebracht werden, darstellen.

Amphibolitfazielle Bedingungen herrschten während der Bildung des Lepontischen Doms im gesamten Untersuchungsgebiet seit dem Ende des Deckenvorschubs (D4). Druck- und Temperaturbestimmungen aufgrund der Mineralzusammensetzungen und Mineral-paragenesen, sowie detaillierter geothermobarometrischer Untersuchungen ergaben ~580°C und ~9,6 kbar während der Lepontinischen Phase. Aufgrund der chemischen Zonierung der Granate wird ein semi-quantitatives Modell für die Druck-und Temperaturentwicklung des Untersuchungsgebietes vorgestellt.

# Table of contents

# Table of figures

3 CRYSTALLIZATION-DEFORMATIONS RELATIONSHIPS

# 1 INTRODUCTION

## 1.1 GEOGRAPHICAL SETTINGS

The studied area consists of 75 square kilometres of mountainous territory situated between the Toggia Lake, the Vannino-Busin area and Fäldbach (Fig. 1.1). The greater part of the area lies within the Italian High Val Formazza and a smaller part lies within the Swiss Binntal. The entire region is situated in the Lepontine Alps. The studied terrain is shown in figure 1.1, which is part of sheet 265 "Nufenenpass" of the "Landeskarte der Schweiz" 1:50'000. The Binntal can be reached by road from Brig via the Gomsertal during the winter and in addition to this, in the summer, it can be reached from the East via the Furka-, the Grimsel- or the Nufenen-pass. The High Val Formazza is reached by road from Domodossola via the Val Antigorio. As several walking paths exist (CROSA LENZ & FRANGIONI 1996), it is possible to reach the area on foot, however, although very pleasant the walks across the mountains are fairly long.

The studied region lies south of the Nufenen massif, which is a watershed dividing the rivers flowing northwards into the Rhone Valley from those flowing southwards, the Ticino and the Toce, into the Pô Valley. It is delimited to the north by the divide line, which coincides with the border between Switzerland and Italy between the Blinnenhorn and the Passo San Giacomo. All the lakes of the area owe their existence directly or indirectly to the effects of glacial erosion; most of them have been artificially enlarged in connection with a hydroelectric scheme.

In the entire region a local Valser German is spoken, along with Italian in Italy. The older population of the region are Valser people.

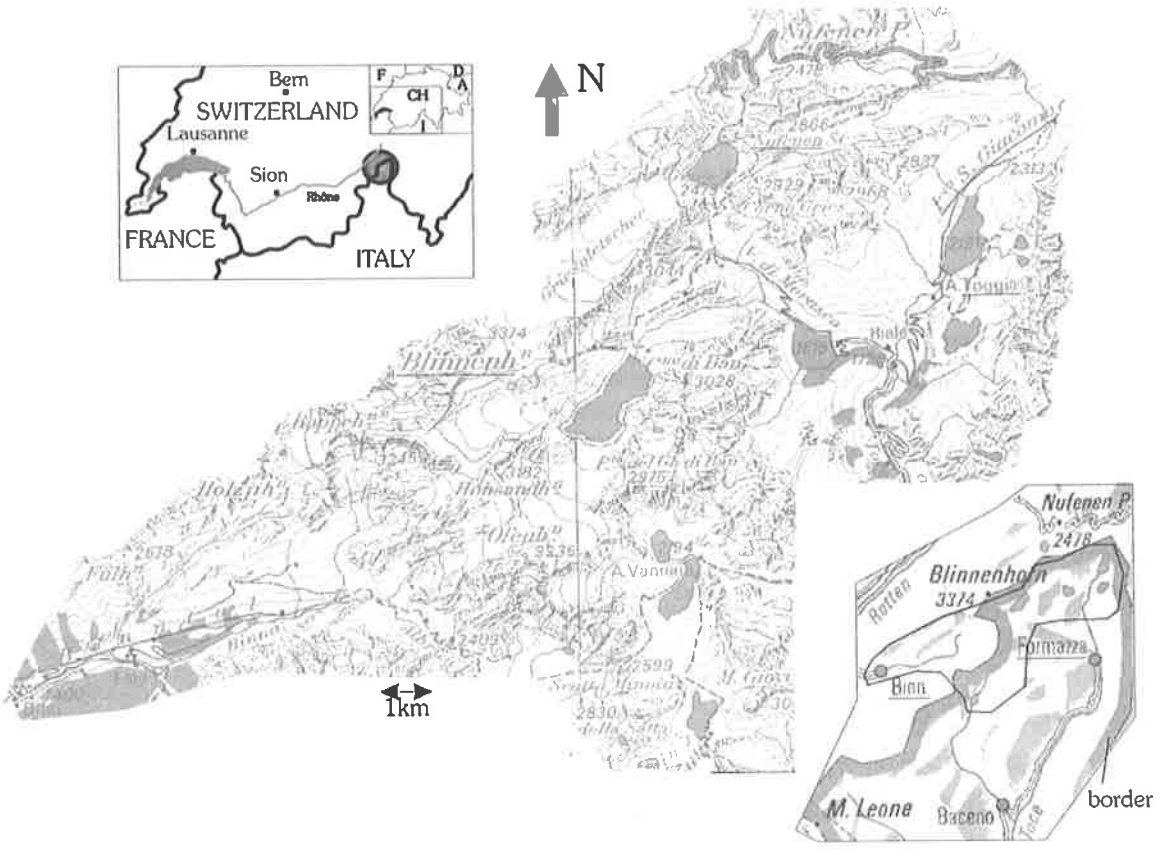


Figure 1.1 Geographical situation.

## 1.2 GENERAL GEOLOGICAL SETTINGS

### 1.2.1 General overview

The Alps are an arcuate mountain belt stretching from the Ligurian Sea to Vienna in Austria. They are composed mainly of pre-Triassic crystalline basement gneisses and sedimentary Mesozoic to Tertiary cover series, intensively folded and metamorphosed in some areas. The Alpine belt is conveniently divided into several broad structural units: a foreland basin, the Prealps nappes, the Helvetic and Ultrahelvetic nappes, the Penninic nappes (subdivided into Lower, Middle and Upper domains) and the Austro- and South- Alpine domain (Fig. 1.2, 1.3). This present superposition of the nappes results from the opening and closing of the Alpine Tethys Ocean, which affected several paleogeographic domains. The following paleogeographic domains are recognized on a transect in the western Alps (ESCHER et al. 1995), proceeding from the North to the South: the European continental domain, the Valaisan sedimentary unit, the Briançonnais exotic terrane, the Alpine Tethys oceanic domain and the Austro- and South-Alpine continental domain (SPICHER 1980, ESCHER et al. 1993, 1997 and references herein, STAMPFLI 1993, MARCHANT & STAMPFLI 1997, STAMPFLI et al. 1998, STECK et al. 2001). The entire structure of the European Alps results from a SE-directed subduction of the Alpine Tethys preceding the Tertiary collision between the European and Adriatic plates (MARCHANT 1993).

The studied area is situated in the Lower Penninic domain of the Central Alps and belongs to the so-called Lepontine or Simplo-Ticino Dome.

### 1.2.2 The Central Alps

In order to understand the regional structural relationships better, the tectonic model proposed by STECK et al. (2001) is briefly summarised as follows:

The formation of the Alps may be considered as a succession of three main stages (DAL PIAZ et al. 1972, DEBELMAS et al. 1980, HUNZIKER et al. 1989, STECK & HUNZIKER 1994, RUBATTO et al. 1998, AMATO et al. 1999, GEBAUER 1999). The alpine orogenesis began in the Late Cretaceous (eoalpine phase, **80 My→60 My**) with the subduction of the Austroalpine units. The first high-pressure metamorphism, associated to this underthrusting, is followed by the rapid exhumation of high-pressure rocks. The next mesoalpine phase (?**50 My → 30 My**) is characterized by the closing and the subduction of the Alpine Tethys. This second subduction is responsible for the second high-pressure metamorphism (**50-40 My**, Zermatt-Saas and Monte Rose nappes), which is also followed by rapid exhumation of the subducted rocks. The nappe stacking then reached its paroxysm and ends with a Barrovian metamorphism (middle-pressure metamorphism **38-25My**). The Penninic and Helvetic nappes were continuously created by detachment, accretion and extrusion of the upper part of the European crust and Briançonnais terrane subducting below the Cretaceous to early Tertiary orogenic wedge. From 34-30 My, the Alpine belt developed under simultaneous NW- and SE- directed thrusting associated to dextral strike-slip shear faults. The Oligocene magmatism (32-26 My) marks the limit between the mesoalpine and neoalpine phase (**30 My→ present**). The uplift of the Lepontine gneiss dome started some 30 My ago, and was concomitant with early south directed backfolding and backthrusting. It reached the Simplon region some 18-15 My ago (HUNZIKER et al. 1992).

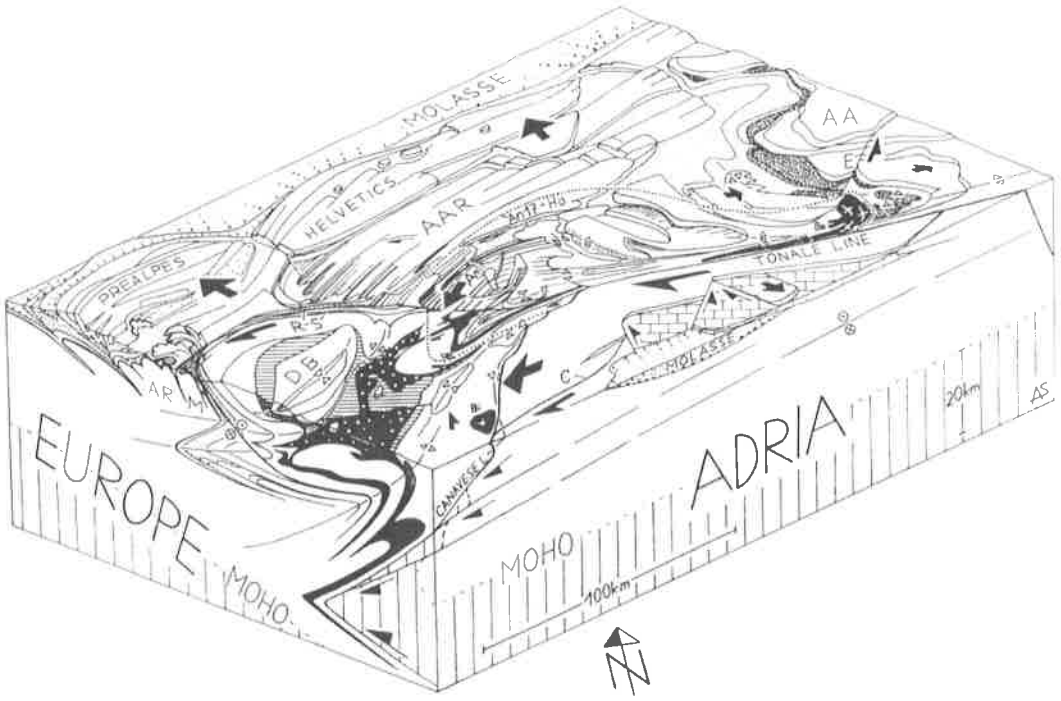


Figure 1.2 The Central Alps with the Lepontine Gneiss Dome and related deformational structures of Oligocene-Quaternary age (after STECK & HUNZIKER 1994).

In the Alps, the peak of metamorphism, which post-dated the SE-directed subduction of the nappes, is dated to 38 My (HUNZIKER 1969, HUNZIKER et al. 1992). In the Central Alps, this event went on gradually to a second Barrovian metamorphism (→25 My), also called the Lepontine metamorphism (WENK & KELLER 1969). The latter induced a concentric pattern of the regional isograds (HUNZIKER et al. 1992 and references therein, TODD & ENGI 1997). This event has been dated to 38-35 My by HUNZIKER (1969), and then JÄGER (1973), to 27-20 My by KÖPPEL & GRÜNENFELDER (1975), to 29-23 My by DEUTSCH & STEIGER (1985) and to 29.6-26.7 My by VANCE & O'NIONS (1992). It is well preserved because of the late and quick cooling of the Lepontine Dome. The existence of a first high pressure event in this region is still yet to be proven; such relicts were found only up to now in the Campo Lungo area to the east (BECKER 1993), and in the Simplon region to the west (HAMMERSCHMIDT & FRANCK 1991).

### 1.2.3 The High Val Formazza – Binntal area

The studied area lies in the Lepontine Alps and belongs to the Lower Penninic domain (Fig. 1.3, 1.4). The Lepontine Alps extend, structurally, southward and above the external Aar-Gotthard massifs and are delimited westwards by a major late extensional fault, the Simplon line (BEARTH 1956, HUNZIKER 1969, HUNZIKER & BEARTH 1969, STECK 1980, 1984, 1990, MANCKTELOW 1985 and 1990, MANCKTELOW & PAVLIS 1994), and southwards by the Insubric line. The eastern limit corresponds to the Bergell intrusion (HANSMANN 1996).

The rocks consist of polymetamorphic refolded basement gneisses separated by thin intercalations of Mesozoic to Tertiary cover series (STUDER 1844, GERLACH 1869, SCHARDT 1903, SCHMIDT & PREISWERK 1908, ARGAND 1911). For instance ARGAND (1911) described from base to top the following succession of pre-Triassic basements separated by sedimentary rocks for the Lepontine Alps:

- nappe n°O: Verampio – nappe n°1: Antigorio – nappe n°2: Lebendun - nappe n°3: Monte Leone – nappe n°4: Grand Saint-Bernard (here the Berisal)

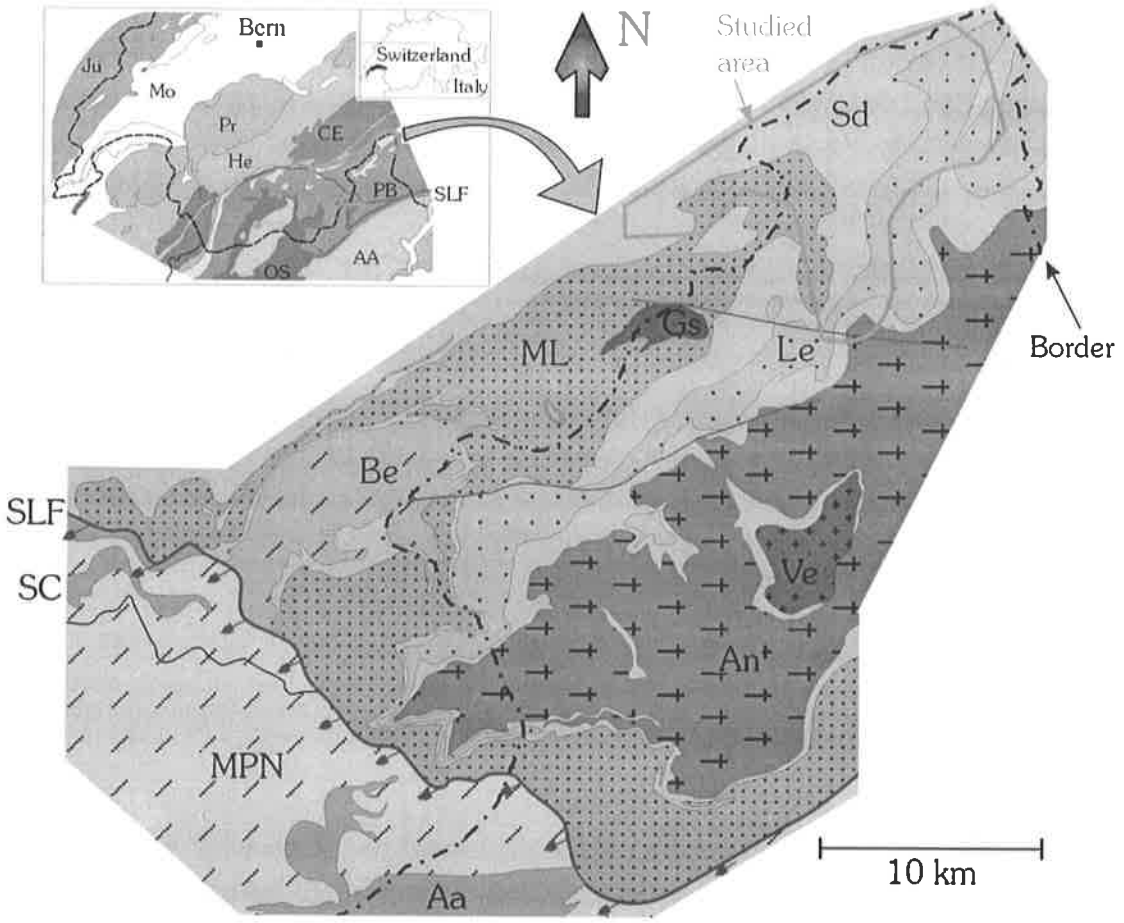


Figure 1.3 Tectonic sketch of the Central Alps (modified after SPICHER 1980, MANCKTELOW & PAVLIS 1994, STECK et al. 1999 and 2001, and new fieldwork). (AA: Austroalpine, CE: external crystalline massif, He: Helvetics, Ju: Jura, Mo: Molassic basin, OS: ophiolite and sediments of the Alpine Tethys, PB: Penninic basements, Pr: Prealps, / Aa: Antrona nappe, An: Antigorio nappe, Be: Berisal series, SC: Sion-Courmayeur zone (Valaisan), Gs: Geisspfad complex, MPN: middle penninic nappes, Le: Lebendun nappe, ML: Monte Leone nappe, Sd: undifferentiated Mesozoic to Tertiary cover, SLF: Simplon Line, Ve: Verampio nappe).

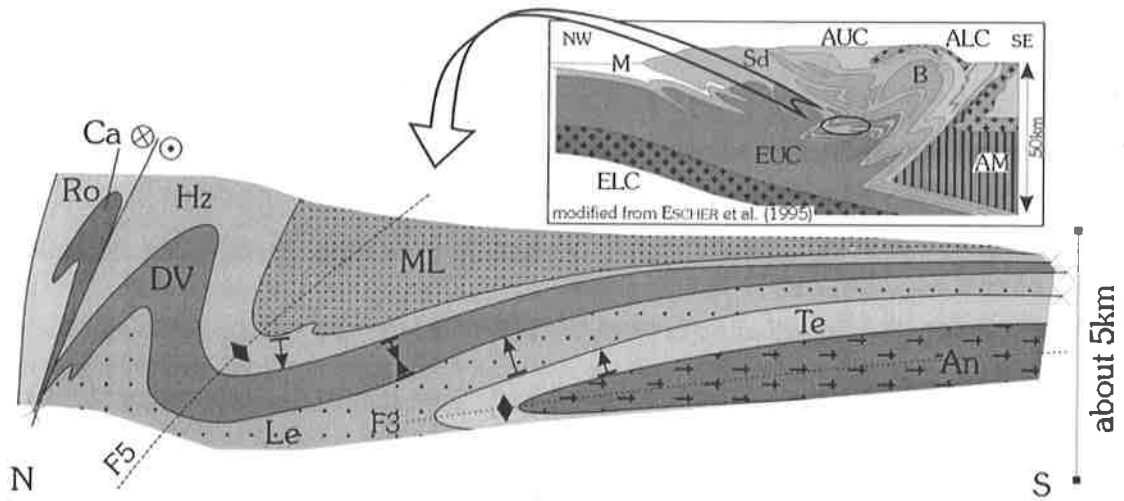


Figure 1.4 General cross-section of the studied area; inset a larger scale section of the Alps. (ALC: Adriatic lower crust, AM: Adriatic mantle, AUC: Adriatic upper crust, B: Briançonnais terrane, ELC: European lower crust, EUC: European upper crust, M: Molassic basin, Sd: undifferentiated Mesozoic to Tertiary covers / An: Antigorio basement, Ca: Camosci nappe, Le: Lebendun nappe, ML: Monte Leone basement, Ro: Rosswald, Hz: Holzerspitz series, Te: Teggiolo cover, V: Pizzo del Vallone nappe). The arrows indicate the polarity. F3 and F5 are described in the chapter VI.

Since ARGAND (1911) proposed his model, several geologists have mapped the Lepontine Alps (HEIM 1922, BADER 1934, WENK 1955, JOOS 1969, HANSEN 1972, MILNES 1974, BOLLI et al. 1980, SPICHER 1980, STECK 1984, LEU 1986, STECK 1987, CANEPA 1993, STECK 1991, BIANCHI et al. 1998, STECK 1999 and 2001). The succession of ARGAND (1911) is still accepted but the names and tectonics limits vary greatly, according to the authors, especially where sedimentary covers are concerned. Some comparisons have been made for the studied area (Tab. 1.1, 1.2).

The results of the detailed lithostratigraphic study, linked to the precise geological mapping presented in this work, allow the following superposition, which will be exposed and defended in this work (Chapter II and VII, Fig.1.4) to be deduced. At the base the normal limb of the Antigorio nappe outcrops: it is composed of the Antigorio pre-Triassic basement gneisses and its Mesozoic to Tertiary sedimentary cover called the Teggiolo zone. Above the Teggiolo zone lies in a normal position the Mesozoic series of the Lebendun nappe. The latter is overlaid by the Pizzo del Vallone nappe; this nappe is composed of Mesozoic to Tertiary sediments intruded by mafic dykes and containing large discontinuous extrusive metabasaltic bodies. This newly described nappe outcrops between the Lebendun nappe and the Monte Leone nappe-fold. The inverted limb of the Monte Leone nappe, which begins with its Mesozoic and Tertiary cover series called the Holzerspitz series, surmounts the Pizzo del Vallone nappe. On the northern part of the area, thanks to a structural discontinuity, the Camosci nappe and the Rosswald series are found.

| JOOS (1969) | HANSEN (1972) | CANEPA (1993) | LEU (1986) | BOLLI et al. (1980) | This work |
|---|---|---|---|---|---|
| Monte Leone | Monte Leone | Monte Leone | Monte Leone | Monte Leone | Monte Leone |
| Veglia zone | Veglia zone | Veglia zone | Fäldbach-Zone | Triassic levels Holzerspitz-Serie | Holzerspitz series |
| Lebendun M. | | Monte Cazzola series | Sabbione-Zone | Fäldbach-Zone | Pizzo del Vallone nappe |
| Lebendun P+B | Lebendun cover Lebendun | Lebendun nappe | Lebendun-Decke | | Lebendun nappe |
| Teggiolo zone | Teggiolo zone | Teggiolo zone | Teggiolo-Zone | | Teggiolo zone |
| Antigorio | | Antigorio | Antigorio | | Antigorio |

Table 1.1 Nomenclature of the lower Penninic nappes (Verampio omitted) outcropping south of the rio del Sabbione strike slip faults ( ——— = tectonic contact, - - - = stratigraphic contact, and in grey-shaded the units considered as pre-Triassic basement by the authors).

| Lithostratigraphy (this work) | HANSEN (1972) | LEU (1986) | BIANCHI and al. (1998) | This work |
|---|---|---|---|---|
| Calcschist | Bedretto zone | Rosswald series | Bedretto Zone | Rosswald series |
| Dolomitic & calcareous series | | Sabbione Zone | | Camosci nappe |
| Graphitic & detritic series | | Termen zone | | |
| Termen Zone | Termen Zone | | | |

Table 1.2 Nomenclature of the lower Penninic nappes outcropping north of the rio del Sabbione strike slip faults ( ——— = tectonic contact).

## 1.3 BRIEF HISTORY

In the early studies (STUDER 1844, GERLACH 1869, SCHARDT 1903, STELLA 1903, LUGEON & ARGAND 1905, SCHMIDT & PREISWERK 1908, ARGAND 1911), the Lepontine Alps were described as a series of gneissose pre-Triassic basements separated by synclines of Mesozoic to Tertiary sediments. Several geological questions were raised and can be sum up as follows:

- understanding of the structural deformation in the Lepontine Alps as well as their associated metamorphic crystallisation (WENK 1955, HIGGINS 1964, JOOS 1967 and 1969, HUNZIKER 1969, HANSEN 1972, STECK 1984, 1987 and 1990, LEU 1986);

- determination of the origin and the Paleozoic or Mesozoic age of the Lebendun paragneiss, which is a thick series of conglomeratic gneisses exposed in a nappe structure for over 50 kilometres. (STUDER 1851, LUGEON 1901, SCHMIDT 1907, ARGAND 1911, BURCKHARDT 1942, NABHOLZ 1954, STAUB 1958, RODGERS & BEARTH 1960, HIGGINS 1964, JOOS 1967, LEU 1986, SPRING et al. 1992).

- study of the correlations at a greater scale between the Western and Eastern Alps (SCHARDT 1906, HEIM 1922, JENNY 1924, PREISWERK and GRUTTER 1924, BOSSHARD 1925, NIGGLI et al. 1936, STAUB 1958, SPICHER 1980). The Lepontine Alps represent the poorly understood link between the Eastern and Western Alps. As the tectonic limits and the paleogeographic signification were interpreted in different ways according to the various authors (Tab. 1.1, 1.2), several solutions were proposed.

- proposition of tectonic models, construction of detailed cross-section and dating of the successive mineral crystallisation (HIGGINS 1964, HALL 1972, MILNES 1973, 1974A and 1974B, STECK 1984, 1987, 1990, MERLE 1987 and 1989, STECK et al. 1999 and 2001, LEU 1986, HUNZIKER et al. 1992, STECK and HUNZIKER 1994).

## 1.4 PROBLEMATIC AND GOALS

Initiation of this work followed two mutually exclusive observations:

- BOLLI et al. (1980) separated a green-rock bearing nappe from the Monte Leone cover (Tab. 1.1). Such a distinction was lately refuted by LEU (1986);
- PASTORELLI et al. (1995) and KNILL (1996) considered the Mesozoic green-rocks outcropping respectively in the Geisspfad-Devero and Binntal areas as emplaced in the "Valaisan" transform zone, or coeval to the opening of the "Valaisan" ocean (both term referring to the plate limit which made the drift of the Briançonnais terrane possible). And yet the so-called "Trilogie Valaisanne" series (BURRI 1979) was never described in these areas. Moreover at the same time CANNIC (1996) dated the green-rocks supposed to belong to the Valaisan ocean in France, and obtained a Paleozoic age.

These two observations were the starting point of this PhD. The latter focussed initially on fieldwork and drafting of a detailed geological map. New goals were defined in due course according to the field results. Finally, I decided to discuss the following topics:

| | |
|---|---|
| - Geological goals: | 1) detailed geological map |
| | 2) stratigraphic study of the Mesozoic series (Chapter II) |
| | 3) structural history (Chapter VI) |
| | 4) crystallisation-deformation relations (Chapter III) |
| - Mineralogical goals: | 1a) geochemistry of the green rocks (Chapter V) |
| | 1b) dating of the green rocks |
| | 2a) P-T evolution (Lepontine thermal doming) (Chapter IV) |
| | 2b) dating of the Lepontine thermal doming |
| | 3) geochemistry of the micaschists |
| - Geodynamic goals: | 1) restoring of the Helvetic passive margin (Chapter VII) |

# 2 STRATIGRAPHY

## 2.1 INTRODUCTION

The lower Penninic nappes are the deepest structural units outcropping in the Alps (Fig. 1.3); they represent the southeastern continuation of the European plate (ESCHER et al. 1997, MARCHANT & STAMPFLI 1997). The polymetamorphic refolded basement gneisses are separated by thin Mesozoic to Tertiary cover series, all commonly grouped under the general term "Bündnerschiefer" (GERLACH 1869, SCHMIDT & PREISWERK 1908, ARGAND 1911). The youngest metasediments are not often preserved, but the study of the older Mesozoic rocks, presented herein, provides enough information to infer their respective paleogeographic position and to propose a coherent geodynamical model.

This chapter presents the systematic lithostratigraphic description of all the nappes studied during this work, followed by a chronostratigraphic interpretation. The discussion paragraph (II.7) focuses on the specific problems, limits and characteristics of the Holzerspitz series, Pizzo del Vallone and Camosci nappes; they are then compared to non-Simplo-Ticino units (paragraph II.8).

General remarks:

- the thicknesses mentioned on the figures are always the thicknesses measured on the field;
- as no datable fossils were found, all levels are "dated" by comparison of their lithology with other external nappes (paragraph II.2.4, II.3.6, II.4.4, II.5.3, II.6.3 and II.8);
- the Rosswald series is not described here. It is present on the geological map only as the northern limit of the studied area. The reader interested in the subject should refer to BOLLI et al. (1980).

## 2.2 THE HOLZERSPITZ SERIES (THE MONTE LEONE COVER SERIES)

### 2.2.1 Introduction and nomenclature consideration

The Monte Leone nappe consists of a pre-Triassic basement surmounted by its autochthonous Triassic to Upper Cretaceous/Tertiary sedimentary cover called Holzerspitz series (Tab. 1.1).

As presented in the introduction (Tab. 1.1, paragraph I.2.3) the name and the upper tectonic limits of this cover differ according to the various authors (BADER 1934, STAUB 1956, JOOS 1969, HANSEN 1972, STRECKEISEN et al. 1978, BOLLI and al. 1980, LEU 1986, JEANBOURQUIN & BURRI 1991, CANEPA 1993). For instance, CANEPA (1993) differentiated the various lithologies present between the Monte Leone and Antigorio basements, but he interpreted the whole stack as a single cover series folded in a giant synclinal structure.

The name chosen in the present study for the Monte Leone cover is the "Holzerspitz Series" (BOLLI et al. 1980) because:

- the upper tectonic limit of BOLLI et al. (1980) and of this work are in agreement. However, I have simply slightly changed the original definition by considering that the Triassic levels form the lower boundary in stratigraphic contact with the basement;
- the series is well exposed at this locality, a mountain in the East flank of the Binntal.

The most commonly used term of Fäldbach was rejected because:
- the upper tectonic limit as defined by LEU (1986) does not correspond to the upper limit mapped in this work. The main differences are that; i) LEU (1986) incorporated the Rosswald series and ii) did not separate the Pizzo del Vallone nappe
- the unit outcropping at the locality of Fäldbach (a now destroyed alpine farm house), is the newly defined Pizzo del Vallone nappe (paragraph II.3.1).

### 2.2.2 Nappe structure

The Monte Leone cover is well represented only in its inverted limb. Indeed, the normal limb systematically shows an extremely reduced or even absent cover series because of i) the thinning due to alpine tectonics and ii) probable original stratigraphic hiatuses. The studied area encompasses only the inverted limb. Consequently the studied sections are amongst the most complete that one can log (Fig. 2.1).

### 2.2.3 Lithostratigraphic description

The main lithostratigraphic sections are shown in figure 2.1. These were logged over the whole studied area (except column D which comes from the lower part of the Binntal) and show significant lateral variations, both in thickness and in facies. Thus, instead of describing each section individually, 4 groups are defined and described hereafter. Each of these groups is bound by a characteristic unconformity respectively UC1, UC2 and UC3 (Fig. 2.10, paragraph II.7.3).

**Group Hz-I**: lies in stratigraphic continuity directly on the pre-Triassic basement. The representative succession of rocks is, from base to top, a white quartzite, a micaceous to quartzo-dolomitic calcareous marble (→10-15% quartz + dolomite), a white and blue dolomitic marble and lenses of gypsum. The quartzite bed is discontinuous, but where it outcrops, it is always in contact with the Monte Leone basement gneisses. The calcitic marble and the dolomitic marble alternate. The calcitic marble is always subordinated to the dolomitic marble and restricted to the base of the group. The nature of the dolomitic marble changes upward: from blue platted at its base, it becomes massive and white or cream, may contain discontinuous conglomeratic layers (dolomitic pebbles in a dolomitic matrix) and is locally mineralised (KNILL 1996). The group Hz-I ends with a garnet poor micaschist, which is not always present. Even if this group is always figured on the representative stratigraphic columns (Fig. 2.1), it is locally totally eroded and group Hz-II or even Hz-III lie directly on pre-Triassic basement.

**Group Hz-II**: begins with a conglomerate. At its base, the latter is monogenic and consists of dolomitic pebbles in a dolomitic matrix. It evolves gradually upward into a polygenic conglomerate formed by gneissic, quartzitic and dolomitic pebbles and its matrix becomes increasingly quartzo- micaceous and sometimes a little bit calcareous. The pebble size then decreases while the matrix becomes increasingly calcareous. It is followed by an impure marble or calcschist, in turn surmounted by a garnet micaschist (see description in paragraph III.5). The latter may disappear locally and emersion traces are then observed: a paleokarst is conserved in the Holzerspitz section (Fig. 2.1C).

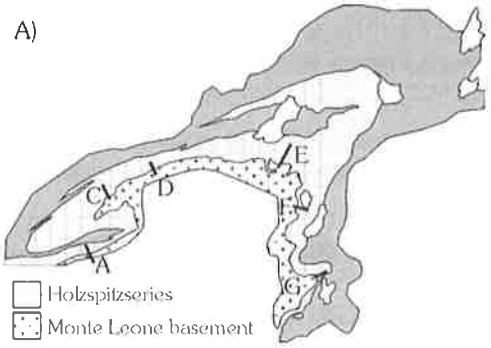


Figure 2.1 A) Localisation of the lithostratigraphic sections B) Lithostratigraphic sections ordered according to their paleogeographic position. UC1, UC2 and UC3 are explained in the paragraph II.7.3 (Fig. 2.10). Section B comes from the lower Binntal (657'800 / 134'300).

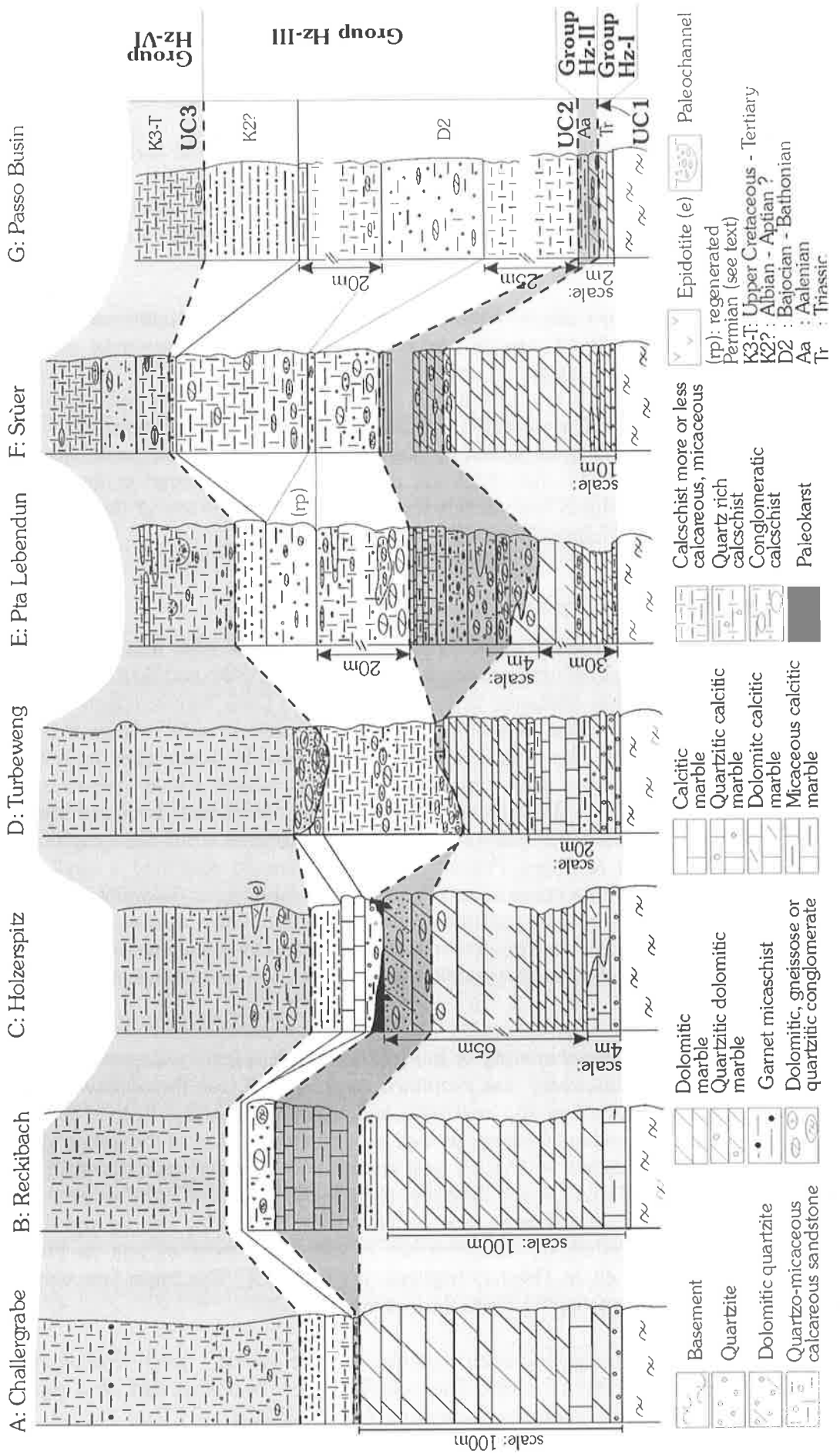
A: Challergrabe
B: Reckibach
C: Holzerspitz
D: Turbeweng
E: Pta Lebendun
F: Srüer
G: Passo Busin
Group Hz-VI
Group Hz-III
Group Hz-II
Group Hz-I
K3-T
UC3
K2?
D2
UC2
Aa
Tr
UC1
scale: 100m
scale: 100m
65m
4m
scale:
20m
20m
4m
30m
scale:
20m
(rp)
scale:
10m
20m
25m
2m
Basement
Quartzite
Dolomitic quartzite
Quartzo-micaceous calcareous sandstone
Dolomitic marble
Quartzitic dolomitic marble
Garnet micaschist
Dolomitic, gneissose or quartzitic conglomerate
Calcitic marble
Quartzitic calcitic marble
Dolomitic calcitic marble
Micaceous calcitic marble
Calcschist more or less calcareous, micaceous
Quartz rich calcschist
Conglomeratic calcschist
Paleokarst
Epidotite (e)
Paleochannel
(rp): regenerated Permian (see text)
K3-T: Upper Cretaceous - Tertiary
K2? : Albian - Aptian ?
D2 : Bajocian - Bathonian
Aa : Aalenian
Tr : Triassic

**Group Hz-III**: is mainly a pile of polygenic conglomerates. In the first basal 10 metres, its matrix is calcareous micaceous metasandstone, which quickly grade upward into a calcschist. At the same time, the size and the proportion of pebbles decrease. All the lithologies of the two underlying groups, as well as the basement, are represented in the pebbles. A conglomeratic quartzitic metasandstone bed is interlayered in this succession (noted "rp" in figure 2.1). It has a characteristic yellow patina and is very hard and massive. Its composition and aspect simulate a regenerated Permian. The dolomitic, quartzitic and gneissic pebbles are badly sorted. The whole succession ends with a quartzitic marble rarely conglomeratic (gneissic pebbles) that changes gradually over a few metres into a garnet micaschist (see description in paragraph III.5) containing hard nodules that I called "garnetite".

**Group Hz-IV**: consists of a thick pile of monotonous calcschist, which is conglomeratic at its base. Pebbles of all the previous levels can be reworked, even though the dolomitic ones always dominate. In the Holzerspitz section an epidotite was found (e on Fig. 2.1C). Upward, the monotonous calcschist deposit is interrupted only by small to medium sized paleochannels, thin layers of garnet micaschist or fine quartzitic metasandstone. The basal conglomeratic calcschist was deposited in a fluvial setting, as shown by plurimetric to pluridecimetric paleochannels that deeply cut into the group Hz-III and which are particularly well preserved in the Turbeweng section (Fig. 2.1D). Neither flysch nor wildflysch were observed at the top of this group, which marks the upper limit of the Holzerspitz series.

### 2.2.4 Chronostratigraphic interpretation

**Group Hz-I**: it contains the Triassic rocks commonly found in the Alps (ELLENBERGER 1958, MASSON et al. 1980, BAUD 1987 and reference therein, EPARD 1990 and SARTORI 1990). The first white quartzite is classically attributed to the Late Permian - Early Triassic epoch: its presence is a good argument in favour of the autochthony of the Holzerspitz series in relation to the Monte Leone pre-Triassic basement. The next layers of a calcitic marble surmounted by a dolomitic marble are specific of the studied area. They display neither Helvetic affinity (where such beds are unknown, EPARD 1990) nor Briançonnais affinity (where similar beds have a thickness that can easily reach 100 m, BAUD & SEPTFONTAINE 1980). This supposes a paleogeographic position where both influences were recorded. POLACK (1983) has already described a similar Triassic succession, but for the Verampio cover series (Fig. 7.6). The monogenic dolomitic conglomerate (middle to upper part of Group H-I) is tentatively attributed to the late Ladinian – Carnian weak extensional phase recognised in the Briançonnais domain (MEGARD-GALLI & FAURE 1988). The terminal thin-bedded garnet micaschist has similarities with the non-metamorphic "Rhetian" facies of the Western Alps.

**Group Hz-II**: the polygenic conglomerate of this group records a quite widespread extensional episode, during which the basement was submitted to erosion. It was then followed, over the whole area, by the deposition of an impure marble and a garnet micaschist, both of which reflect a quiet, clearly marine depositional setting, as well as a temporary stop of the tectonics activity. Such lithologies and depositional setting are well known and recorded everywhere in the Alps and have a Late Liassic to Aalenian age (MASSON et al. 1980, BAUD 1987 and reference herein, EPARD 1990 and SARTORI 1990). I propose a similar age for the calcitic marble and the garnet micaschist, whereas the underlying conglomerate would correspond in age to the Liassic extensional phase (nappe de la Brèche, STEFFEN et al. 1993). The important variation in thickness and in facies of the group Hz-II has three causes:

- the highly variable paleogeography (extensional type setting), which implies important lateral variations of detrital input. The paleokarst can be interpreted as a sign of the emersion of tilted block geometry (paragraph 7.4, Fig. 2.1C);

- the next erosive event, called UC2 (Fig. 2.1, 2.10) was so important that it could erode the whole group Hz-II;
- later alpine deformation would stretch or constrict the cover differently according to its variable competency.

**Group Hz-III**: a second important tectonic activity is reflected by the deposition of polygenic conglomerates forming 100 m to 500 m wide lenses disposed longitudinally one after the other. The basal limit UC2 shows evidence of aerial to subaerial erosion (fluviatile paleochannels and karst) and is locally responsible for the disappearance of the group Hz-II and Hz-III. An episode of extensive karstification is known in the lower Dogger of the Internal Briançonnais (BAUD et al. 1979, HÜRLIMANN et al. 1996), and the "conglomérats du Lédery" were deposited at the same time in the Niesen anppe; so I propose a similar age for UC2 (which would be an any case younger than the Aalenian, Fig. 2.1). The change toward monotonous calcschist deposit, locally conglomeratic, reflects a progressive decrease in the tectonic activity, only interrupted by an input of terrigeneous clastics resulting in a regenerated Permian bed. The calcschists grade upward into a pure calcitic (locally conglomeratic) marble: such a pure calcitic marble is generally attributed, in the Alps, to the Malm epoch. The platform was then flooded and a graphitic shale (garnet micaschist) was deposited. I attribute it to the middle Cretaceous epoch because this epoch is marked by a globally high sea level and the whole Helvetic domain recorded, a southward trend toward deeper facies (MASSON et al. 1980).

**Group Hz-IV**: its basal level UC3 is erosive (paragraph II.7.3). The basal conglomeratic part contains pebbles coming from all the previous described levels, but also an epidotite coming most probably from the Pizzo del Vallone nappe. This suggests that rocks coming from other nappes are reworked here as pebbles and point to a new type of tectonic activity (inversion?). The following thick succession of calcschist proves a continual fine detrital input: the absence of a specific marker level prevents me from proposing a better constricted age other than Late Cretaceous to Tertiary.

## 2.3 THE PIZZO DEL VALLONE NAPPE

### 2.3.1 Introduction and nomenclature consideration

It is the green rocks bearing nappe. The majority of authors did not separate this nappe from the Monte Leone nappe. However LÜTHY (1967) informally introduced the name of "Fäldbach Zone" for the latter. BOLLI et al. (1980) added a tectonic limit between the Fäldbach Zone and the Holzerspitz series. Later the name of Fäldbach Zone became ambiguous, since LEU (1986) did not accept the tectonic limit recognised by LÜTHY (1967) and BOLLI et al (1980), but did use the same name for the Monte Leone cover series. The main results of this work are:

- the green rocks bearing unit is separated from the Monte Leone cover series by a tectonic contact;
- the mapped tectonics limits are in agreement with the work of BOLLI et al. (1980).

Instead of using BOLLI's nomenclature (the Fäldbach zone having unfortunately two definitions) this work introduces a new name, the Pizzo del Vallone nappe, whose upper and lower limit are formally defined below.

### 2.3.2 Nappe structure

The oldest levels outcropping over the studied area are either a cornieule or a dolomitic marble attributed to the Late Triassic time. This means that this nappe is detached from its pre-Triassic basement and is only made up of Mesozoic to Tertiary rocks (Fig. 2.2).

This nappe forms a "synclinal de raccord" between the Monte Leone and the Lebendun nappes (Fig. 6.9): it lies in an inverted position below the Monte Leone inverted limb, and in a normal position above the Lebendun nappe. The thickness of the nappe varies a lot, depending mainly on the thickness of the magmatic bodies, the total amount of detrital input and the lateral variations of facies. An ideal stratigraphic scheme, summarising all the relations observed on the field, is presented in figure 2.2.

### 2.3.3 Lithostratigraphic description

**Group V-I**: the first levels consist either of a cornieule, of rare big lenses of gypsum, or of a dolomitic marble. They are followed by an impure calcitic marble. The latter contains quartzitic and dolomitic detrital grains in various proportion (→20-25% quartz + dolomite), and an interbed of discontinuous light green micaceous quartzite rich in millimetric pyrite crystals.

**Group V-II**: A first conglomerate is then found mainly above an erosive contact, although locally the observations of a progressively greater proportion of detritic grains in the underlying marble could point to a more transitional contact. The conglomerate is best developed in the Fäldbach but also near the little lake situated between the Lago del Sabbione and the Gemelli di Ban (670'980 / 140'210). It is conglomeratic at its base and consists of a quartzitic dolomitic marble containing dolomitic pebbles. It then evolves upward into a polygenic conglomerate (consisting of gneissic, quartzitic and dolomitic pebbles), while the matrix becomes a quartzo-micaceous microsandstone. This first detritic sequence is followed by another similar succession, also beginning with a monogenic conglomerate. But the latter significantly consists of pebbles of gneisses. The matrix is a quartzo-micaceous microsandstone, which becomes finer and more mature upsection, finally giving way to a layer of fine blue micaceous quartzite. This sequence is in turn followed by a conglomeratic quartzitic marble, consisting of dolomitic pebbles, detritic dolomitic grains and 25 to 40 % of quartz grains. The whole unit ends with a non-calcareous garnet micaschist (microquartzitic shale), rarely present over the mapped area because most of it is eroded by time.

**Group V-III**: The next metasandstone, the "**Sabbione metasandstone**" (see description in paragraph III.3), is characteristic of the Pizzo del Vallone nappe. It is easily recognizable due to the presence of many ferromagnesian minerals, discontinuous stratiform fine levels of calcitic marble or of quartzite, and metric paleochannels. This metasandstone is conglomeratic; it reworks essentially dolomitic pebbles, a few pebbles of garnet micaschist, quartzite and gneisses may be found locally. Its mineralogy is variable, but it mostly contains randomly oriented metamorphic porphyroblasts of amphibole, kyanite, and staurolite... (paragraph III.3, Fig. 3.2). The Sabbione metasandstone becomes finer and more mature upward (Fig. 2.2). This level was already recognised by ETTER (1984) in the Toggia area.

The Sabbione metasandstone is, at its base, locally crosscut, at the same time as the underlying marble, by mafic dykes; some cooling rims are preserved. These dykes are the first signs of a magmatic activity, which becomes evident with the overlying extrusive discontinuous basaltic bodies, capped by a metavolcanoclastic level interbedded in the upper part of the Sabbione sandstone (see below).

Figure 2.2: Schematic stratigraphy of the Pizzo del Vallone nappe. The mafic rocks are coloured in greyish. UC1, UC2 and Uc3 are the main unconformities (paragraph II.7.3).

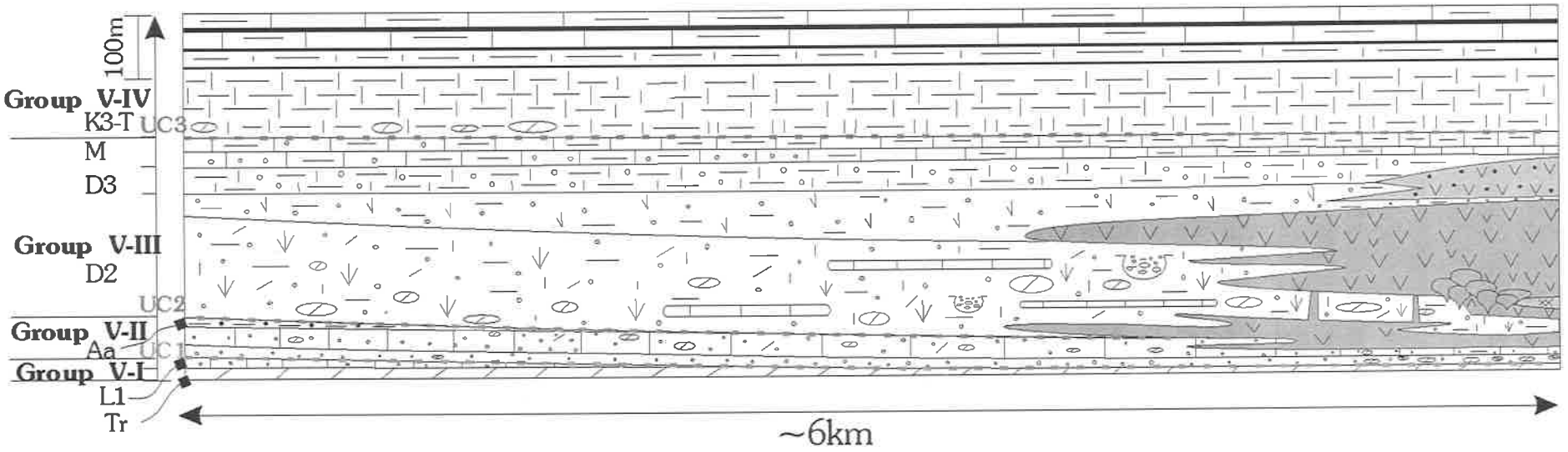


Dolomitic marble, cornieule
Calcitic marble
Quartzitic calcitic marble
Quartzo-dolomitic calcitic marble
Quartzo-micaceous calcitic marble
Quartzite

Garnet micaschist
Sabbione sandstone (basal coarser part)
Sabbione sandstone (upper finer part)
Dolomitic, quartzitic, gneissose pebbles
Paleochannel

Dolerite (dyke or sill)
Basalts and metapillows-lavas
Cumulat
Interstratified volcanoclastic

Calcschist more or less calcareous, micaceous
Micaschist

K3-T: Upper Cretaceous - Tertiary
M : Malm
D3 : Callovo-Oxfordian
D2 : Bajocian - Bathonian
Aa : Aalenian
L1 : Lower Liassic
Tr : Triassic

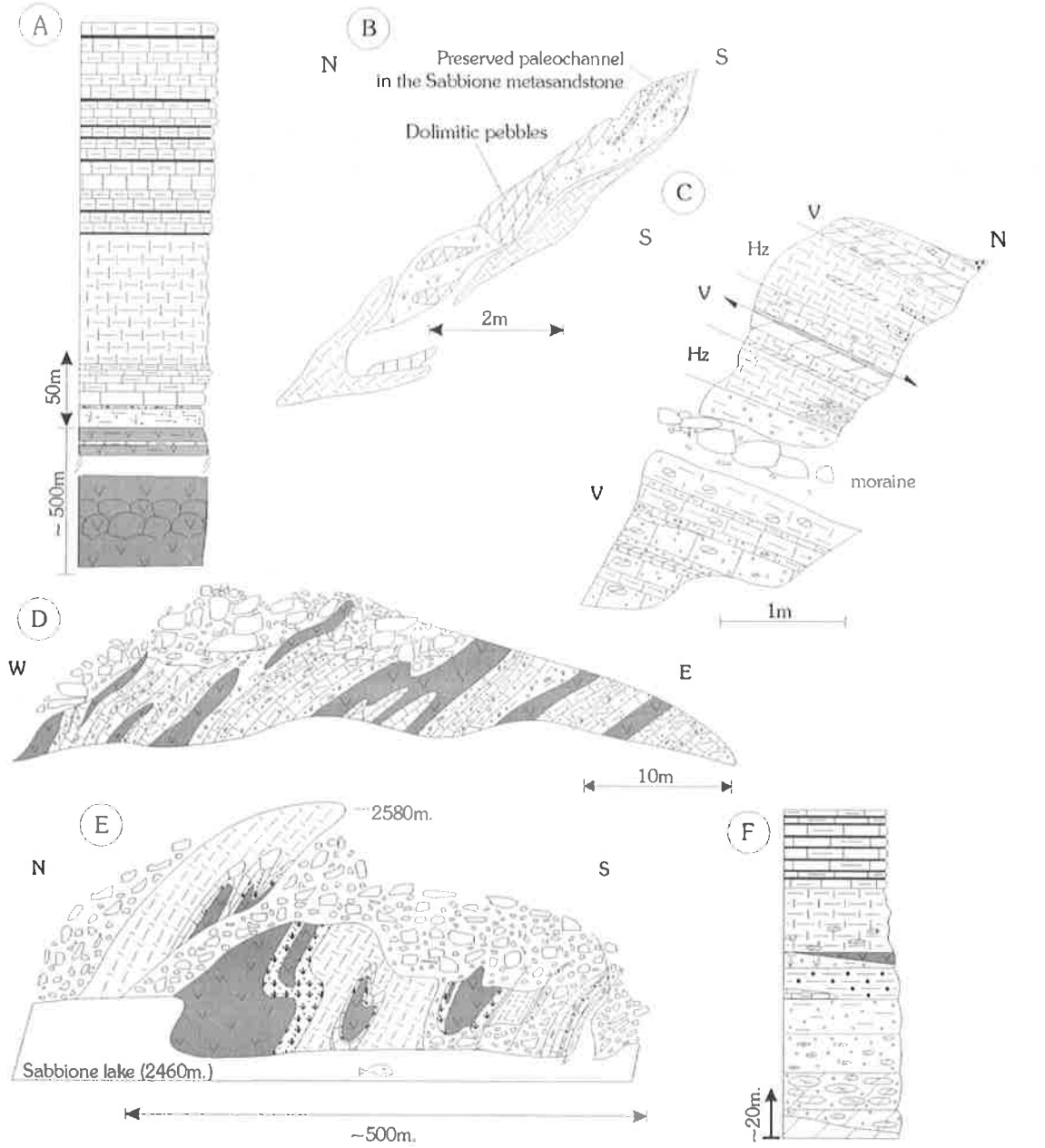


Figure 2.3 The Pizzo del Vallone nappe. A) Stratigraphic section of the upper part of the nappe (left side of the Lago del Sabbione). B) Outcrop of the Sabbione metasandstone southeastern shore of the lago del Sabbione. C) Outcrop showing the isoclinally folded contact between the Holzerspitz series (younger levels) and the Pizzo del Vallone nappe (Group Hz-I and Hz-II) on the left bank of the lago del Sabbione (668'480 140'450). D) Dykes in the quartzitic marble and the Sabbione metasandstone (left bank of the Lago del Sabbione). E) View of the east shore of the lago del Sabbione. F) Synthetic section of the Pizzo del Vallone nappe in the Fäldbachtal. The legend is the same for figure 2.2; Hz: Holzerspitz series, V: Pizzo del Vallone nappe.

A calcareous graphitic micaschist containing epidote or plagioclase porphyroblasts (graphitic marlstone) overlies the Sabbione metasandstone. The contact between the two is clear-cut (especially where the metasandstone laterally gives way to the metavolcaniclastic), although it may be gradual at the decimetric scale. Locally the calcareous graphitic micaschist may smell foul when hit with the hammer. It is overlaid by a quartzitic calcitic marble or by fine alternation of thin beds of calcareous quartzite and of thin quartzitic calcitic marble that may change into a pure calcitic marble. The contact with the calcareous graphitic micaschist is gradual.

**Group V-IV**: two types of basal contact are observed: it is either clear-cut (erosive?), or gradual, the underlying calcitic marble becoming micaceous and grading into a calcschist containing rare dolomitic pebbles at its base. In both cases, the calcschist unit ends with a final calcareous metaflysch: an impure greenish quartzitic marble alternates with a dark non-calcareous fine micaschist (Fig. 2.3A+F).

### 2.3.4 The mafic bodies

The size and shape of the individual basaltic bodies differ, but the lithological igneous succession is the same. The outcrops that show the best magmatic succession are located west of the Lago del Sabbione, close to the Rifugio "Claudio e Bruno".

The oldest igneous rocks consist of dykes and/or sills (Fig. 2.3D) intruding the conglomeratic quartzitic calcitic marble and the Sabbione sandstone, as well as rare epidotites. The latter is a very fine-grained, almost aphinitic, massive and hard rock, which if not for its characteristic pistache-green colour, can be mistaken in the field with a quartzite. Microscopically it is made of submillimetric secondary pistachite and plagioclase minerals in granular texture. This rock is interpreted as a metamorphosed vitric tuff. The basaltic bodies sensu strictu are recognizable thanks to the presence of basal metacumulates (paragraph IV.5), which display a more primitive geochemical signature (paragraph V.2.3, Fig. 5.3A). The majority of the mafic bodies are composed of fine-grained or microgabbroic metabasalt, metapillows, and some metabreccias (see description in paragraph III.6, Fig. 2.3, 2.3E). The metapillows prove the submarine volcanic emplacement. The field relations show evidences of multiple magma injections, but this is likely to have occurred over a short period of time because no sediment were deposited in between. The final volcanoclastics metasediments are either layered with the upper part of the Sabbione sandstone, in which case the different stages of tectonic deformations are well recorded, or are massive. A quartzitic matrix supports the amphiboles, epidotes and some plagioclase.

The term "mafic body" is used because of the discontinuity of the green rocks outcrops. Actually this discontinuity may be stratigraphic (several lateral mafic suites pulses) and/or tectonic (boudinage).

### 2.3.5 Lateral variations and continuation of the nappe in the Saflischpass–Rosswald area

The mafic bodies are best developed in the Sabbione area: their sizes decrease westward in the Binntal and southward in the Vannino-Busin area, indicating that these two regions were paleogeographically more distant from the magmatic centre. Similarly the Sabbione metasandstone thickness decreases toward the Binntal area as if this region was paleogeographically situated in a more distal position than the Sabbione area.

The mineralogy of the Sabbione metasandstone reflects the nature of the detritic supply, which varies from terrigenous and calcareous (dolomitic and quartzitic) to volcanic (relative enrichment in metamorphic ferromagnesian minerals which can be locally so important that the rock simulates a mesocratic basalt). The metasandstone can evolve from one type to another in only a few metres (e.g. from an essentially regenerated dolomite to a quartzo-micaceous rocks or from the latter to a regenerated basalt).

The Sabbione metasandstone outcrops up to the Saflischpass, where it is associated to big lenses of gypsum (similar situation as in the Toggia area) and to green rocks, which have preserved their magmatic texture (paragraph V.2.2). It would be interesting to follow the Pizzo del Vallone nappe westwards toward Visp, to see whether this nappe continues or whether it disappears, giving way to the Monte Leone nappe.

### 2.3.6 Chronostratigraphic interpretation

**Group V-I and V-II**: this nappe is detached from its basement, but comparisons with other stratigraphic column show that it begins with the typical upper Triassic dolomitic marble now well recognised in the Alps (BAUD & SEPTFONTAINE 1980, MASSON et al. 1980, EPARD 1990). Such an argument suggests that the pre-Triassic basement of the Pizzo del Vallone nappe was of continental nature.

The overlying impure calcitic marble, interbedded with impure quartzite (group V-II) can be related to similar succession typical of the Liassic epoch (BAUD & SEPTFONTAINE 1980, MASSON et al. 1980, DOLIVO 1982 and BUGNON 1986). The incoming of conglomerate is similarly typical of the Prepiemontais Liassic succession. The graphitic garnet micaschist (microquartzitic shale) can be linked to the Aalenian high-stand (JENKYNS 1988) during which similar deposit are known almost everywhere in the Alps (schistes à miches...).

**Group V-III**: then the conglomeratic Sabbione metasandstone was deposited. The conserved metapaleochannels indicate a relative shallow-water environment of deposition. The fact that the Sabbione metasandstone becomes more mature and finer up sequence means that the basin was gradually filled in. The magmatic activity is coeval to this sandstone deposit. It is therefore younger than the Aalenian age since the Sabbione metasandstone was deposited after the garnet micaschist attributed to the Aalenian age.

The deposition of a graphitic calcareous micaschist suggests that the environment became flooded shortly preceding the onset of a carbonate platform, which allowed the pure marble to be deposited. Such an evolution is consistent with the Late Dogger to Malm epoch. Indeed, at that time the Alps were submerged and a carbonate platform developed nearly everywhere (BAUD & SEPTFONTAINE 1980, MASSON et al. 1980, DOLIVO 1982, SARTORI 1990, HÜRLIMANN et al. 1996). The graphitic calcareous micaschist and the pure calcitic marble are hence attributed to the Callovo-oxfordian to Kimmeridgian age. This implies that the Sabbione metasandstone, as well as the magmatic activity are older than the Callovo-oxfordian age; they are therefore attributed to the Bajocian-Bathonian.

**Group V-IV**: the monotonous calcschist sequence, conglomeratic at its base and surmounted by a calcareous metaflysch is attributed to the Cretaceous-Tertiary epoch. No specific levels permit the attribution of a more precise age.

## 2.4 THE CAMOSCI NAPPE

### 2.4.1 Introduction and nomenclature considerations

HANSEN (1972), and later BIANCHI et al. (1998), distinguished a tectonic unit they called Bedretto Zone (Tab. 1.2). Later PROBST (1980) and LEU (1986) showed that the Bedretto zone was in fact composed of three tectonic units. For the first two tectonic units, LEU (1986) used the name of Rosswald series (as defined by BOLLI et al. 1980) and of Termen Zone (LISKAY 1966). For the last tectonic unit, LEU (1986) used the term Sabbione Zone (introduced by ETTER 1984).

In this work the Rosswald series corresponds tectonically, as well as stratigraphically, to the definition of BOLLI et al. (1980) and LEU (1986). But this work shows that the Sabbione Zone and the upper part of the micaschist of the Termen Zone of LEU (1986) are in stratigraphic continuity and thus correspond in fact to a single tectonic unit. This single tectonic unit is defined herein as the Camosci nappe (paragraph II.4.3, II.7.3). The name is derived from the "ghiacciao dei Camosci" which corresponds to the western termination of the Camosci nappe.

### 2.4.2 Nappe structure

The oldest levels of this nappe, outcropping over the studied area, are either a cornieule or a dolomitic marble attributed to the Triassic (paragraph II.4.4.). This nappe is detached from its pre-Triassic basement and only made of Mesozoic sediments.

The tectonic limits of the Camosci nappe are discussed in the paragraph II.7.2.

### 2.4.3 Lithostratigraphic description

I subdivided the Camosci nappe into 4 main units. They are called Dolomitic unit, Calcareous unit, Graphitic unit and Detritic unit (Fig. 2.4, 2.8).

**Dolomitic unit**: a dolomitic marble that may contain a few phyllosilicates (→10%) outcrops above the basal discontinuous cornieule. The dolomitic marble is locally mineralised (sulphides). Up sequence the proportion of detrital quartz increases to reach 10 %. This succession either continues with the progressive interfingering of a lustrous black micaschist or is capped by a quartzitic to arkosic metasandstone, which is locally conglomeratic. The latter is light yellowish and can locally record (e.g. in the "ghiacciao dei Camosci" area) as much as three superposed schistosities (Fig. 3.1A). Its thickness varies from ~1m to ~100 m, mainly due to alpine folding.

**Calcareous unit**: the contact with the underlying Dolomitic unit is either gradual or clear-cut. Whenever in contact with the lustrous micaschist (rare), the contact is clear-cut. But when it is in contact with the metasandstone, a transitional passage from the metasandstone to a quartzitic calcitic marble is observed over 5 metres. Upsection the marble becomes gradually purer until it gives way to a pure calcareous recrystallised marble. The latter is laterally discontinuous but may reach 20 metres in thickness at its most central part. The detritic fraction (quartz. dolomite, micas) then increases again. Most of the marbles contain up to 20% of quartz and about 10% of phyllosilicates. A quartzitic level follows which gradually interfingeres with subordinated thin levels of calcitic marble. These marble interbeds progressively thicken and dominate upon the quartzitic layers. The subordinated layers, the quartzite as well as the calcitic marble, are often boudinaged probably due to the alpine deformations. A quartzitic calcitic marble surmounts this series: the latter may contain discontinuous thin levels of quartzitic and dolomitic metasandstone. A 1 m-thick discontinuous quartzitic level ends this Calcareous unit.

**Graphitic unit**: is characterized by important lateral variations of facies (Fig. 10.2).

The clearest succession is found in the western part of the nappe. A black graphitic micaschist (metashale, see microscopic description in paragraph III.4) containing porphyroblasts of garnets, immediately follows the Calcareous unit; the contact is clear-cut. It may contain rare thin levels of a calcareous graphitic micaschist (metamarls). BIANCHI et al. (1998) found various heavily recrystallized bioclasts in the black micaschist.

The eastern part is more complex. A calcareous graphitic micaschist (metamarls, see microscopic description in paragraph III.4) containing porphyroblasts of plagioclase or epidote (paragraph III.4) overlies the Calcareous unit. The contact is gradual: thin levels (3 cm) of calcareous micaschist alternate with the calcitic marble; the latter becomes thinner upsection, whereas the calcareous micaschist thickens. Some graded bedding can be observed, indicating the local polarity (Fig. 2.4). Up sequence, thin levels of black micaschist are interbedded within the calcareous micaschist.

The lateral transition between the western and eastern part of the Graphitic unit is made over less than 2 m. A very hard and dark 50 cm-thick rock composed of graphite (50%), carbonate (29%), muscovite (12%), opaque (8%) and some accessory minerals, represents the transitional stage between the calcareous micaschist and the black micaschist.

**Detritic unit**: the contact with the Graphitic unit is always clear-cut. Strikingly, the Detritic unit is in contact only with the calcareous micaschist and never with the black micaschist. The detrital input shows a clear evolution: the deposit begins with a hard, grey argillaceous-rich quartzitic metasandstone that becomes richer in dolomitic detritic grains toward the top. It simulates a paragneiss and contains locally centimetric pyrite crystals. This deposit suddenly ends with the abrupt shedding of a very quartz- and clay- poor dolomitic metasandstone. The whole unit has a maximum thickness of 20-25 m.

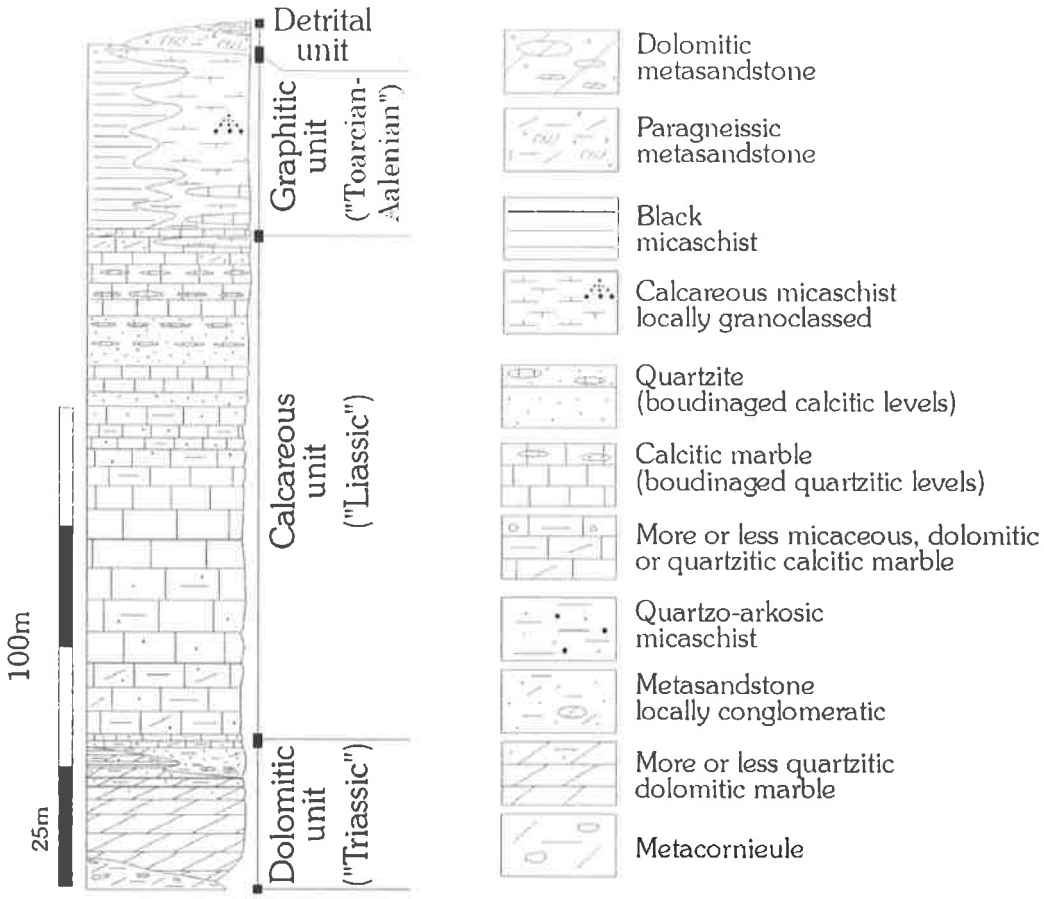


Figure 2.4 Synthetic section for the Camosci nappe (For the age attribution see the paragraph II.4.4).

## 2.4.4 Chronostratigraphic interpretation

This nappe is detached from its basement, but comparisons with other sections show that this lithostratigraphic column has a clear Helvetic s.l. affinity (Fig. 7.7, paragraph II.8.2, MASSON et al. 1980, DOLIVO 1982, BUGNON 1986, LEU 1986 and EPARD 1990). Such an affinity implies that the pre-Triassic Camosci basement was of continental nature. Following these comparisons, the successive units can be correlated as follows.

**Dolomitic unit**: contains the stratigraphically lowest levels of this nappe. The cornieule is discussed in paragraph II.7.3. On the basis of facies comparison with the Helvetic domain, the dolomitic marble would be the equivalent of Norian lithologies (e.g. Formation des Arandellys, EPARD 1990) and the quartzitic metasandstone of the Rhetian (e.g. Formation de Besoëns, EPARD 1990).

**Calcareous unit**: was probably deposited on a carbonate platform subjected to recurrent detrital input. A more important detritic episode resulted in the deposition of two quartzitic levels. This

episode points toward the erosion of a continental Triassic cover series and/or basement gneisses. The comparison with Helvetic stratigraphic sections allows to propose a Liassic age for the Calcareous unit. The two quartzitic levels would correspond to similar Helvetic deposit of respectively Lotharingian and Domerian age (DOLIVO 1982, BUGNON 1986).

**Graphitic unit**: the environment of deposition deepened suddenly and the Camosci platform flooded, resulting in the simultaneous deposition of marls and shales (calcareous micaschist and black micaschist). Such a flooding surface is recorded everywhere in the Alps, and elsewhere in the world (JENKYNS 1988). It is attributed to the Toarcian /Aalenian age.

**Detritic unit**: this unit ends the Camosci section. It reflects an erosion cutting in progressively older deposits, initially reworking terrigenous elements followed by dolomitic levels. The paragneissic metasandstone of the base of the unit is quite similar to the "Schistes mordorés" (Bajocian-Bathonian age) of the Wildhorn and a Dogger age is attributed to the whole unit. Once again Triassic levels are eroded.

The Camosci nappe would thus end with deposit of Dogger age. Why are younger levels not present? Three solutions are envisaged:

- they were never deposited;
- they were later eroded;
- they were translated in a more external position of the Alps.

These points will be discussed in the paragraph VII.3.1.

## 2.5 LEBENDUN NAPPE

### 2.5.1 Introduction and nappe structure

For over half a century (SCHARDT 1903, ARGAND 1911, PREISWERK 1918, BURCKHARDT 1942, JOOS 1969 and LEU 1986), the Lebendun gneisses have been considered to form the pre-Triassic basement of one of the great recumbent anticlines of the Pennine Alps (nappe n°2 of ARGAND 1911), and this despite the resulting contradictions.

In 1960, RODGERS & BEARTH proposed a different interpretation that resolved the incoherencies. In their view this nappe was a series of younger Mesozoic "flysch-like sediments" associated to the Bündnerschiefer, which was subsequently folded together with the Bündnerschiefer into a recumbent syncline between the Antigorio and Monte Leone nappe. Recent studies confirmed the Mesozoic age of this series on the basis of lithostratigraphic and structural arguments (SPRING et al. 1992, CANEPA 1993, DELLA TORRE 1995, DELEZE 1999). DELLA TORRE (1995) and DELEZE (1999) clarified the stratigraphy of the nappe. They divided it in three stratigraphic units called: "unité du Lebendun basal", "unité du Lebendun conglomératique" and "unité du Lebendun sommital". In the area of the present study only the "unité du Lebendun conglomératique" and "unité du Lebendun sommital" outcrop (Fig. 2.5B). However, instead of using their nomenclature, I will refer to the respectively equivalent term of "Paragneiss conglomeratici" and "Scisti Bruni", both of which were previously defined just south-west of the present studied area by CANEPA (1993).

It is not clear, over the studied area, whether the Scisti Bruni are older or younger than the coarser detritic paragneisses. However, in the Cristallina area, DELEZE (1999) found a clear polarity argument showing that the "unité du Lebendun sommital" (equivalent of the Scisti Bruni) is the younger unit. As I have made no convincing observations on the studied area, I have therefore assumed the polarity proposed by DELEZE (1999).

### 2.5.2 Lithostratigraphic description

**Paragneiss conglomeratici**: is composed of paragneiss old sedimentary origin, which has a variable granulometry. The basal part is finer than the upper part (Fig. 2.5). However, everywhere, detrital grains (quartz, feldspath. micas...), and/or centimetric gneissic pebbles are observable together; they are mainly badly to poorly sorted. This reconstituted gneiss is massive, hard and light-coloured. Locally, decimetric grey layers, that record a greater proportion of biotite, are interbedded. A very weak almost anecdotic fraction of the pebbles consists of calcitic marble or dolomitic marble. HIGGINS (1964) and DELEZE (1999) also mentioned the presence of sporadic metabasaltic pebbles. At the point 672'150/133'900 outcrops a 50 cm-thick by 30 m-long discontinuous bed of white impure conglomeratic calcitic marble. The bed consists of 8% of pebbles, sand-sized detritic grain (35-40%) in a sparitic matrix (55-60%). The pebbles consist entirely of the same granitic elements than those found in the surrounding conglomeratic paragneiss. The sand-size fraction consists of 60% of feldspar, 25% of quartz, and 10% of metamorphic biotite and of 2% of accessory minerals. The plagioclase is remarkably fresh and unaltered and often shows a preserved myrmekitic texture. Its lower and upper contacts are sharp (Fig. 2.6C).

The contact between the Paragneiss conglomeratici and the Scisti Bruni is variable. It can be gradual, schistose or abrupt. In the first case, the transition is observed over 2-4 metres, in which the paragneiss becomes progressively richer in biotite, while the size and the quantity of pebbles decrease rapidly until they disappear completely. Where the contact is schistose (e.g. 671'950/133'970), the Scisti Bruni and the paragneissic blend together; the contact is thus difficult to place.

**Scisti Bruni**: are composed of fine detritic levels, which have a composition that evolves up sequence. The first layers, composed of a light blue micaceous metasandstone, are the Scisti Bruni s. str. (LEU 1986, CANEPA 1993). They have a brown-rusted patina due to the presence of little grains of altered sulphide. Aligned authigenic pyrite minerals can reach 5-10% of the rock. A small mineralisation consisting of several huge pyrite minerals, reaching 8 cm in size, aligned in the schistosity was observed. A fine layering results from the alternance of quartz-rich and biotite-rich thin beds, which induce differences in hardness and colour. Up sequence the metasandstone gradually becomes carbonaceous and transforms itself into a calcschist. Dark graphitic garnet micaschist are locally interbedded in the calcschist. Exceptionnally the calcschist may even turn locally into a white-blue calcitic marble. Such a transition is readily observable on the left side of the road, when going up, between the Cascata del Toce and the village called Riale. The calcschist is generally rich in accessory minerals and contains randomly oriented porphyroblasts of amphibole. The section ends with a light-green quartzitic marble interbedded with a more or less dark micaceous calcschist.

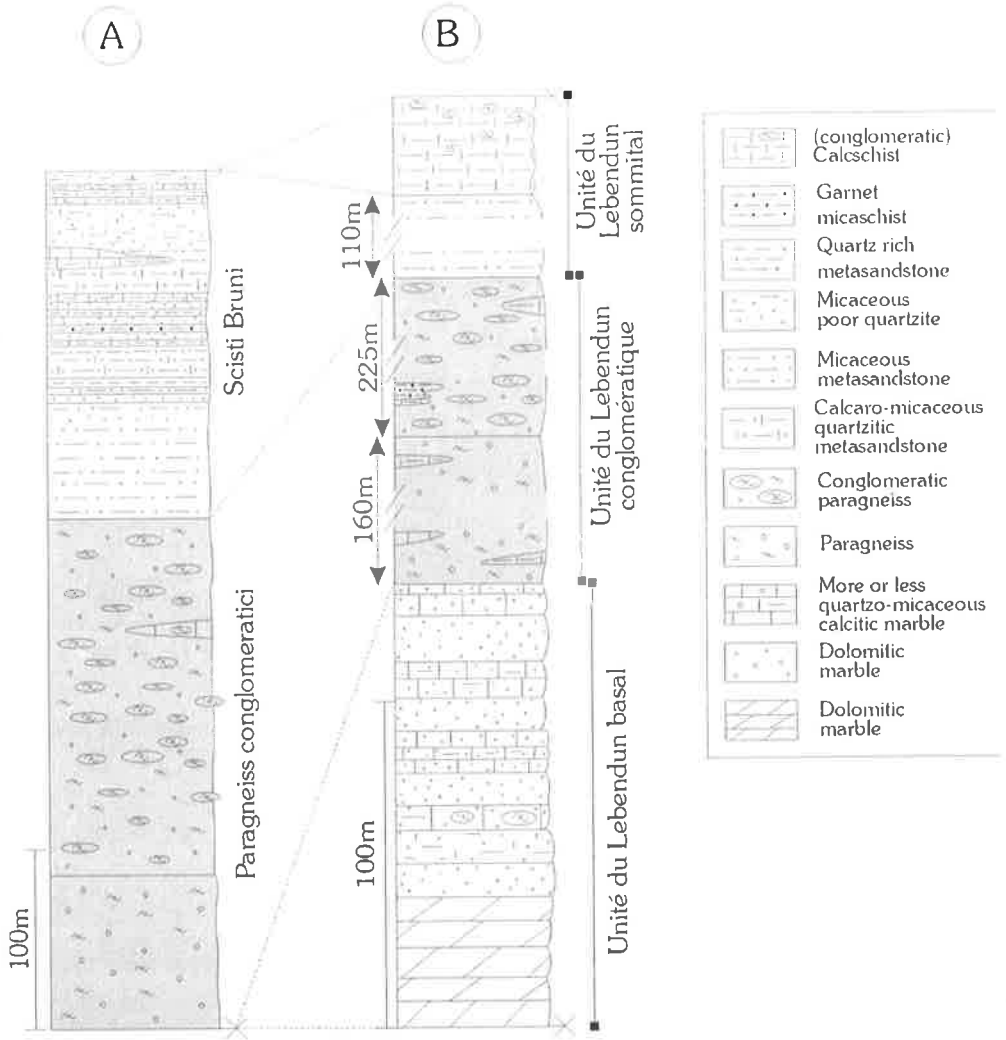


Figure 2.5 Lithostratigraphy of the Lebendun nappe. A) Synthetic section (this work). B) Type-section, Lago Sfundau (DÉLÈZE 1999).

### 2.5.3 Sedimentological and chronostratigraphic interpretation

**Paragneiss conglomeratici**: the granulometry of the paragneiss changes, but the nature of the detrital supply remains the same through the whole unit. In the opposite case, if the source was to be distant, this conglomerate would have been contaminated by or mixed with detrital supply coming from of one or more others sources. The unique layer of conglomeratic impure calcitic marble, interlaid in this sequence, displays all the characteristics of a debris-flow: very poor sorting, matrix-supported pebbles floating in the middle of the bed and a sand-sized fraction showing a very weak transport (sphericity, high proportion of unaltered plagioclase, perfect preservation of original igneous texture). All the detritic elements, from the coarsest to the smallest, point toward a single source, similar to that of the paragneiss. Hence the whole sequence is interpreted as an important accumulation of successive debris-flows (absence of granoclassed beds, absence of the Bouma sequences), with very little transport. The source was most likely a Variscan or older granitic basement eventually intruded by basic intrusions and on which must have rested a tegument of Triassic dolomite. The presence of the calcareous bed points to a marine depositional setting as well as to some episodical carbonate construction. The Paragneiss conglomeratici is of post-Triassic age because dolomitic marble is reworked within it and was deposited during an active tectonic period. No further field criteria enable me to deduce a more precise age; more precise age correlations are given in paragraph II.8.

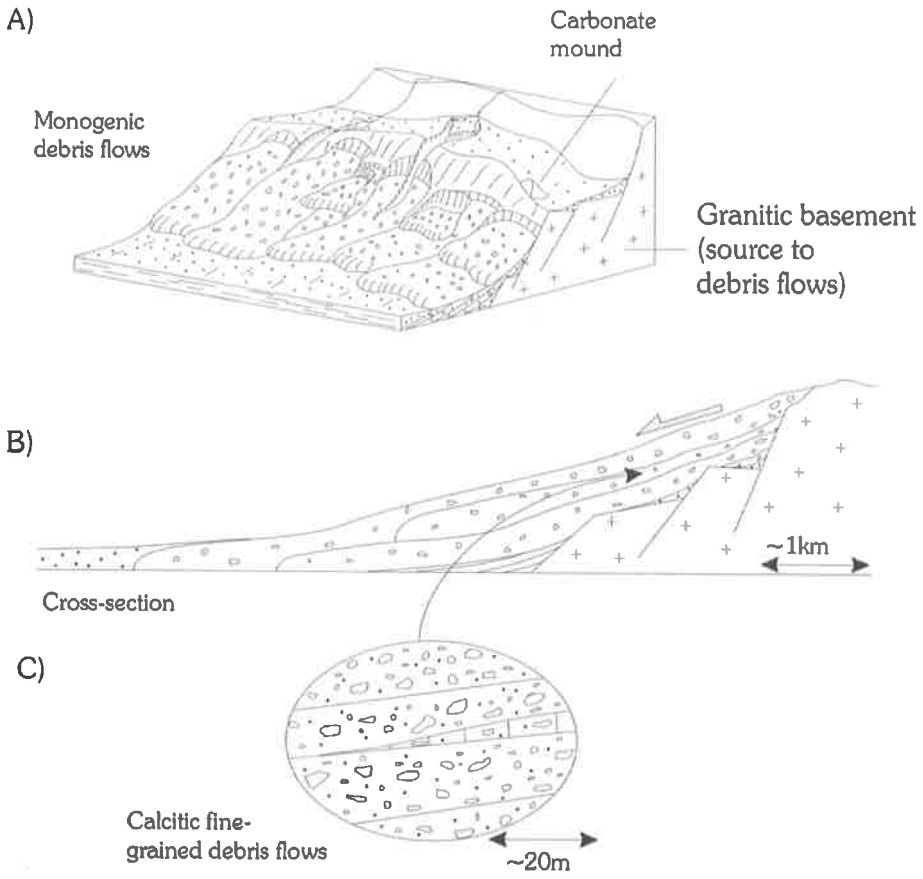


Figure 2.6 Proposed environment of deposition for the Paragneiss conglomeratici of the Lebendun nappe.

**Scisti Bruni**: this succession was deposited in stratigraphic continuity. Although the deposition from the debris-flow stopped rather abruptly, the input of detritic quartz grains continued. The environment became weakly oxygenated or even anoxic: the Scisti Bruni s.s. probably results from the metamorphism of silty sandstone deposited in an $O_2$-poor marine environment. The disappearance of pyrite and the transitional appearance of calcite up sequence point toward a renewed oxygenation of the environment. With the exception of the discontinuous pure calcitic marble, generally attributed to the Malm, no particular lithofacies is specific of a particular age. The only possible suggestion is that this interbedded pure calcitic marble is Late Jurassic in age.

## 2.6 THE TEGGIOLO ZONE (THE ANTIGORIO COVER SERIES)

### 2.6.1 Introduction and nappe structure

The Teggiolo zone is the autochthonous cover of the Antigorio basement. Both terms are encompassed in the Antigorio nappe (CASTIGLIONI 1958, SPRING et al. 1992, CANEPA 1993, ESCHER et al. 1993, STECK et al. 2001).

Over the mapped area, the Antigorio nappe represents the structurally lowest nappe and only its normal limb outcrops. The cover series begins here with a conglomeratic calcitic marble that directly overlies the basement. A stratigraphic contact is suggested by the presence of reworked basement gneisses in this first sedimentary deposit.

In order to study older Triassic levels of the Teggiolo zone (i.e. the dolomitic beds), one section in the Val Vannino was logged (Fig. 2.7A). Figure 2.7 shows the lateral lithofacies variations of the nappe over an even broader area.

## 2.6.2 Lithostratigraphic description

**Unit 1**: does not outcrop over the mapped area, but it was studied in the Val Vannino (Fig. 2.7A). Two discontinuous white quartzite beds lie directly above the Antigorio gneisses. A quartzitic dolomitic marble then follows, which contains some thin interbedded layers of a quartzite similar to the lowest levels. Up sequence the quartzitic dolomitic marble changes into a calcareous dolomitic marble. Then a discontinuous micaceous calcitic marble precedes brownish calcschists, which are conglomeratic at their base: they contain dolomitic grains and pebbles and belong either to unit 2 or 3.

**Unit 2**: begins with a conglomeratic slightly micaceous calcitic marble that lies directly on the pre-Mesozoic basement (Fig. 2.7B). It is overlaid by a micaceous quartzite that contains gneissic pebbles at its base. Its oxide content, although weak, is sufficient to give the rock a dark patina. The upper contact of this unit is abrupt, while the lower is locally erosive. Although the intense alpine deformations flattened the contacts, signs of erosion are visible along the lower contact.

**Unit 3**: is made of the alternating thin quartzite and even thinner calcitic quartzite.

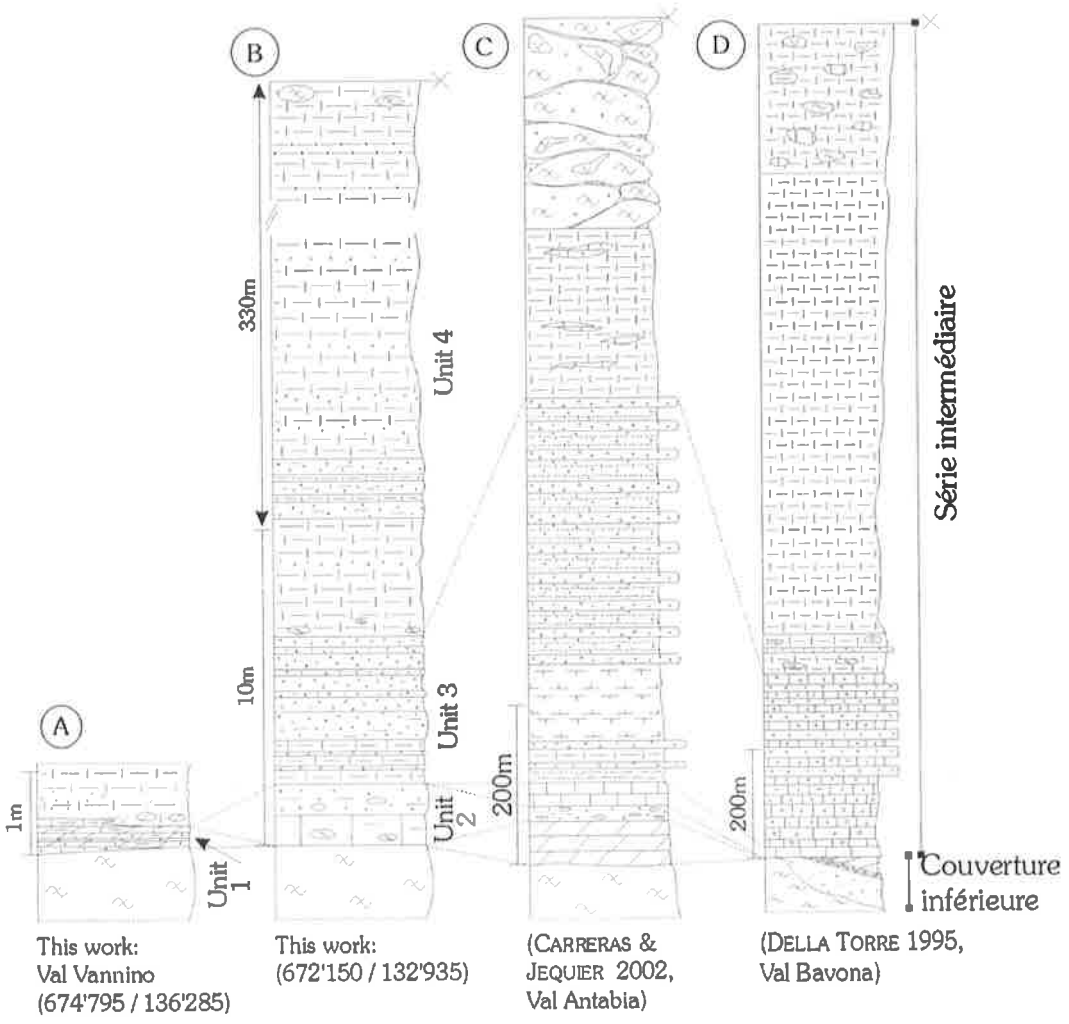


Figure 2.7 Stratigraphic profiles of the Teggiolo cover (for the legend see figure 2.1).

**Unit 4**: begins with a thickness of 5 m of calcschist that is conglomeratic at its base. The latter contains often-refolded gneissic pebbles. It is surmounted by a 10 m thick sequence of quartz-rich calcschist interbedded with thin micaceous quartzite. It is followed by a very thick monotonous series of calcschist. This calcschist may be locally rich in detrital quartz (up to 30%), or interbedded with pluridecimetric beds of non-calcareous garnet micaschist. The unit ends with the apparition of gneissic boulders that can reach 3 m in width. CARRERAS & JEQUIER (2002) described a terminal block-supported wildflysch, in the area of the Tamierpass (not present in the studied area), in which the blocks are reworked blocks of the Lebendun Paragneiss conglomeratici (Fig. 2.7C).

### 2.6.3 Chronostratigraphic interpretation

**Unit 1**: the first quartzite indicates that the Teggiolo zone is autochthonous. The next alternance of quartzite and of quartzitic dolomitic marble, as well as the absence of a calcitic marble, suggests a Helvetic affinity (MASSON et al. 1980, EPARD 1990). But the pure dolomitic marble (Norian age), which follows these deposits in the Helvetic domain, is absent here. Correlations with sections studied by DELLA TORRE (1995) and CARRERAS & JEQUIER (2002) determine the Helvetic affinity of this cover. In the Val Bavona, for instance, DELLA TORRE (1995) observed a complete sequence, with similar alternance overlaid by pure dolomitic marble (Fig. 2.7D). Therefore the levels are attributed to the pre-Norian Triassic epoch. In the Teggiolo zone important lateral variations of thickness characterise the Triassic levels: they are either absent (eroded) or can reach 40 m in thickness (Fig. 2.7C).

**Unit 2**: where it lies directly in contact with the Antigorio gneisses (Fig. 2.7B, 2.7D), it reworks the latter, proving that the cover is autochthonous. This unit is very thin (>5 m) and the micaceous calcitic matrix points toward a marine depositional setting.

**Units 3+4**: simulate a flysch formation, rarely interrupted by thin conglomeratic calcschist levels. No clues exist that enable the possibility of dating this succession. CARRERAS & JEQUIER (2002) described a pure calcitic marble that lies between units 2 and 3. They attributed it either to the Liassic epoch or to the Malm epoch, but clearly favour the second solution. This would imply that unit 3 and 4 are younger than Malm. Its resemblance with Group Hz-IV of the Holzerspitz series and with Group V-IV of the Pizzo del Vallone nappe is also an argument in favour of a Cretaceous to Tertiary age attribution.

## 2.7 DISCUSSION

### 2.7.1 Why has the Pizzo del Vallone been separated from the Holzerspitz series?

The Holzerspitz series and the Pizzo del Vallone nappe show striking similarities, as well as some significant differences (Fig. 2.1, 2.2). For instance, only the Pizzo del Vallone nappe contains green rocks. The main observations that lead, stratigraphically, to the individualisation of these two nappes are exposed as follows:

- during mapping, it was difficult but important to decipher whether the various conglomerates should be differentiated and then how to differentiate them. With this aim in mind, the nature of the pebbles of each level was systematically noted along with the mineralogy of the matrix. During this process, the Sabbione metasandstone stood out as a very specific and characteristic formation. Its association with the green rocks and its richness in ferromagnesian minerals were helpful characteristics. This metasandstone was never observed in the Holzerspitz series;

- the green rocks never outcrop close to the Monte Leone basement. They never intrude the pre-Triassic Monte Leone gneisses or the Triassic levels that are directly in contact with the Monte Leone gneisses. They are always separated from the Monte Leone basement by an entire cover series. Field mapping shows that the green rocks are systematically associated to the Sabbione metasandstone, and this over the whole area (Annexe 2A);
- discontinuous levels of cornieule and dolomitic marble, both attributed to the Triassic epoch, always outcrop in the same structural position between the Monte Leone pre-Triassic gneisses and the Sabbione metasandstone. This cornieule and the dolomitic marble are always in tectonic contact with the upper part of the group IV of the Holzerspitz series. Moreover the recurrence of a Triassic series inside the younger calcschists cannot be stratigraphic. Such outcrops were observed, for instance, in both sides of the southern part of the Lago del Sabbione, or close to the Rifugio Somma Lombardo.

In conclusion, the green rocks are always associated with the Sabbione metasandstone. The green rocks and the Sabbione metasandstone are separated from the Monte Leone basement by the Holzerspitz series and by a second series of Triassic rocks (the base of the Pizzo del Vallone nappe). The Monte Leone nappe and the Pizzo del Vallone nappe are two different nappes, separated by a tectonic contact. The Pizzo del Vallone nappe is structurally situated under the Monte Leone nappe: its older levels are always in contact with the youngest levels of the Holzerspitz series.

The Monte Leone nappe and the Pizzo del Vallone nappe must be separated. Nevertheless the similarities of the stratigraphic sections indicate a close paleogeographic origin. Since only the Pizzo del Vallone nappe contains green rocks, it would seem that it was the nappe closest to the magmatic activity.

### 2.7.2 Limits of the Camosci nappe

In this work, the Camosci nappe has been individualised from the Rosswald series and Holzerspitz series. The following arguments were decisive.

**Contact with the Holzerspitz series**: the tectonic contact is locally underlined by cornieule. It was reactivated at some point by the late rio del Sabbione strike-slip fault which is the most striking structural feature of the area. All the previous authors acknowledged this tectonic limit.

**Contact with the Rosswald series**: the calcschists of the Rosswald series are in contact with the Dolomitic unit of the Camosci nappe (Fig. 2.8, 2.9). The contact between these two lithologies is often outlined by a cornieule, whose nature is not obvious. The cornieule can either underline a thrust plane or can be caused only by a random Quaternary surface alteration. Here I clearly favour the first hypothesis (the cornieule as being the result of an alteration developed preferentially on a thrust plane, Fig. 2.8A) because:

- the alpine schistosity is recorded by the matrix and is concordant with the local schistosity (e.g. with outcrops lying at, or within less than 10 m from the cornieule). The schistosity clearly predates the alteration;
- since the rocks are younging upward from the Dolomitic unit to the Detritic unit as discussed in paragraph II.4.3 and II.4.4, the adverse hypothesis of a stratigraphic contact between the Dolomitic unit and the calcschists would result in a stratigraphic improbability (Fig. 2.8B). It would indeed imply that the calcschists are older than the Dolomitic unit, i.e. of a pre-Triassic age. Yet these calcschists are generally accepted as

having a middle to upper Mesozoic age (e.g. PANTIC & GANSSER 1977). Besides, a lower pre-Triassic ca 1.2 km-thick calcschist unit has never been described anywhere;

-historically, the Bedretto Zone corresponds to the whole undifferentiated succession, with the dolomite and the marble considered as Triassic and the remaining lithologies as Jurassic (HANSEN 1972). This scenario would imply two series too radically different on both sides of the implied Triassic anticline (Fig. 2.8C).

LEU (1986) proposed a tectonic contact between the Calcareous unit and the Graphitic unit on the basis of facies correlation with the micaschist of the Termen Zone (LISKAY 1966, Fig. 7.6). As described in the introduction (paragraph II.4.1) this contact is clearly gradual especially where the calcareous facies of the Graphitic unit is present (interfingering of calcareous marble, Fig. 2.4).

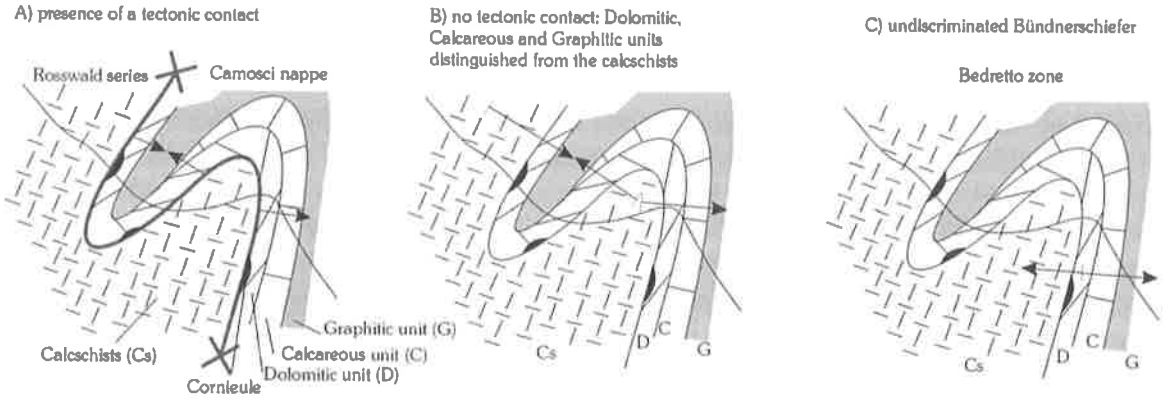


Figure 2.8 Schematic sketches showing the relation between the calcschists, the Dolomitic unit and the position of the cornieule. A), B) and C): three hypotheses discussed in the text.

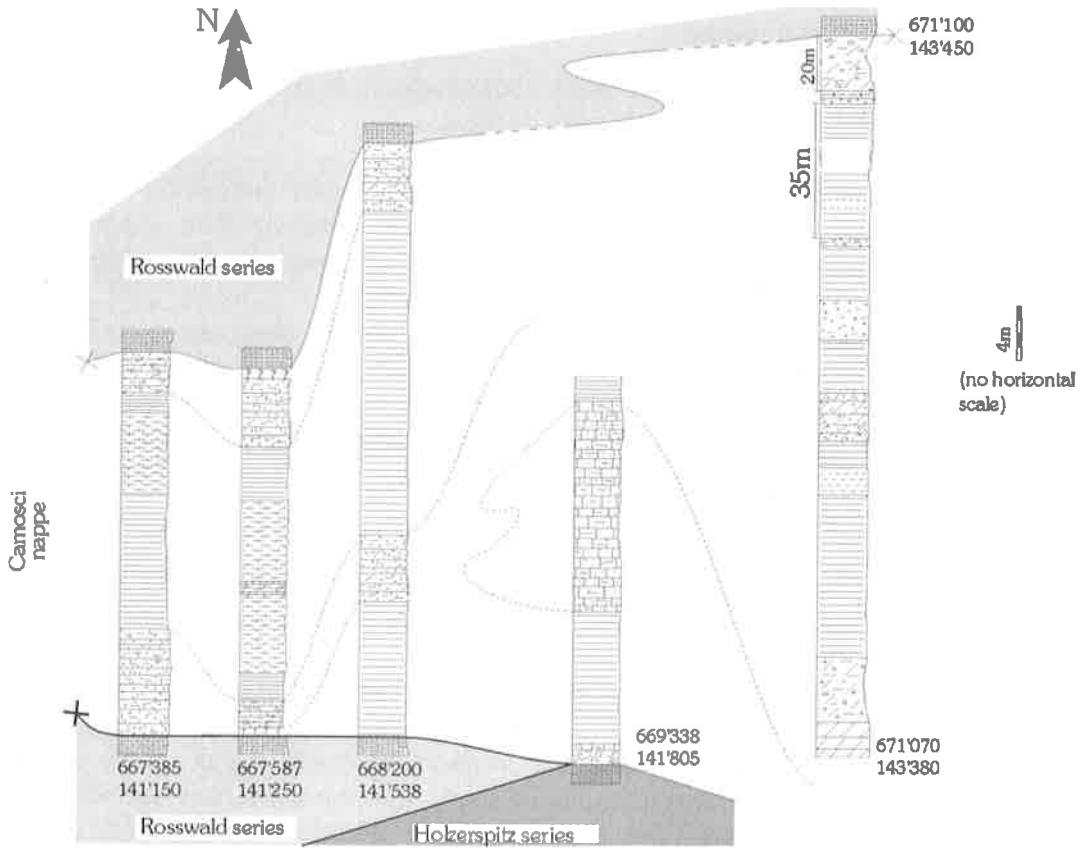


Figure 2.9 Some sections logged along the Camosci thrust plane (for the legend, see figure 2.4).

### 2.7.3 General stratigraphic comparisons between the studied nappes

All these nappes (the Monte Leone, Pizzo del Vallone, Lebendun, Antigorio and Camosci nappes) have important similarities but significant differences too.

In the studied area, all nappes contain (Fig. 2.10):

- Triassic levels (except for the Lebendun nappe, but SPRING et al. (1992) and DELEZE (1999) described such levels); this proves that these covers were deposited on a continental basement;
- more or less well-developed monogenic to polygenic conglomerates. The great abundance of granular to plurimetric pebbles of Triassic rocks and older basement gneisses is a common important point between all these nappes. It proves that a continental basement and a Triassic cover were submitted to erosion. Three situations are envisaged:

- the erosion of an unknown distant basement supplying all the detritic material;
- the erosion of their own basement (for instance the Monte Leone and Antigorio basement) supplying enough material;
- a combination of these two solutions.

Nevertheless, the presence of both monogenic to polygenic conglomerates and regenerated detritic layers ("Permian") shows not only that the nappe originated from an active depocentre basin but that the deposits were very proximal (conglomerate-rich fans) and close to abrupt reliefs.

The main differences can be summarized as follows:

- only the Camosci nappe shows a clear Helvetic s.l. affinity. Comparisons with typical Helvetic covers (Fig. 10.6, MASSON et al. 1980, DOLIVO 1982, BUGNON 1986, EPARD 1990) suggest a Triassic to Dogger age for this nappe (paragraph II.4.4);
- only the Monte Leone and the Antigorio nappes include a preserved pre-Triassic basement, above which lies the autochthonous sedimentary cover series (respectively the Holzerspitz series and the Teggiolo zone). Their basement-cover contact shows that the Triassic levels are often eroded. The other nappes are detached; thus, it is impossible to decipher if the oldest levels were ever deposited, or if they were eroded as well;
- only the Pizzo del Vallone nappe contains intrusive and extrusive green rocks. This indicates that it laid very close to the centre of magmatic activity;
- the Lebendun nappe and the Teggiolo zone contain principally gneissic pebbles while the Holzerspitz series and the Pizzo del Vallone nappe contain principally dolomitic pebbles. The Teggiolo zone is also the series with the most important lower Mesozoic hiatus;
- the youngest levels of the Camosci nappe is missing, but the youngest levels of the Holzerspitz series and of the Pizzo del Vallone nappe is equally missing. No terminal wildflysch was ever observed.

The detailed lithostratigraphic study associated to the chronostratigraphic interpretation suggests correlations between all these nappes (Fig. 2.10). As the nappes supposedly arise from a close paleogeographic position (they form stacked tectonic units displaying numerous lithostratigraphic similarities), I based my correlations upon two criterions:

- presence of conglomeratic levels;
- deposition of a calcitic marble and of a graphitic micaschist.

Three major unconformities, called UC1, UC2 and UC3 can be recognized laterally. Two sections were added (DELEZE 1999, JEQUIER & CARRERAS 2002) because they supplied useful information, which enable correlations to be made.

Following the chronostratigraphic interpretations, the UC1 and UC2 unconformities are attributed respectively to the middle - upper Liassic epoch and to the Bajocian-Bathonian times (Fig. 2.1, 2.2, paragraph II.2.4, II.3.6). They are best observed in the Monte Leone and Pizzo del Vallone nappe.

The UC1 unconformities are recognizable only in the Monte Leone and Pizzo del Vallone nappes. It is followed by the deposition of a basal monogenic conglomeratic sandstone that grades into a polygenic conglomeratic sandstone (Fig. 2.1, 2.2). UC1 is responsible for the lateral erosion of the Lower Liassic and/or Triassic levels. In the Monte Leone nappe, for instance, the dolomitic marble thickness varies from 100 m to 0 m.

The second unconformity, UC2, is the main one. It is recorded in all nappes and often erodes the UC1 unconformity, as well as the Triassic levels. In the Pizzo del Vallone nappe, UC2 is the lower limit of the Sabbione metasandstone deposit (Fig. 2.2, 2.10). The L1 and L3-Aa levels (Fig. 2.10) are mostly eroded, except in the lowest outcropping unit, the Camosci nappe, where they are well preserved (Fig. 2.4).

The depositional sequence between UC2 and UC3 shows the evolution of an active depocentre that became starved, inactive and finally flooded (Fig. 2.1, 2.2, 2.10).

The third unconformity, UC3, is recorded by all the nappes in which this young sequence is present (Fig. 2.10). UC3 is clearly erosive (Fig. 2.1B). Once again the paleoenvironment is tectonically active. In the Holzerspitz series, for instance, there is at least one bloc of epidotite, which is probably reworked from the Group V-III of the Pizzo del Vallone nappe (paragraph II.2, II.2.4).

The presence of these unconformities, the lateral variations of facies as well as the high amount of conglomeratic levels points to a paleogeographic environment of extensional tectonic and of tilted blocks. Moreover an active centre of tholeiitic basaltic volcanism erupted in this region (Chapter V).

Fig. 2.10 Synthetic stratigraphic columns of the studied area, ordered according to their paleogeographic position. The syn-rift sequence is coloured in greyish. The major unconformities are noted UC1, UC2 and UC3 (see text). The letters T, L1, L2, L3-Aa, D2, D3, M, K2 and K3-T delimit coeval levels (Tr is for the undifferentiated Triassic rocks, L1 for the lower Liassic rocks, L2 is for the middle Liassic rocks, L3-Aa for the upper Liassic-Aalenian rocks, D2 for the Bajocian – Bathonian rocks, D3 for the Callovo-Oxfordian rocks, M for the Malm rocks, K2 is for the Albian - Aptian rocks, and K3-T for the upper Cretaceous - Tertiary rocks).

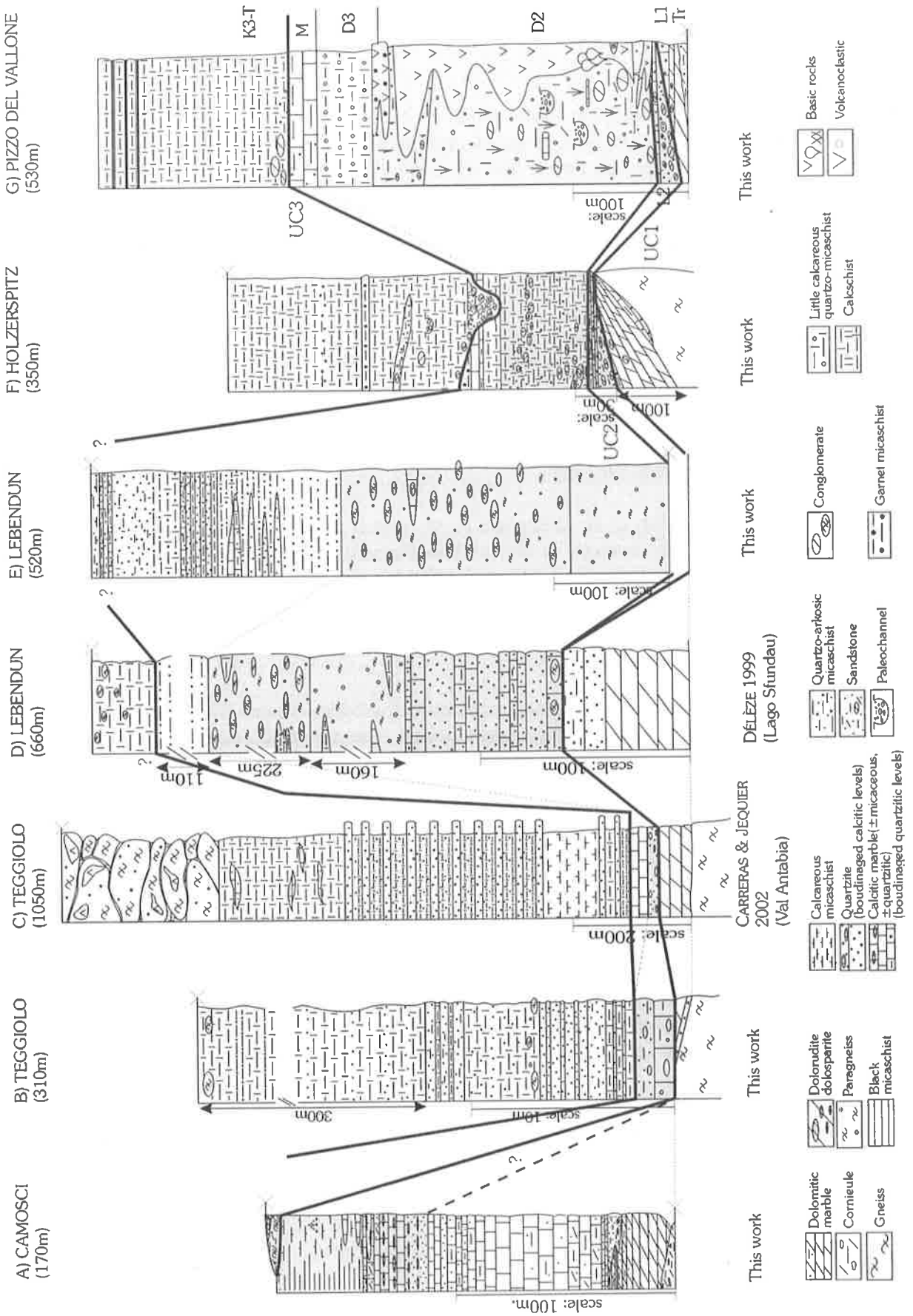
A) CAMOSCI (170m)
B) TEGGIOLO (310m)
C) TEGGIOLO (1050m)
D) LEBENDUN (660m)
E) LEBENDUN (520m)
F) HOLZERSPITZ (350m)
G) PIZZO DEL VALLONE (530m)
K3-T
M
D3
D2
L1
Tr
UC3
UC2
UC1
scale: 100m
scale: 200m
scale: 10m
scale: 30m
110m
225m
160m
300m
?
This work
DÉLÈZE 1999 (Lago Sfundau)
CARRERAS & JEQUIER 2002 (Val Antabia)
Dolomitic marble
Cornieule
Gneiss
Dolorudite dolosparite
Paragneiss
Black micaschist
Calcareous micaschist
Quartzite (boudinaged calcitic levels)
Calcitic marble(±micaceous, ±quartzitic) (boudinaged quartzitic levels)
Quartzo-arkosic micaschist
Sandstone
Paleochannel
Conglomerate
Garnet micaschist
Little calcareous quartzo-micaschist
Calcschist
Basic rocks
Volcanoclastic

## 2.8 STRATIGRAPHIC COMPARISONS WITH PENNINIC UNITS OUTSIDE OF THE SIMPLO-TICINO DOME

The stratigraphic study shows that these nappes are rich in conglomerates. However, the two structurally lowest nappes, the Camosci and Antigorio nappes, contain fewer conglomerates than the Pizzo del Vallone, the Monte Leone and the Lebendun nappes. Several other nappes of the Alps are conglomerate-rich. Some are described here after.

### 2.8.1 Nappes with a similar internal organisation

The Brèche nappe (SCHARDT 1893) lies in the French and Swiss Prealps. It consists of Mesozoic sediments that were deposited within the most internal parts of the Briançonnais platform; this part corresponds to a rapid transition between the European thinned crust and the partly oceanised Alpine Tethys domain (STEFFEN et al. 1993). A detailed sedimentological study indicates the existence of both marginal and basinal deposits (Fig. 2.11A+B). The sediments were most probably deposited in a pull-apart rift system which evolved into a continental margin (Early Jurassic to early Cretaceous). Current bedding and detritic grain analysis reveal several supply areas from the west to the north.

The Starlera nappe (BAUDIN et al. 1995) is a cover, which is now completely detached from its basement (Fig. 2.11C). It outcrops in the middle Penninic zone of eastern Switzerland. This nappe comes from a more internal part than the Tambo and Suretta nappes and was emplaced during an early Alpine phase of thin-skinned thrusting. As it is hardly distinguishable from the "Schistes Lustrés" of the Avers nappe, the authors envisaged an emplacement inside the Avers sedimentary basin.

The Niesen nappe is a lower Penninic nappe found in the Swiss Prealps (BADOUX & HOMEWOOD 1978). The petrology of the reworked elements as well as current directions enable the deduction that this nappe has been deposited south of the shoulder of the Helvetic margin in a proximal position. It was deposited during the Aalenian to Bathonian age in a deep-sea fan environment related to the Alpine Tethys Ocean passive margin (RINGGENBERG et al. 2002). The last level of this nappe, the Niesen flysch (ACKERMANN 1986) was deposited during the major movements of the Late Cretaceous inversion processes.

LEFEVRE (1982) described the internal Briançonnais and the Ultrabriançonnais (MORET 1954, DEBELMAS & LEMOINE 1957) in the Cottiennes Alps. He showed that the Ultrabriançonnais is characterized by a Norian to upper Bathonian erosion and hiatus (sub-aerial erosion, dissolution and block falls), and a transgressive Malm often deposited directly upon the Werfenian quartzite. This erosion cleared away 800 m to 1000 m of middle-upper Triassic and locally much of the lower Triassic and Permian, providing a large amount of material to the pré-Piémontais nappes.

### 2.8.2 Comparisons

The Starlera, Brèche and Niesen nappes have i) a paleogeographical common point: they were deposited on the northern margin of the Alpine Tethys, and ii) sedimentological similarities: they contain huge quantities of breccias. The Niesen nappe was probably deposited in a more external position than the Startera and Brèche nappes. The nature of the matrix varies from principally calcareous (Brèche nappe and Starlera nappe, associated to the Briançonnais terrane) to highly quartz-rich (Niesen nappe, associated to the Helvetic realm).

Two main detrital events are recognizable: Liassic-Dogger and Cretaceous-Tertiary. However, these main events are subdivided, for instance, STEFFEN et al. (1993) described four characteristic events in the lower Breccias of the proximal Brèche (Fig. 2.11A).

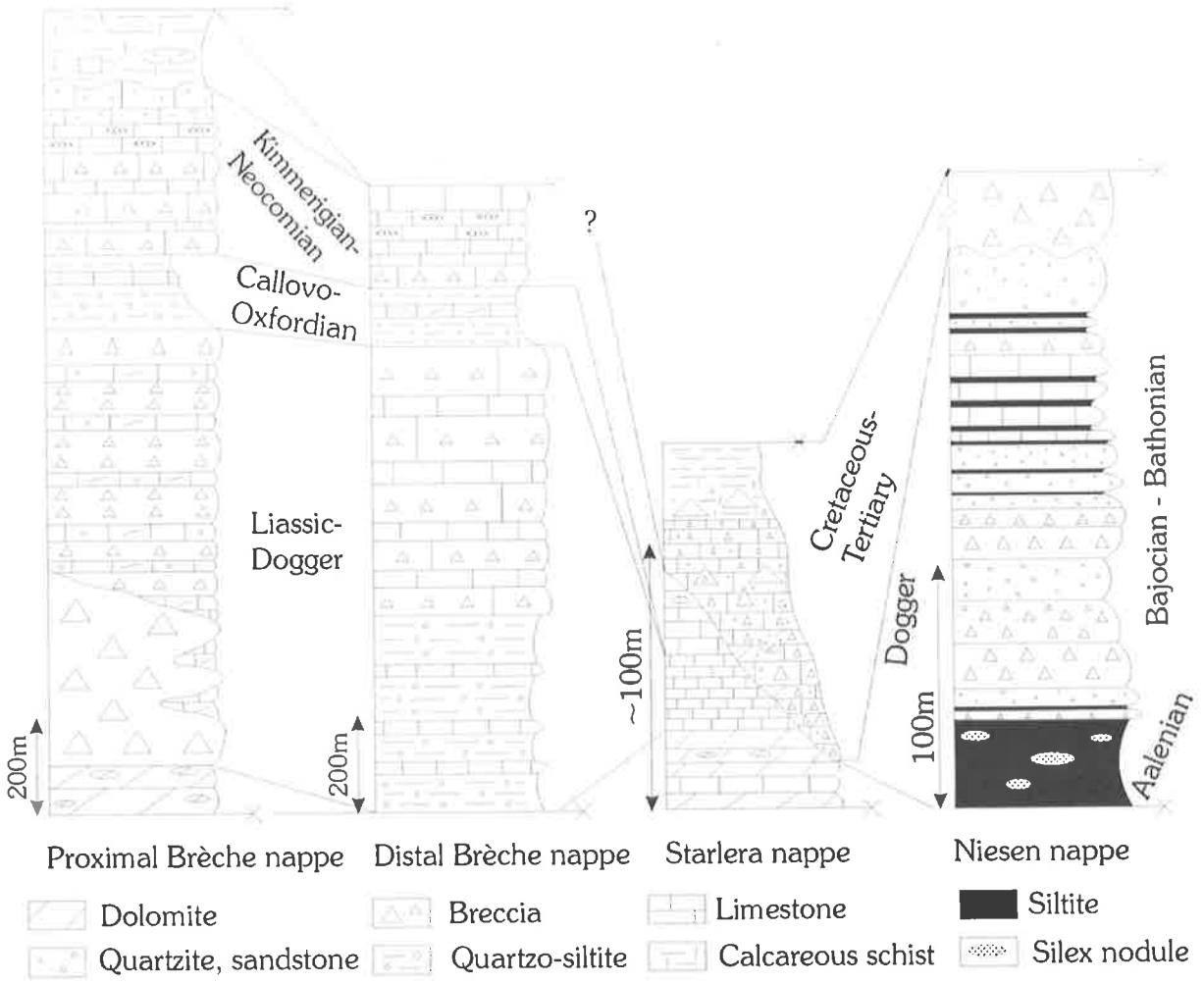


Figure 2.11 Schematic stratigraphy of various prépiémontais nappes. A)+B) STEFFEN et al. 1993, C) BAUDIN et al. 1993) and D) the Niesen nappe after RINGGENBERG et al. 2002.

The Monte Leone, Pizzo del Vallone and Lebendun nappes have similar internal structures. Indeed they all contain thick series of conglomerate. The chronostratigraphic attributions point toward a possible Liassic, Dogger and Cretaceous to Tertiary age, respectively for the successive conglomeratic episodes (Fig. 2.10). Moreover the Lebendun nappe is analogous to the Niesen nappe, while the Monte Leone nappe is similar to the Starlera and Brèche nappe. The internal organisation of the Pizzo del Vallone nappe is also similar but in addition it contains green rocks. Comparisons with the Ambin massif would be more appropriate (ALLENBACH & CARON 1986).

These comparisons indicate that the lower Penninic Monte Leone, Pizzo del Vallone and Lebendun nappes are comparable to sedimentary sequences directly related to the opening of the Alpine Tethys. The Antigorio nappe has a somewhat reduced or even absent Triassic to Dogger succession (Fig. 2.7, 2.10, CARRERAS & JEQUIER 2002) reminiscent of the series of the Ultrabriançonnais nappes (LEFEVRE 1982); the Antigorio nappe could be a longitudinal paleotectonic equivalent of the Ultrabriançonnais nappes.

I would like to stress here, that the Camosci nappe seems to be particular in so much that it has a unique Helvetic s.l. affinity. At the same time it is the most external tectonic unit.

# 3 CRYSTALLIZATION-DEFORMATION RELATIONSHIPS

## 3.1 INTRODUCTION

The crystallization-deformation results proposed here are based upon microscopic observations of thin-sections. As these were made from oriented samples, the microscopic structures observed can be directly linked to large-scale structures. The successive phases of deformation are described in the chapter VI, but as not all deformation were penetrative, only the three have been recognised in thin sections: they are the two penetrative schistosities S2 and S3, and a crenulative cleavage S4 (Fig. 3.1). The metamorphism (Chapter IV) during which the various porphyroblasts crystallized began during S4 (dynamic) but went on after S4 (static): it is so coeval to post S4. This metamorphism is also called the Lepontine metamorphism.

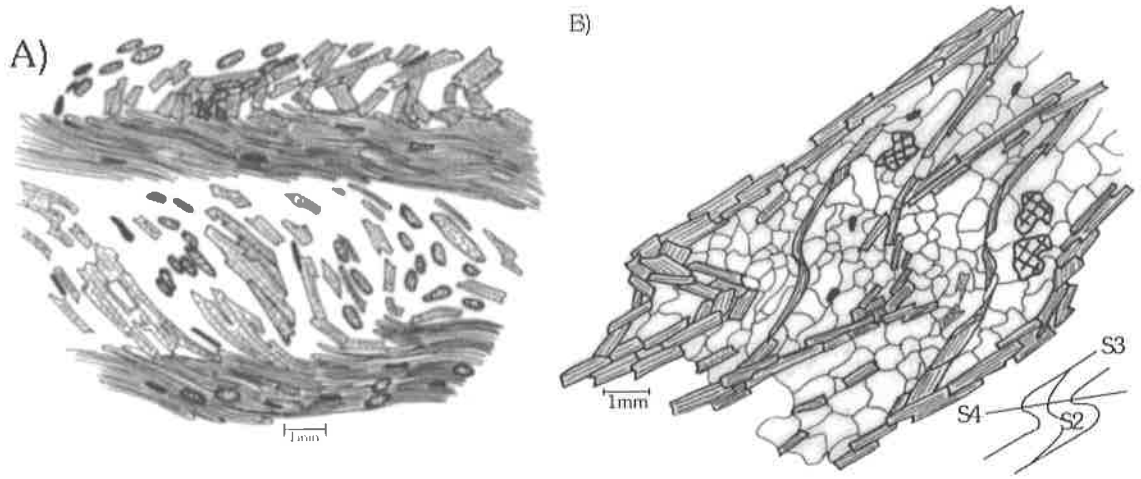


Figure 3.1 A) Fine alternations of muscovite- and quartz-rich layers (upper part of the detrital unit of the Camosci nappe, sample EC269, 672'760/143'060). The main schistosity S3 was refracted according to variations in bedding competence and has been refolded by the following crenulation phase S4. B) Impure quartzite in the dolomitic unit of the Camosci nappe may have recorded 3 phases of deformation (Sample EC231, 669'300/142'120). The microlithons are crenulated.

As the observed deformation phases postdated the nappe stacking, there is no sense in presenting the results nappe by nappe. To avoid useless repetitions, the results have been here summarised and classified according to lithologies. Only the lithologies useful for the metamorphic study are here presented, although completed by some observations or important points.

## 3.2 THE DOLOMITIC MARBLE

Except in the Lebendun nappe, this lithology is common at the base of all nappes. Where the dolomitic marble is pure, no useful conclusions can be drawn: the dolomite grains recrystallized, more or less obscuring all previous fabrics. However, the dolomitic marble often contains a small fraction of quartz, which allowed the tremolite to grow in some places. The first occurrence of

tremolite approximately coincides with the beginning of the amphibolite facies and tremolite-bearing marbles are characteristic for the lower to middle amphibolite facies (BUCHER & FREY 1994). Although dolomite recrystallization erased evidence of successive earlier schistosities, the random orientation and unpredictable distribution of tremolite indicate that this crystallization was late and contemporaneous with the peak of temperature of the Lepontine metamorphism.

## 3.3 THE SABBIONE METASANDSTONE

The Sabbione metasandstone, as noted in paragraph II.3.3, is an extremely variable unit; its chemistry and mineralogy may change in a few meters depending on the source of the detrital components, the tectonic activity and the magmatic influx. As result, the dolomitic conglomerates can change laterally into a fine micaceous quartzite or may incorporate discontinuous fine bands of pure calcitic marble. Such variations allowed a wide variety of minerals to crystallize (Tab. 3.1). For instance, an originally aluminous quartzitic matrix containing dolomitic pebbles is now composed by dolomite, kyanite, quartz, biotite and epidote. Such associations are restricted to limited areas, and are atypical, but permit the pressure-temperature conditions reached by the metasandstone to be relatively precisely determined (paragraph IV.2). The first two schistosities are normally difficult to see, because they are obscured by the relatively large minerals, which grew after S4 (Fig. 3.2). However, where S2 and S3 have been observed, it is clear that the metamorphic conditions were prograde until the metamorphic peak. The minerals, which formed synchronously with the peak of temperature of the Lepontine metamorphism are randomly distributed, include garnet, staurolite, kyanite, tremolite, tschermakitic hornblende and tschermakite. These minerals are all typical of the middle amphibolite facies.

| Quartz | Carbonate | Feldspath | Epidote | White micas |
|---|---|---|---|---|
| >1-70 | 0-45 | 0-25 | 1-30 | >1-50 |
| Biotite | Chlorite | Amphibole | Garnet | Staurolite |
| 1-50 | 0-15 | 0-50 | 0-4 | 0-2 |
| Kyanite | Rutile | Tourmaline | Opaque | Accessory |
| 0-15% | >1-2 | 0-5 | >1-4 | >1 |

Table 3.1 Variations in the minerals content of the extremely variable Sabbione metasandstone.

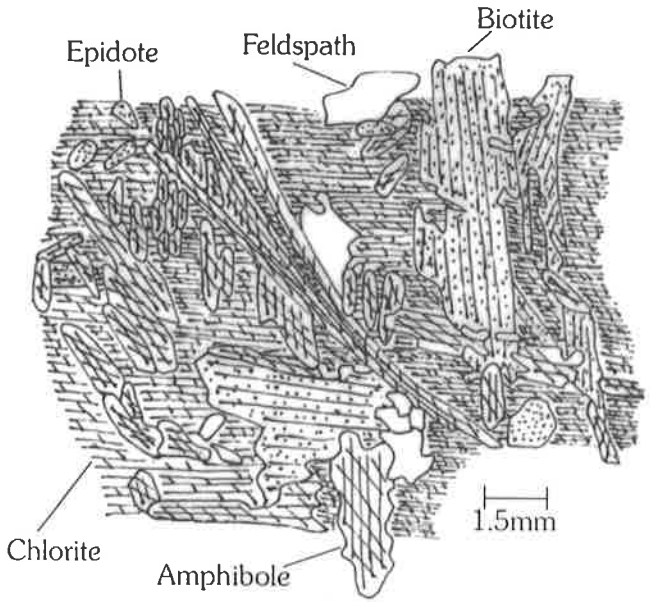


Figure 3.2 Late porphyroblasts, coeval to the Lepontine metamorphism (Chapter IV), are well developed and randomly oriented in the Sabionne metasandstone (sample EC186, 668215/140545). They overprint the main schistosity here outlined by chlorite.

## 3.4 THE VARIOUS MICASCHISTS OF THE CAMOSCI NAPPE

Three kinds of micaschist outcrop in the Camosci nappe: the lustrous micaschist of the Dolomitic unit, and the two micaschists of the Graphitic unit (paragraph II.4.3). They all have rather similar mineralogy but significantly different modal percentages of each mineral (Tab. 3.2). Moreover, only the calcareous micaschist contains calcite, although in varying proportions.

The Rhetian schists are essentially fine-grained micaschists that are foliated because of their high content in graphite and phyllosilicates. Their association with dolomitic marble creates marked contrasts in colour. They are rich in muscovite, biotite and quartz, and contain micro-porphyroblasts of epidote surrounded by two schistosities (S2 and S3), and micro-porphyroblasts of staurolite overgrowing the main schistosities (Tab. 3.3). The crenulation cleavage has not been recorded in these samples. They have a strong resemblance to the black micaschist, but the absence of garnet as well as the association with dolomitic marble is characteristic.

The black micaschist splits into foliated compact bands several centimetres thick. When it contains a greater proportion of quartz it is harder. It may be lighter on fresh surfaces than where weathered but, even with a hand lens, the minerals are undistinguishable because of their small size and dark colour. Only garnets are identifiable on fracture due to their brilliant lustre or on weathered surfaces where they stand out because of their greater hardness. Most outcrops are metres sized overhangs due to the steep dip and resistance to erosion. In thin sections staurolite and, to a lesser extend, garnet clearly overgrow the crenulated S2 and S3 schistosities.

The calcareous micaschist is not particularly useful for metamorphic investigation but, as it is directly associated to the black micaschists and as it develops particular mineralogical associations, it is briefly described here. Theses micaschists outcrop on the east side of the Camosci nappe demonstrating the existence of lateral variations in the sedimentary facies. Moreover they also exhibit internal compositional variations. The porphyroblasts type varies: both plagioclase and epidote have been seen, probably depending on whether the rock chemistry is more sodic or ferric, but the two never coexist. In the valle di Morasco, where the calcareous micaschists are thickest, the carbonate content may increase and at the same time carbonaceous microturbidites appear. In that case both porphyroblastic phases disappear, suggesting that the calcium was completely used up by the growth of calcite, because of the lack of aluminium. Such variations are similar in the basal alternations with the quartzitic marble, where important structural observations can be made; the schistosities are refracted and the lineations refolded (paragraph VI.3.4)

The crystallization-deformation relationships show prograde conditions. Garnet, biotite, muscovite and plagioclase all crystallized during S2 and S3. Only garnet and staurolite clearly overgrew all the three schistosities, although some others minerals have a thin border overgrowing the crenulated S3 fabric. Primarily, S4 only crenulated the two earlier schistosities and little neocrystallization occurred during this phase. Some garnets and biotite porphyroblasts show sign of rotation contemporaneous with S4 formation: the wavelength of folds in S3 varies from outside to inside the garnet or biotite porphyroblasts. A few late chlorite grains are the only indication of the onset of the retrograde metamorphism after the growth of staurolite, a typical mineral of the amphibolite facies. The micaceous quartzitic metasandstone from the detrital unit (paragraph II.4.3) contain amphiboles, which grew during the metamorphism, also indicating that the Camosci nappe, despite its northern situation, also reached the amphibolite facies.

More precise investigations have been done on sample EC179, a black micaschist; they are presented in chapter IV.

| | Rhetian schists | Black micaschist | Calcareous micaschist |
|---|---|---|---|
| Graphite | 5-9% | 10-15% | 2-8% |
| Quartz | 6-15% | 30-50% | 10-35% |
| Muscovite | 60-65% | 10-30% | 4-20% |
| Biotite | 6-20% | 6-18% | 5-15% |
| Plagioclase | >1% | >1% | 1-30% |
| Epidote | >1% | >1% | 1-35% |
| Carbonate | >1% | >1% | 1-50% |
| Staurolite | 4-6% | 2-3% | 0% |
| Garnet | >1% | 3-10% | 0% |
| Opaque | 1% | 3-6% | 2-8% |
| Tourmaline | 0% | 1% | 1% |
| Chlorite | 1-3% | 0% | 0% |
| Rutile | 0-2% | >1% | 1% |
| Accessory | >1% | >1% | >1% |

Table 3.2 Percentage of the minerals in the various micaschists of the Camosci nappe.

| Minerals | Size (mm) | | S2 | | S3 | Dt S4 | |
|---|---|---|---|---|---|---|---|
| Garnet | 2-5 | | | | | | |
| Biotite | ->4 | | | | | | |
| Muscovite | ->4 | | | | | | |
| Quartz | ->3 | | | | | | |
| Plagioclase | 1-7 | | | | | | |
| Opaque | ->2 | | | | | | |
| Rutile | ->1 | | | | | | |
| Chlorite | ->1 | | | | | | |
| Epidote | ->7 | | | | | | |
| Staurolite | 1-2 | | | | | | |
| Carbonate | ->3 | | | | | | |
| Accessory | ->1 | | | | | | |
| Graphite | | | | | | | |
| Tourmaline | ->1 | | | | | | |

Table 3.3 Summary of the crystallization-deformation relationships observed in the various micaschists of the Camosci nappe (S2 and S3 are the first two penetrative schistosities, S4 the crenulative schistosity, and Dt the Lepontine metamorphism).

## 3.5 THE GARNET MICASCHISTS

The Holzerspitz series and the Pizzo del Vallone nappe contain levels of garnet micaschist. Obviously each level recorded the same metamorphic history (Tab. 3.4); however, kyanite only appears in the micaschist sampled south of the lago del Sabbione, south of the kyanite-in isograd (Fig. 3.6).

Except in the micaschists containing kyanite, the garnets porphyroblasts are both texturally and chemically zoned (Fig. 4.1). The garnet cores are free of inclusions but towards the rim the garnets incorporate thin, refolded graphitic layers and fine-grained quartz. The transition is clear-cut, but irregular and simulates a flower-shaped transition, caused by the garnets overgrowing

arcuate graphite accumulations termed cleavage domes (FERGUSON et al. 1980). This texture has also been observed in the garnetites (CARRUPT & RICE, in prep). Localized microprobe profiles show a continuous chemical zoning across this boundary (Fig. 4.1), indicating that garnet growth was uninterrupted; it first pushed back the graphite and then included it. The Fe/(Fe+Mg) ratio indicates that garnet grew during prograde metamorphic conditions and the bell-shaped profile of spessartine is typical of the staurolite zone (SPEAR 1993). The grossular percent varies more than that of other oxides. The garnets in sample EC27, a micaschist containing well-developed kyanite crystals (Fig. 3.3), have a weak chemical zoning, proving either that they have crystallized late but continuously or, and more likely, that they have been rehomogenized.

Plagioclase grains (commonly 1-4mm) contain inclusions and are generally zoned; the anorthite percentage initially decreases and then increases. Most crystallized during the static phase and are in equilibrium with late assemblage. The smaller plagioclases, which predate the crenulation schistosity S4, are free of inclusions and aligned in the principal schistosity S3. Biotites crystallized in several stages too, but have only preserved their textural zoning (Fig. 4.1). No chemical zoning has been observed, demonstrating that they are fully recrystallized. The relationships and textures of white micas indicate at least 3 stages of crystallization. Staurolite is either situated close to the garnets and/or associated with biotite and/or kyanite; it has never been found as an inclusion. The refolded thin layers of graphite it overgrew prove its post S4 crystallization age. The hornblende found in EC137 also overgrew S3 and S4. Zoned epidote, (piemontite to clinozoïsite$_{0.70}$ and pistachite$_{0.30}$) are randomly distributed among quartz, muscovite and plagioclase; they crystallized before S4 and probably before S3. Some prograde chlorites have been preserved as inclusions in ECB16, EC27 and EC31, constraining the prograde P-T path.

| Minerals | Size (mm) | % | ->S2 | S3 | ? | Dt S4 | Dt |
|---|---|---|---|---|---|---|---|
| Garnet | 2-15 | 7-20 | | | | | |
| Biotite | 2-7 | 7-10 | | | | | |
| Muscovite | ->4 | 15-30 | | | | | |
| Quartz | ->3 | 20-25 | | | | | |
| Plagioclase | 1-4 | 0-15 | | | | | |
| Ilmenite | ->3 | 0-2 | | | | | |
| Rutile | ->2 | 0-1 | | | | | |
| Chlorite | ->2 | 0-4 | | | | | |
| Epidote | ->1 | 0-2 | | | | | |
| Staurolite | 1-3 | 0-4 | | | | | |
| Kyanite | ->5 | 0-3 | | | | | |
| Amphibole | ->22 | 0-1 | | | | | |
| Graphite | | 0-3 | | | | | |
| Tourmaline | ->1 | <1 | | | | | |

Table 3.4 Grain size and modal percentage of the minerals, and observed relationships between deformation and mineral crystallization in garnet micaschists. (S2 and S3 are the first two penetrative schistosities, S4 the crenulative schistosity, and Dt the Lepontine metamorphism).

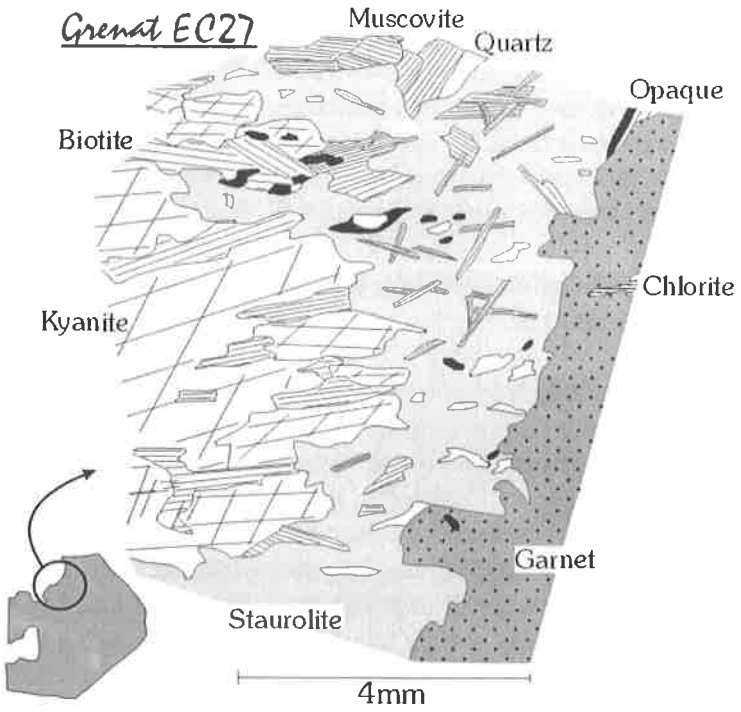


Figure 3.3 Barrowian sequence recorded in the garnet micaschist EC27 (671'420/135'330).

## 3.6 THE MAFIC ROCKS

Mafic rocks were only found in the Pizzo del Vallone nappe. They are massive, generally hard and of course green, except for the differentiated metabasalts, which are richer in plagioclase. The schistosities are differently recorded depending on the texture of the original rock. Different textures, such as coarse-grained (microgabbroic), fine-grained, cumulate with phenocrysts have been recognized in the various metabasalts (Fig. 3.4). The microscopic texture of these rocks is nemato(porphyro)blastic with oligoclasic to andesitic poikiloblasts of plagioclase. The proportion of amphibole-epidote-plagioclase is variable (Tab. 3.5), and depends on the more or less good preservation of the various schistosities. However S3 is always more or less visible.

Several generations of zoned amphiboles have been distinguished (Fig. 3.5). Amphiboles of pre-S2 age are randomly distributed but lie oriented in the principal schistosity S2. Most of the amphiboles, however, are coeval of D3 and D4. Younger amphiboles have a more marked and intense colour. Indeed the few amphiboles contemporaneous of D4 have a dark blue-green colour indicating that metamorphic conditions increased from D2 to D4, to reach the peak. In the sample EC57, some dark kaersutite amphiboles remain, these being relicts of the primary magmatic mineralogy (paragraph IV.5). As EC57 has not been completely overprinted during metamorphism, ghosts of olivine, now completely replaced by dolomite, can be seen. Epidote is present but to a lesser extend than in the Sabbione and Vannino areas or in the Binntal, showing the existence of a metamorphic gradient. However in altered chilled margins, the epidote coupled with plagioclase or green biotite can form up to the 80% of the rocks. Rutile, the Ti-bearing mineral, is also variable and is either present in the rock with a modal percentage around 3-5%, or it is wholly absent.

| Minerals | Size max. (mm.) | % | ->S2 | S3 | ? | Dt S4 |
|---|---|---|---|---|---|---|
| Amphibole | 2*0.6 | 5-88 | | | | |
| Plagioclase | 0.7 | 2-32 | | | | |
| Epidote | 0.8 | 0-38 | | | | |
| Biotite | 3*1 | 0-25 | | | | |
| Opaque | 0.6 | 0-5 | | | | |
| Garnet | 0.8 | 0-2 | | | | |
| Rutile | 0.4 | 0-5 | | | | |
| Chlorite | 2*0.3 | 0-50 | | | | |
| Quartz | 0.3 | 0-4 | | | | |
| Carbonate | 3*1.8 | 0-15 | | | | |
| Accessory | 0.3 | ->4 | | | | |

Table 3.5 Summary of the crystallization-deformation relationships observed in the metabasalts (S2 and S3 are the first two penetrative schistosities, S4 the crenulative schistosity, and Dt the Lepontine metamorphism).


Figure 3.4 The boundary between the metabasalt and the volcanoclastic sediments of the Pizzo del Vallone nappe (Sample EC238, 668'900/141280), with a well-developed S4 crenulation. D4 refolded the amphibole rich layers (S3) but allowed biotite crystals (S4) to crystallize in the volcanoclastic layers.

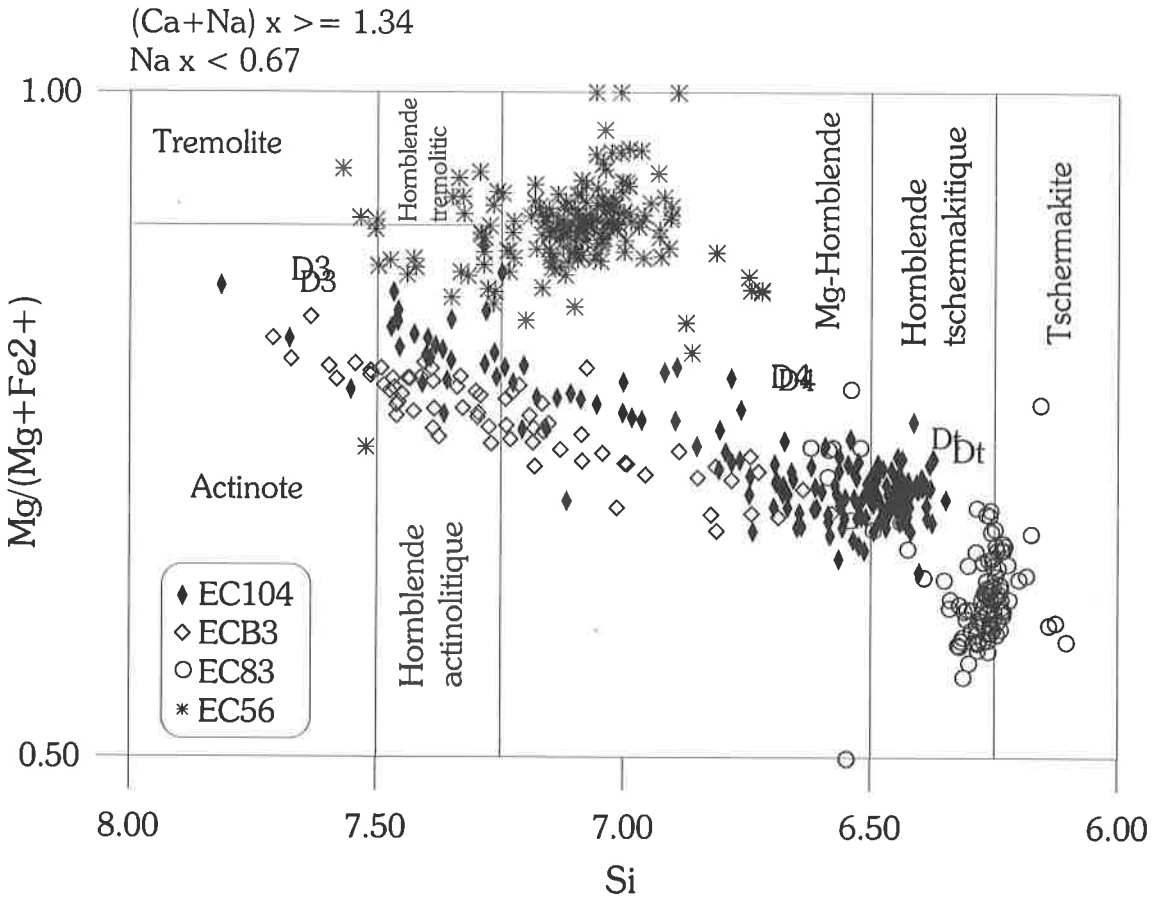


Figure 3.5 Variations of composition of the amphiboles depending on their crystallization age. D3, D4 and Dt are roughly situated to see the general prograde trend. (EC104 is a fine-grained metabasalt collected in the Sabbione area, ECB3 is a fine-grained metabasalt collected in the Binntal, EC83 is a metavolcanoclastite rich in amphibole collected in the Sabbione area, and EC56 a differentiated metabasalt collected in the Sabbione area, close to the sample EC104).

## 3.7 Discussion

The textures differ according to the mineralogy of the samples: micaceous quartzites are lepidoblastic, the metabasalts are nematoblastic, containing variable amounts of poikiloblasts of plagioclases and the garnet micaschists are granolepidoporphyroblastic. Despite these differences several common points exist in most of the investigated samples.

S2 is a slaty cleavage generally fully transposed (and thus lost) during later cleavage forming events but conserved and recognisable in relic fold hinges. It is still quite well preserved in micaceous quartzites (Fig. 1B) and graphite rich layers, where the S3 overprint was not very strong. S3 is the main schistosity; it is parallel to bedding, except of course in D2 fold hinges or where it is refracted (Fig. 3.1A). Where S2 has been preserved, S3 clearly crenulates S2 and microlithons are observable (Fig. 3.1B); in such case, S2 and S3 are approximately equivally well developed in the rock. Otherwise, S2 probably disappeared during S3 growth by solution transfer, recrystallization and grain growths (Passchier & Throuw 1998). S3 is preferentially best developed in more pelitic samples and its intensity may change abruptly at lithological boundaries. The development of S4 varies depending on the rocks type (Fig. 3.1B, 3.4): D4 crenulated or only folded the previous schistosities depending on the competency of the rock.

The peak of temperature of the Lepontine metamorphism which caused much porphyroblastesis, occured after D4 (Fig. 3.2, Tab. 3.4) although, in detail, the crystallization had already began during D4. Porphyroblasts overgrowing S4 not deflect this fabric and there are no strain shadows. However, deflection of S4 and folded S3 are visible inside the porphyroblasts, although rarely. Microprobe profiles across such porphyroblasts (Fig. 4.1) show no abrupt changes of composition, proving that growth was continuous contemporaneously with and after D4.

The minerals coeval to D3, D4 and Dt respectively show well-preserved prograde conditions in all rock-types. The kyanite zone is reached in metapelite and the amphibolite facies in metabasalts, with tschermakite crystallizing, in the southern part of the area. The kyanite isograd crosscuts thrustings (Fig. 3.6) again demonstrating that the Lepontine metamorphism was late, as shown by the structural study. A more precise quantification of the P-T conditions is given in chapter IV.

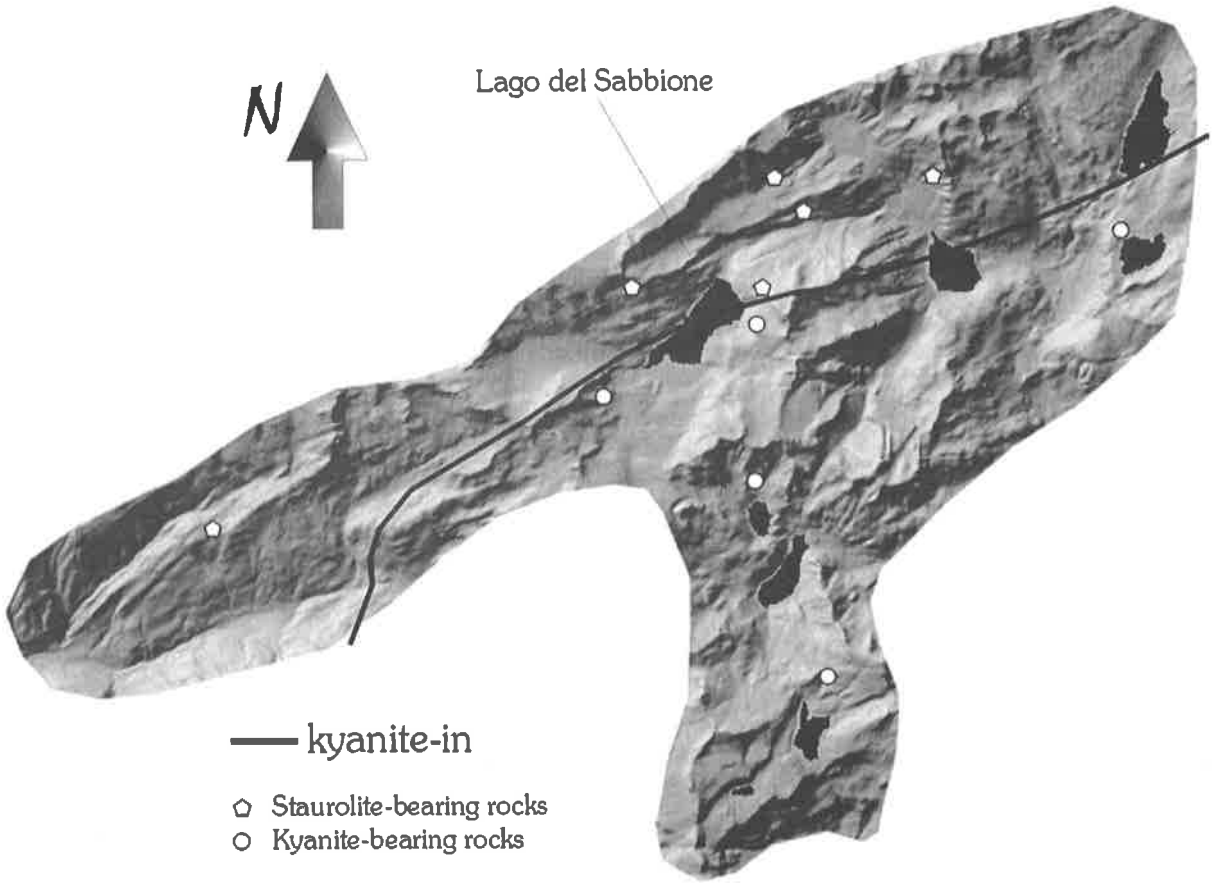


Figure 3.6 Localisation of the kyanite-in isograd.

# 4 THERMOBAROMETRIC INVESTIGATIONS

## 4.1 INTRODUCTION

Oriented samples from the Holzerspitz series, the Pizzo del Vallone and Camosci nappes, with a mineralogical assemblage suitable for determining P-T values and no mineral texture indicating disequilibria, were investigated. All samples were replaced in the structural frame to ensure that the same metamorphism was always measured: the last static phase Dt occurring after nappes emplacement (paragraph III.1, VI.3.4, Tab. 3.3, 3.4, 3.5).

The various graphitic aluminous garnet micaschists of the Holzerspitz series (Fig. 2.1) were investigated (ECB16-EC27-EC31-EC97-EC137). As the principal levels of the Pizzo del Vallone nappe are of detrital nature, a discontinuous micaschist (EC204) as well as metabasalt bodies (ECB3-EC104) and volcanoclastic metasediments (EC83-EC152-EC232) were analysed to determine the consistency of the results between the pelitic and mafic sequences. Only one micaschist of the Camosci nappe (EC179) was investigated because it is the only one that has a suitable mineralogical assemblage.

The nappes are characterised by several superposed deformations. The relations of crystallisation-deformation are summarised in chapter III (Fig. 3.3, 3.4, 3.5) and the tectonics is presented in chapter VI (Fig. 6.1, 6.2, 6.3, 6.4). However, a short summary is useful here.

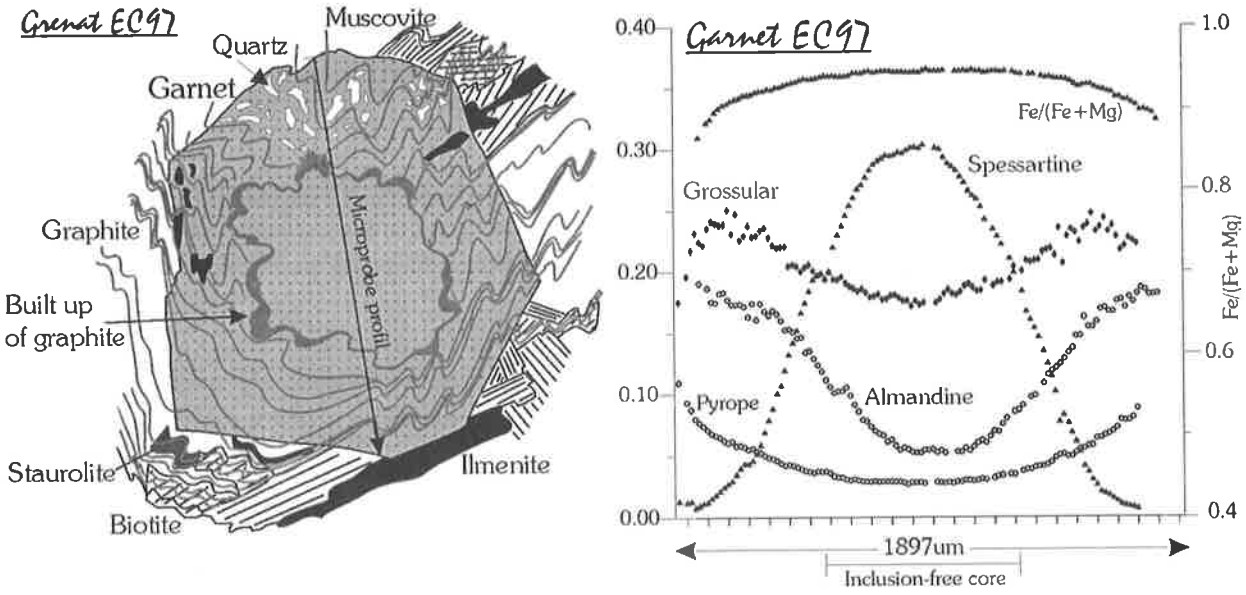


Figure 4.1 A) Texturally and chemically zoned garnet (Sample EC97, 670'090/141'650) in a garnet micaschist of the Holzerspitz series. B) Microprobe profile across the garnet.

The earliest recognisable schistosity is rarely visible but is even so attributable to the isoclinal folds F2. A second folding phase, the main phase, produced the isoclinal folds F3. Its associated schistosity S3 is strongly penetrative, printed over all the area and moreover parallel to the stratification, except of course in fold hinges F3. The next folding phase D4 induced a crenulative cleavage S4. Few minerals crystallised during this phase, but it hardly distorted the previous structures. The studied phase Dt acted during and after D4. It permitted well-developed porphyroblasts to overgrow the schistosities and thus, preserve older structures. This phase is essentially static, but small rotations of garnets are visible (Fig. 4.1). The main porphyroblasts coeval to Dt are garnet, staurolite, kyanite and tschermakite crystals. This assemblage is typical of the amphibolite facies. The area initially underwent the chlorite and garnet zone, in other words the greenschist facies, and later reached the staurolite and kyanite zone, that is to say the amphibolite facies (Fig. 3.3). The last backfoldings distorted previous structures and most probably the isograds as well. Only rare fibres of retrograde chlorite crystallized after Dt.

## 4.2 ANALYSES

### 4.2.1 Preliminary considerations

A first pressure-temperature quantification has been done using the conventional calibrations, for instance the garnet-biotite thermometer (SPEAR 1993, and references therein). However, depending on the chosen calibration, the results varied a lot (Tab. 4.1). Moreover, SPEAR (1993) demonstrated that the presence of a third mineral might interfere in the cation exchange. For instance, the presence of staurolite changes the relation between garnet and biotite.

| Sample | Assemblage | $P_S$ | $T_S$ | $T_{Gt\text{-}St}$ | $P_{Th}$ | $T_{Th}$ |
|---|---|---|---|---|---|---|
| EC179 | Gt-Bt-St | | | 515 | 9.5 | 540 |
| ECB16 | Gt-Bt | 6.9 | 480 | | 8.8 | 572 |
| EC97 | Gt-Bbt-St | 7.75 | 510 | 588 | 8.9 | 547 |
| EC31 | Gt-Bt-St-Ky | 8.1 | 550 | 637 | 9.6 | 574 |
| EC27 | Gt-Bt-St-Ky | 6.0 | 625 | 678 | 7.6 | 594 |

Tab.4.1 Comparison of the values (without the calculated errors because not provided by all methods, see Table 4.2) obtained by different methods: $P_S$-$T_S$: pressure, temperature respectively after a chosen calibration proposed by the SPEAR's software / $T_{Gt\text{-}St}$: temperature after FED'KIN & ARANOVICH's equation (1991) / $P_{Th}$-$T_{Th}$: pressure and temperature after THERMOCALC.

Due to the two above-cited reasons, pressure and temperature were determined by a second method, which considers all of the contemporary equilibrated minerals. I used the software THERMOCALC version 2.75, along with HP98 (HOLLAND & POWELL 1998 http://www.esc.cam.ac.uk/astaff/holland/thermocalc.html), an internally consistent thermo-dynamic dataset

THERMOCALC considers the whole mineralogical assemblage (HOLLAND & POWELL 1998). It calculates all possible reactions using the end-members of the equilibrated minerals (calculated by the software AX, HOLLAND & POWELL 1999) and propagates the error by the least square method and the average P-T method (HOLLAND & POWELL 1994). Optimal P-T conditions are, thus, determined for the equilibrium (Annexe 4A, Tab. 5.2). Moreover, the calculated errors on P and T allow the construction of an ellipse of errors (HOLLAND & POWELL 1994).

| N° | P(Ax) | T(Ax) | σfit | fit (66%) | P | ΔP | T | ΔT | corr | react. | Alt. |
|---|---|---|---|---|---|---|---|---|---|---|---|
| EC179 | 9.2 | 540 | 1.42 | 1.29 | 9.5 | 2.3 | 540 | 58 | -0.207 | 9 | 2730 |
| ECB16 | 8.4 | 570 | 1.45 | 1.30 | 8.8 | 1.4 | 572 | 52 | 0.954 | 8 | 2656 |
| EC97 | 9.2 | 570 | 1.54 | 1.11 | 8.9 | 1.3 | 547 | 51 | 0.821 | 6 | 2505 |
| EC31 | 9.4 | 590 | 1.49 | 1.05 | 9.6 | 0.7 | 574 | 20 | 0.286 | 7 | 2440 |
| EC137 | 10.1 | 600 | 1.42 | 1.18 | 9.8 | 1.3 | 590 | 41 | 0.820 | 10 | 2550 |
| EC27 | 8 | 590 | 1.45 | 0.86 | 7.6 | 0.7 | 594 | 19 | 0.293 | 7 | 2510 |
| EC204 | 9.4 | 610 | 1.49 | 1.44 | 9.5 | 1.1 | 618 | 20 | 0.586 | 7 | 2040 |

Table 4.2 Results provided by THERMOCALC for X ($H_2O$)=0.8. The columns P(Ax) and T(Ax) are the parameters enter in the DosAx program (http://www.esc.cam.ac.uk/astaff/holland/ax.html); ΔP and ΔT are the errors calculated on P and respectively T by THERMOCALC, "Corr" is the coefficient of correlation; "React." represents the number of linearly independent reactions considered by THERMOCALC; and "Alt." the altitude of sampling.

All the equilibrated phases, as well as others, were analysed to determine the precise chemistry/mineralogy of the rocks. For each sample an average of the composition of the borders of all equilibrated phases was made. At the same time, controlling that the standard deviation of each oxide measured is not too great ensured that the minerals are chemically in equilibrium (Annex 4A). To determine the metamorphic history, the garnet zoning was also investigated (Fig. 4.1, 4.3).

Acquisition was carried with the use of the Camera SX50 microprobe of the University of Lausanne. The measured minerals are garnet (Gt), biotite (Bt) and muscovite (Ms), plagioclase (FP), ilmenite (Ilm), rutile (Rt), quartz (Q), epidote (Ep), amphibole (Amph), chlorite (Chl), staurolite (St) and kyanite (Ky). In order to take into account a maximum number of oxides, several petrogenetic grids were used:

- KMASH, KFASH and KFMASH calculated for Q-Ms-H2O in excess (Jean-Claude Vannay, personal communication)
- CKNASH (SPEAR 1993) where the stability domains of white micas and epidotes is represented.

### 4.2.2 Thermobarometric results: the garnet micaschists

The investigated metapelites all plot together in the zone of coexisting epidote and staurolite, according to the mineralogical assemblage (Fig. 4.2, Tab. 3.4).

EC27 is a good example. In fact, it preserved a good sequence of barrowian metamorphism (Fig. 3.3) and its anorthite content, at around 86%, is high. This signifies that here the mineralogical observations are extremely well concordant with the petrogenetic grid. Indeed EC27 plots in the coexisting garnet-staurolite-kyanite field (Fig. 4.2) but mostly along the reaction curve that produces Ca-rich plagioclase through the breakdown of epidote. EC27 and EC137 were collected close to each other. But EC27 was sampled five metres westward of a thrust plane. So the pressure differences between these two samples may be explain by the proximity of this thrust plane; the latter allowed EC27 to react longer during the retrograde history, probably due to fluid circulation.

EC97, EC31 and EC137 are aligned on the same north-south cross-section. A small increase of P-T from north to south, that is to say from an external to a more internal position, is calculated. This small increase is coherent with the structural considerations. Indeed the static metamorphism Dt occurred before the onset of backfoldings; thanks to the present cross-section of the Alps (Fig. 1.4) it is possible to form a good idea of the nappe stack at this time. A slight increase of the P-T

conditions southward is, thus, coherent due to the slight increase of the thickness of the nappe stack southward.

ECB16, EC97 and EC204 are roughly aligned on the same west-east cross-section. The temperature, and in a lesser way the pressure, increase respectively from EC97 and ECB16 to EC204 according to their structural position. Moreover the axes are strongly east pitching in the area where EC204 was collected, and EC204 was collected at a lower altitude than the two other samples.

Sample EC179 has a great ellipse of error because it does not contain plagioclase and so the pressure cannot be constrained well. However, as it contains staurolite in equilibrium it is obvious that only the right part of the ellipse (staurolite in), the part that is consistent with the P-T values obtained for the other investigated samples, has a signification.

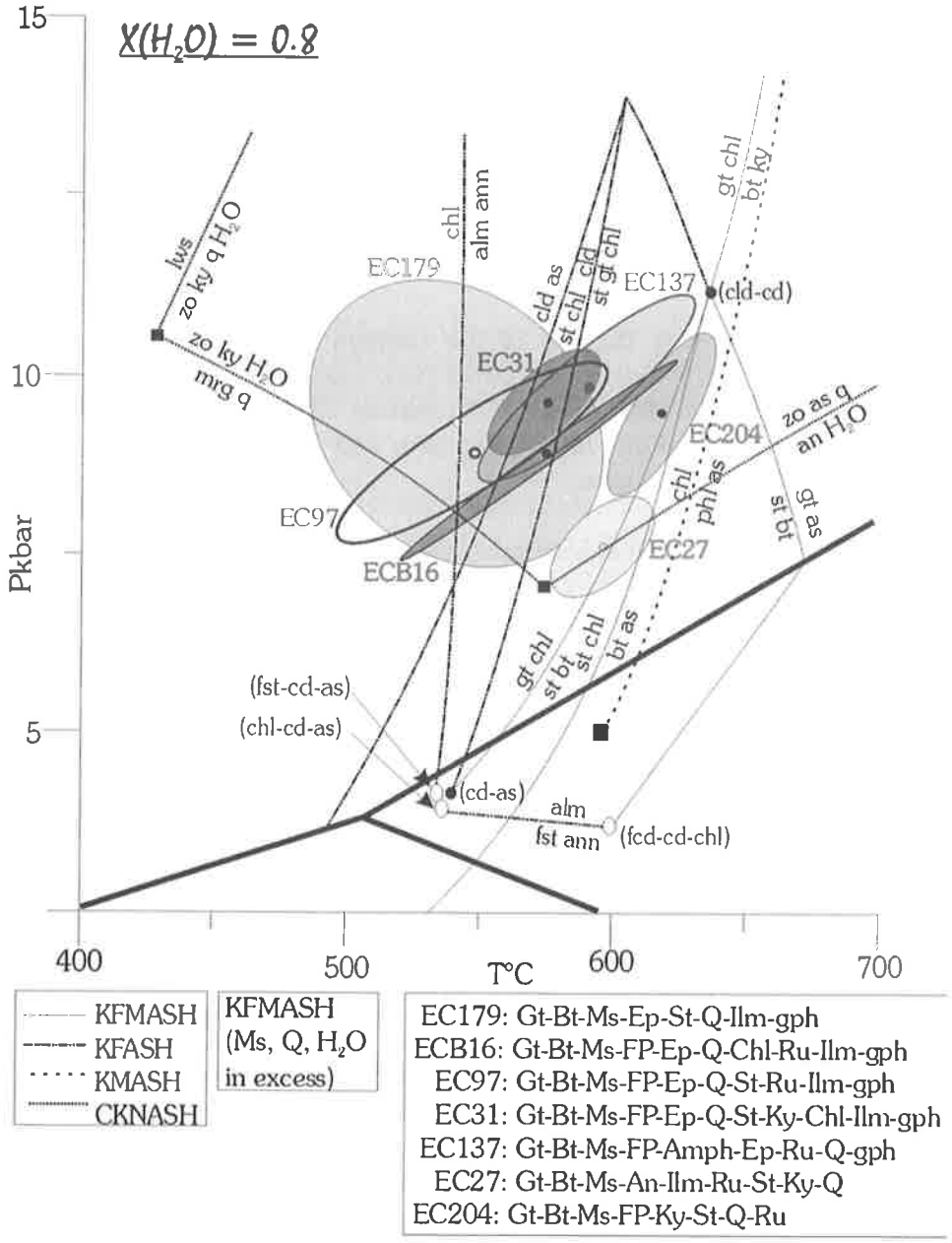


Figure 4.2 P-T calculated by THERMOCALC (Tab. 4.2) for the analysed samples. Jean-Claude VANNAY (personal comm.) calculated the reactions for the KFASH, KMASH and KFMASH systems, SPEAR (1993) for the CKNASH system. The minerals abbreviations are in annexe 4B.

### 4.2.3 Thermobarometric results: metabasalts and volcanoclastic metasediments

In the various metabasalts, the number of minerals in equilibrium is unfortunately too low to obtain enough linearly independent reactions in order to use THERMOCALC. However, it is sufficient to determine that the assemblage coeval of the peak of the Lepontine metamorphism is characteristic of the amphibolite facies (Tab. 3.5).

In the investigated metabasalts, Ti is above all contained by rutile and amphiboles. So the thermometer based on the Ti-content of amphiboles (COLOMBI 1989) should provide good results, because no mineral is susceptible to have a Ti-cation exchange with the amphiboles. The obtained temperature for EC83-EC104-EC152-EC203 and EC232 are coherent within themselves (Tab. 4.3A) and coherent with the temperature obtained for the micaschists. For instance, the closing temperature of EC137 was calculated by THERMOCALC and by the Ti-content thermometer (Tab. 4.2, 4.3A). The results are reproducible. Likewise EC137 and EC152, which were collected relatively close one another, on both side of the Holzerspitz – Pizzo del Vallone tectonic contact plane, give similar results.

In some samples, several generations of amphiboles are preserved. The Ti thermometer was applied to amphiboles coeval to S2, S3 and S4. The results show that the amphiboles crystallised from S2 to the end of Dt in an environment of increasing temperature (Tab. 4.3B).

Several minerals containing Al are likely to disrupt the use of the barometer, which is based on the Al-content of amphibole (ANDERSON & SMITH (1995). However, I decided, all the same, to use it on the amphiboles coeval to the late Lepontine metamorphism Dt. It was not applied to older amphiboles due to the mobility of this cation. The results are again consistent with those obtained for the micaschists (Tab. 4.2, 4.3A).

| A) | EC83 | EC104 | EC203 | EC152 | EC232 | EC137 |
|---|---|---|---|---|---|---|
| $T°_{Ti\text{-}amph}$ | 578 | 573 | 583 | 613 | 582 | 593 |
| $P_{Al\text{-}amph}$ | 10.7 | 9.7 | 10.5 | 9.9 | 9.3 | 10.0 |

| B) | ECB3 (S4) | EC83 (S3) | EC104 (S3) | EC232 (S2) | EC232 (S3) |
|---|---|---|---|---|---|
| $T°_{Ti\text{-}amph}$ | 548 | 547 | 537 | 520 | 565 |

Table 4.3 A) P-T obtained for the rim of the porphyroblasts (end of Dt, Tab. 3.5) after COLOMBI (1989). For EC137, I use the same average composition of amphibole than in THERMOCALC. EC203 is a garnet amphibole micaschist that does not contain enough minerals in equilibrium for applying THERMOCALC. B) Temperature calculated for the amphiboles respectively coeval to S2, S3 and S4.

### 4.2.4 P-T paths from garnet zoning (Gibb's modelling)

The quantification of the P-T values of the peak of metamorphism Dt is good, coherent and moreover reproducible. But as the garnets in the metapelites are, as said above, chemically well zoned (Fig. 4.1), it was possible, thanks to a backward process known as Gibb's modelling (SPEAR et al. 1984, SELVERSTONE et al. 1984), to calculate the successive P-T conditions recorded by the garnets. To do this the degree of freedom of the system must be less than the number of variables: so only ECB16, EC31 and EC97 are usable (Fig. 4.3 and Annexe 4C). To obtain better curves and to avoid mixing two different thermodynamic datasets, three P-T values were calculated with a Spear's software (Tab. 4.1). As the calculation is based on the final coeval mineral assemblage, the software has complete control upon the successive mineral assemblage, that it recalculated each time the curve crosscut a reaction curve, for instance the breakdown of staurolite. Consequently the successive P-T values obtained are only semi-quantitative. Thus, the history and the interpretation of the relative shape of the curves correspond to the relative history.

$P_{max}$ is reached before $T_{max}$. As a consequence it appears that dP/dT varies according to the grossular variations (Fig. 4.1, Annexe 4C). Firstly, the garnets recorded a compressive regime, visible because of the near isothermal increase of pressure until $P_{max}$ was reached. Then, a relaxation or decompression allowed the temperature to increase contemporaneously with a slight decrease in pressure. The resulting P-T curves are simple, but coherent with the P-T path that could be envisaged for such an environment of tectonic exhumation (SPEAR 1993).

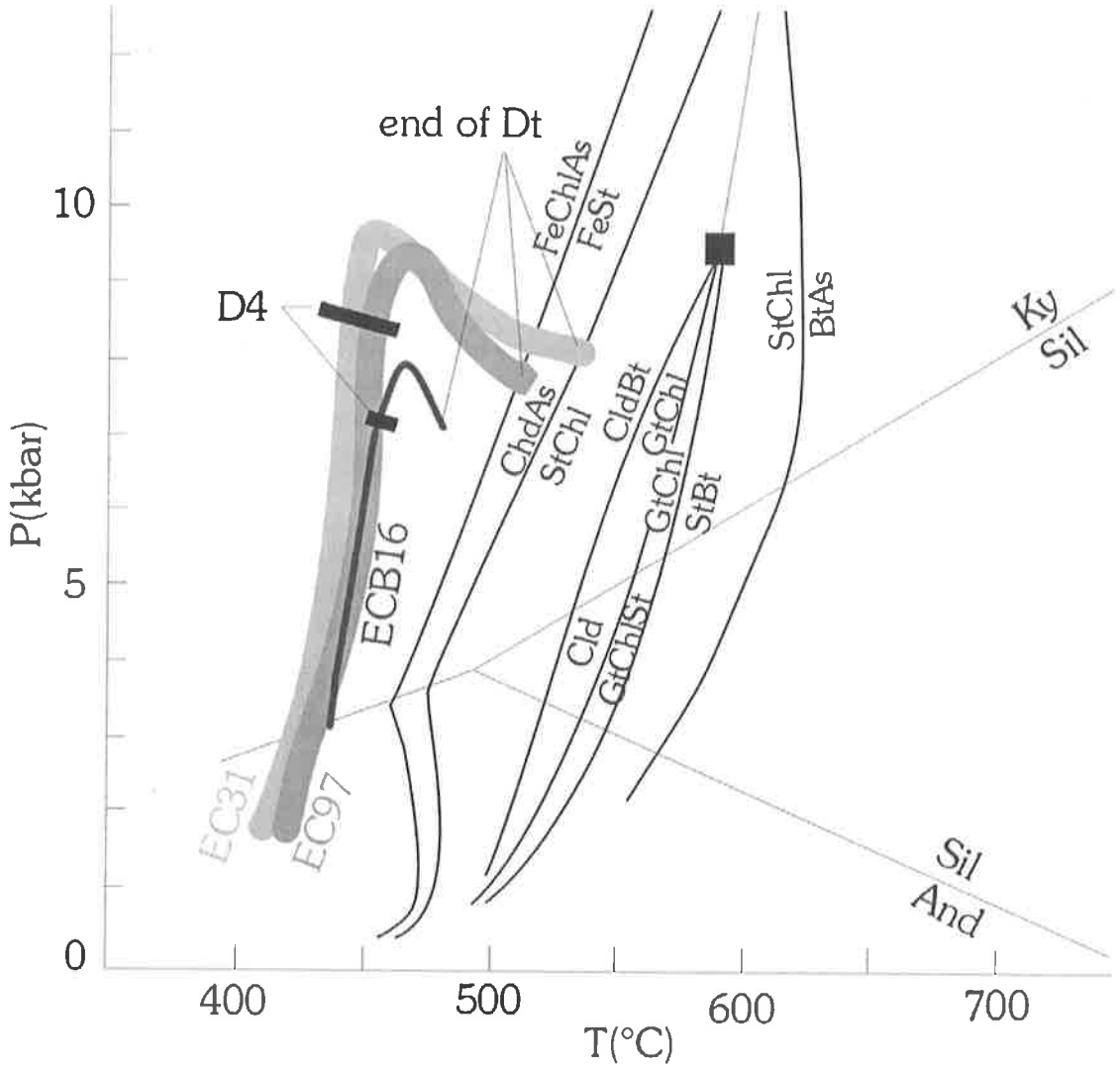


Figure 4.3 Gibb's modelling for the sample ECB16, EC97 and EC31 (after SPEAR et al. 1984). The results are reported on a petrogenetic grid proposed by SPEAR (1993).

### 4.2.5 Concluding remarks

The micaschists, metabasalts and volcanoclastic metasediments give consistent results for the last static phase of crystallisation. The obtained P-T values are well constrained and coherent with the observed mineralogical assemblage:

- EC137 has been investigated twice, and the two methods give the same results;
- a slight increase in the values is detectable from north to south;
- the calculated metamorphic P-T path is consistent with the idea that I had for this region and it is also coherent with the models that I have for an environment of tectonic exhumation.

## 4.3 COMPARISONS

Previous workers have already established the metamorphic values reached during the Lepontine metamorphism for a larger area (KLAPER & BUCHER-NURMINEN 1987, KAMBERS 1993, TODD & ENGI 1997, DELEZE 1999). Nevertheless, the P-T values they proposed for the High Val Formazza and Binntal do not correspond with the mineralogical assemblage they described (Fig. 4.4, 4.5). DELEZE (1999) is the exception: the values he proposed for the Cristallina region are higher than those of all other authors. However, it is hazardous to compile or compare P-T values provided by different authors. But, with the help of THERMOCALC I recalculate the P-T values for some rocks published with their chemical composition (Fig. 4.4, 4.5, Annexe 4D). TODD & ENGI (1997), who proposed a metamorphic map of the whole Lepontine Alps, published so few chemical compositions, I can only recalculate the P-T values for one sample, that of Ma9464. Fortunately this rock was sampled near the area investigated by DELEZE (1999), and located not far from his sample called M36.

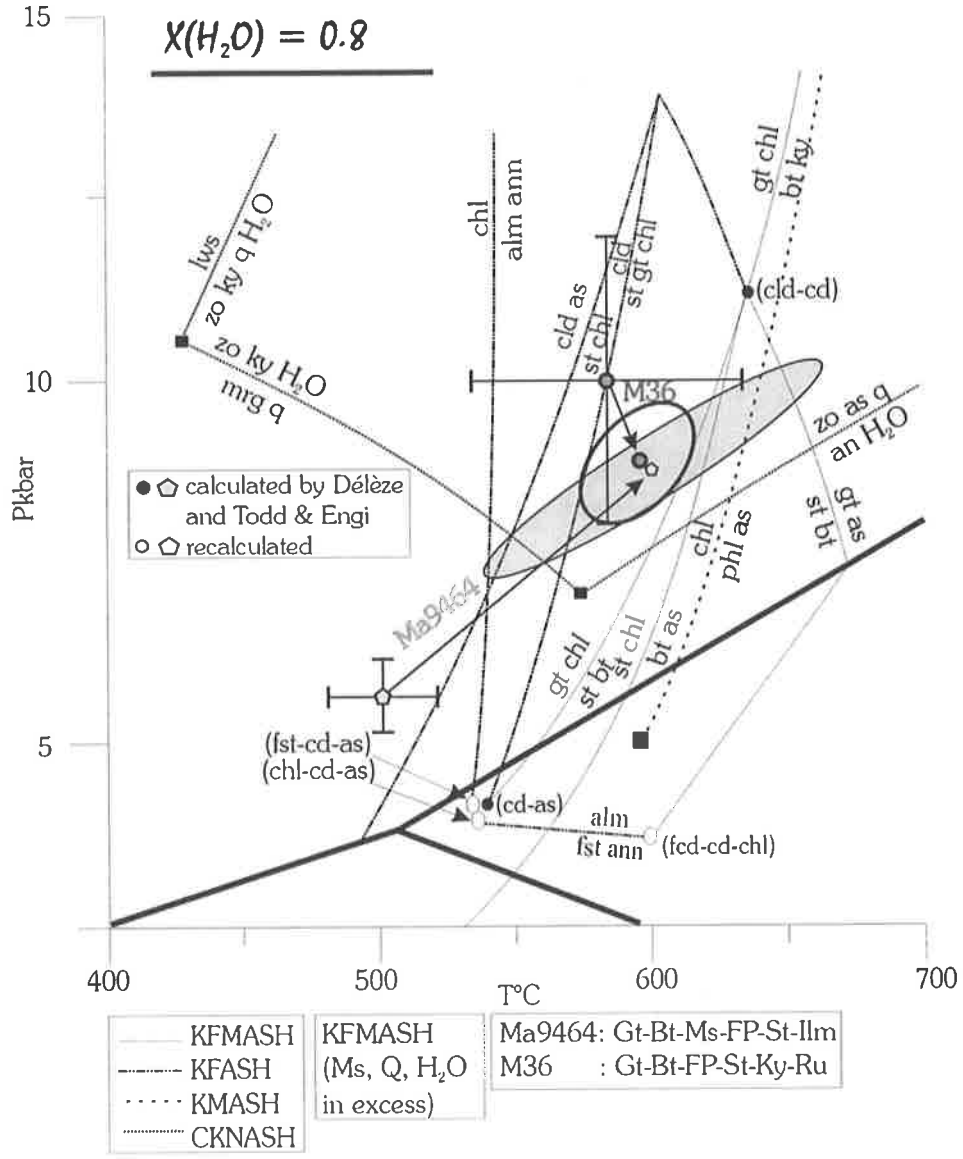


Figure 4.4 The P-T values calculated by THERMOCALC for MA9464 (TODD & ENGI 1997) and for M36 (DÉLÈZE 1999). These two samples were sampled not too far away from one another. The P-T values calculated by the authors are also reported on the grid. Jean-Claude VANNAY (personal communication) calculated the reactions for the KFASH, KMASH and KFMASH systems, SPEAR (1993) for the CKNASH system. The mineral abbreviations are in annexe 4B.

Figure 4.4, 4.5 reports some P-T values calculated by the above-cited authors and the P-T values recalculated with THERMOCALC. The sample mineralogical assemblage does not correspond to the mineralogical assemblage read on the petrogenetic grid. For instance, when the sample Ma9464 contains staurolite crystals, the P-T values determined by TODD & ENGI (1997) are too low to allow the staurolite to crystallise.

KAMBERS (1993) studied an area close to the one I studied. In the same way and for the same reasons I recalculated the P-T values for some samples he investigated (Fig. 4.5, Annexe 4D). All the samples contain epidote crystals but when plotted on a petrogenetic grid none are in the epidote stability field. THERMOCALC provides better-constrained values; they are more consistent with the petrogenetic grid.

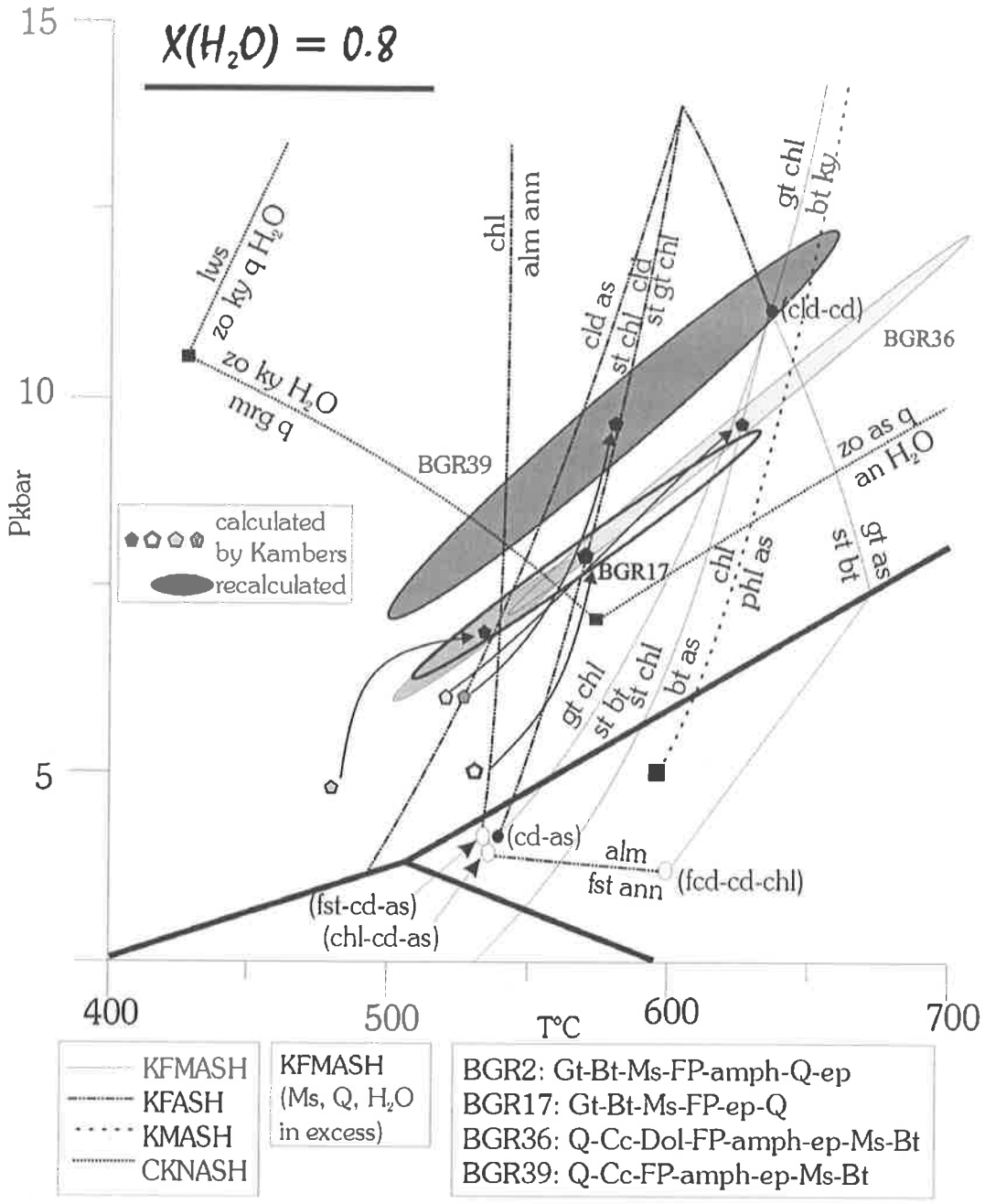


Figure 4.5 P-T values recalculated for some samples of KAMBERS (1993). Jean-Claude VANNAY (personal communication) calculated the reactions for the KFASH, KMASH and KFMASH systems, SPEAR (1993) for the CKNASH system. The mineral abbreviations are in annexe 4B.

## 4.4 CONCLUSION

### 4.4.1 Discussion

The P-T conditions reached at the end of Dt in the micaschists, metabasalts and volcanoclastic sediments are similar. Nevertheless the absolute values are greater than previously calculated for this area. These differences suggest three possible propositions:

1) a different metamorphism was investigated. Such a proposition seems improbable because the used minerals for determining the P-T values are identical, and in this work only the borders were taken into account;
2) the samples record and preserve the metamorphic history differently depending on the area where they were collected. In this case correlations and comparisons would only have a limited signification;
3) the choice of the method is crucial. Actually it represents an important step.

The new calculated P-T values from this work are not likely to contradict previous predictions about the concentric pattern of the isobars and isotherms in the Lepontine Alps (HUNZIKER et al. 1992, TODD & ENGI 1997). But the absolute values must be recalculated to erase the incoherencies between the observed mineralogical assemblage and the calculated P-T conditions (Fig. 4.4, 4.5). At least in the studied area, the reached pressure was higher than 9 kbar.

### 4.4.2 And the structural framework!

Thermobarometry is a wonderful tool. However, even if the results are consistent and reproducible, they must be integrated into the structural framework in order to permit the detection of incoherencies. To test the results, I used different cross-sections of the Central Alps (ESCHER et al. 1988, 1993, 1997 and MARCHANT & STAMPFLI 1997), and consider that this metamorphism occurred during Middle to Late Oligocene (JÄGER 1973, KÖPPEL & GRÜNENFELDER 1975, DEUTSCH & STEIGER 1985, VANCE & O'NIONS 1992, HUNZIKER et al. 1992).

The inverted limb of the Monte Leone nappe is presently situated more or less 27 km below the top of the nappe stack. It was buried slightly more deeply before the backfoldings. Younger movements along the old discrete Simplon low angle normal fault (30° SW) are calculated to be of at least 15 km (HUNZIKER & BEARTH 1969, MANCKTELOW 1985, GRASEMANN & MANCKTELOW 1993).

Therefore, 27 km added to 7.5 km (=15 km*sin30°) signifies that the area was around 35 km below the surface when the peak of metamorphism occurred. Considering an average density of 2.65g/cm$^3$ for the overlying sedimentary-ophiolitico-gneissose column, the pressure supported by rocks situated in the inverted limb of the Monte Leone nappe was at least 9 kbar. Considering a gradient of 0.27 kbar/1 km, gradient commonly accepted for such an environment, I obtain 9.3 kbar.

Taking 35 km as the depth range from which the present studied area was exhumed since the start of the uplift/cooling cycle, in other word after $T_{max}$, leads to time-averaged rates of uplift for the Oligocene-Neogene ranging from 1.06 km/1 My to 1.52 km/1 My. These values are in general agreement with present day uplift rates for this region (GUBLER et al. 1981). So structural, geophysical and thermobarometric investigations lead to similar conclusion.

### 4.4.3 Summary

During the Lepontine metamorphism, the studied area reached ~580°C and ~9.6 kbar. The metamorphic conditions increase slightly from the north to the south of the area according to the structural position, and the mineral isograds crosscut the thrusting plane. The kyanite-in isograd (Fig. 3.6) is similar to the one proposed by KLAPER & BUCHER-NURMINEN (1987). Staurolite is found in all nappes outcropping south of the Rosswald series. Two micaschist were collected in the Teggiolo zone. They were not investigated because the garnet was not in equilibrium: its outer rim reacted with the matrix.

The thermodynamic history preceding the Lepontine metamorphism Dt is well recorded in the garnet. $P_{max}$ was reached before $T_{max}$. $P_{max}$ corresponds to the end of the NW-directed thrusting (Fig. 4.3), that is to say to the end of D4. The temperature was equilibrated after the pressure.

## 4.5 SPECIAL OBSERVATION

Some cumulates are still recognizable at the base of the basaltic bodies of the Pizzo del Vallone nappe (paragraphs II.3.3, V.2.2): large crystals of dolomite replace previous crystals of olivine in a dark green matrix. In the matrix, the magmatic core of some amphiboles was preserved: in fact, they are Ti-rich amphiboles called kaersutite.

The thermometer based on the Ti-content of amphiboles (COLOMBI 1989) applied to these kaersutites shows that these amphiboles most probably crystallised during the magmatic activity. The temperature of crystallisation varies from 425° C to 1400° C: the borders having recrystallized during the alpine metamorphism(s).

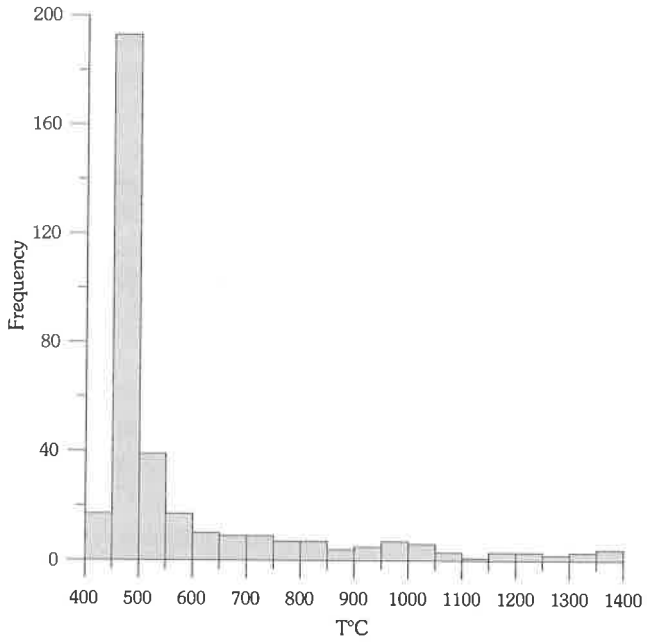


Figure 4.6 Histogram of the calculated temperatures of crystallization for the amphiboles of EC57 (COLOMBI 1989). The original core of some amphiboles is preserved.

# 5 GEOCHEMISTRY

## 5.1 INTRODUCTION

The mafic rocks of the Pizzo del Vallone nappe were analysed to determine their nature(s) and their paleogeographic setting.

Major, minor and trace elements for all samples were analysed at the "Centre d'Analyses Minérales" (CAM) of the Lausanne University (UNIL) by X-ray fluorescence (XRF) methods using a Philips PW 1400 spectrometer (Sc-Mo tube). Major and minor elements were measured on glass beads and common trace elements on powder pellets. The spectrometer calibration was based on international standards from the U.S. Geological Survey, ANRT-France and NIM-South Africa. Rare Earth Elements (REE) were analysed by a VG Plasma Quad Inductively Coupled Plasma/Mass Spectrometer, in the XRAL Laboratories, Toronto, Canada. A $Na_2O_2$ fusion technique was used to ensure total dissolution of the sample.

## 5.2 BASIC ROCKS OF THE PIZZO DEL VALLONE NAPPE

### 5.2.1 Introduction

The stratigraphic study of the Pizzo del Vallone nappe indicates the presence of both dolerites and large extrusive basaltic bodies respectively intruded or interbedded within the sedimentary cover series. The thickness and the width of the mafic bodies are extremely variable (paragraph II.3.4, III.6, V.2.3).

In order to highlight, or not, a possible evolution of the geochemical signature at outcrop scale but also at map scale, samples were collected over the whole area. However, as the Sabbione metasandstone was recognized in the Saflischpass, I also collected some mafic rocks outcropping around the Saflischpass in order to make comparisons on a larger scale; indeed the Saflischpass represents the westward continuation of the Pizzo del Vallone nappe.

The collected rocks may be subdivided into seven groups:

1) mafic rocks of the Vannino-Busin area: EC132-EC152-EC153-EC154-EC226;
2) mafic rocks of the Binntal area: ECB1-ECB2-ECB3-ECB19-ECB42;
3) mafic rocks of the Saflischpass: ECR12-ECR14-ECR15;
4) dolerites (EC185-EC199-EC200) and cumulate (EC57) of the Sabbione area;
5) mafic rocks of the Sabbione area: EC40-EC41-EC42-EC43-EC44-EC45-EC49- EC55-EC58-EC71-EC74-EC85-EC87-EC103-EC196-EC197;
6) cooling rim and reaction border of the Sabbione area: EC167-EC188;
7) differentiated basalts of the Sabbione area: EC56-EC192.

Such distinctions have been made because the location is primordial in order to detect eventual lateral magmatic variations at map scale. Moreover, as most of the green rocks outcrop in the Sabbione area, finer subdivisions were made for this area.

The sample EC132 is a volcanoclastic metasediment that simulates a green rock; its mafic detritus fraction is high (%Cr = 59 ppm). As it is the "more basic" rock that I have found in the Vannino area, it was also analysed, postulating that the ratio between the typical magmatic elements should be preserved.

### 5.2.2 Outcrops of mafic bodies

The mafic rocks are already described in the paragraph II.3.4 and III.6. Therefore, only some important field observations are reported here.

The intrusive dykes are recognisable due to preserved cooling rims, chilled margins, reaction borders and bedding unconformities; they are easily observable at the base of the basic bodies. A volcanoclastic sequence covers the extrusive basaltic flows suggesting the rapid cooling of the mafic rocks, a phenomenon expected in such an extrusive environment. No evidence of contact metamorphism in the sediments overlying the mafic bodies is observed. All the mafic rocks belong to the same magmatic suites.

**The Vannino-Busin area**: the mafic rocks form only restricted outcrops scattered within the Sabbione sandstone. They are fine- to medium- grained, and it is not uncommon to see 1 cm long crystals of biotite, coeval to the static metamorphic event and randomly oriented in the matrix, inserted between the amphibole crystals.

**The Binntal area**: the outcrops of green rocks are thin and continuous over long distances. The collected samples contain medium-sized amphiboles floating in a fine-grained matrix principally made of epidotes and feldspaths.

**The Saflischpass area**: the basalts from the Saflischpass form pluridecametric mafic bodies confined and wrapped by the Sabbione metasandstone, which is in contact with two big lenses of gypsum. Some basalts have conserved their magmatic texture (STRECKEISEN et al. 1998): indeed variolite, hyaloclastite, metapillows are currently still observable proving that they emplaced in an aquatic environment. The basaltic rocks are rich in medium-sized amphiboles and green biotites floating in a plagioclase rich matrix.

**The Sabbione area**: the biggest mafic bodies outcrop in the Sabbione area. They are made up of various metabasalts, principally made of amphiboles and plagioclase, and to a lesser extent of epidotes, biotites and titanite:

- common fine-grained basalts;
- basalt with a microgabbroic texture;
- cumulate: the primitive shape of the cumulative olivines (EC57) is still well recognizable even if brownish crystals of Mg-calcite replace them now;
- dolerite: beautiful minerals may crystallize at the contacts between the dolerites and the dolomitic pebbles of the Sabbione metasandstone;
- fine-grained pillow-lavas, although well deformed.

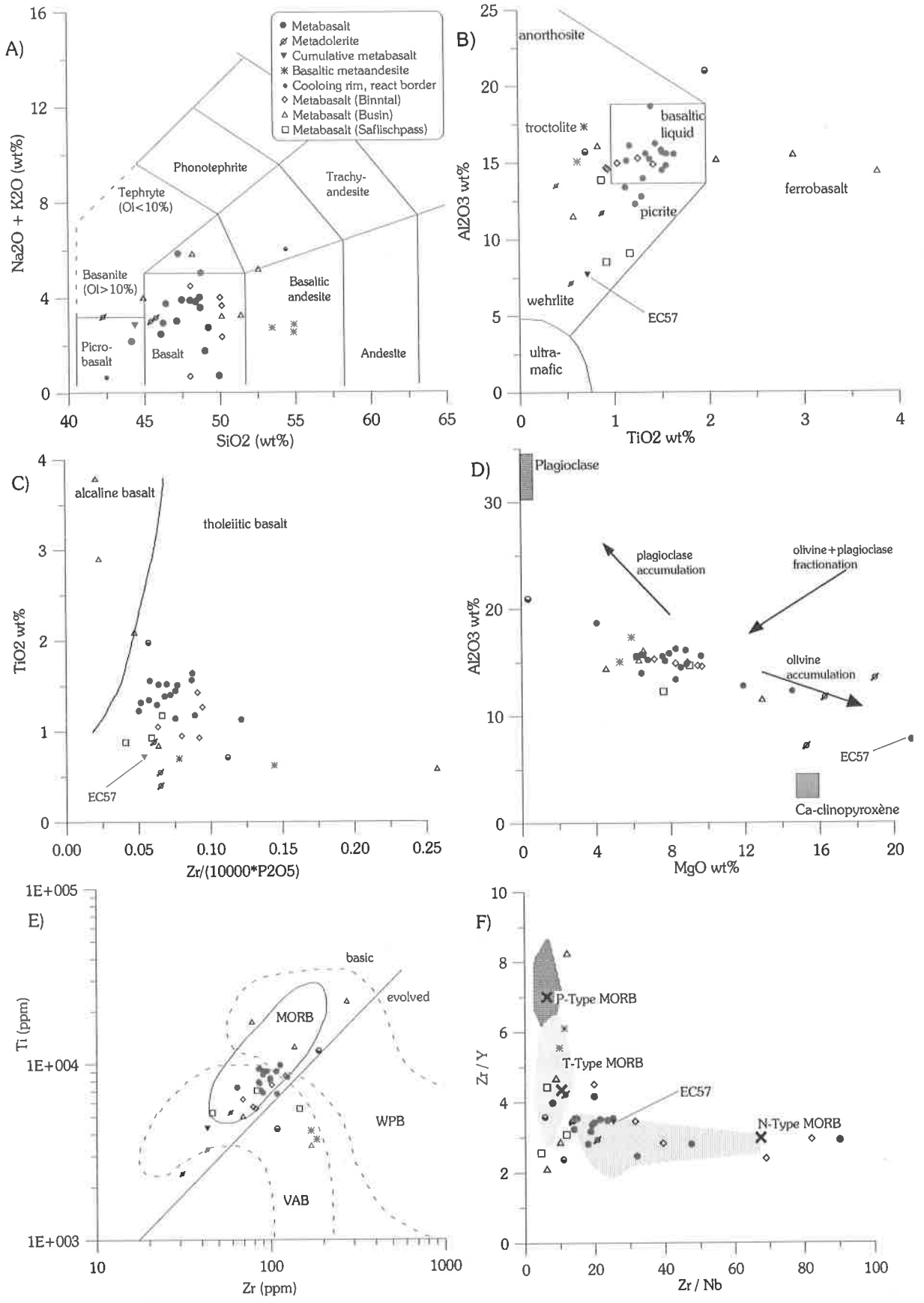


Figure 5.1 Denomination of the various metabasalts: A) after LE MAITRE et al. 1989, B) after PEARCE 1984, E) after WINCHESTER & FLOYD 1976, D) after PERFIT et al. 1980 E) after PEARCE 1982 (VAB: volcanic-arc basalt, WPB: within-plate basalt) and F) after PEARCE 1983.

### 5.2.3 Major and trace elements

As no bimodal distribution is obvious (Annexe 5A, Fig. 5.1), a correlation matrix was calculated (Annexe 5.C) to highlight the correlated elements. It is a pre-requisite to detect possible element mobility of the green rocks deformed and metamorphosed during an orogenesis before studying the element behaviour. Four groups of correlated elements were deduced: $TiO_2$-$Al_2O_3$-Ga-Pb-Sr-Y-S, $K_2O$-Ba-Rb, MgO-Cr-Ni-Co-Hf, and $SiO_2$-La-Nb-Zr-Th-Ce-Nd-U. Fortunately the elements presumed to have the same magmatic behaviour are correlated; they were not disturbed by the metamorphism. Hf is the exception; this incompatible high field strength element (HFSE) is strangely correlated with transitional and compatible elements. So either it had an uncommon behaviour (in which case more specific analyses have to be done) or the source is enriched in this element, or more likely it was measured wrongly. For some samples the loss on ignition (L.O.I) is high and associated with enrichment in CaO and depletion in $Na_2O$ and $K_2O$, suggesting a chemical metasomatic change in connection with a hydration event.

The studied rocks are basaltic to andesite-basaltic tholeiites (Fig. 5.1A+B) that are quartz normative, or hypersthene to hypersthene-olivine normative (KELSEY 1965 and COX et al. 1979); however, the mobility of alkalis implies that these results should be considered cautiously. Some basalts, enriched in Ti (Fig. 5.1B+C), are ferrobasalts. The Ti/Zr ratio allows the distinction of the basic from evolved melts (Fig. 5.1E): only points plotting above the line separating the basic from the evolved melts should be used to distinguish basalts (PEARCE et al. 1981).

The samples crystallise from a basaltic liquid that evolved (Fig. 5.1). So the dolerites, the cumulate, the basalts and the differentiated basalts were systematically plotted in the various diagrams to see the evolution. The magmatic differentiation occurred by olivine fractionation, and in a lesser way by Ca-clinopyroxene and plagioclase fractionation (Fig. 5.1D). This conclusion is confirmed by the study of the $Al_2O_3/TiO_2$ and $CaO/TiO_2$ ratios (SUN & SHARASKIN 1979). These mafic rocks are tholeiites (Fig. 5.1C), which have a T-MORB-like composition (Fig. 5.1F, 5.2); they represent a cogenetic magmatic series.

The dolerites and the cumulative basalt (EC57) are well distinguishable from the common and more differentiated basalts due to strong depletion in incompatible elements. The Cr and Ni depletion is easily observable and attributable to the olivine and clinopyroxene fractionation (Fig. 5.2, Annexe 5A). The Cr-depletion and Nb/Ce enrichment in the samples EC56-EC192-EC132 may be interpreted either by a great fractionation of the initial magmatic liquid (EC56-EC192) or by an important contamination by detritic fractions (EC132).

The multi-element diagrams normalised to MORB (Fig. 5.2) highlight the following significant points for the green rocks outcropping in the Sabbione area:

- the common basalts from the Sabbione area (Fig. 5.2B-D) have a flat profile from Nb to Sc, only showing weak Cr (and strangely Hf!) enrichments;
- the differentiated basalts (Fig. 5.2D) have strong enrichments in Th-Nb-Ce and Ti-Sc-Cr depletions. The liquid probably fractionated and underwent a weak crustal contamination. Moreover some zircons were dated, and all are inherited, proving the existence of crustal contamination (CARRUPT 2002, CARRUPT et al. in prep.);
- the cumulate EC57 (Fig. 5.2A) is enriched in Cr (and Hf!) but depleted in all others elements relatively to MORB, precisely because of its cumulative nature. Nevertheless the typical flat profile from Nb to Sc is also recorded;
- the dolerites (Fig. 5.2A) have a signature similar to the cumulative basalt but which is intermediate between the cumulative and common basalts. The incompatible elements (Nb-Ce) are present in greater quantity than in the cumulate EC57.

The cooling rim and reaction borders will not be discussed here precisely because of the contamination that obviously occurred during their emplacement (fluids, surrounding sediments...).

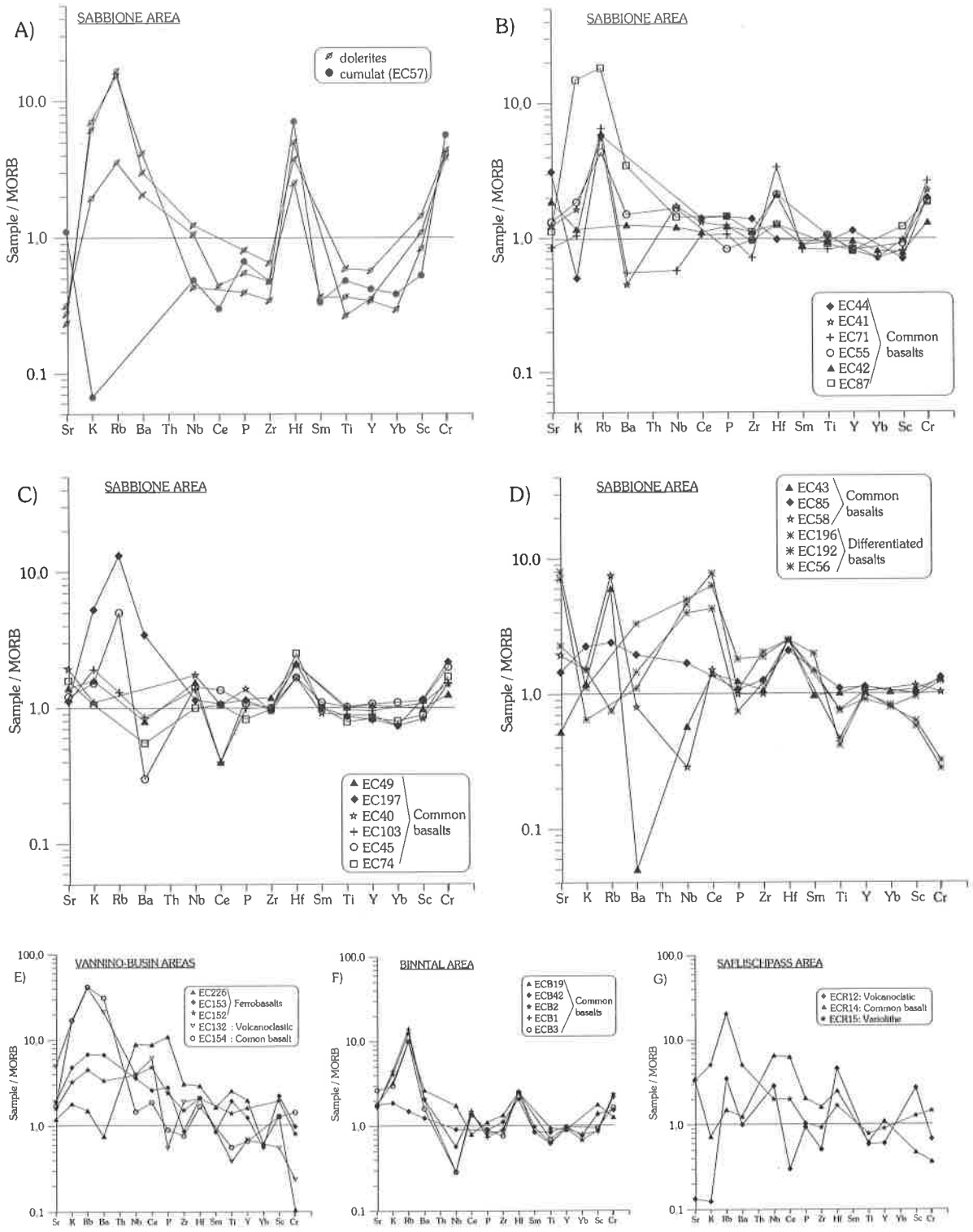


Figure 5.2 MORB normalized trace elements patterns for mafic rocks of the Pizzo del Vallone nappe. Normalization values are after PEARCE 1983, Sc and Cr from PEARCE 1982. In A) are the dolerites and the cumulate, in B) to D) are the common and differentiated basalts, in E) F) and G) are the basalts from respectively the Vannino-Busin area, the Binntal area and the Saflischpass.

The basalts from the Binntal (Fig. 5.2F) have a similar geochemical signature to those of the Sabbione area: the flat profile from Ce to Sc is observable. Nevertheless they may be poorly enriched in Nb; this indicates further fractionation or crustal contamination. The basalts from the Vannino-Busin area (Fig. 5.2E) are all highly enriched in Nb and Ce and to a lesser degree in P and Zr (4 HFSE); this tendency towards E-MORB may suggests a slight plume influence or a greater fractionation for these ferrobasalts. The signature of the basalts of the Saflischpass is transitional between those of the basalts from the Vannino-Busin and the Binntal areas.

### 5.2.4 Rare earth elements

The multi-element diagrams normalised to Rare Earth Elements (REE) (Fig. 5.3A) highlight the following significant points for the green rocks outcropping in the Sabbione area:
- the common basalts (Fig. 5.3) have a rather flat profile from light REE (LREE) to heavy REE (HREE);
- the cumulative basalt EC57 and the dolerite EC200 have the identical flat profile but are depleted in all REE; these two samples have a more primitive composition (less olivine fractionated);
- the differentiated basalts are strongly enriched in LREE, suggesting crustal contamination and/or a more advanced fractionating stage: the Eu negative anomaly specifically favours plagioclase fractionation. EC 196 has a transitional signature between the common and differentiated basalts.

The basalts from the Busin and Binntal areas also have a flat profile from LREE to HREE, although a weak enrichment in La and Ce is detectable. EC132 (volcanoclastic metasediment) and two ferrobasalts of the Busin area (Fig. 5.1A) are enriched in LREE.

The common flat profile from Gd to Lu visible on all patterns implies the absence of residual garnet in the source. Moreover, it suggests a similar magmatic source for all these mafic rocks. For the common basalts of the Sabbione, Binntal and Busin areas, the $(La/Sm)_N$ ratios vary from 0.75 to 1.5. The latter ratio indicates a T-MORB or continental tholeiitic affinity. The LREE enrichments are due to fractional crystallisation and/or to crustal or lithospheric contamination of the magma.

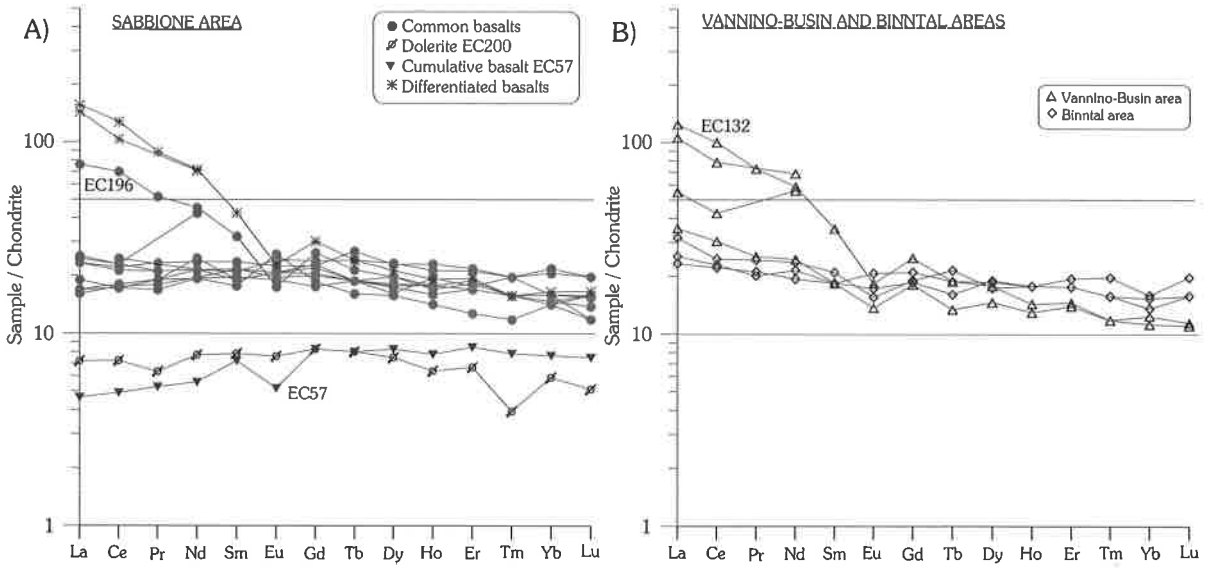


Figure 5.3 Chondrite normalized REE patterns for A) basalts of the Sabbione area, B) the Vannino-Busin and Binntal areas. Normalization values are after SUN & MACDONOUGH (1989).

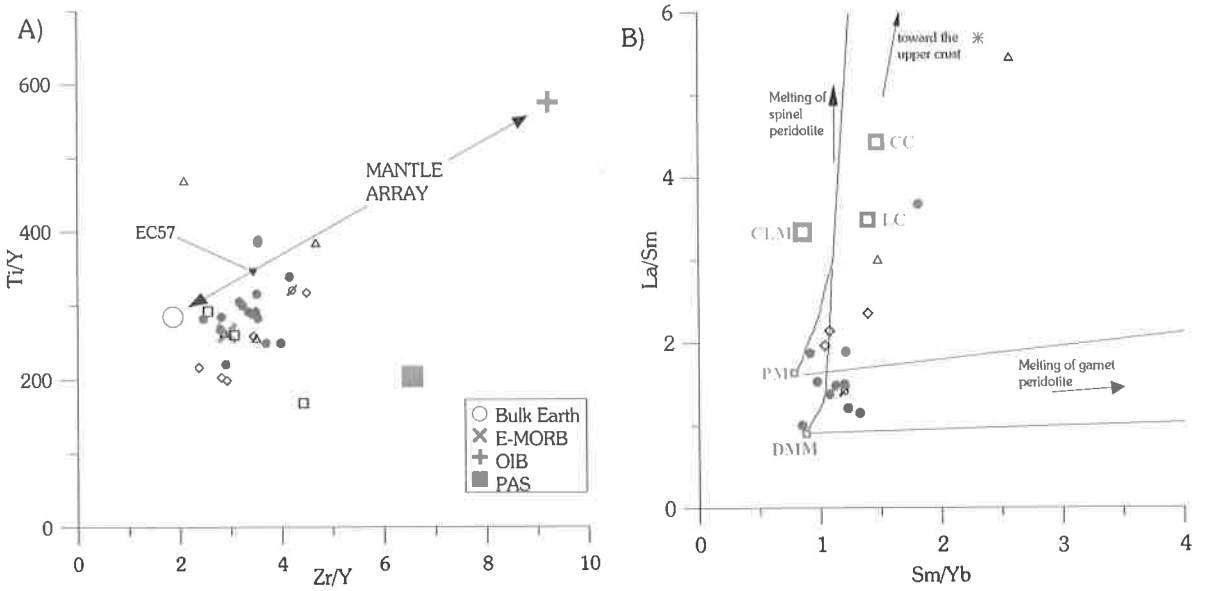


Figure 5.4 A) Diagram proposed by BREWER et al. (1992) which allows the localisation of the sample compared with the Bulk Earth composition, the E-MORB, the Oceanic Island Basalt (OIB) and the Post-Archean Average Shale (PAS), B) Batch melting trends for garnet and spinel peridotite calculated using the partition coefficients, modal abundances and primitive (PM) and depleted (DMM) mantle trace element ratios of MCKENZIE & O'NIONS (1991). Arrows denote the effect of decreasing melt fraction. Median composition of the CLM (MCDONOUGH, 1990), lower (LC), upper (UC) and bulk continental crust (CC) (TAYLOR & MCLENNAN, 1981) are shown for comparison.

In conclusion, the olivine and Ca-clinopyroxene fractionation explains the evolution from dolerites and/or cumulative basalts to the common basalts found everywhere. Further plagioclase fractionation and crustal / lithospheric contamination explain the evolution from the common basalt to the more differentiated basalts. As the investigated rocks belongs to the same cogenetic series, the source is supposed to have a stable signature across the supposed short-time episode of magmatic activity. The common flat profile from Nb to Sc, when normalized to MORB, as well as the common flat profile from La to Lu, when normalized to chondrite, show that the source had a composition close to that of an enriched mantle.

To explain the LREE enrichment, various degrees of fractionation and a second contamination with crustal or lithospheric material enriched in LREE (Fig. 5.4A, 5.4B) are invoked. The evidence for contamination is clear (inherited zircons) but it is not so easy to distinguish whether this contamination was due to interactions of magma directly with the crust or whether the magma was derived from a mantle already contaminated by crustal material, for example during a previous subduction event.

## 5.3 COMPARISON WITH PREVIOUS WORKS DONE IN THE LEPONTINE ALPS

Several authors (PASTORELLI 1994, PASTORELLI et al. 1995, KNILL 1996, BIANCHI et al. 1998 and BIANCHI et al. 2001) have already investigated the green rocks present in the Mesozoic sediments outcropping below the Monte Leone basement gneisses. They obtained geochemical signatures that are identical to those presented here (flat profiles) but their interpretations are different.

PASTORELLI (1994) and PASTORELLI et al. (1995) included in the Monte Leone nappe, the Monte Leone basement gneisses, the ultramafic Geisspfad complex and a Mesozoic sedimentary cover which locally contains basaltic rocks. They interpreted the Geisspfad peridotite as a slice of subcontinental mantle, emplaced at the earth surface during pre-Alpine rifting. This extensional tectonics was accompanied by intrusion of MORB-type magmas along the contact between the mantle and the upper crust (basalts and gabbros) but also in the Mesozoic sedimentary cover (synsedimentary volcanic activity). According to the authors this area underwent evolution as a passive continental margin (active tectonic depositional environment that enhanced the erosion of Triassic beds) of the North Penninic Ocean, in other words the Valais Ocean.

KNILL (1996) analysed the metabasalts intruded in the Mesozoic sedimentary cover in the Binntal, to understand the relations they have with the polymetallic sulfide mineralization, which is well developed in the Triassic dolomitic marble of the Monte Leone nappe. He attributed these Mesozoic basalts to the Triassic epoch (because the Mesozoic amphibolites occur close to or in contact to the mineralised Triassic dolomitic marbles) and interpreted their geochemical signatures as typical of fast spreading ridges. Thus he concluded that the rifting of the North Penninic Ocean started in its western part in Triassic time. Besides, KNILL (1996) assumed that the ophiolites of Visp belong to the Mesozoic cover of the Monte Leone nappe.

For BIANCHI et al. (1998) the Monte Leone cover series is defined by a basal Triassic part (gypsum-anhydrite, dolomitic marbles and local quartzite levels), locally absent, and by a calcschist sequence representing a high energy depositional environment: the mafic bodies are associated with this sequence. They interpreted the chemical analyses as showing a basaltic-tholeiitic trend with a WPB affinity and presumed these basalts to be of Early Jurassic age. BIANCHI et al. (2001) specified that the volcanic activity occurred during Late Triassic – Early Liassic time.

It seems clear that we all agree on one point: the green rocks of the High Val Formazza – Binntal area are either intrusive or extrusive, and linked to a rifting event. However, I do not agree about the age of the magmatic activity, and/or about the rifting event.

The proposition made by KNILL (1996) is highly improbable. Although the basalts intrude the Triassic rocks, this does not necessarily imply that they are Triassic in age; in fact, the basalts also intruded younger levels (paragraph II.3.3, V.2.2, calcschist sequence of BIANCHI et al. 1998). So the occurrence of Mesozoic amphibolites close to or in contact with the mineralised Triassic dolomitic marbles is not an argument in favour of a Triassic magmatic activity, but rather younger than Triassic. The magmatic activity should at least be attributed to the Early Liassic epoch; moreover it is probably younger (II.3.3, II.3.6). Indeed as described in this work, and in Bianchi et al. (1998), the extrusive rocks are found in levels younger than Triassic.

KNILL (1996) and PASTORELLI (1994) postulated this magmatic activity as the result of the North Penninic Ocean rifting. This interpretation is improbable because where it is dated, the volcanic activity of the North Penninic Ocean is older than Triassic (CANNIC 1996, GIROUD & MEILHAC 2002). Where its age is deduced from the stratigraphical study and field investigations, it is attributed either to a pre-Triassic age (GIROUD & MEILHAC 2002) or to the Cretaceous age (ANTOINE 1971, 1972 and LOUBAT 1968). In addition, the field relations show that the basalts of the North Penninic basin are always associated to dark graphitic and siliceous schists, relations never described in the Mesozoic metasediments outcropping below the Monte Leone crystalline basement. The present work associates the green rocks to the Alpine Tethys rifting (or Piemont-Ligurian).

To understand the evolution of the European-Briançonnais margin and to discuss the tectonic and magmatic evolution of the Piemont-Ligurian basin, BIANCHI et al. (2001) investigated four sectors of the Western Alps: the Bourg d'Oisans basin (Dauphine-Alps), the Lepontine domain (south European continental margin, Nufenen-Sabbione area), the southern Italian Cottian Alps (Prepiemontais), and the Versoyen zone (North Penninic basin). However, these areas did not belong to the same rifting event. Moreover, the proposition of a Late Triassic – Early Liassic volcanic activity is highly improbable because the green rocks are not associated to the Triassic dolomitic marble of the Monte Leone nappe, but to the "calcschist sequence" (BIANCHI et al. 1998, paragraph II.3.3, II.7.1, Fig. 2.9).

## 5.4 COMPARISONS WITH BASIC ROCKS RELATED TO INITIAL STAGES OF RIFTING

Over the studied area no true N-MORB has been analysed, and a T-MORB like signature is not characteristic of a single tectonic environment. For instance FIECHTNER et al. (1992), who studied continental tholeiites related to the initial opening of the Atlantic Ocean in the Atlas rift system in Central Morocco, remarked that most of the tholeiitic basalts plot in the field of ocean ridge or sea-floor basalts, even if they are continental tholeiites. So in order to better constrain the paleogeographic position of the Pizzo del Vallone nappe, I have compiled data from different parts of the world related to an initial stage of rifting. The next paragraphs briefly sum up the geological settings of these latter zones.

In eastern Canada, two periods of magmatism are associated with the early Mesozoic continental rifting prior to the opening of the Central Atlantic Ocean (PE-PIPER et al. 1992, Fig. 6.5A, 6.5B). The Anisian to Early Hettangian rifting was accompanied by minor alkalic dykes (Coastal New England (CNE) province), when basins formed by extension and were filled by thick terrigenous clastics and evaporites; the igneous activity was of such a limited extent that it is missing in most places. The Late Hettangian to Bajocian postrifting phase (Eastern North America (ENA) dolerite province) was accompanied by both flows and dykes penetrating up to 400 km landward of the hinge line; the lava flows may locally overlie an angular unconformity. Basalts from the CNE province are mildly alkaline to transitional olivine normative diabase, and the mafic rocks from the ENA province are tholeiitic basalts (most are quartz normative and some are olivine normative). The total volume of observed early Mesozoic magmatic products is small, and was probably emplaced over relatively short time intervals. The next incipient formation of oceanic crust in the Bajocian was marked by local development of thick volcanogenic sequences at the ocean-continent boundary.

In the Prealps, the Gets wildflysch (BILL et al. 1997, 2000) contains remnants or relics of an embryonic oceanic crust of the Alpine Tethys (Fig. 5.5C, 5.5D). The Gets wildflysch with its mafic and ultramafic lenses is an ophiolitic mélange, inferred to come from a proximal part of the accretionary prism at the foot of the active SE margin of the Alpine Tethys Ocean. The chemical features of these two groups are consistent with those of basalts related to the onset of oceanic spreading, an embryonic stage of the opening of the Alpine Thetys.

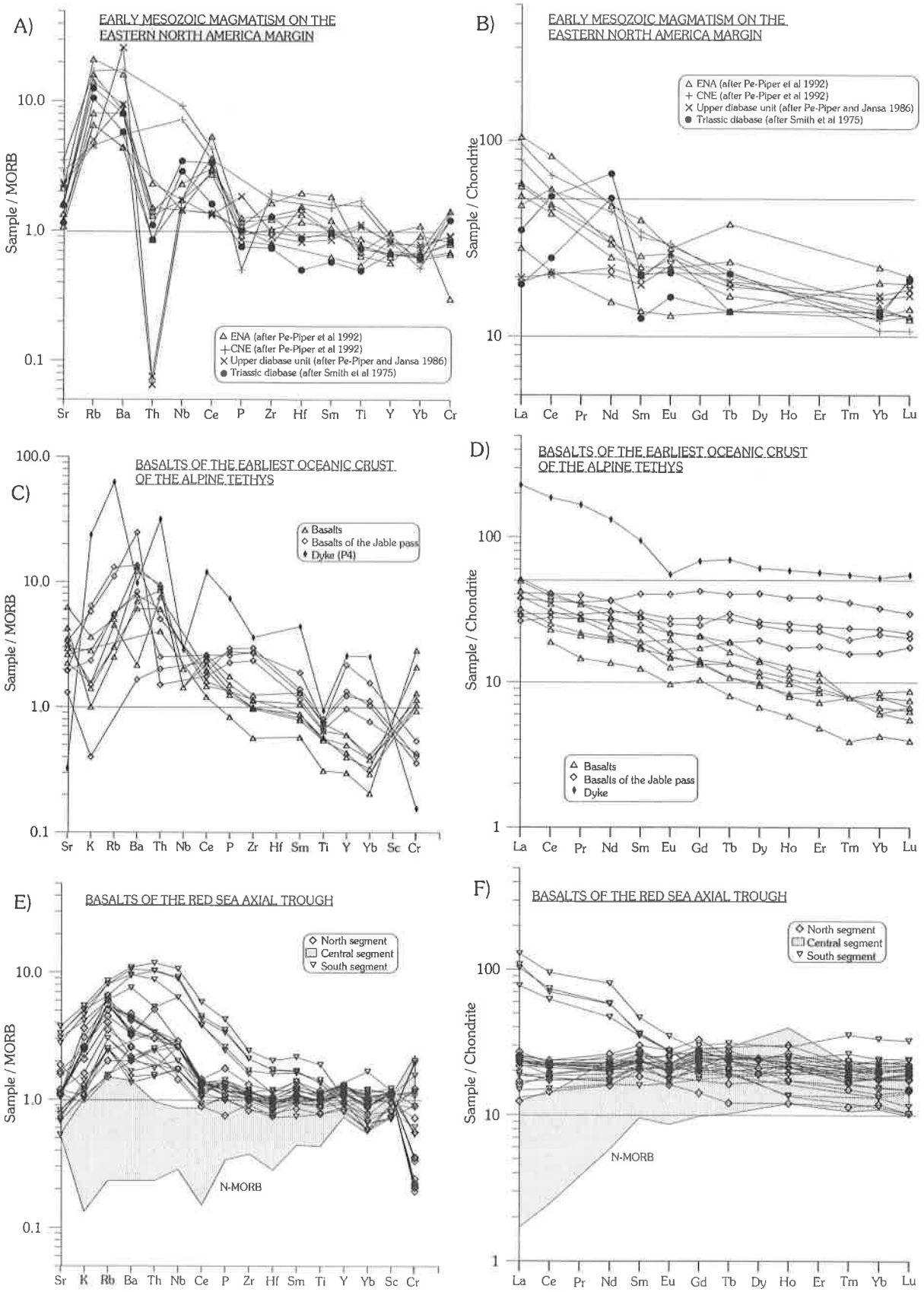


Figure 5.5 MORB (after PEARCE 1983 and 1982) and chondrite (normalization values are after SUN & MACDONOUGH 1989) normalized patterns for the mafic rocks of various regions. A) and B) are for the North America margin (PE-PIPER et al. 1992, PE-PIPER & JANSA 1986, SMITH et al. 1975) C) and D) are for the earliest oceanic crust of the Alpine Tethys (BILL et al. 2001), E) and F) are for the Red Sea axial trough (ALTHERR et al. 1988).

The Red Sea is an embryonic ocean, which offers the chance to study the transition from a continental to an oceanic rift. The Red Sea axial trough magnetic anomalies suggest that sea-floor spreading began in an area around 17°N and from there propagated to the north; presently the northern part has not yet reached the sea-floor spreading stage (Fig. 5.5E, 5.5F). The presence of a large mantle plume affects the chemical composition of basalts from both the central and southern part of the axial trough. It allows N-MORB to crystallise already in the central part, which is most advanced in the transition from a continental to an oceanic crust from a petrological point of view only. Here, only the basalts coming from the northern part of the Red Sea are interesting for a comparison. Because the sea-floor spreading stage in that area as not started yet, basalts tend to be more differentiated than in the central segment and are olivine or quartz normative. After ALTHERR et al. (1988) the variations of the chemical composition, from alkaline to tholeiitic basalts, are caused by different degrees of partial melting within the mantle source, which is heterogeneous on a small scale but homogeneous on a large scale: the increasing degrees of partial melting of the enriched components become more diluted by the depleted components.

The common basalts of the Pizzo del Vallone nappe have a rather flat profile from Ce to Cr when normalized to MORB (Fig. 5.2B, 5.2C, 5.2D, 5.2F), and from Sm to Lu when normalized to chondrite (Fig. 6.3). Such a signature is comparable with the signature of the basalts of the eastern North America margin, the Gets nappe and the northern part of the Red Sea. The multi-element diagrams normalised to MORB (Fig. 5.5A, 5.5C, 5.5E) show that the profile are flat in their second part, but may also display a negative Y and Yb anomaly and/or enrichment in Nb, P, Zr (and Hf) suggesting a crustal contamination. The enrichment in Sr, K, Rb and Ba may be linked to crustal contamination but also to their high mobility under various alterations episodes. The pattern of the curves suggests an overall T-MORB affinity.

The REE chondrite-normalized patterns show that most of the samples have a first flat to steady-decreasing LREE spectrum, and a second flat HREE spectrum: the normalized values are between 10 and 50 (Fig. 5.3, 5.5B, 5.5D, 5.5F). Some basalts have a particularly strong LREE enrichment suggesting crustal contamination, and some basalts of the Gets nappe have a low HREE content suggesting the presence of residual garnet in the source and/or a small degree of partial melting. The Nd positive anomaly associated to the Sm negative anomaly is in favour of orthopyroxene crystallization. The basalts are T-MORB-like basalts, which underwent a more or less great degree of partial melting.

## 5.5 DISCUSSION

The green rocks of the Pizzo del Vallone nappe have a geochemical signature similar to the geochemical signature of syn-rift basalts. They are basaltic tholeiites evolving into andesite-basaltic tholeiites, which have a T-MORB-like affinity. Many chemical details can be related to variations in the percentage of olivine, clinopyroxene and plagioclase fractionation, and/or to variations in the percentage of contamination (either within the continental crust or within inhomogeneous subcontinental lithospheric mantle, DUNCAN 1987, DUPUY et al. 1988). Here it is difficult to determine in what degree the geochemical composition variability represent variations in fractionation, in crustal contamination or in partial melting, because the chemical composition of the magmatic minerals is unknown.

The stratigraphic records are consistent with active tectonic extensional rifting. In fact, the Sabbione metasandstone (paragraph II.3.3) that contains principally Triassic pebbles recorded an extensional event and was deposited before and during the magmatic activity. The total amount of magmatic rocks is low, localized for its major part in the Sabbione area, and probably

emplaced over a short time interval. PE-PIPER et al. (1992) mentioned the same characteristics for the Mesozoic magmatic products on the eastern Canadian margin; SMITH et al. (1975) added that dykes might extend several kilometres into the subsiding basins, and are most commonly between 60 and 600 metres long and no thicker than about tens of meters. Generally, they are approximately conformable to the bedding and are finer grained towards the borders. Sometimes thick basalt flows may overlay the dykes and sills. These descriptions are concordant with the observations made for the Pizzo del Vallone nappe. Indeed the shapes of the basaltic outcrops vary from Busin to the Binntal, likely depending on the orientation of the basaltic bodies relative to the topography, and according to the alpine deformations. Moreover, the presence of an upper volcanogenic level is also concordant (although not exclusive) with the onset of oceanic spreading (PE-PIPER et al. 1992).

The geochemical signature of the green rocks and the stratigraphic records favour a rifted margin (CARRUPT et al. 2002). Indeed the association of detrital levels (mainly the Sabbione sandstone) with magmatic rocks having a T-MORB-like signature can be easily explained, invoking an active extensional tectonic event associated with a magmatic event. Moreover, the presence of a basal Triassic level in the Pizzo del Vallone nappe suggests that the nappe originated from a continental crust (paragraph II.3); this fact associated with the absence of ultrabasic rocks prove that the studied magmatic bodies do not represent an ophiolitic sequence. The results of the geochemistry associated to field observations show that the mafic rocks evolve first by mineral fractionation and then in a lesser way by crustal contamination. The presence of pillow specifies the submerged nature of the environment of extrusion, and the final volcanoclastic sequence interbedded with the upper part of the Sabbione metasandstone are in favour of a shallow water depth.

# 6 TECTONICS

## 6.1 INTRODUCTION

The aim of this chapter is to describe the successive phases of deformation that affected the area, in order to determine the successive positions of the nappes through time. The tectonics results are not the only elements considered; the stratigraphical results (paragraph II.7.3, II.8) allows the evolution across time of the area to be determined rather precisely.

## 6.2 METHODOLOGY

The tectonics results proceed from the systematic measurement on the field of the stratification S0, schistosities, the axial surfaces, the fold axes, the various lineations (Fig. 6.2, 6.3) and from the study of superposed folds (Fig. 6.1, 6.4). The construction of cross-sections (Fig. 6.5) allows to better understand the succession of deformations (Fig. 6.6), as well as to correlate the small to large structures, and in order to discover a possible cause for them. However some investigated folds were impossible to associate to a precise deformation. Indeed the characteristics of the deformations are sometimes similar because they were all reoriented by the younger deformations, and thus, in the absence of superposed folds, some folds become indistinguishable. Moreover transitional stage most likely existed between the successive deformations.

A late fracturing is visible over the entire area, but it will not be discussed here even if it is responsible for some present instabilities; it can be related to the continuing Alpine deformation.

## 6.3 RESULTS

The orientation of the stratification S0 varies greatly over the area (Fig. 6.2, 6.5, 6.7, 6.8, Annexe 6A, 6B), clearly showing that this region has been refolded several times.

### 6.3.1 First deformation D1:

This deformation is the oldest recognized phase. Neither schistosity nor folds can be associated to it. On the field it is recognizable through the presence, over the whole area and in all lithologies, of elongated eyes of quartz or discontinuous quartz veins parallel to the stratification (LISKAY 1965, DELEZE 1999). They are folded by the following deformation, and thus recorded good superposed folds (Fig. 6.1).

### 6.3.2 Second deformation D2:

Centimetre to decimetre isoclinal to closed synschistose (S2) folds characterise the deformation D2. S2 is parallel to S0 apart from those close to the fold hinges. But, as few hinges remain recognizable, most of the time due to the refolded eyes of quartz, it is not easy to determine if a lineation is associated to this deformation. The axes A2 and the axial surfaces SA2 were reoriented by the following deformations (Fig. 6.2 S2, 6.3 A2). I identified this deformation mainly in the Pizzo del Vallone nappe and in the Holzerspitz series in the Sabbione area. A lot of structures are understandable in this area because it represents a tectonic knot.

### 6.3.3 Third (main) deformation D3:

This deformation is characterised by synschistose (S3) isoclinal to tight folds (Fig. 6.2 S3, 6.3 A3). The shape varies according to the competency of the lithology. The associated mineral lineation L3 is underlined by phyllosilicates, quartz, amphiboles (hornblende) and calcite depending on the rock chemistry. The fold size varies from centimetres to decametres. Except for obviously those close to the hinges, the schistosity S3 is parallel to the stratification. Thin levels of graphite underlined mostly S3. This deformation is the main one, and it is recorded over the whole area.

### 6.3.4 Fourth (crenulative) deformation D4:

The folds coeval to this deformation are similar and accompanied by a crenulative schistosity S4, penetrative in the sediments but rough in metabasalts and gneisses (Fig. 6.2 S4, 6.3 A4). A lineation of intersection with S3 and S0 is often visible but a mineral lineation L4, underlined by phyllosilicates, is rarely observable, except in the micaschists. The size varies from decimetres to hectometres. Sometimes the folds are limited, at their base, by a thrust plane. The dip and dip direction of axial surfaces and axes are similar to those of D2; the differentiation between the folds F3 and F4 is only possible on the field, and is easier where superposed folds are observable (Fig. 6.4). The folds are similar but also submitted to a weak flexure slip detectable when analysing the behaviour of the principal lineation L3 (Fig. 6.1C): for instance: SA4=308/70 \ A4=65→256 with L3=100/54 \ 060/24 \ 040/70 \ 072/16 remaining in the plane: 154/80, and so a=068/24 (a is the direction of tectonic transport, MCCLAY 1987).

These four deformations developed during the "procharriage"; thus the following deformations recorded the "retrochariage" history (backfolding). The amphibolite thermal metamorphism (TODD & ENGI 1997, this work) is coeval to- and postdates the deformations D4 (Tab. 3.3, 3.4, 3.5).

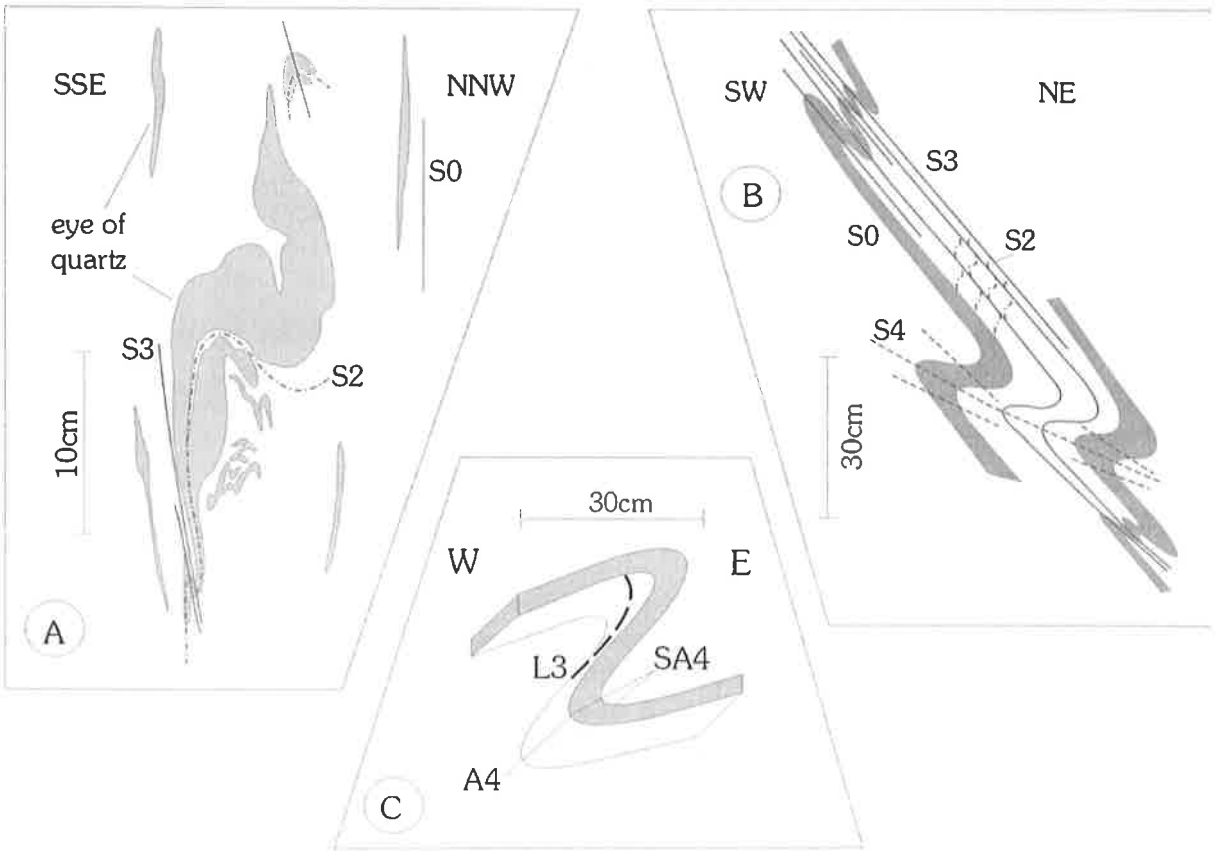


Figure 6.1 Superposed folds: A) in garnet micaschist (Holzerspitz series, 670'465/141'880), B) in alternations of calcitic marble and quartzite (Camosci nappe, 668'820/141'629), C) L3 folded by D4 (Camosci nappe, 671220/142620).

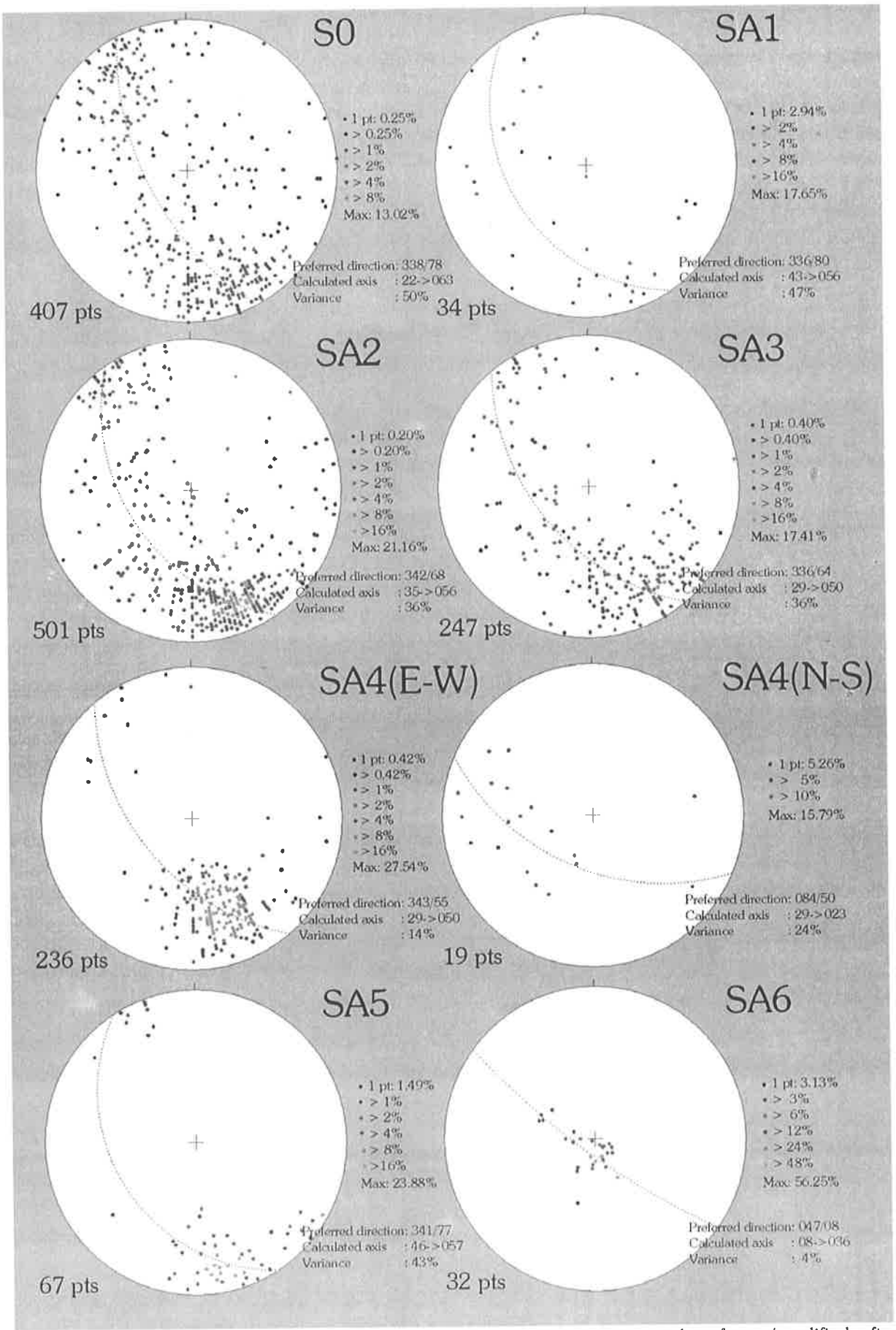


Figure 6.2 Stereographic projection of the stratigraphy and the various axial surfaces (modified after GEOrient 8.0, HOLDCOMBE 2001, http://www.earthsciences.uq.edu.au/~rodh/index.html).

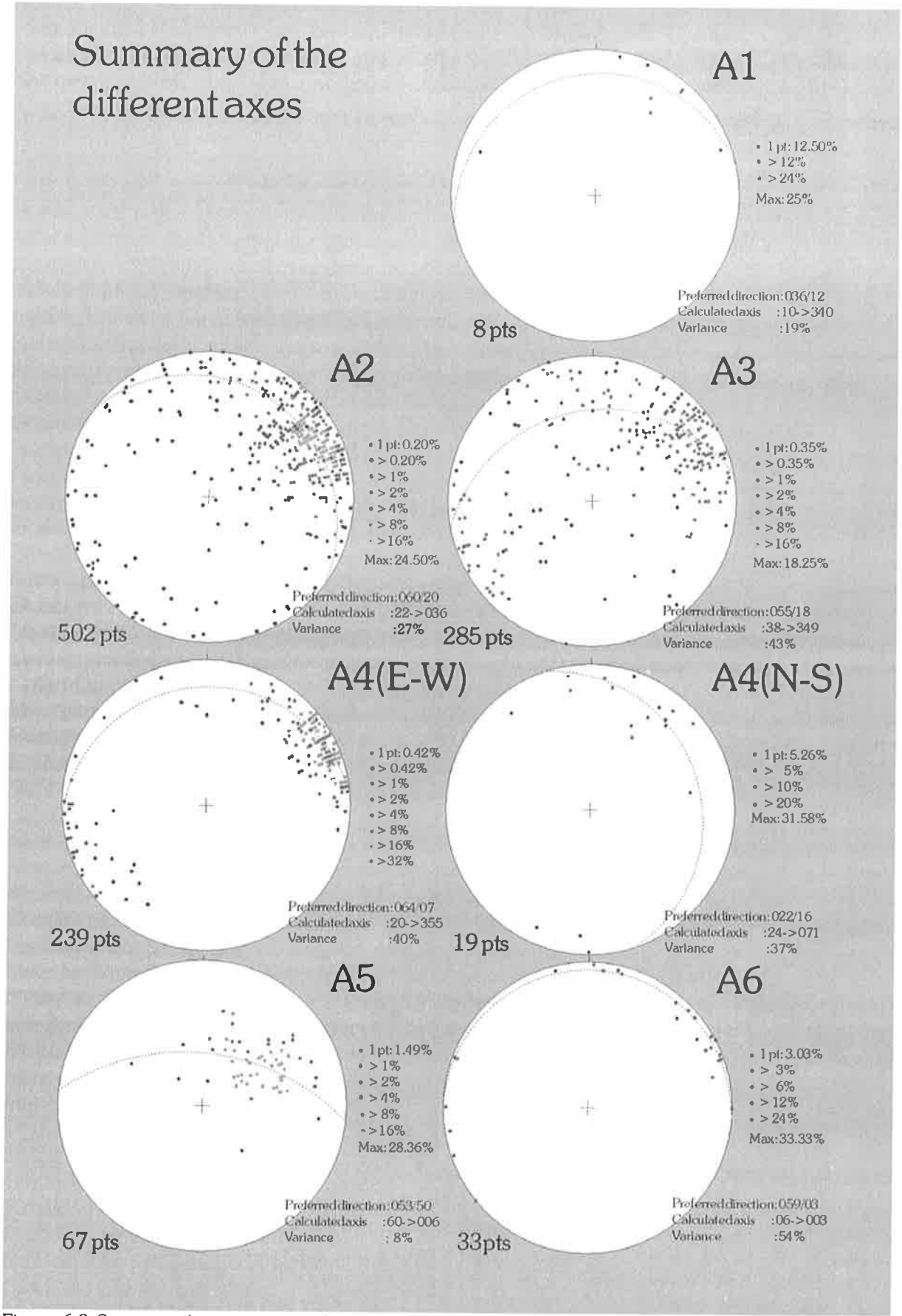


Figure 6.3 Stereographic projection of the lineations and the various axes (modified after GEOrient 8.0, HOLDCOMBE 2001, http://www.earthsciences.uq.edu.au/~rodh/index.html).

### 6.3.5 Fifth (backfolding) deformation D5:

The backfolds are similar to concentric (depending on the lithology the interlimb angle α varies from 35° to 75°) and can be considered as cylindrical at a local scale (Fig. 6.2 S5, 6.3 A5). Their sizes vary from decimetres to hectometres. Field measurements indicate that these folds were created under similar folding because the recumbent lineation L3 remains in a plane (for instance: SA5=110/52 and A5=30→060 with L3=052/08 \ 070/02 \ 100/04 remain in the plane: 075/04, and so a=146/02; McCLAY 1987). No schistosity is coeval with this phase except in the more schistose rocks. Rare fibres of chlorites, crystallising in the metabasalts or retromorphosing some biotites or amphiboles in various lithologies, marked the beginning of the retromorphosis history. This deformation postdates the peak of metamorphism and strongly reorients all the previous structures (Fig. 6.2, 6.3).

These backfolds are visible everywhere, but particularly in the Binntal where plurihectometric folds are easily seen in the landscape thanks to the presence of white dolomitic marbles. Another hectometric fold F5 is also clearly observable from the south, in the Corno di Nefelgiù. The orientations of the axes and axial surfaces (Fig. 6.2 S5(N-S), 6.3 A5(N-S)) are very different than those of the backfolds in the Binntal, Toggia or Sabbione areas (Fig. 6.2 S5(E-W), 6.3 A5(E-W)). The structural study near the lago di Morasco clearly shows that they are backfolds F5 (Fig. 6.7) reoriented by the deformation D6. Excepted in the Nefelgiù area, the folds have a south-vergence. The study of the regional deformation allows the correlation of this phase with the Berisal syncline active after 12 My (STECK & HUNZIKER 1994 and STECK et al. 2001).

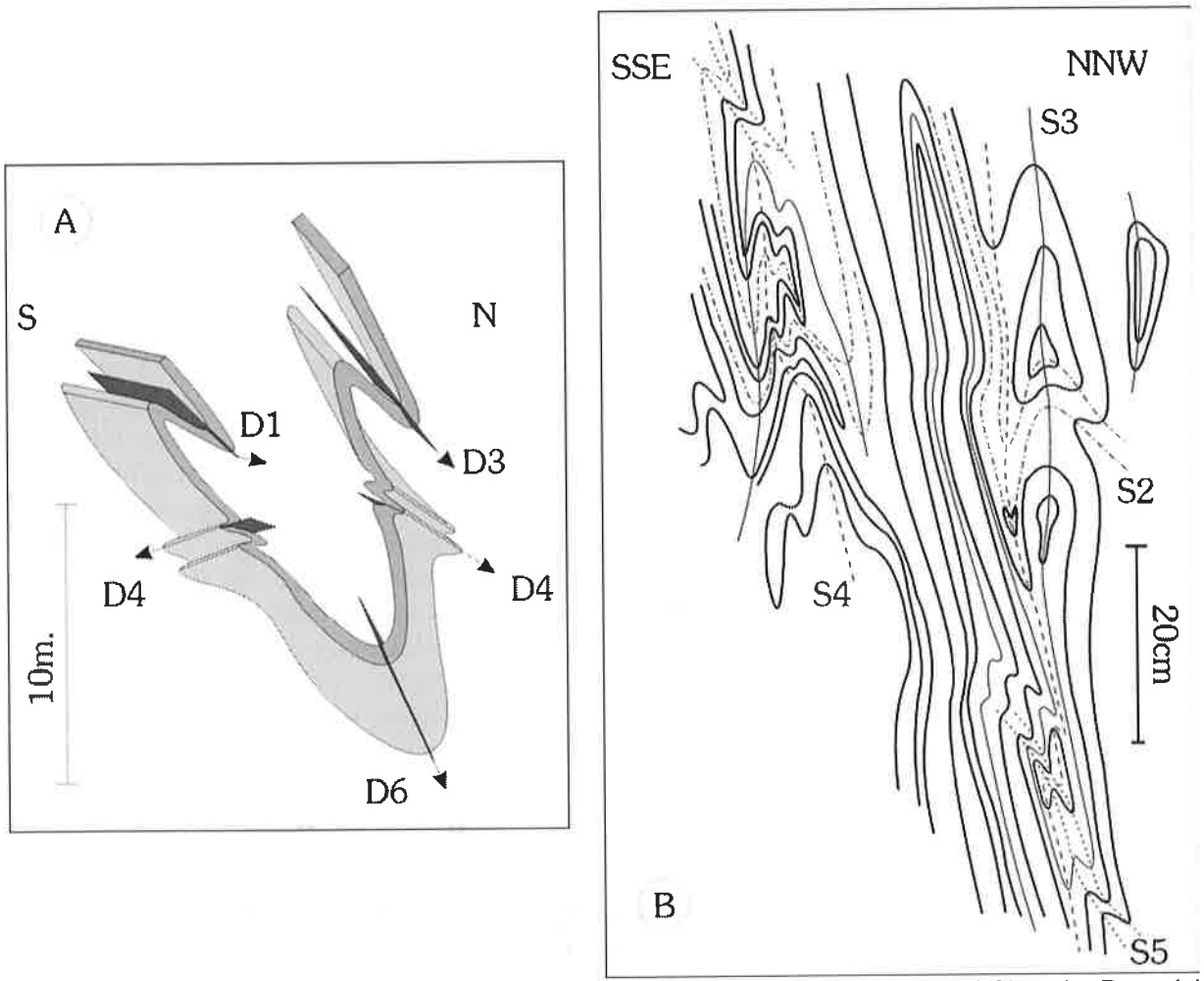


Figure 6.4 Superposed folds found: A) in the Holerspitz series (671'030/138'800) and B) in the Pizzo del Vallone nappe (670'800/140'430).

### 6.3.6 Sixth (shearing) deformation D6:

This deformation is a large dextral shearing phase understandable when following the axial trace of the backfolds (Fig. 6.7A). The induced folds are open to closed, and moderately to steeply sloped (Fig. 6.2 S6, 6.3 A6). A weak schistosity is associated when the folds developed in schistose rocks. These folds are especially well observable in the Morasco area, and in a lesser way along the Nefelgiù valley and around the Corno di Ban. The parameters of the deformation change, obviously due to the different orientations (RAMSAY 1967) of the stratification (especially due to the backfolds) before the shear acted. The complementary part of this shearing zone should be found just southward or southeastward of the investigated area, where the stratification becomes steeper, or in the Wandfluhorn area (HUNZIKER 1966).

### 6.3.7 The late deformation D7

This late ductile deformation D7 is a sort of collapse that marks the end of the retrocharriage. The axes and axial surfaces are subhorizontal and the opening angle $\alpha$ is around 150°. So the only effect of these decametric folds is to gently reorient the stratification and the axial surfaces of the preceding deformations.

### 6.3.8 Brittle dextral transform faults

Two dextral transform faults exist in the north of the area; they extend from the Gries Valley towards the Blinnenhorn (Annexe 6B): they are called the **Rio del Sabbione** strike slip faults. It is most likely a fault that ends eastward in a horse tail type zone. They are easy to follow on the map thanks to the stratigraphical study and the geological mapping, but they outcrop in few places. The very low number of observations (4) does not permit the rotational component to be determined but of course one does exist. The measurements are follows: F=338/88, f=24→068, south up \ F=342/76, f=02→070, south up \ F=348/68, f=10→071, south up \ F=350/76, f=06→082, south up / with F=fault and f=fiber.

### 6.3.9 Different natures of tectonic contact

Three different tectonic contacts were found over the area:

- underlined by cornieule: the Monte Leone - Pizzo del Vallone thrust as well as the Camosci - Rosswald thrust can be followed because of the presence of Mesozoic cornieule representing the oldest level of the Pizzo del Vallone and Camosci nappes respectively. These thrust planes were most likely to be the place where the main movements occurred, certainly several times and in various directions during history;
- underlined by a transform fault: the Holzerspitz – Camosci tectonic contact is essentially due to the Rio del Sabbione strike slip faults. The latter continue and are responsible westward for the Rosswald – Holzerspitz and Rosswald – Pizzo del Vallone tectonic contacts, and eastward for the Pizzo del Vallone – Camosci tectonic contact (Annexe 6.B). They then disappear eastward within the Lebendun nappe;
- nothing special: the shorter mapped thrust is the Antigorio – Lebendun thrust. However on the field the latter is not recognizable: indeed all seem to conform, and could be in stratigraphic continuity. So this thrust was placed simply to agree with previous works, centred on this contact (DELLA TORRE 1995, SPRING et al. 1992).

### 6.3.10 Remark

Around the Punta Lebendun, the Hohsandhorn and the Holzerspitz, old faults outcrop (Fig. 6.5, Annexe 6.B). They are refolded but recognizable thanks to the non-symmetrical splitting of the stratigraphical succession, and the displacement of the basement against the cover. They probably represent small-scale synthetic or antithetic faults that developed within the already differentiated tilted-blocks coeval to the Alpine Tethys rifting (Paragraph 7.4).

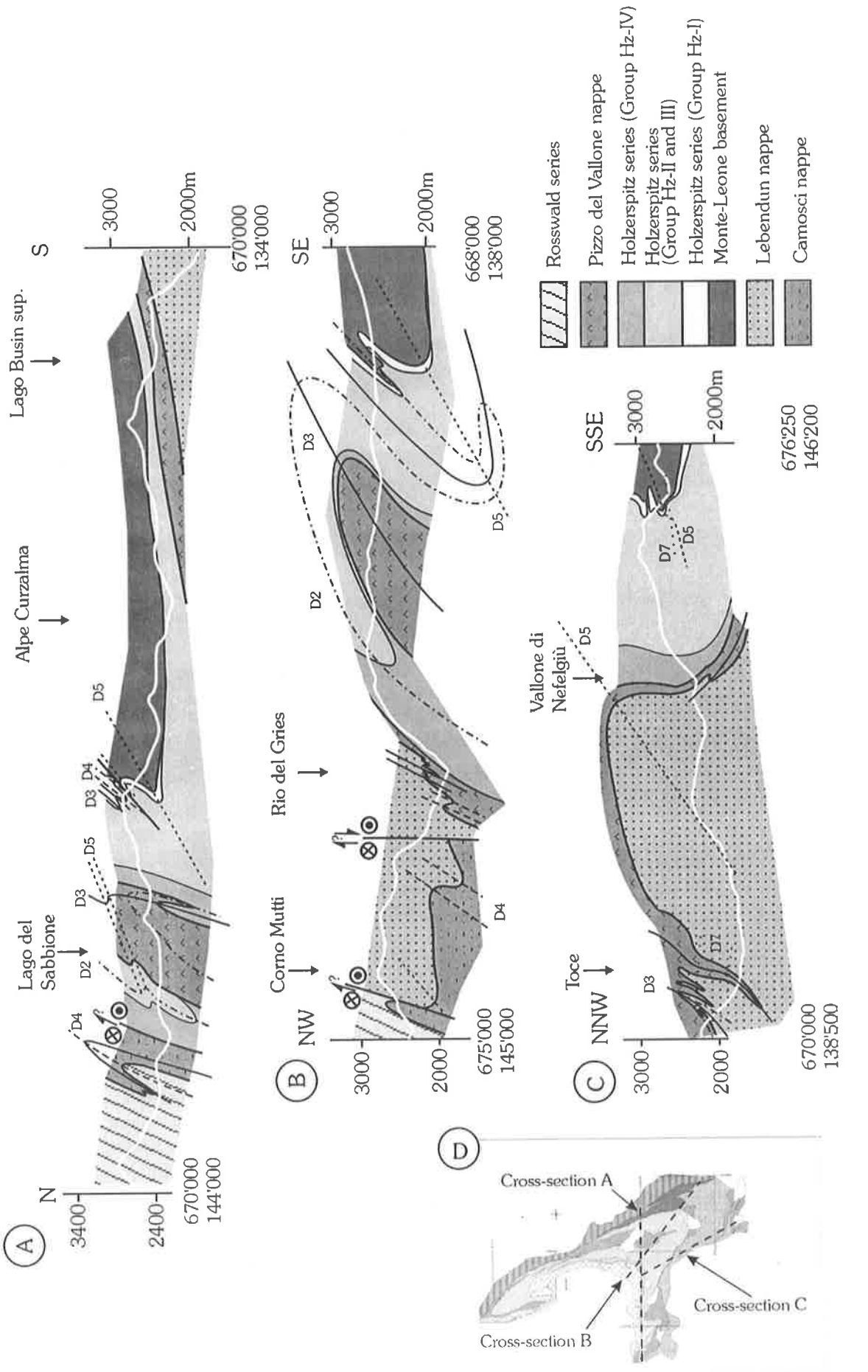


Figure 6.5 A), B) and C) Differently oriented cross-sections, D) location of the cross-sections.

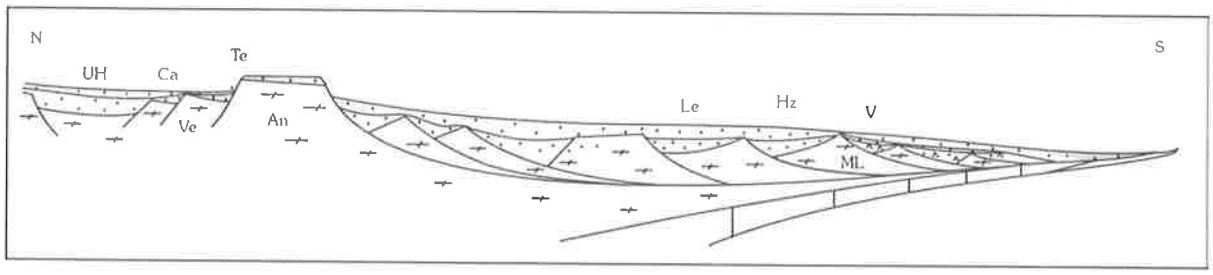


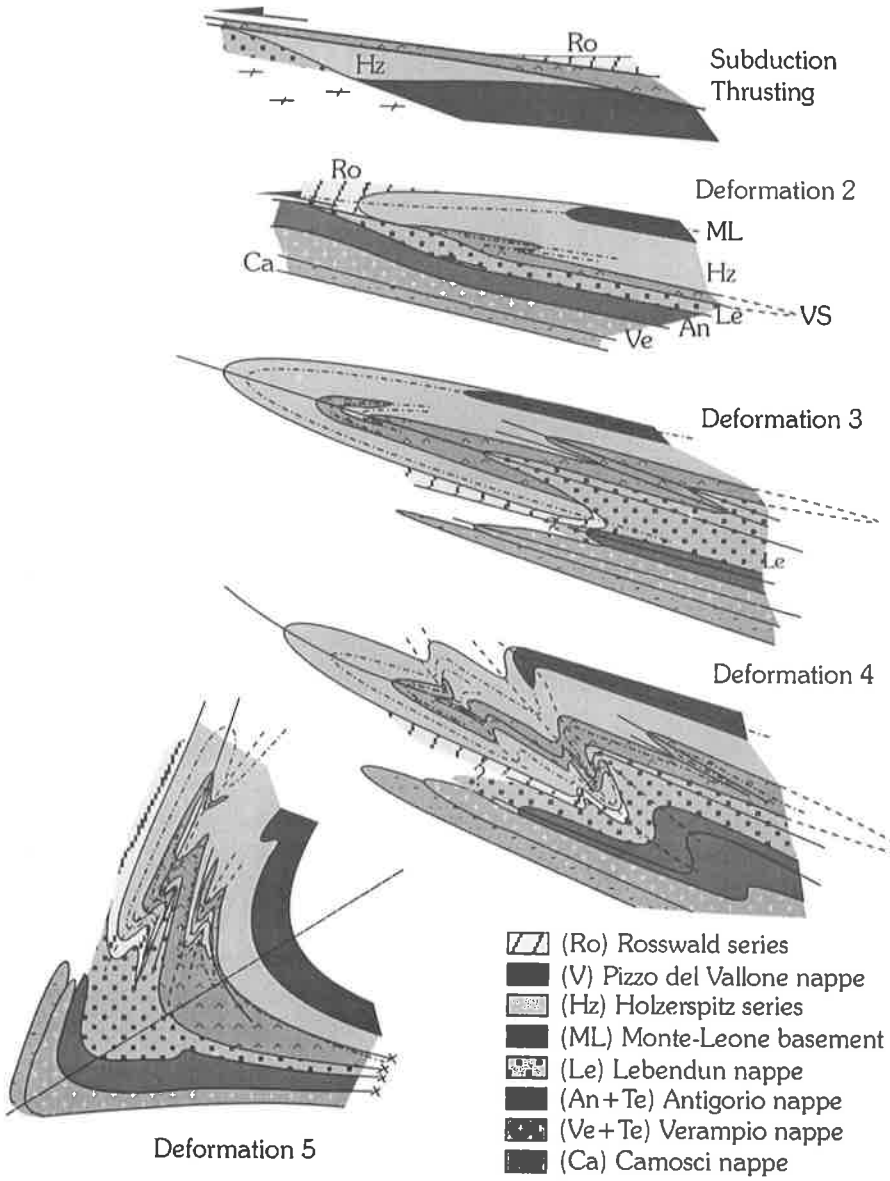


Figure 6.6 Proposed schematic evolution of the area based on field observations (not to scale; UH: ultrahelvetic covers). The paleogeographic interpretation is explained in paragraph 7.2.

## 6.4 DISCUSSION

The Pizzo del Vallone nappe is of more internal origin than the Monte Leone nappe (that is to say this cover deposited south of the Monte Leone cover) even though the Pizzo del Vallone nappe outcrops now below the Monte Leone nappe (Fig. 6.9). When drawing the successive deformations (Fig. 6.6), it appears that the tectonic results associated to the stratigraphical constraints give a coherent history.

No relics of the eoalpine stage were found in this region. The oldest deformations still recorded are contemporaneous of the initial stages of procharriage that is to say the mesoalpine phase. The procharriage happened in four successive stages (D1, D2, D3 and D4) that developed under shearing deformations.

The neoalpine phase began with the backfolding D5, well marked in the landscape especially by big folds. On a regional map (Fig. 1.2) the axial surface trace of this fold 12-11 My old (STECK & HUNZIKER 1994) can be easily followed from the Berisal area to the Lago del Sabbione. This trace then curves due to the arriving deformations resulting from the dextral shear zone D6 that strongly reorients all the previous structure in the eastern part of the studied area (Annexe 6B). Indeed the N-S orientations of axes and of the stratigraphy S0 in the Nefelgiù-Vannino area are results from it. This shear zone represents an initial complication in the correlation between the western and eastern part of the Central Alps, and it is likely that other(s) shear zone(s) also exist(s).

STECK (1984) mentioned that the Wandfluhhorn antiform refolded the main alpine schistosity, and developed after the metamorphism culmination, and that it is likely to be contemporaneous of an early backfolding. So this fold has probably formed before the deformation D5. It would be interesting to study the field relations between D4, D5 and the Wandfluhhorn antiform.

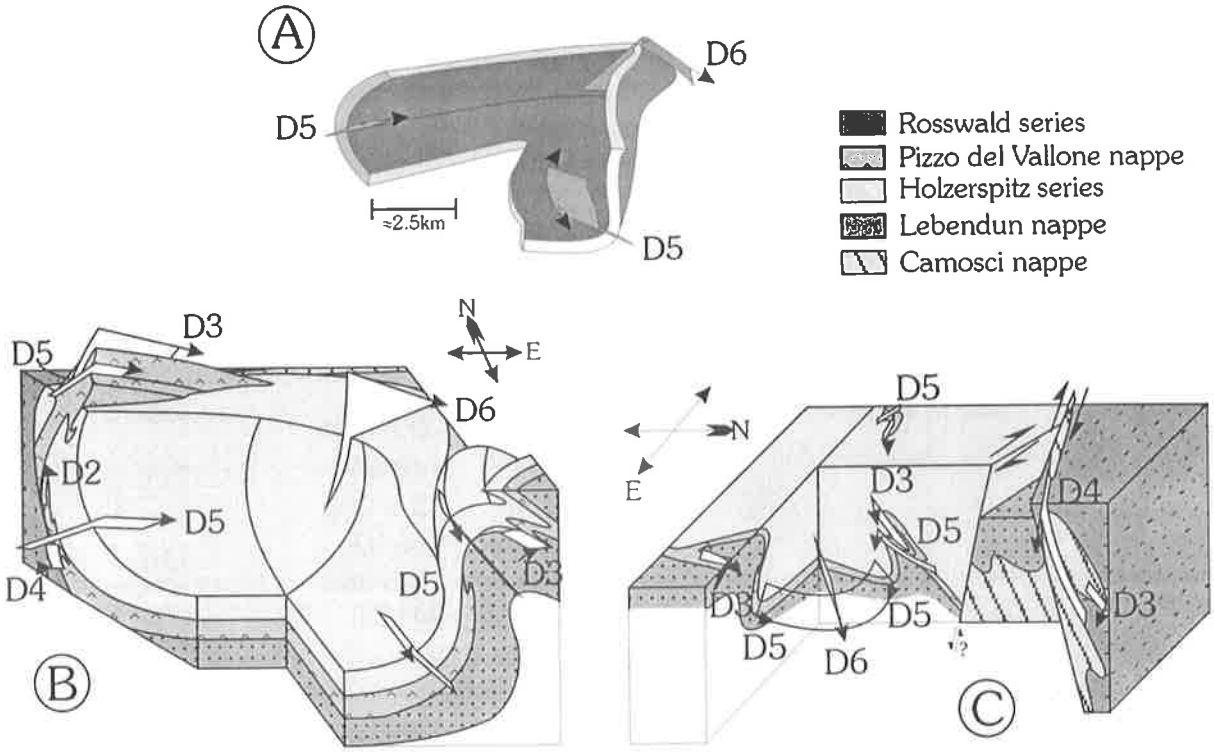


Figure 6.7 3D diagram for the area (not to scale): A) schematic sketch of the refolded backfold D5, B) area viewed from southwest, C) area viewed from east.

The dextral rio del Sabbione faults D7 are clearly visible in the valle del Gries where triple points are noticeable. The terminal collapse D7 is difficult to place, but it is probable that it acted before but also after the dextral shear zone D6. In conclusion it appears that the main dextral shear zones of the central Alps acted quite far away from the mapped area, but even so the dextral constraint affected the entire Lepontine dome, because they surround it.

To conclude the structural history, the consistency between the observations and the interpretations was tested. To do so, firstly, I constructed, a hand-made history to highlight the observed heterogeneities (Fig. 6.6), and then a second succession was calculated by a computer program (REY 2001) to see if the anticipated structures really were plausible (Fig. 6.8). Indeed it is not easy to draw three or more phases of folding manually and in addition the result is not guaranteed. Strictly speaking, the calculated block-diagram (Fig. 6.8) will not represent reality, but reflects the observed geometry. To have an idea of the approximate values of the axial surfaces and axes of the D5 and D4 deformation I successively unfolded the zone and recalculated the values by approximating the deformation; they were supposed to be similar. As D4 is similar to isoclinal, it is unfortunately impossible to calculate an approximation of the original values of the D3 and D2 deformations; this is why I used the statistical values calculated by GEOrient 8.0 when doing the stereographic projections (Fig. 6.2, 6.3; http://www.earthsciences.uq.edu.au/~rodh/index.html). The calculated values provided to the computer are as follows: SA5: 345/40, A5: 04→070, SA4: 150/52, A4: 11→065. The result is that both reconstructions are coherent, but above all they are also consistent with the constructed cross-sections (Fig. 6.5), 3D-diagram (Fig. 6.7), and the observed superposed folds (Fig. 6.1, 6.4). The geometry is similar and the vergences are coherent.

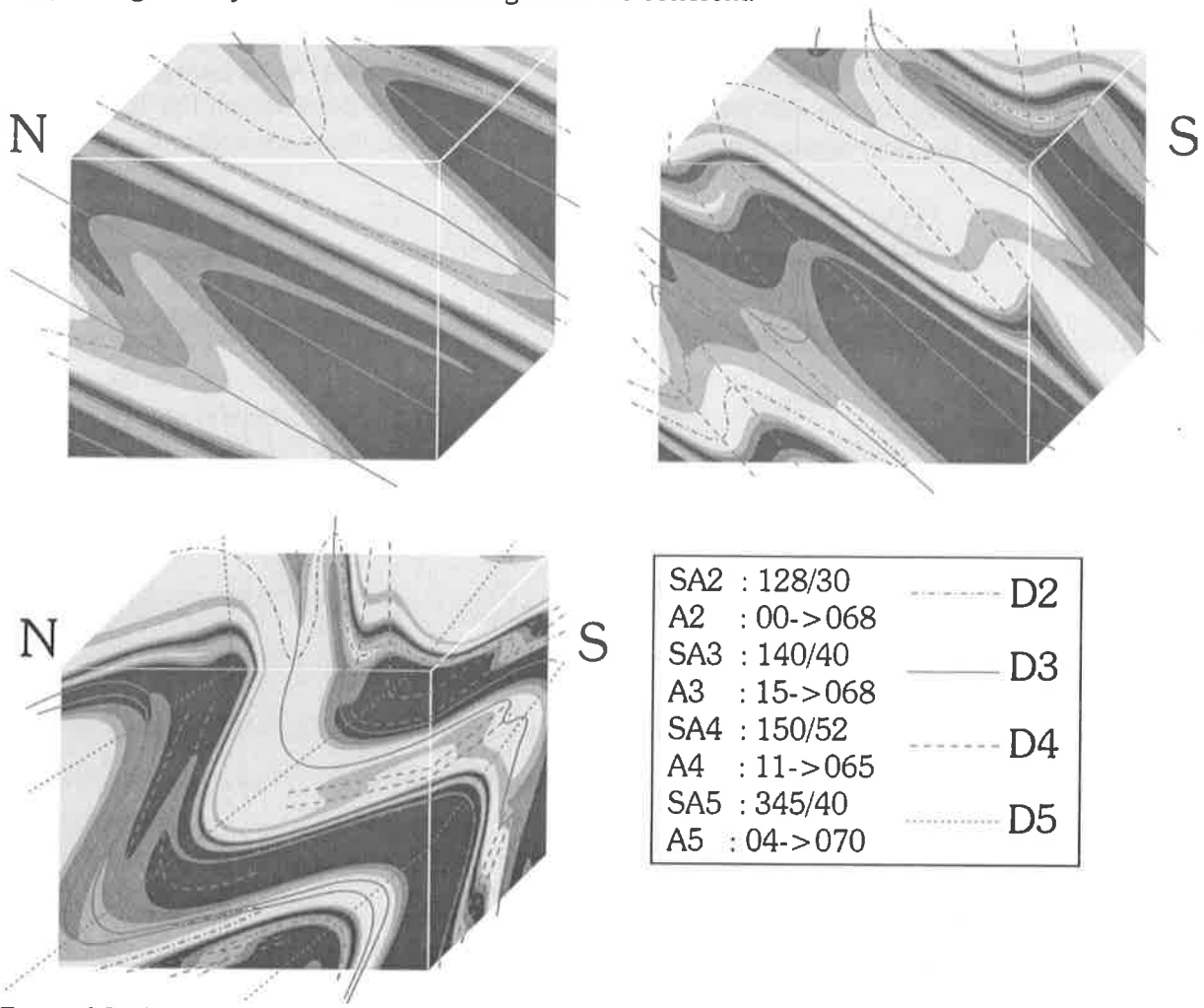


Figure 6.8 Bloc diagram calculated by a computer program (Shear2F, REY 2001) with the localisation of the various axial traces.

## 6.5 Remark about the Pizzo del Vallone nappe

The Pizzo del Vallone nappe lies below the Holzerspitz series in an inverted position. In the Binntal and Sabbione areas its inverted flanks does not completely outcrop because either the erosion is not advanced enough or late tectonic discontinuities hide the primary links. The relations between the Lebendun and Pizzo del Vallone nappes, however, are observable from the Busin area up to the Castel region: the Pizzo del Vallone nappe lies in a normal position above the Lebendun nappe. Moreover when following the Pizzo del Vallone – Lebendun thrust it seems clear that the levels of the Pizzo del Vallone nappe are faintly discordant with the thrust (Fig. 6.9), suggesting a synclinal closure southward.

The structural and stratigraphical relations suggest a more external position for the Lebendun and Monte Leone nappes relative to the Pizzo del Vallone nappe. To explain such relations, the latter must have initially overthrust the Holzerspitz series and then the southern part of the Lebendun cover (Fig. 6.6), before being folded several times.

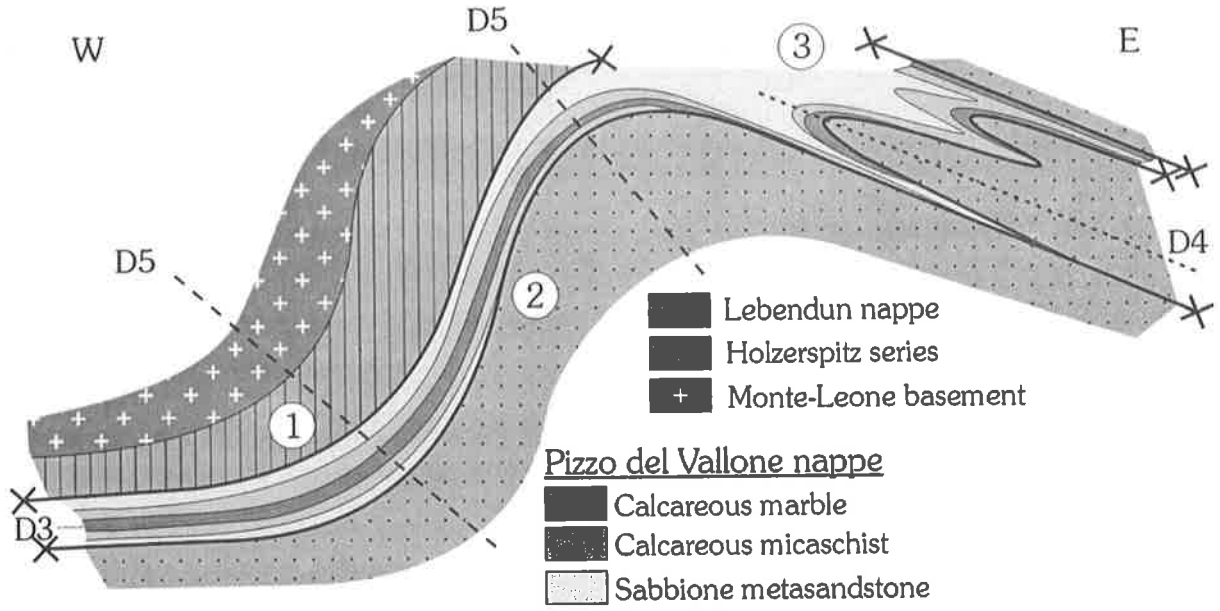


Figure: 6.9 Synthetic E-W cross-section of the eastern part of the studied area. The thickness of the levels is exaggerated in order to highlight the structural relations. 1 represents the Busin area, 2 the Nefelgiù area and 3 the Castel area.

# 7 DISCUSSION - CONCLUSION

## 7.1 SUMMARY OF THE MAIN RESULTS

This chapter will focus on the principal conclusions obtained from the stratigraphic (lithostratigraphic description and chronostratigraphic interpretation), the metamorphic (P-T values reached at the end of the Lepontine metamorphism), the geochemical (type of volcanism) and the structural (Alpine deformations) studies.

### 7.1.1 Stratigraphic and geochemical studies

The Pizzo del Vallone nappe is a newly defined nappe. It consists of a Mesozoic series (Fig. 2.2) completely separated from its pre-Triassic basement. The lithostratigraphic section is characteristic of the typical succession described on tilted blocks adjoining an axial rift valley. The green rocks are continental tholeiites, which have a T-MORB like signature; they are variously enriched in LREE (Fig. 4.3A+B).

The Monte Leone Mesozoic to Tertiary cover, called the Holzerspitz series, is characterized by important lateral variations of facies (Fig. 2.1). The basal quartzite is in favour of the autochthony of the Holzerspitz series in relation to the Monte Leone crystalline basement. However, the Triassic levels (Group Hz-I, Fig. 2.1) are atypical: they have a transitional signature between the common Triassic levels of the Helvetic s.l. realm (EPARD 1990) and of the Briançonnais platform (BAUD & SEPTFONTAINE 1979, JAILLARD et al. 1986) or even of the Austro-alpine domain (DRUCKMAN et al. 1982, CONTI et al. 1994, VENTURINI et al. 1994). Several discontinuous detritic levels containing mainly dolomitic pebbles reveal (Fig. 2.1) that this cover was deposited in a high-energy environment, crosscut by rivers and affected by extensional tectonics.

The lithostratigraphy of the Lebendun nappe shows the most striking differences when compared to the other nappes (Fig. 7.1). Thus it is not surprising that it created great controversies between authors during the XXth century (paragraph I.3). Even if the major part of this nappe simulates a granite or an orthogneiss, it is in fact a Mesozoic detrital stacking miming a Paleozoic basement (RODGERS & BEARTH 1960, Fig. 2.5). Active normal faults continuously creating space allowed the deposition of such a thick and very coarse detrital sequence. Thanks to the presence of very rare calcareous debris flow, the whole series can be consistently interpreted as a fan.

The Teggiolo zone also varies laterally (Fig. 2.7). But in contrast to the Holzerspitz series, or the Pizzo del Vallone nappe, it contains fewer conglomeratic layers; the latter are dominated by the quartzitic and gneissic detritism. A basal quartzite confirms the autochthony of this cover relatively to the Antigorio basement. The Triassic levels are almost always absent, most probably due to erosion and, when preserved, have a Helvetic s.l. affinity. The major part of the section is made of a thick monotonous succession of calcschist, which was deposited after UC3.

The Camosci nappe is separated from its pre-Triassic basement, the latter being admittedly of continental nature. This nappe has a clear Helvetic s.l. affinity: Triassic, Liassic and Dogger layers are easily recognisable (MASSON et al. 1980, EPARD 1990). However, the levels younger than Dogger are missing, most likely transported during the Alpine orogenesis into a more external position, probably in the Prealps in or close to the Infra-Niesen zone (for instance, La Lenk nappe, LEMPICKA MÜNCH 1996, Fig. 7.7). The internal lateral variations of facies (Fig. 7.2) imply a deposition in a paleoenvironment of tilted blocks.

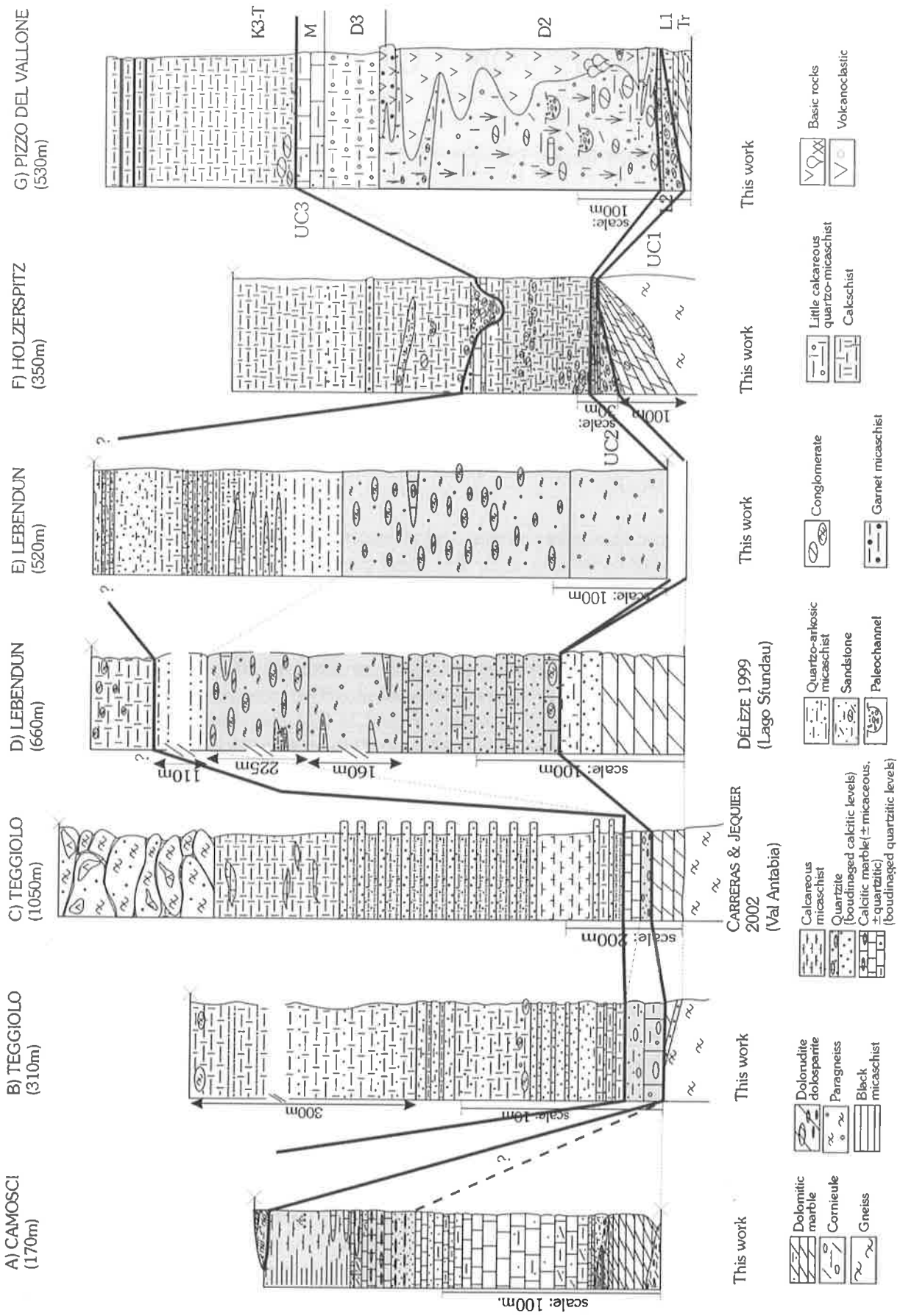


Figure 7.1 Figure 2.10 is redrawn here in order to show a graphic summary.

The major discontinuities UC1, UC2 and UC3 (Fig. 7.1) are best observable, and were initially defined in the Holzerspitz series and in the Pizzo del Vallone nappe, but they are also recorded in the other nappes.

The two principal conglomeratic levels are younger than UC1, which is attributed to the Middle- or to the Late Liassic epoch, and younger than UC2, attributed to the Dogger epoch.

The conglomerates, which were deposited above UC3 (attributed to the Upper Cretaceous), are different. The proportion of pebbles is of lesser importance than the proportion of pebbles found in the conglomerates that were deposited above the discontinuities UC1 and UC2. Moreover, the tectonic process responsible for this detritism is different because for the first time lithologies of others nappes are reworked as pebbles (Fig. 2.1). These conglomeratic levels most likely result from tectonic inversion processes.

The studied nappes have the following characteristics (paragraph II.7.3):

- important lateral variations of facies and of thickness;
- richness in monogenic and polygenic conglomeratic levels;
- atypical, reduced or eroded Triassic sequence (except for the Camosci nappe);
- they are bound by the same unconformities noted UC1, UC2 and UC3 (Fig. 7.1);
- the Pizzo del Vallone nappe contain tholeiitic green rocks typical of a rifting magmatic activity.

Such characteristics suggest a paleogeographic environment of tilted blocks, or a by-pass type margin. The geochemical results show that these tilted blocks are associated to lithospheric extension linked to intra-continental rifting.

### 7.1.2 Results of the stratigraphic and geochemical comparisons with others areas

The studied nappes have lithostratigraphic sections that show strong similarities with nappes deposited on the northern part of the Alpine Tethys (paragraph II.8).

The Pizzo del Vallone nappe is similar to the more internal nappes of pré-Piémontais origin outcropping in the Ambin masssif (ALLENBACH & CARRON 1986). The green rocks found in the Pizzo del Vallone nappe have a geochemical signature comparable to and typical of the geochemical signature of mafic rocks found in a syn-rift sedimentary sequence (paragraph VI.4, ALTHERR et al. 1988, SMITH et al. 1975, PE-PIPER & JANSA 1986, PE-PIPER et al. 1992, BILL et al. 1997, 2000). The green rocks form a cogenetic series, which evolved by olivine, plagioclase and clinopyroxene fractionation (paragraph V.2). The more differentiated basaltic end-member are contaminated and enriched in L-REE (crustal contamination). Some comparisons with rocks having a similar geochemical signature are proposed in chapter V (paragraph V.4), but further comparisons could be envisaged, such as the southeastern Brazilian margin (FODOR & VETTER 1984), the Iberian abyssal plain (CORNEN at al. 1996), and the Labrador Sea (CLARKE et al. 1989).

The Monte Leone nappe resembles best, the Brèche nappe (STEFFEN et al. 1993), the Starlera nappe (BAUDIN et al. 1995), or the more external nappes outcropping in the Ambin massif (ALLENBACH & CARRON 1986), that have a pré-Piémontais origin.

The Lebendun nappe is similar to the Niesen nappe at least in facies (SCHARDT 1983, BADOUX & HOMEWOOD 1978, RINGGENBERG et al. 2001).

The Antigorio nappe is similar to the Ultrabriançonnais nappes (LEFEVRE 1982). Indeed the oldest Mesozoic sediments are mostly absent or extremely reduced.

The Camosci nappe has a clear Helvetic s.l. affinity (Fig. 7.7). The Dolomitic and Calcareous units are typical of the Helvetic basin (MASSON et al. 1980, DOLIVO 1982, BUGNON 1986, EPARD 1990).

### 7.1.3 Structural study

Several ductile deformations affected the region. The oldest recorded deformations are likely coeval to the initial stages of procharriage (mesoalpine phase). No relic of a previous deformation associated to a high-pressure deformation coeval to the subduction was found. The procharriage happened in four successive stages and was followed by the backfolding D5 (neoalpine phase), which is easily recognisable in the landscape thanks to hectometric folds. The following dextral shear zone phase strongly incurved the previous structures and complicated the understanding of the structural relationships between the Central and Eastern Alps; the structure of the whole Lepontine Alps mainly results from the existence of several dextral shear zones (STECK & HUNZIKER 1994 and references herein). The folds coeval to D7, the final folding, were probably induced by the late vertical decompression that allowed the late exhumation of the Lepontine Alps.

### 7.1.4 Metamorphic study

The Lepontine metamorphism is in part younger, in part coeval to the deformation D4. The metamorphic assemblage finished crystallising after the end of the procharriage under the amphibolite facies, more precisely under ~580° C - ~9.7 kbar. Thus, only few places preserved the sedimentological information. The hard nodules scattered in the garnet micaschist or in the cooling rims are good examples of preserved primary sedimentological and igneous texture. No relic of a first high-pressure metamorphism was found.

## 7.2 PALEOGEOGRAPHIC SUCCESSION

Even if the region was strongly deformed and metamorphosed, it is possible to establish the paleogeographical succession of the studied nappes. From the internal to the external part it was as follows (Fig. 7.2):

Camosci – (Verampio) Antigorio – Lebendun – Monte Leone – Pizzo del Vallone - Rosswald

This paleogeographic succession was established considering the following points.

The normal limb of the Pizzo del Vallone nappe lies structurally above the Lebendun nappe and its inverted limb lies below the Monte Leone nappe (Fig. 1.4). Moreover its internal structure shows that the youngest levels are always located southward in contact with the Monte Leone nappe (paragraph VIII.5). This implies an initial decollement and overthrusting of the Pizzo del Vallone nappe above the Monte Leone and the Lebendun nappes (Fig. 6.6).

The Monte Leone nappe is structurally the highest nappe. Even if the dolomitic pebbles dominate, the Holzerspitz series is richer in quartzitic or gneissic detritic input than the Pizzo del Vallone nappe. This is interpreted as the Holzerspitz series having a more proximal position than the Pizzo del Vallone nappe. Its lithostratigraphic section is transitional between those of the Pizzo del Vallone and the Lebendun nappes, although it shows more similarities with the Pizzo del Vallone nappe.

The Lebendun nappe contains the thick and monotonous unit of Paragneissic conglomeratici that resembles a thin succession found in the Monte Leone cover and which is attributed to the Dogger (paragraph II.2.3, Group Hz-III (rp), Fig. 2.1). They derive from the same source and may be issued from the same detritic episode, even if the latter is far less developed in the Holzerpsitz series, where the conglomeratic quartzitic metasandstone is thinner and more mature. As this detritic episode was not recorded by the Pizzo del Vallone nappe, this suggests that the source was situated north of the Lebendun nappe, that the Holzerspitz series was mainly a by-pass area and that the Lebendun nappe was the main depocentre. DELEZE (1999) noticed a similitude of the detrital elements found in the Paragneiss conglomeratici with the Maggia pre-Triassic basement.

The Antigorio nappe was a structural high, which separated the Helvetic s.l. basin from the very distal European margin (Lebendun, Monte Leone and Pizzo del Vallone nappes, Fig. 7.4, 7.5), at least from the Liassic to the Dogger epoch (Fig. 2.7, 7.1, 7.7). The presence in the terminal wildflysch of reworked pebbles derived from the Lebendun nappe (CARRERAS & JEQUIER 2002) is an argument in favour of a more external position for the Antigorio nappe in relation to the Lebendun nappe (the inversion basin presumably lies to the north of the inverted blocks).

The Camosci nappe is interpreted as being the most external nappe due to its structural position and its clear Helvetic s.l. affinity (paragraph II.4.3, II.8.2, Fig. 2.4). It comes from under the Lebendun and the Antigorio nappes (Fig. 1.4).

The Rosswald series outcrops only on the northern part of the area, in front of all the above-cited nappes, and never below (Fig. 1.4). This favours a more internal origin for this nappe, and the Alpine shortening made it overthrust the other nappes. However, only a detailed geological mapping of the nappes outcropping above the Monte Leone nappe will allow the origin of this nappe to be deduced more precisely. Its age is unknown, but the nappe could represent a late Cretaceous or a Tertiary Alpine flysch.

The present superposition (Fig. 1.4) is the result of a tectonic juxtaposition, and it cannot be excluded that important parts of the margin were lost forever during the subduction (STAMPFLI et al. 1998). Indeed the tectonic sketch of the Swiss Alps (SPICHER 1980) suggests that nappes may be missing between the Antigorio and Lebendun nappes in the studied area (Fig. 8.6, 7.4D).

## 7.3 GEOMETRIC CONSIDERATIONS

### 7.3.1 The Camosci nappe

The lithostratigraphic study shows that lateral variations of facies are common in the Camosci nappe (paragraph II.4.3, Fig. 2.4). The goal of this paragraph is to provide a model for that phenomenon in agreement with the field relationships, and to provide an interpretation. The differently observed successions are summarized in figure 7.2.

From sections A to D (Fig. 7.2) no particular problem appears in reference to the position and the order of the various schematic sections; only the stratigraphical gap between the Dolomitic and Graphitic units is impossible to evaluate. So the age attribution for the base and top of the Graphitic unit in section A and B are arbitrarily chosen. But as these columns show only relative chronostratigraphic relations, the approximation does not create incoherency.

The interpretation becomes more difficult with the appearance of the submittal Detritic unit. Indeed, it represents the last recognized unit (Fig. 2.4), and it is always only in contact with the

calcareous micaschist and never with the black micaschist (paragraph II.4.3). So three explanations (sections E1 to E3) are possible:

-section E3: the Detritic unit was deposited over the calcareous micaschist but after a sedimentary hiatus;
-section E2: the Detritic unit was deposited in continuity above the calcareous micaschist;
-section E1: the Detritic unit was deposited in continuity above the calcareous micaschist and moreover eroded its top.

In all three sections, the Detritic unit was deposited in stratigraphic continuity, but a sedimentary hiatus cannot be excluded for section E3 nor an erosive base that eroded the top of the Graphitic unit in section E1.

These three solutions are not mutually exclusive and could coexist in different parts of the basin. The favoured solution is the following (Fig. 7.2). The Detritic unit was deposited perhaps everywhere but above all in a proximal position. It probably eroded the older levels. Its richness in detrital dolomite in its upper part not surprisingly coincides with the area of preferential alpine detachment plane.

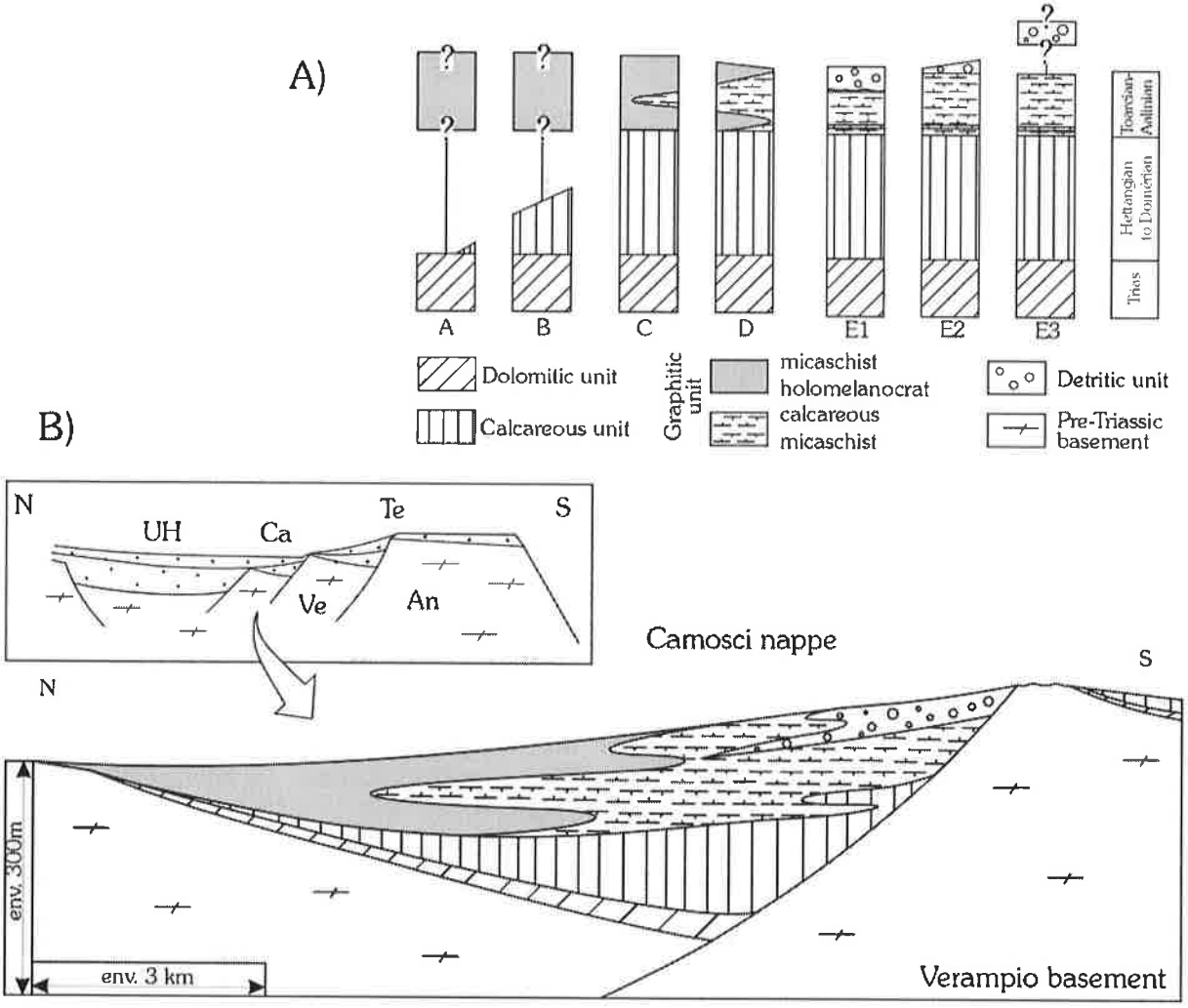


Figure 7.2 A) Schematic sections of the Camosci nappe ordered following the field relationships and B) Proposed model for the Camosci nappe (An: Antigorio basement, Ca: Camosci nappe, Te: Teggiolo zone, UH: Ultra-Helvetic covers, Ve: Verampio basement).

The abrupt variation of facies (Fig. 2.4, 7.2) between the western and eastern part of this nappe, i.e. between the calcareous micaschist and the black micaschist, probably reflects a series of transgressive or flooding surfaces recording eustatic sea-level variations (paragraph II.4.3). The calcareous micaschist was deposited in a more proximal position than the black micaschist, since the latter are devoid of any carbonate. Moreover as the more proximal Detritic unit is only in contact with the calcareous micaschist, this also argues in favour of a more proximal position of the latter in relation to the black micaschist (paragraph II.4.3, II.4.4).

The unfolding of the Camosci nappe, therefore, provides the succession of the schematic sections proposed in the figure 7.2. The fact that the micaschist facies of the graphitic unit are structurally in the most external position led me to orient the "Camosci tilted block" as shown in the figure 7.2.

### 7.3.2 The Monte Leone nappe

The lithostratigraphic description shows that the Holzerspitz series is characterized by important lateral variations of facies and by great quantities of conglomeratic levels (paragraph II.2.3). Moreover, the three discontinuities UC1, UC2 and UC3 are recognizable.

The stratigraphic sections presented in figure 2.1, linked to the observations made at the outcrop scale and from the map allow me to deduce that the Holzersptiz series was deposited on a northward-dipping surface represented by the crystalline basement of the Monte Leone nappe (Fig. 7.3). Once again a tilted blocks model is proposed, based on the following relationships:

- the thickness of the Group Hz-I varies a lot over the mapped area. Moreover, the thickness of this group also clearly decreases toward the Saflischpass, to the west-southwest.
- the thickness of the Group Hz-II decreases toward the south;
- the amount of pebbles in the basal conglomerate of the Group Hz-III regularly decreases toward the paleosouth;
- the quartzitic metasandstone of the Group Hz-III either overlies the thick succession of conglomeratic levels and calcschist, or unconformably overlies the Group Hz-II toward the south;
- a calcitic marble was deposited upon the quartzitic metasandstone only southward.

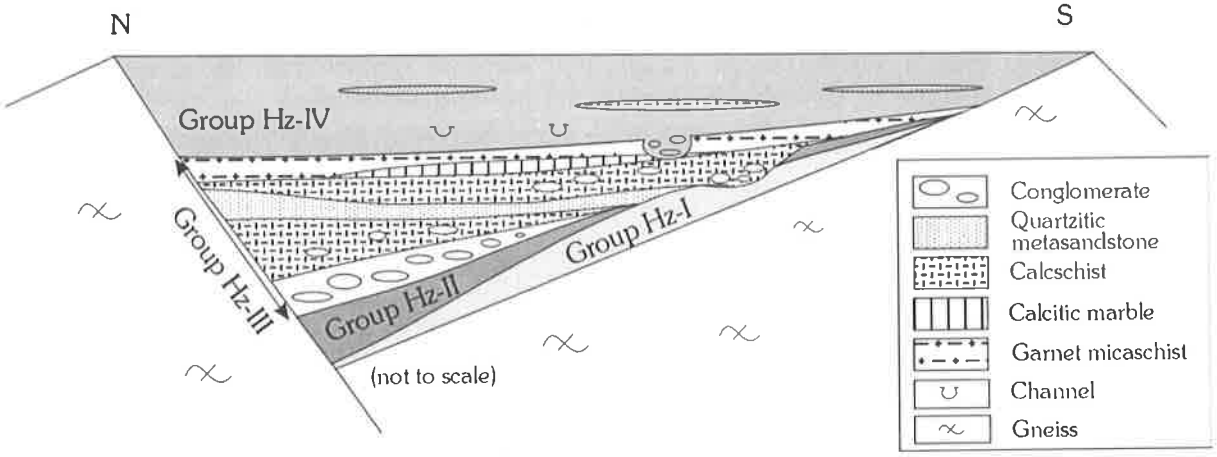


Figure 7.3 Schematic reconstitution of the environment of deposition of the Holzerspitz series.

### 7.3.3 The Pizzo del Vallone, Lebendun nappes and Antigorio nappes

The same type of considerations for the Monte Leone nappe (thickness variations, proximal versus distal position) can be made for the Pizzo del Vallone nappe. They lead to the conclusion that the Pizzo del Vallone nappe was deposited on a north-dipping tilted-block of continental origin.

The Lebendun nappe is reduced over the mapped area in relation to its westward continuation; only the paragneiss conglomeratici and the Scisti Bruni are present. Although it was impossible to specify the original dip orientation of the Lebendun block, if the working hypothesis of a depositional setting similar to the Monte Leone nappe is accepted, the Lebendun block (Fig. 7.4) was nevertheless oriented by analogy with the Monte-Leone and Pizzo del Vallone tilted blocks. Indeed, the Lebendun nappe has an origin close to the one of the Monte Leone nappe, that is to say south of the Antigorio basement.

The Teggiolo zone contains the most reduced cover series, with very few preserved levels younger than UC3. This suggests that it was a structural high separating the south-dipping tilted blocks to the South, from the north-dipping tilted blocks to the North, whose infill shows affinities with the Helvetic s.l. basin. The Antigorio block is hence regarded as the shoulder of the Alpine Tethys (paragraph VII.4, Fig. 7.4, 10.5, SPRING et al. 1992).

## 7.4 PALEOGEOGRAPHY

It is now established that the studied nappes have a present superposition that is the result of the Alpine orogenesis. Despite the high metamorphic grade it was possible to describe the environment of deposition, to deduce the relative paleogeographic succession of these nappes (paragraph VII.2) and to propose a model in which the Mesozoic to Tertiary metasediments were deposited during an extensional phase linked to a rift in a paleoenvironment of tilted blocks (paragraph VII.3). It was shown that the Camosci nappe has a Helvetic s.l. affinity, the Antigorio nappe has an Ultrabriançonnais affinity, and the Pizzo del Vallone, Monte Leone and Lebendun have a Prépiémontais affinity. This clearly indicates that the studied area lay north of the Alpine Tethys ocean and represents a complete south European passive margin segment, including part of the most internal rim basin, the rift shoulder as well as proximal to distal oceanward-facing tilted block series (paragraph VII.3)

Before formulating conclusions, I have to specify that I prefer envisaging a simple paleogeography and a slightly more complicated tectonic history than to complicate the paleogeography in order to simplify the tectonic history. Indeed, creating new ocean(s) implies creating two more passive margins for which there are no known evidence (paragraph VII.5).

These results together allow me to draw the time evolution of the internal European margin (Fig. 7.4), east of the pre-drift oriental termination of the Briançonnais terrane (Fig. 7.5). To visualize the relations on a greater scale, I used and modified the paleogeographic reconstruction proposed by STAMPFLI et al. (2001). Two schematic paleogeographic maps (Fig. 7.5) were added to situate the nappes cited in this manuscript, along with some others as well, in order to establish an idea of their relative paleogeographic position at the time of Dogger and Early Cretaceous epochs respectively.

As it is most likely that some parts of the European margin were lost forever during the subduction (STAMPFLI et al. 1998), I have added some unknown blocks to the margin between the Antigorio and Lebendun blocks (Fig. 7.4D). Indeed, the tectonic sketch of the Central Alps

(SPICHER 1980) suggests that nappes outcropping eastward, such as the Maggia or Adula nappes, are missing in the studied area.

## 7.5 THE VALAISAN CONTROVERSY

Some authors (LEU 1986, PASTORELLI et al. 1995, KNILL 1996) suggested that the green rocks of the Pizzo del Vallone nappe were somehow linked to two other well-known metabasaltic bodies of the Western Alps; the metapillow lava of Visp (Sion-Courmayeur zone, BURRI 1958, 1979, BURRI et al. 1993, 1994) and the Petit-Saint-Bernard suite (Complexe du Versoyen, ANTOINE 1971, 1972, CANNIC 1996). All these occurrences of metabasic rocks were interpreted as being related to the opening of a very oblique ocean (sometimes seen as deep California Baja-type pull-apart oceanic domain, KELTS 1981) called the Valaisan ocean or North Penninic ocean. Although such a transform zone was invoked (and is necessary) to permit the eastward movement of the Briançonnais terrane, the Pizzo del Vallone green rocks cannot be linked to the Visp and Petit-Saint-Bernard occurrences.

- the mafic rocks of the Petit-Saint-Bernard are now dated to the upper Paleozoic (294±1 My, U-Pb on zircons, CANNIC 1996, and 296±30 My, U-Pb on zircons, GIROUD & MEILHAC 2002), whereas the green rocks of the Pizzo del Vallone nappe are clearly Mesozoic;
- the green rocks of the Petit Saint-Bernard are always associated to black, non or very little calcareous schists. Such an association was never observed in the studied area, where the green rocks are associated with proximal marine, mainly terrigenous detritics;
- in the Petit-Saint-Bernard area (France), a very characteristic sedimentary unit, the "Flysch de la Tarentaise" is overthrust by the mafic rocks of the "Complexe du Versoyen" (ANTOINE 1971, 1972, CANNIC 1996). This sedimentary unit can be followed up to the Visp area, and is known in Switzerland as the "trilogie valaisanne" (BURRI 1979). This "trilogie valaisanne" was typically associated to the hypothetic "Valaisan ocean". However, it does not exist at all in the studied area;
- the Rosswald series only outcrop in front of the studied area and never below (Fig. 1.4). As previously stated (paragraph VII.2), this series is the most internal nappe outcropping over the mapped area. Its lithological succession shows some similarities with Group Hz-IV and Group V-IV in so far as that they are all flysch s.s. (probably Late Cretaceous to Tertiary in age). Moreover, the Rosswald series is identical to the "flysch de Saint-Christophe", which is a formation of the "trilogie valaisanne" (Sion-Courmayeur zone). The Rosswald series seems, thus, to be linked to the Valaisan sedimentary unit and is rooted south of the studied area.

Figure 7.4 Cross-sections of the southern European margin at different time: A) Middle to Late Triassic, B) Late-Liassic - Aalenian and C) Late Malm. The blocks are oriented according to the present position of the various stratigraphic columns that I studied on the field. Shown inset are the paleoreconstruction of STAMPFLI et al. (2001) to have an idea of the paleogeographic evolution of this margin (Ab: Alboran, Ad: Adria s.str., Ap: Apulia s.str., Br: Briançonnais, BY: Beyshehir, Ca: Calabride, Da: Dacides, Db: Dent Blanche, Gt: Getic, He. Helvatic rim basin, Hr: Hronicum, IA: Izmir-Ankara, Ky: Kabylies, Lg: Ligerian, Li: Ligurian, Lo: Lombardian, Me. Meliata, Mg: Magura margin, Mk: Mangyshlak, MS: Margna-Sella, Pa: Panormides, Pal.T: Paleotethys, sB: sub-Betic rim basin, Se: Sesia, Si: Sicanian, SM: Serbo-Macedonian, TD: Trans-Danubian range, Ti: Tirolic-Bavaric, Tt: Tatric, Tz: Tizia, Va: Valais, Ve: Veporic). D) interpretation of the whole southern European margin, including the parts that were lost forever during the subduction. Actually present day passive margins are made of a greater quantity of tilted blocks between the oceanic part and the shoulder (An: Antigorio basement, Ca: Camosci nappe, V: P. del Vallone nappe, Le. Lebendun nappe, ML: Monte Leone basement, Hz: Holzerspitz series, Te: Teggiolo zone, UH: ultra-Helvetic covers, Ve: Verampio).

Figure 7.4: legend on previous page

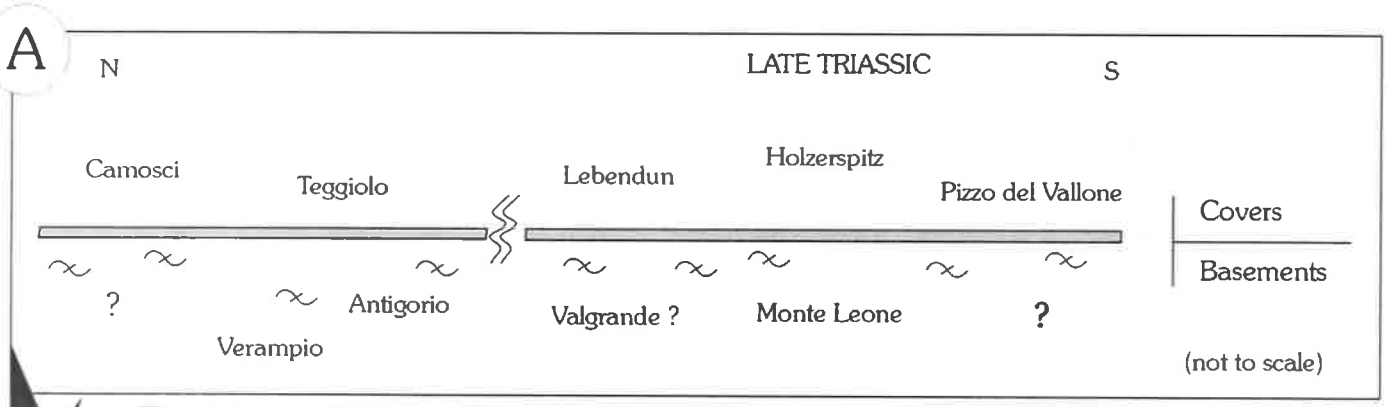


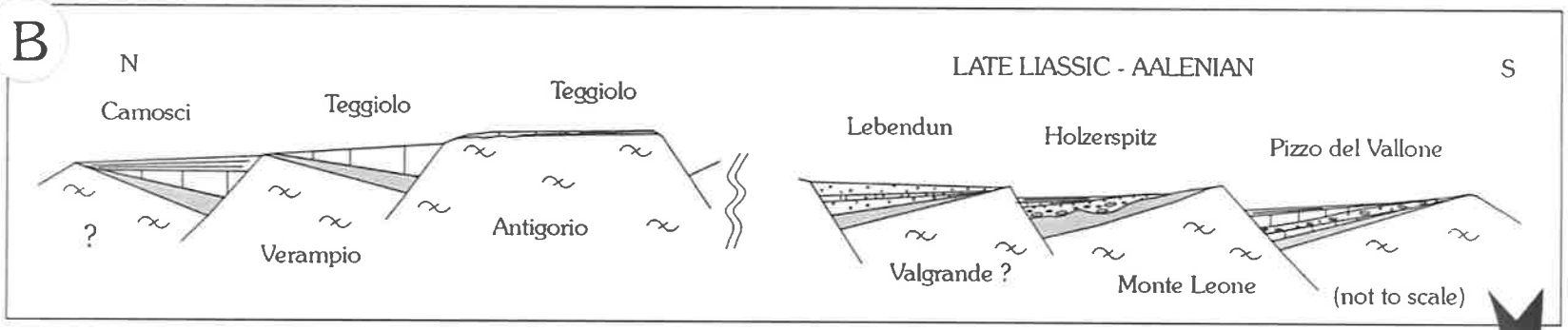



Reconstructed paleogeographical succession:

A) Late Triassic
and
B) Late Liassic - Aalenian

A discontinuity is placed where present information misses.

The paleogeographic maps are from STAMPFLI et al. (2001).

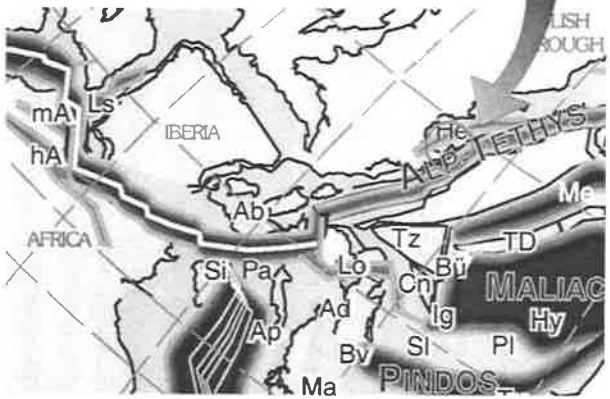

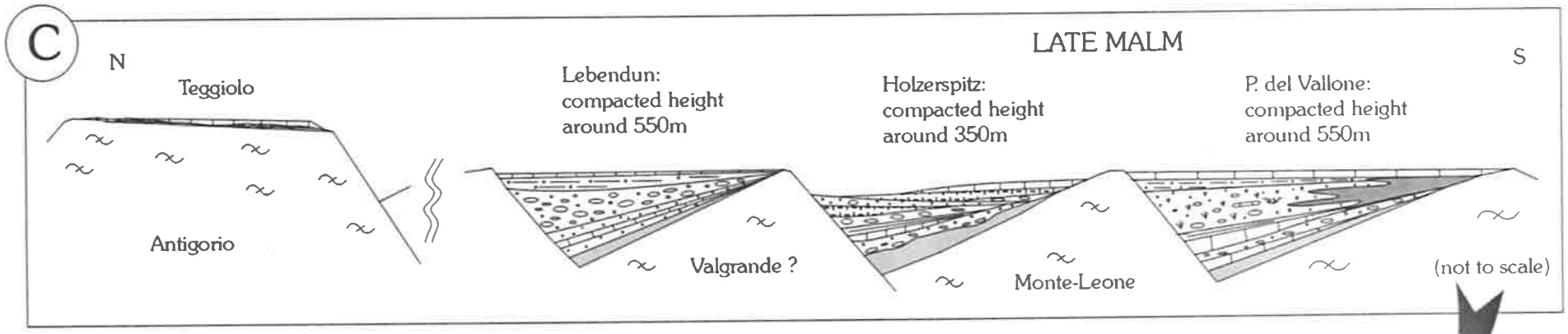


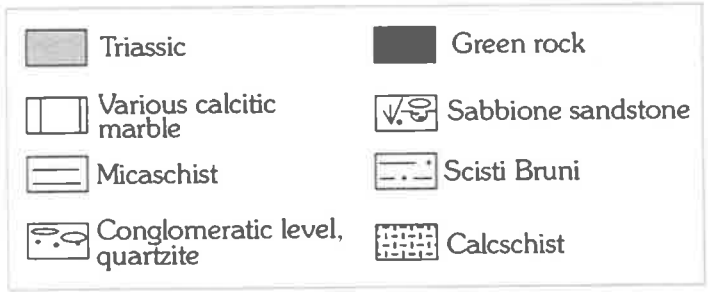


Reconstructed paleogeographical successsion:

C) Late Malm
and
D) Late Malm, but the whole margin is reconstructed.

A discontinuity is placed where present information misses.

The paleogeographic map is from STAMPFLI et al. (2001).

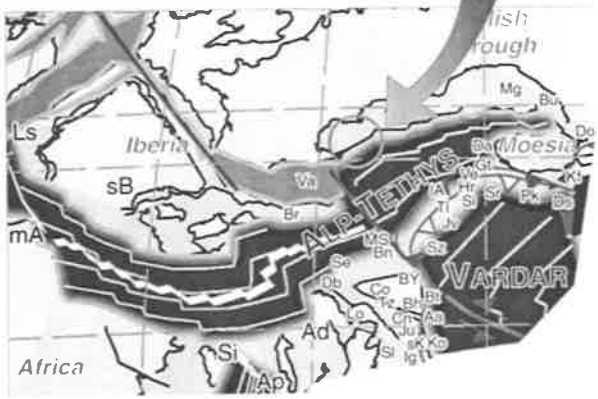


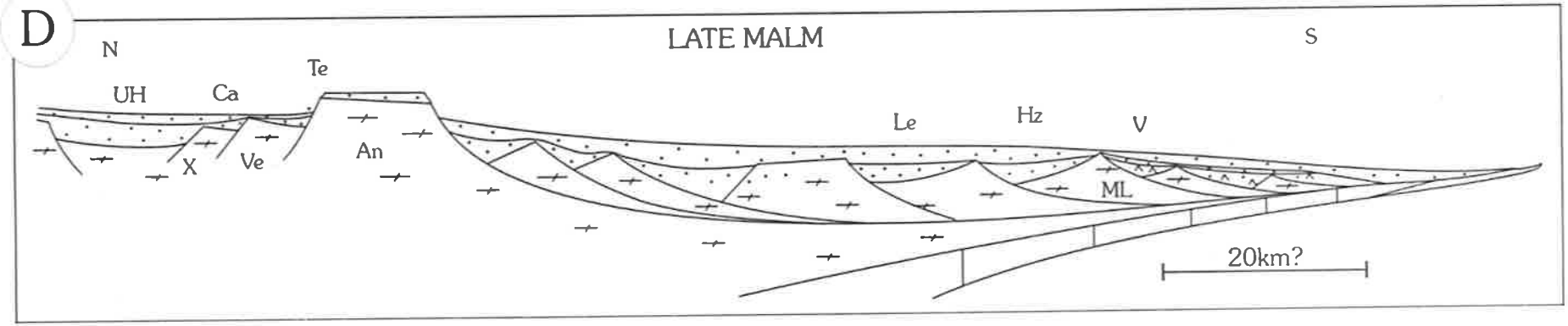


Figure 7.4: continued

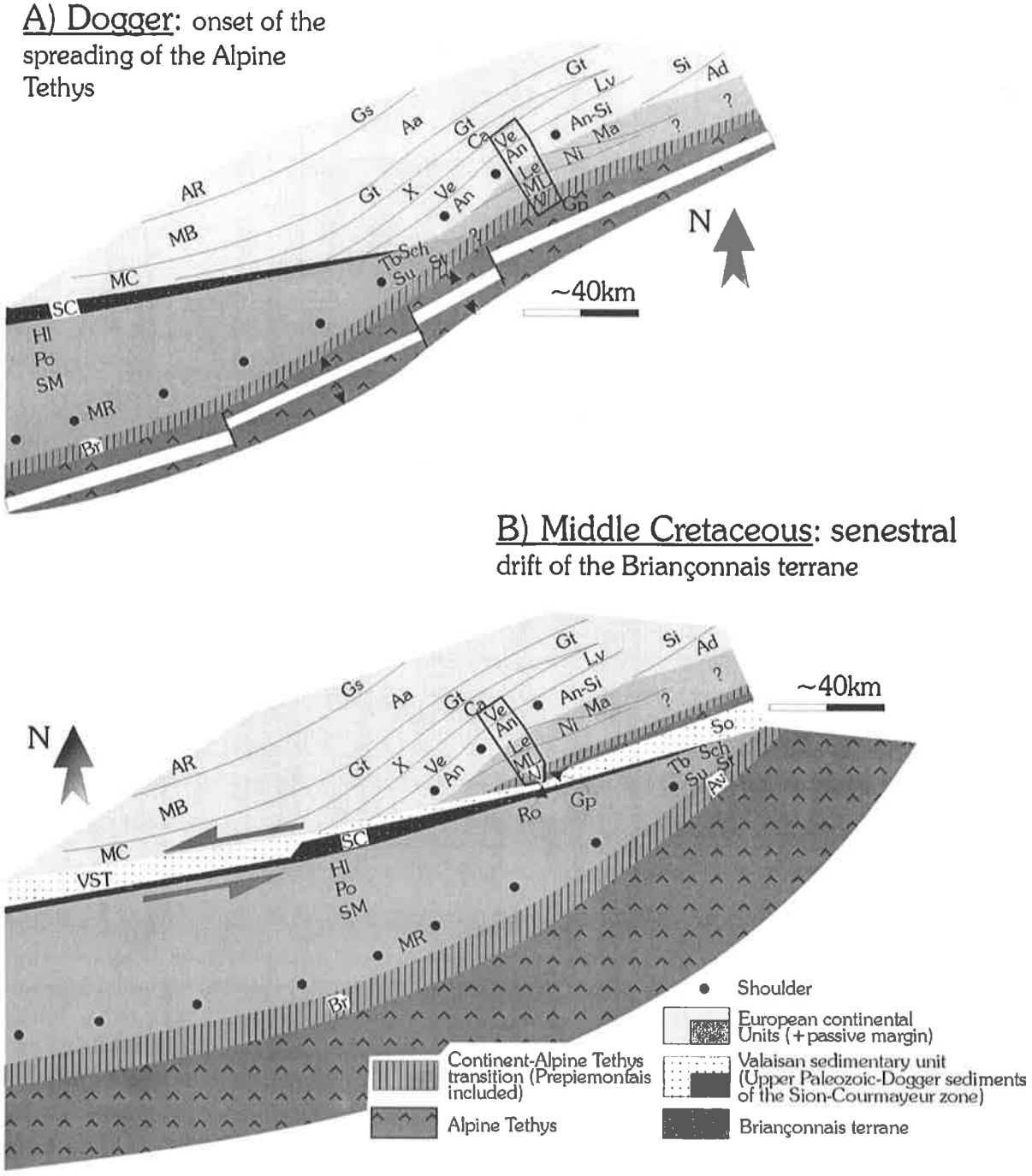


Figure 7.5 Schematic maps of the paleogeographic environment (Aa: Aar massif, Ad: Adula nappe, An: Antigorio nappe, Ar: Aiguilles Rouges massif, Av: Avers nappe, Br: Brèche nappe, Ca: Camosci nappe, Gp: GeisspfadGs: Gastern massif, Gt: Gotthard massif, Hl: Houiller basin, ML: Monte Leone nappe, Le: Lebendun nappe, Lv: Leventina nappe, Ma: Maggia nappe, MB: Mont Blanc massif, MC: Mont Chetif basement, ML: Monte Leone nappe, MR: Mont Rose nappe, Ni: Niesen nappe, Po: Pontis nappe, Ro: Rosswald series, SC: Sion-Courmayeur zone without the Valaisan sediments, Sch. Schams nappes, Si: Simano nappe, SM: Siviez-Mischabel nappe, So: Sosto Schists, St: Starlera nappe, Su: Suretta nappe, Tb. Tambo nappe, V: Pizzo del Vallone nappe,Ve. Verampio nappe, VST: Valaisan trilogy, X: X-basement (ESCHER et al. 1995).

Figure 7.6 Stratigraphic columns of the southern European margin according to their paleogeographic position (for the legend, see figure 10.1). Keys to paleontological data: 1.=*Saxoceras* or *Schlotheimia* (indicating an Hettangian age); 2.=*Arietitidae* (Sinemurian); 3.=*Hildoceras bifrons* (Toarcian); 4.=*Peltoceras* and *Peltoceratoïde* (Oxfordian); 5.=*Leitoceras* (Aalenian); 6.=*Protopeneroplis* and *Archeosepta platierensis* and *Bositra buchi* (Bathonian); 7.=*Protopeneroplis striata* and *Archeosepta platierensis* (Bathonian).

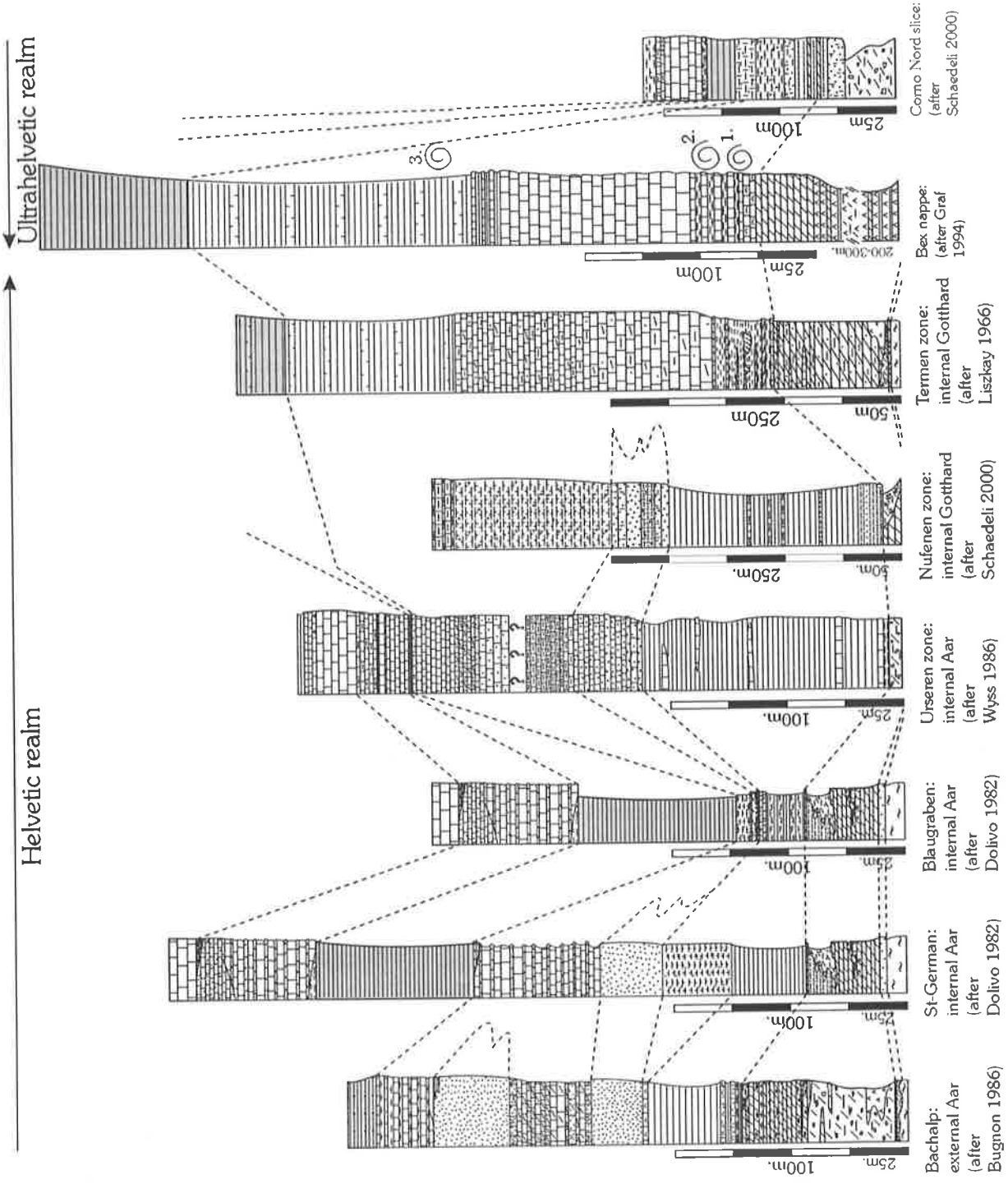

Figure 7.6: continued

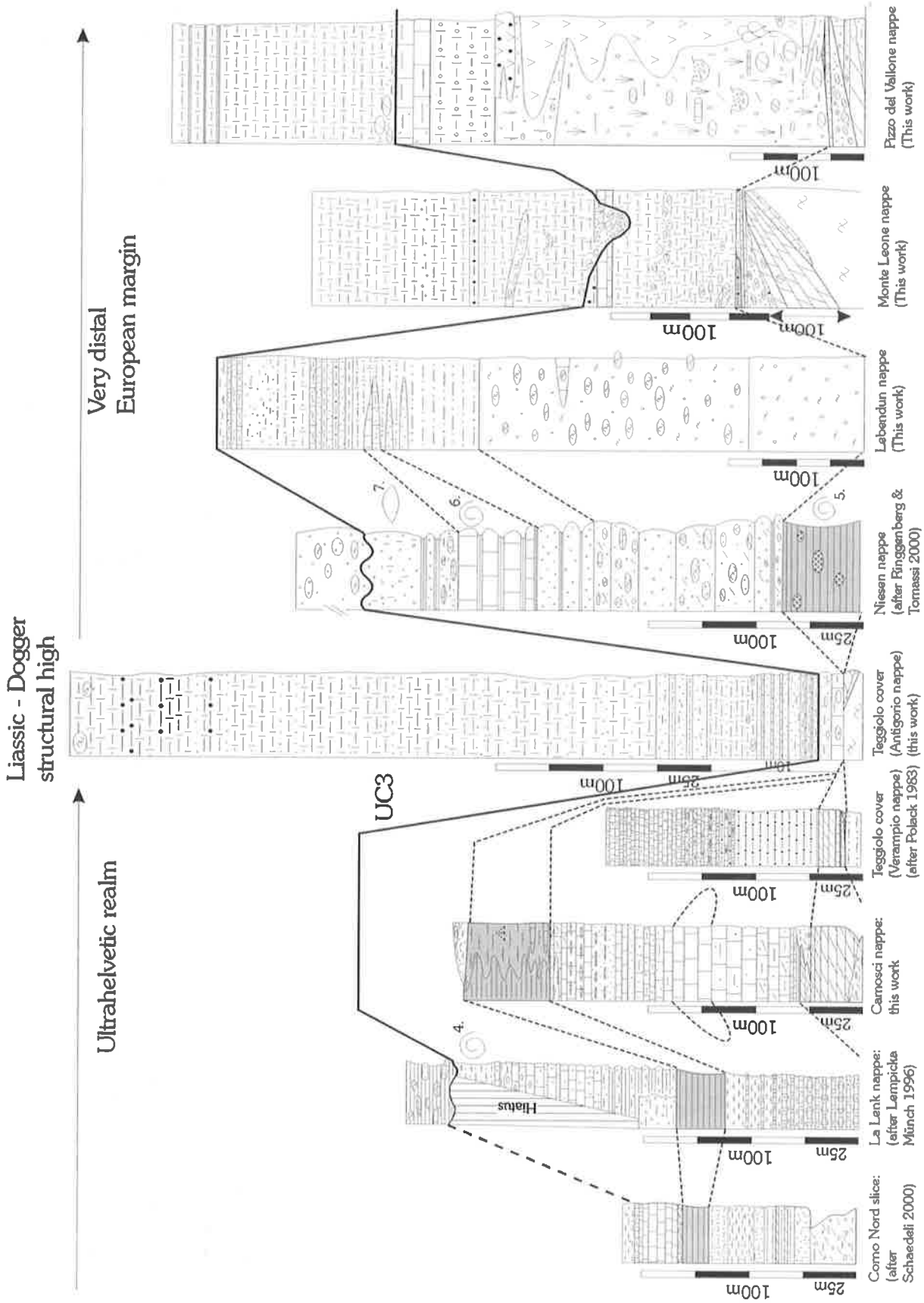

## 7.6 On a Greater Scale

This study leads up to the paleogeographic reconstruction of the very distal south European passive margin linked to the Alpine Tethys rifting. The Camosci nappe is the most external nappe outcropping over the studied area, but it is also the most internal nappe of the Helvetic s.l. rim basin that laid north of the Antigorio rift shoulder (Fig. 7.1, 7.4, 7.5).

To conclude this PhD work, a bibliographic research was done to establish a schematic overview of the southern European margin on a greater scale. Indeed, the juxtaposition and the comparisons of several stratigraphic sections allow some of the non-Briançonnais cover series now outcropping in the Prealps (Submédiane, Niesen and Infraniesen zones) to be resituated in their paleogeographic position and also to clarify certain points in the Helvetic domain (Helvetic s.l. nappes, Fig. 7.6). We can, thus, imagine how the margin may have looked before the alpine deformations (structural highs and basins alternated, Fig. 7.7):

- the nappes, which were deposited on the northern (St-German in Dolivo 1982, Bachalp in Bugnon 1986) and southern (La Lenk nappe in Lempicka Münch 1996, the Camosci nappe this work) sides of the Helvetic basin s.l., are more similar, but slightly different from those which were deposited in the deepest central part of the basin (the Urseren zone in Wyss 1986, the Nufenen zone in Schaedli 2000, the Termen zone in Liskay 1966 and the Bex nappe in Graf 1994). This means that the more internal Ultrahelvetic covers resemble the more external Helvetic covers best (Lotharingian and Domerian quartzite, Fig. 7.6, 7.7);
- the Camosci nappe has clear affinities with La Lenk nappe (Lempicka Münch 1996), in other words with the Infra Niesen zone. They were probably deposited very close to one another. The weak metamorphic grade recorded in the La Lenk nappe also implies that this nappe came from the internal Ultrahelvetic basin (Lempicka Münch 1996);
- the Niesen nappe has a controversial paleogeographic origin. However, the stratigraphic similarities (Badoux & Homewood 1978, Ringgenberg et al. 2001) with the Lebendun nappe, as well as its structural position, imply that these two nappes have a close paleogeographic origin. Moreover, the Niesen nappe underwent a weak anchizonal metamorphism (Lempicka Münch 1996) also suggesting an internal origin.

With reference to the studied area, the Infra-Niesen zone (La Lenk nappe, Lempicka Münch 1996) was deposited immediately north from the Camosci nappe, and the Niesen nappe has to be rooted in a paleogeographic position similar to that of the Lebendun nappe, in-between the Monte Leone and the Antigorio nappes.

The remaining question is, what was deposited south of the studied area?

The Submédiane zone (McConnel & de Raaf 1929) is an upper Cretaceous to Eocene chaotic wildflysch outcropping in the Prealps. However, it is not clearly rooted now. The only conclusion that seems clear is that it has a more internal origin in relation to the Niesen nappe. The following points help to constrain its origin:

- Weidmann et al. (1976) noticed the presence in the melange of slices coming from various units (Niesen and Préalpes Médianes nappes), the most abundant blocks consist of upper Jurassic pelagic limestone interbedded with calcareous debris flows. This, added to the similarity of some slices with Ultrahelvetic, north Penninic or Subbriançonnais facies, allowed the authors to root this zone between the Briançonnais and Ultrahelvetic nappes (already proposed by Badoux 1965), in the southern part of the Sion-Courmayeur zone.

- STAMPFLI (1993) considered the Submédiane zone as coming from a continent-ocean transition zone that was situated south of the south Helvetic margin. Moreover he proposed to link the Trom spilites to the Valaisan event, whereas the reworked ultrabasic pebbles are likely coming from the erosion of a lower part of the oceanic Alpine Tethys crust.
- GRAF (1994) has compared the reworked material of the Submédiane zone with those of the external Préalpes Médianes Plastique nappe. He concluded that the two nappes are coeval and similar, but at the same time different. He proposed that the Sub-Médiane zone was deposited in a basin less subjected to tectonic activities and in a lateral rather different environment than the external Préalpes Médianes nappes.

All this information implies that the Submédiane zone was probably deposited north of the Subbriançonnais but south of the studied region. It could be interpreted as the accretionary prism that developed north of the Briançonnais terrane, thus, explaining the great diversities of tectonic slices found in it.

The Sion-Courmayeur zone is the most important tectonic element coming from the transform zone associated to the eastward Briançonnais terrane drift, often called the Valaisan ocean (paragraph VII.5, TRÜMPY 1955, BURRI 1958, ANTOINE 1972, JEANBOURQUIN & BURRI 1991). The Pierre Avoi unit, youngest unit of the Sion-Courmayeur zone, is middle Eocene – Oligocene chaotic melange (BAGNOUD et al. 1998).

The Submédiane zone and the Pierre Avoi units i) are both contemporaneous of the early underthrusting of the European margin under the Briançonnais terrane, ii) and represent both the accretionary prism. In relation to the studied area and from the above-mentioned relationships, the Submédiane zone and the Pierre Avoi unit originated south from the Pizzo del Vallone nappe. In fact, the Rosswald series was deposited south from the Pizzo del Vallone nappe, and is identical to the "flysch de Saint-Christophe", which belongs to the Sion-Courmayeur zone (paragraph VII.2, VII.5). Following this statement, the Sion-Courmayeur zone originated south from the Pizzo del Vallone nappe, and the Submédiane zone originated even further south.

The studied area represents the south European passive margin, with elements from the rift shoulder up to the very distal blocks, which recorded the opening of the Alpine Tethys. The late Briançonnais drift affected a domain located southward but is not recorded in the mapped area. The beginning of the northward convergence of the Briançonnais during the Late Cretaceous time is recorded by the UC3 unconformity (inversion processes, Fig. 7.1).

The studied area is, therefore, directly linked to the opening of the Alpine Tethys, but the late Briançonnais drift separated it from the Alpine Tethys. Indeed, the studied area was paleogeographically situated, since the Late Cretaceous time, in-between the Sion-Courmayeur and the Infraniesen zone.

## 7.7 FINAL WORDS AND PERSPECTIVES

Up to now the metabasalts of the studied area were mostly considered as relicts of the northern transform zone associated to the Briançonnais terrane drift (PASTORELLI et al. 1995, KNILL 1996), and were attributed to the Monte Leone autochthonous cover (LEU 1986, BIANCHI et al. 1998). However, this study supplies facts against these interpretations; previous authors have previously proposed, although somewhat partially, the same conclusions (JOOS 1969 and BOLLI et al. 1980).

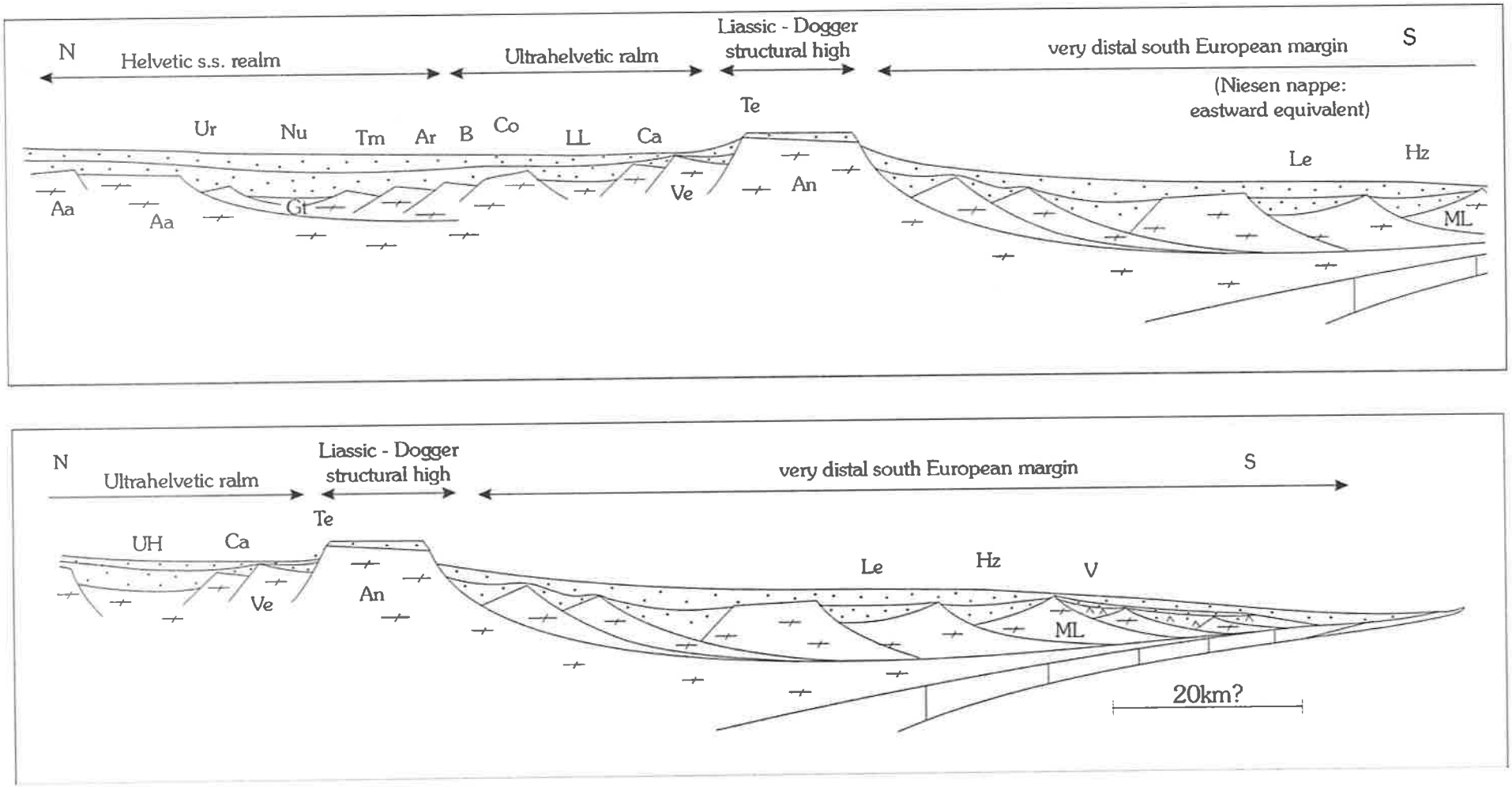


Figure 7.5 Schematic overview of the south European margin at Dogger age. (Aa: Aar massif, An: Antigorio basement, Ar: Arveyses nappe, B: Bex nappe, Ca: Camosci nappe, Co. Corno zone, Gt: Gothard massif, Hz: Holzerspitz series, Le: Lebendun nappe, LL: La Lenk nappe, ML: Monte Leone basement, Nu: Nufenen zone, Te: Teggiolo cover, Tm: Termen zone, Ur: Urseren zone, Ve: Verampio basement, X: X-basement).

The important conclusions highlighted by this work can be summarised into the seven following points:

1- the Antigorio nappe, which represented the Alpine Tethys rift shoulder, has a very reduced cover series over the mapped area. The thickness of the levels, which were deposited before the unconformity UC3 (attributed to the Late Cretaceous or Tertiary epoch) is of 3 m, whereas the thickness of the levels younger than UC3 reaches more or less 300m;

2- the cover series, which were deposited south of the Antigorio shoulder (Lebendun nappe, Holzerspitz series and Pizzo del Vallone nappe), have a specific stratigraphic signature characterised by a great abundance of conglomeratic levels. Geometric and stratigraphic reconstructions are systematically in agreement with a deposition in a half-graben setting (tilted block);

3- the Pizzo del Vallone nappe, newly defined here, is the only nappe that contains intrusive and extrusive mafic rocks; they are continental tholeiites with a T-MORB like signature contemporaneous to the deposition of the Sabbione metasandstone attributed to the Dogger. The green rocks were emplaced during the Alpine Tethys rifting;

4- the Camosci nappe, newly defined here, has a clear Helvetic s.l. affinity. It is the most external nappe outcropping on the mapped area; the beginning of mapping in the Rosswald-Saflischpass area shows that the Pizzo del Vallone nappe could be rooted on the Eisten gneiss;

5- the Lepontine metamorphism began before D4 (dynamic) and continued after D4 (static). Modern methods of investigation permitted the P-T conditions of ~580°C ~9.6 kbar, reached during the peak of metamorphism, to be determined. Such values are higher than previously established;

6- a late dextral shear zone noted D6 and well observable in the Morasco area, strongly incurved the previous structures. The latter were rotated from a general WSW-ENE trend to a NNE-SSW trend thus complicating the tectonic correlations between the Western and Eastern Alps. The axial traces of the backfolds D5, for instance, are incurved (Annexe 6B): the axes have a WSW-ENE orientation in the Binntal and Sabbione areas, but they have a NNE-SSW orientation in the Vannino and Busin areas.

The lower Penninic nappes outcropping in the Binntal – Val Formazza area formed the very distal south European passive margin linked to the opening of the Alpine Tethys rifting. Such results, admittedly resolve some problems, but also create new ones. The following specific points could be interesting to pursue:

1- continuation of the mapping of the Pizzo del Vallone nappe to determine its longitudinal extension;
2- the study of the relations (if possible) between the Pizzo del Vallone nappe and the Bosco series, series that also contains green rocks;
3- the pursuit east of the axial trace of the Berisal synform, in order to understand its relations with the Wandfluhhorn antiform;
4- an attempt to possibly discover new Mesozoic volcanic rocks, that could contain datable zircons;
5- and the dating of the Mesozoic rocks via isotopic methods.

# BIBLIOGRAPHY

ACKERMANN A. (1986): Le flysch de la nappe du Niesen. Eclogae geol. Helv., 79/3, 641-684.
ALLENBACH B. and CARON J.M. (1986): Relations lithostratigraphiques et tectoniques entre les séries mésozoïques de la bordure sud-ouest du massif d'Ambin (Alpes Occidentales). Eclogae geol. Helv., 79/1, 75-116.
ALTHERR R., HENJES K.F., PUCHELT H. and BAUMANN A. (1988): Volcanic activity in the Red Sea axial trough; evidence for a large mantle diapir?. Tectonophysics, 150/1-2, 121-133.
AMATO J.M., JOHNSON C.M., BAUMGARTNER L.P. and BEARD B.L. (1999): Rapid exhumation of the Zermatt-Saas ophiolite deduced from high-precision Sm-Nd and Rb-Sr geochronology. Earth Planet. Sci. Lett., 171/3, 425-438.
ANDERSON J.L. and SMITH D.R. (1995): The effects of temperature and f(O2) on the Al-in-hornblende barometer. Am. Mineral., 80/5-6, 549-559.
ANTOINE P. (1971): La zone des Brèches de Tarentaise entre Bourg-Saint-Maurice (Vallée de l'Isère) et la frontière italo-suisse. Mémoire 9, Trav. Lab. géol. Univ. Grenoble.
ANTOINE P. (1972): Le domaine pennique externe entre Bourg-Saint-Maurice (Savoie) et la frontière italo-suisse. Géol. Alpine, 48/I, 5-40.
ARGAND E. (1911): Les nappes de recouvrement des Alpes Pennines et leurs prolongements structuraux. Beitr. Geol. Karte Schweiz, N.F., 31, 1-26.
ARGAND E. (1916): Sur l'arc des Alpes Occidentales. Eclogae geol. Helv., 14, 145-204.
BADER H. (1934): Beitrag zur Kenntnis der Gesteine und Minerallagerstätten des Binnentals. Schweiz. mineral. petrogr. Mitt., 14, 319-441.
BADOUX E. and HOMEWOOD P. (1978): Le soubassement de la nappe du Niesen dans la région du Sépey (Alpes Vaudoises). Bull. Soc. Vaud. Sc. Nat., 353/74, 15-23.
BAUD A. (1987): Stratigraphie et sédimentologie des calcaires de Saint-Triphon (Trias, Préalpes, Suisse et France). Mém. Géol. Lausanne, 1, 322p.
BAUD A., MASSON H. and SEPTFONTAINE M. (1979): Karst et paléotectonique jurassique du domaine brainçonnais des Préalpes. Symp. sédimentation jurassique W-europ., Paris 1977, A.S.F. Publ. spéc. 1, 441-452.
BAUD A. and SEPTFONTAINE M. (1980): Présentation d'un profil palinspatique de la nappe des Préalpes médianes en Suisse Occidentale. Eclogae geol. Helv., 73/2, 651-660.
BAUDIN T., MARQUER D., BARFETY J.-C., KERCKHOVE C. and PERSOZ F. (1995): Nouvelle interprétation stratigraphique de la couverture mésozoïque des nappes de Tambo et de Suretta: mise en évidence d'une nappe de décollement précoce (Alpes centrales suisses). C. R. Acad. Sci., série I, 321, 401-408.
BEARTH P. (1956): Geologische Beobachtungen im Grenzgebiet der lepontinischen and penninischen Alpen. Eclogae geol. Helv., 49, 279-290.
BECKER H. (1993): Garnet peridotite and eclogite Sm-Nd mineral ages from the Lepontine Dome (Swiss Alps); new evidence for Eocene high-pressure metamorphism in the Central Alps. Geology (Boulder), 21/7, 599-602.
BIANCHI G.W., MARTINOTTI G. and OBERHÄNSLI R. (1998): Metasedimentary cover sequences and associated metabasites in the Sabbione lake zone, Formazza Valley, Italy, northwest Alps. Schweiz. mineral. petrogr. Mitt., 78/1, 133-146.
BIANCHI G.W., OBERHÄNSLI R. and MARTINOTTI G. (2001): Magmatism and tectonics during the initial opening of the Piemont-Ligurian Ocean. Della Tetide alle Alpi – Convegno scientifico in memorie di Giulio Elter, Cogne, Valle d'Aosta, 2p.
BILL M., BUSSY F., COSCA M., MASSON H. and HUNZIKER J.C. (1997): High-precision U-Pb and 40Ar/39Ar dating of an Alpine ophiolite (Gets nappe, French Alps). Eclogae geol. Helv., 91/1, 43-54.
BILL M., NÄGLER T. and MASSON H. (2000): Major, minor, trace element, Sm-Nd and Sr isotope compositions of mafic rocks from the earliest oceanic crust of the Alpine Tethys. Schweiz. mineral. petrogr. Mitt., 80/1, 131-145.

BILL M., O'DOGHERTY L., GUEX J., BAUMGARTNER P.-O. and MASSON H. (2001): Radiolarite ages in Alpine-Mediterranean ophiolites; constraints on the oceanic spreading and the Tethys-Atlantic connection. Geol. Soc. Am. Bull., 113/1, 129-143.

BOLLI H., BURRI M., ISLER A., NABHOLZ W., PANTIC N.K. and PROBST P. (1980): Der nordpenninische Saum zwischen Westgraubünden and Brig. Eclogae geol. Helv., 73/32, 779-797.

BOSSARD L. (1925): Der Bau der Tessiner Kulmination. Mit tektonischer Übersichtkarte. Eclogae geol. Helv., 19, 504-521.

BOURBON M. (1980): Evolution d'un secteur de la marge nord-thétysienne en milieu pélagique: la zone briançonnaise près de Briançon entre le début du Malm et l'Eocène inférieur. Thesis Univ. Strasbourg, 337p.

BREWER T.S., HERG J.M., HAWKESWORTH C.J., REX D. and STOREY B.C. (1992): Coast Land dolerites and the generation of Antarctic continental flood, 68. In: STOREY B.C., ALABASTER T. and PANKHURST R.J. (Eds), Magmatism and the causes of continental break-up, Geol. Soc. Spec. Publ., 68. London, 185-208.

BUGNON P.-C. (1986): Géologie de l'Helvétique à l'extrémité sud-ouest du massif de l'Aar (Loèche, Valais). Thesis Univ. Lausanne, 106p.

BURCKHARDT C. (1942): Geologie und Petrographie des Basodino-Gebietes. Schweiz. mineral. petrogr. Mitt., 22, 99-186.

BURRI M. (1958): La zone de Sion-Courmayeur au Nord du Rhône. Beitr. geol. Karte Schweiz, N.F., 71.

BURRI M. (1979): Les formations valaisannes dans la région de Visp. Eclogae. geol. Helv., 72/3, 789-802.

BURRI M., FRANK E., JEANBOURQUIN P, LABHART T., LISZKAY M. and STRECKEISEN A. (1993): Blatt 1289 Brig. Geol. Atals Schweiz 1:25'000, Karte 93.

BURRI M., JEMELIN L. and JEANBOURQUIN P. (1994): Blatt 1289 Brig. Geol. Atals Schweiz 1:25'000, Erlaüterungen 93, 62p.

CANEPA M. (1993): Evoluzione stratigrafica, tettonica e metamorfica di un settore di margine continentale al limite tra Elvetico e Pennidico: il caso delle unità "Pennidiche Inferiori" tra la Val Cairasca e la Val Formazza – Antigorio (provincia di Novara). Thesis Univ. Genova, 141p.

CANNIC S. (1996): L'évolution magmatique et tectono-métamorphique du substratum du domaine valaisan (Complexe du Versoyen, Alpes Occidentales): implications dans l'histoire alpine. Thesis Univ. Grenoble, 215p.

CARRERAS R. and JEQUIER C. (2002): Etude géologique de la zone du Teggiolo au sud du Basodino. Diplôme Univ. Lausannne, Unpubl., 95p.

CARRUPT E. (2002): Geological and mineralogical study of the High Val Formazza – Binntal area (Central Alps): new stratigraphic, geochemical and structural constraints. Thesis Univ. Lausanne, 185p.

CARRUPT E., MASSON H., and GOUFFON Y. (2002): The Sabbione metabasalts: new tectonic, stratigraphic and geochemical constraints on a mid-Jurassic volcanic event (Pizzo del Vallone nappe, Central Alps). Science and the Magic Mountain, Annual Meeting of the Swiss Academy of Natural Sciences (SANW) 2002, Abstracts, 17-18.

CARRUPT E. and RICE A.H.N. (in prep.): Texturally sector-zoned garnets and displaced graphite; Monte Leone Nappe, Central Alps (High Val Formazza), Italy.

CARRUPT E., BUSSY F. and MASSON H. (in prep.): The Sabbione metabasalts (Pizzo del Vallone nappe, Central Alps): evidence of a mid-Jurassic volcanic activity.

CASTIGLIONI G.-B. (1958): Studio geologico e morfologico del territorio di Baceno e Premia (Val d'Ossola, Alpi Lepontine). Mem. Ist. Geol. Mineral. Univ. Padova, XX, 82p.

CLARKE D.B., CAMERON B.I., MUECKE G.K. and BATES J.L. (1989): Petrology and geochemistry of basalts from ODP Leg 105, hole 647A, Labrador Sea and the Davis Strait Area.Proceedings of the ODP, Scientific results, 105, 863-886.

COLOMBI A. (1989): Métamorphisme et géochimie des roches mafiques des Alpes ouest-centrales (géoprofil Viège-Domodossola-Locarno). Mém. Géol. Lausanne, 4, 216p.
CONTI P., MANATSCHAL G. and PFISTER M. (1994): Synrift sedimentation, Jurassic and Alpine tectonics in the Central Ortler Nappe (Eastern Alps, Italy). Eclogae geol. Helv., 87/1, 6-90.
CORNEN G., BESLIER M.-O. and GIRARDEAU J. (1996): Petrology of the mafic rocks cored in the Iberia abyssal plain. Proceedings of the ODP, Scientific results, 149, 449-465.
COX K.G., BELL J.D. and PANKHURST R.J. (1979): The interpretation of igneous rocks. George, Allen and Unwin, London.
CROSA LENZ P. and FRANGIONI G. (1996): Escursionismo in Valdossola: Antigorio-Formazza", Ed. Grossio, Domodossola, 3rd Ed., 238p.
CULLERS R.L. (1988): Mineralogical and chemical changes of soil and stream sediment formed by intense weathering of the Danburg granite, Geogia, U.S.A. Lithos, 21, 301-314.
DAL PIAZ G.V., HUNZIKER J.C. and MARTINOTTI G. (1972): La zona Sesia-Lanzo e l'evoluzione tettonico-metamorphica delle Alpi nordoccidentali interne. Mem. Soc. Geol. Ital., 11, 433-466.
DAL PIAZ G.V., DEL MORO A., MARTIN S. and VENTURELLI G. (1988): Post-collisional magmatism in the Ortler-Cevedale Masif (Northern Italy). Jahrb. Geol. Bundesanst., 131, 533-551.
DEBELMAS J. & LEMOINE M. (1957): Calcschistes piémontais et terrains à faciès briançonnais dans les hautes vallées de la Maira et de la Varaita. C.R.somm.Soc.géol.Fr., 38-40.
DEBELMAS J., OBERHAUSER R., SANDULESCU M. and TRÜMPY R. (1980): L'arc alpino-carpathique. In: J. Aubouin, J. Debelmas and M. Latreille (Editors). Géologie des chaînes alpines issues de la Téthys. Mém. B.R.G.M., 115, 86-95.
DELEZE J.-Y. (1999): Géologie et minéralogie de la région de la Cristallina. Diplôme Univ. Lausannne, Unpubl., 167p.
DELLA TORRE F. (1995): Géologie et minéralogie du pennique inférieur de la région de Robiei, Val Bavona (Tessin). Diplôme Univ. Lausannne, Unpubl., 71p.
DEUTSCH A. and STEIGER R.-H. (1985): Hornblende K-Ar ages and the climax of Tertiary metamorphism in the Lepontine Alps (south-central Switzerland); an old problem reassessed. Earth Planet. Sci. Lett., 72/2-3, 175-189.
DOLIVO E. (1982): Nouvelles observations structurales au SW du massif de l'Aar entre Visp et Gampel. Mat. Carte géol. Suisse, N.S., 157, 65p.
DRUCKMAN Y., HIRSCH F. and WEISSBROD T. (1982): The Triassic of the southern margin of the Tethys in the Levant and its correlation across the Jordan rift valley. Geol. Rundschau, 71/3, 919-936.
DUNCAN A.R. (1987): The Karoo igneous province – A problem area for inferring tectonic setting from basalt geochemistry. J. Volc. Geochem. res., 32, 13-34.
DUPUY C., MARSH J., DOSTAL J., MICHARD A. and TESTA S. (1988): Astenospheric and lithospheric sources for Mesozoic dolerites from Liberia (Africa): trace element and isotopic evidence. Earth Planet. Sci. Lett., 87, 100-110.
ELLENBERGER F. (1958): Etude géologique du pays de Vanoise. Mém. carte géol. France, 561p.
EPARD J.-L. (1990): La nappe de Morcles au sud-ouest du Mont-Blanc. Mém. Géol. Lausanne, 8, 165p.
ESCHER A., MASSON H. and STECK A. (1988): Coupes géologiques à travers la partie centrale des Alpes occidentales suisses. Rapp. Géol. Serv. Hydrol. Géol. Natl. Suisse, 2, 1-11.
ESCHER A., MASSON H. and STECK A. (1993): Nappe geometry in the western Swiss Alps. J. struct. Geol., 15/3-5, 501-509.
ESCHER A., HUNZIKER J.C., MASSON H., SARTORI M. and STECK A. (1997): Geologic framework and structural evolution of the western Swiss-Italian Alps. In: Pfiffner O.A., Lehner P., Heitzman P.Z., Mueller S. and Steck A. (Eds.), Deep Structure of the swiss Alps. Deutike, Vienna, 379-406.
ETTER U. (1984): Die Geologie zwischen Vqalle del Gries und Val Toggia (Novara, Italien). Lizentiatsarbeit Univ. Bern, Unpubl., 88p.
FAVEY S. (1999): Etude géologique et minéralogique du pennique inférieur au val Vannino (Val Formazza, Italie). Diplôme Univ. Lausannne, Unpubl., 185p.

FAVRE P. and STAMPFLI G.M. (1992): From rifting to passive margin; the example of the red Sea, central Atlantic and Alpine Tethys. Tectonophysics, 215/1-2, 69-97.
FED'KIN V.V. and ARANOVICH L.Ya. (1991): A new thermodynamic model of the staurolite-garnet geothermometer. USSR Acad. Sci., 146-150.
FERGUSON C.C., HARVEY P.K. and LLOYD G.E. (1980): On the mechanical interaction between a growing porphyroblast and its surrounding matrix. Contrib. Mineral. Petrol., 75, 339-352.
FIECHTNER L., FRIEDRICHSEN H. and HAMMERSCHMIDT K. (1992): Geochemistry and geochronology of early Mesozoic tholeiites from central Marocco. Geol. Runds., 81/1, 45-62.
FODOR R.V. and VETTER S.K. (1984): Rift-tone magmatism: petrology of basaltic rocks transitional from CFB to MORB, southeastern Brazil margin. Contrib. Mineral. Petrol., 88, 307-321.
FRANK E. (1983): Alpine metamorphism of calcareous rocks along a cross-section in the central Alps: occurrence and breakdown of muscovite, margarite and paragonite. Schweiz. mineral. petrogr. Mitt., 63, 37-93.
FREY M. and MÄHLMANN R.F. (1999): Alpine metamorphism of the Central Alps (Review). Schweiz. mineral. petrogr. Mitt., 79/1, 135-154.
GEBAUER D. (1999): Alpine geochronology of the Central and Western Alps; new constraints for a complex geodynamic evolution. Schweiz. mineral. petrogr. Mitt., 79/1, 191-208.
GERLACH H. (1869): Die Penninischen Alpen. Denkschr. Schweiz naturf. Ges., 23, 132p.
GIROUD N. and MEILHAC C. (2002): Etude géologique de la série du Versoyen et de ses relations avec la série du Petit-Saint-Bernard et la série des Brèches de Tarentaise, Savoie (France). Diplôme Univ. Lausannne, Unpubl., 161p.
GRAF M.-A. (1994): Géologie et métallogénie de la région de Bex-Ollon-Villars (VD). Diplôme Univ. Lausannne, Unpubl., 85p.
GRASEMANN B. and MANCKTELOW N.S. (1993): Two-dimensional thermal modelling of normal faulting; the Simplon fault zone, Central Alps, Switzerland. Tectonophysics, 225/3, 155-165.
GRECO A. (1985): Analisi strutturale della parte frontale del ricoprimento pennidico dell' Antigorio in Val Formazza (Novara, Italia). Schweiz. mineral. petrogr. Mitt., 65, 299-323.
GUBLER E., KAHLE H.G., KLINGELE E., MUELLER S. and OLIVIER R. (1981): Recent crustal movements in Switzerland and their geophysical interpretation. Tectonophysics, 71/1-4, 125-152.
HALL W.D.M. (1972): The structural geology and metamorphic history of the lower pennine nappes, Valle di Bosco, Ticino, Switzerland. Thesis Univ. London, 220p.
HAMMERSCHMIDT K. and FRANCK E. (1991): Relics of high pressure metamorphism in the lEpontine Alps (Switzerland) – $^{40}Ar/^{39}Ar$ and microprobe analyses on white K-micas. Schweiz. mineral. petrogr. Mitt., 71, 261-274.
HANSEN J.W. (1972): Zur Geologie, Petrographie and Geochemie der Bündnerschiefer-Serien zwischen Nufenenpass (Schweiz) and Cascata toce (Italia). Schweiz. mineral. petrogr. Mitt., 52/1, 109-153.
HANSMANN W. (1996): Age determination on the Tertiary Masino-Bregaglia (Bergell) intrusives (Italy, Switzerland): a review. Schweiz. mineral. petrogr. Mitt., 76/3, 421-451.
HEIM A. (1922): Geologie der Schweiz. T2, Tauchnitz, Leipzig, 1018p.
HIGGINS A. K. (1964): The structural and metamorphic geology of the area between Nufenenpass and Basodino Tessin, S. Switzerland. Thesis Univ. London, 251p.
HIGGINS A. K. (1964b): Fossil remains is staurolite-kyanite schists of the Bedretto-Mulde Bündnerschiefer. Eclogae geol. Helv. 57, 151-156.
HOLLAND T.J.B. and POWELL R. (1990): An enlarged and updated internally consistent thermodynamic dataset with uncertainties and $MgO$-$MnO$-$FeO$-$Fe_2O_3$-$Al_2O_3$-$TiO_2$-$SiO_2$-$C$-$H$-$H_2$-$O_2$. J. metamorphic Geol., 8, 89-124.
HOLLAND T.J.B. and POWELL R. (1994): Optimal geothermometry and geobarometry. Amer. Mineral., 79, 130-133.

HOLLAND T.J.B. and POWELL R. (1998): An internally consistent thermodynamic data set for phases of petrological interest. J. metamorphic Geol., 16/3, 309-343.
HOLLAND T.J.B. and POWELL R. (1999): The effect of $TiO_2$ and $Fe_2O_3$ on metapelitic assemblages at greenschist and amphibolite facies conditions; mineral equilibria calculations in the system $K_2O$-FeO-MgO-$Al_2O_3$-$SiO_2$-$H_2$-$Fe_2O_3$. J. metamorphic Geol., 18/5, 497-511.
HUNZIKER J.C. (1966): Zur Geologie und Geochemie des Gebietes zwischen Valle Antigorio (Provincia di Novara) und Valle di Campo (Kt. Tessin). Schweiz. mineral. petrogr. Mitt., 46/2, 473-552.
HUNZIKER J.C. (1969): Rb/Sr Alterbestimmungen aus den Walliser Alpen. Hellglimmer- und Gesamtgesteinsalterswerte. Eclogae geol. Helv., 62, 527-542.
HUNZIKER J.C. and BEARTH P. (1969): Rb-Sr Altersbestimmungen aus den Walliser Alpen. Biotitalterswerte und ihre Bedeutung für die Abkühlungsgeschichte der alpinen Metamorphose. Eclogae geol. Helv., 62, 205-222.
HUNZIKER J.C., DESMONS J. and MARTINOTTI G. (1989): Alpine thermal evolution in the central and western Alps. In: M.P. Coward, d. Dietrich and R.G. Park (Editors), Alpine Tectonics. Geol. Soc. Spec. Publ., 45, 353-367.
HUNZIKER J.C., DESMONS J. and HURFORD A.J. (1992): Thirty-two years of geochronological work in the central and Western Alps: a review on seven maps. Mém. Géol. Lausanne, 13.
HÜRLIMANN A., BESSON-HÜRLIMANN A. and MASSON H. (1996): Stratigraphie et tectonique de la partie orientale de l'écaille de la Gummfluh (Domaine Briançonnais des Préalpes). Mém. Géol. Lausanne, 28, 132p.
JÄGER E (1973): Phases of Alpine metamorphism; the changes of pressure and temperature in time. European Geophys. Soc., Meeting, Abstracts 1, 53p.
JAILLARD E., DONDEY H. and DEBELMAS J. (1986): Reconstitution paléogéographique de la zone briançonnaise de Vanoise (Alpes occidentales); nouveaux arguments pour une origine intra-briançonnaise de l'unité de la Grande Motte. C. R. Acad. Sci., Série II/302, 1091-1094.
JEANBOURQUIN P. (1994): The lower Penninic nappes in the Western Alps; the link between Helvetic and Penninic. J. struct. Geol., 16/6, 895-898.
JEANBOURQUIN P. and BURRI M. (1989): La zone de Sion-Courmayeur dans la région du Simplon. Rapp. Géol. Serv. Hydrol. Géol. Natl. Suisse, 11, 35p.
JEANBOURQUIN P. and BURRI M. (1991): Les métasédiments du Pennique inférieur dans la région de Brigue-Simplon; lithostratigraphie, structure et contexte géodynamique dans le bassin valaisan. Eclogae geol. Helv., 84/2, 463-581.
JENKYNS H.C. (1980): Cretaceous anoxic events; from continents to oceans. J. geol. Soc. London, 137/2, 171-188.
JENNY H. (1924): Die alpine Faltung: ihre Anordnung in Raum und Zeit. Berlin, 176p.
JOOS M.G. (1969): Zur Geologie und Petrographie der Monte-Giove-Gebirgsgruppe im östlichen Simplon-Gebiet (Novara, Italia). Schweiz. mineral. petrogr. Mitt., 49, 277-323.
KAMBERS B.S. (1993): Regional metamorphism and uplift along the southern margin of the Gotthard massif: results from the Nufenenpass area. Schweiz. mineral. petrogr. Mitt., 73/1, 241-257.
KELSEY C.H. (1965): Calculation of the CIPW norm. Mineral. Mag., 34, 276-282.
KELTS K. (1981): A comparison of some aspects of sedimentation and translational tectonics from the Gulf of California and the Mesozoic Tethys, northern Penninic margin. Eclogae geol. Helv. 74/2, 317-338.
KEUSEN H.-R. (1972): Mineralogie und Petrographie des metamorphen Ultramafitit-Komplexes von Geisspfad (Penninische Alpen). Schweiz. mineral. petrogr. Mitt., 52/3, 385-478.
KLAPER E.M. and BUCHER-NURMINEN K. (1987): Alpine metamorphism of pelitic schists in the Nufenen Pass area, Lepontine Alps. J. metamorphic Geol., 5/2, 175-194.
KNILL M.D. (1996): The Pb-Zn-As-Tl-Ba deposit at Lengenbach, Binn Valley, Switzerland. Mat. Géol. Suisse, Série géotechnique, Lief. 90, 56p.

KÖPPEL V. and GRUENENFELDER M. (1975): Concordant U-Pb ages of monazite and xenotime from the Central Alps and the timing of the high temperature Alpine metamorphism; a preliminary report. Schweiz. mineral. petrogr. Mitt., 55/1, 129-132.
KRAMAR N. (1997): La couverture mésozoïque de la région d'Artsinol (Val d'Hérens, Valais): relations avec les nappes du Mont Fort et du Tsaté. Diplôme Univ. Lausannne, Unpubl., 122p.
LEFEVRE R. (1982): Les nappes briançonnaises internes et ultrabriançonnaises dans les Alpes Cottiennes méridionales. Thesis Univ. Paris Sud, 435p.
LE MAITRE R.W, BATEMAN P., DUDEK A., KELLER J., LAMEYRE LE BAS M.J., SABINE P.A., SCHMID R., SORENSEN H., STRECKEISEN A., WOOLLEY A.R. and ZANETTIN B. (1989): A classification of igneous rocks and glossary of terms. Blackwell, Oxford, 193p.
LEMPICKA MÜNCH A. (1996): La géologie de la zone des cols de l'Oberland Bernois entre Geils (Adelboden) et la Sarine. Thesis Univ. Lausanne, 146p.
LEU W. (1986): Lithostratigraphie und Tektonik der nordpenninischen Sedimente in der region Bedretto-Baceno-Visp. Eclogae geol. Helv., 79/3, 769-824.
LISZKAY M. (1965): Geologie der Sedimentbedeckung des südwestlichen Gotthard-Massivs im Oberwallis. Eclogae geol. Helv., 58/2, 901-965.
LOUBAT H. (1968): Etude pétrographique des ophiolites de la zone du Versoyen, Savoie (France) et Province d'Aoste (Italie). Arch. Sc. Genève, 21/3, 265-457.
LUGEON M. (1901): Les grandes nappes de recouvrement des Alpes du Chablais et de la Suisse. Bull. Soc. géol. Fr., 1, 4ème série.
LUGEON M. and ARGAND E. (1905): Sur les grandes nappes de recouvrement de la zone du Piémont. C.R.S. Acad. Sci.
LÜTHY H.-J. (1965): Geologie der gotthardmassivischen Sedimentbedeckung und der penninischen Bündnerschiefer im Blinnental, Rappental und Binntal (Oberwallis). Inauguraldissertation Univ. Bern, 95p.
MANCKTELOW N.S. (1985): The Simplon Line: a major displacement zone in the western Lepontine Alps. Eclogae geol. Helv., 78, 73-96.
MANCKTELOW N.S. (1990): The Simplon Fault Zone. Beitr. geol. Karte Schweiz, 163, 74 p.
MANCKTELOW N.S. and PAVLIS T.L. (1994): Fold-fault relationships in low-angle detachment systems. Tectonics, 13/3, 668-685.
MARCHANT R.H. (1993): The underground of the Western Alps. Mém. Géol. Lausanne, 15, 137p.
MARCHANT R.H. and STAMPFLI G.M. (1997): Crustal and lithospheric structures of the Western Alps: geodynamic significance. In: Pfiffner, O.A., Lehner P., Heitzman P.Z., Mueller S. and Steck A. (Eds.), Deep Structure of the Swiss Alps, Results from NRP20, Birkhäuser AG, Basel, 326-337.
MASSON H., HERB R. and STECK A. (1980): Helvetic Alps of Western Switzerland. Geology of Switzerland, a guide-book, part B, Geological excursions, 109-153.
MCCLAY K. (1987): The mapping of geological structures. Geol. soc. of London handbook, 161p.
MCDONOUGH W.F. (1990): Constraints on the composition of the continental lithospheric mantle. Earth Planet. Sci. Lett., 101/1, 1-18.
MCKENZIE D. and O'NIONS. R.K.: Partial melt distributions from inversion of rare earth element concentrations. J. Petrol., 32/5, 1021-1091.
MEGARD-GALLI J. and FAURE J.-L. (1988): Tectonique distensive et sédimentation au Ladinien supérieur – Carnien dans la zone briançonnaise. Bull. Soc. géol. Fr., 8/IV/5, ,705-715.
MERLE O. (1987): Histoire de la déformation dans les Alpes lépontines occidentales. Bull. Soc. géol. Fr., 8/II/1, 183-190.
MERLE O., COBBOLD P.R. and SCHMID S. (1989): Tertiary kinematics in the Lepontine dome. Geol. Soc. Spec. Publ., 45, 113-134.
MICHARD A. (1967): Etude géologique dans les zones internes des alpes Cottiennes. Thesis C.N.R.S., 260, 401p.
MILNES A.G. (1973): Structural reinterpretation of the classic Simplon tunnel section of the Central Alps. Geol. Soc. Am., 84, 269-274.

MILNES A.G. (1974A): Post-nappe folding in the Western Lepontine Alps. Eclogae geol. Helv., 67/2, 333-348.
MILNES A.G. (1974B): Structure of the Pennine zone (Central Alps): a new working hypothesis. Geol. Soc. Am., 85, 1727-1732.
MORET L. (1954): Problèmes de stratigraphie et de tectonique dans les Alpes françaises. Trav. Lab. Géol. Univ. Grenoble, 31, 1.
NABHOLZ W.K. (1954): Gesteinsmaterial und Gebirgsbildung im Alpenquerschnitt Aar-Massiv-Seengebirge. Geol. Runds., 42/2, 155-171.
NIGGLI P., PREISWERK H., GRÜTTER O., BOSSARD L. and KÜNDIG E. (1936): Geologische Beschreibung der Tessiner Alpen zwischen Maggia- und Bleniotal. Beitr. geol. Karte Schweiz, N.F., 71, 190p.
PANTIC N. and GANSSER A. (1977): Palynologische Untersuchung in Bündnerschiefern. Eclogae geol. Helv., 70/1, 59-81.
PASSCHIER C.W. and TROUW R.A.J. (1998): Microtectonics. Springer Verlag, 253p.
PASTORELLI S. (1994): Il complesso ultramafico di Geisspfad e I suoi rapporti con le rocce incassanti. Diplôme Univ. Torino, Unpubl., 120p
PASTORELLI S., MARTINOTTI G., PICCARDO G.B., RAMPONE E. and SCAMBELLURI M. (1995): The Geisspfad complex and its relationships with the Monte Leone nappe (lower Pennine, Western Alps). Acad. Naz. Sci., detta dei XL, scritti e documenti XIV, 349-358.
PEARCE J.A. (1983): Role of the sub-continental lithosphere in magma genesis at active continenetal margins. In: Hawkesworth C.J. and Norry M.J. (Eds), Continental basalts and mantle xenoliths. Shiva, Nantwich, 230-249.
PEARCE J.A. (1984): A "user-guide" to basalt discrimination diagrams, unpubl.
PEARCE J.A., ALABASTER T., SHELTON A.W. and SEARLE M.P. (1981): The Oman ophiolite as a Cretaceous arc-basin complex: evidence and implications. Phil. Trans. R. Soc. A300, 299-300.
PE-PIPER G. and JANSA L.F. (1986): Triassic olivine-normative diabase from Northumberland Strait, eastern Canada: implications for continental rifting. Can. J. Earth Sci., 23, 1013-1021.
PE-PIPER G. and JANSA L.F. and LAMBERT R.St.J. (1992): Early Mesozoic magmatism on the Eastern canadian margin: petrogenetic and tectonic significance. Geol. Soc. Am. Sp. Paper, 268, 13-36.
PERFIT M.R., GUST D.A., BENCE A.E., ARCULUS R.J. and TAYLOR S.R. (1980): Chemical characteristics of island arc basalts: implications for mantle sources. Chem. Geol., 30, 227-256.
POLACK (1983): la fenêtre de Verampio: étude géologique et pétrographique. Diplôme Univ. Lausanne, 54p.
PREISWERK H. (1918): Geologische Beschreibung der Lepontinischen Alpen. II. Beitr. geol. K. Schweiz, 26.
PREISWERK H. and GRÜTTER O. (1925): Tessinergneis mit tektonischer Kartenskizze. Eclogae geol. Helv., 19, 177-187.
PROBST P. (1980): Die Bündnerschiefer des nördlichen Penninikums zwischen Valser Tal und Passo di San Giacomo. Thesis Univ. Bern, 64p.
RAMSAY J.G. (1967): Folding and fracturing of rocks. Mc-Graw-Hill, New-York.
REY (2001): Shear2F: un logiciel de modélisation tectonique. Thesis Univ. Lausannne, 163p.
REY (2002): Shear2F: un logiciel de modélisation tectonique. Mém. Géol. Lausanne, 47, 52p.
RINNGENBERG Y., TOMASSI A. and G.M. STAMPFLI (2002): The Jurassic sequence of the Niesen nappe in the region of Le Sépey – La Forclaz (Switzerland): witness of the Piemont rifting in the Helvetic paleogeographic domain. Bull. Soc. Vaud. Sc. Nat., 87/4, 353-372.
RODGERS J. and BEARTH P. (1960): Sur la "nappe" du Lebendun. C.R.S. Acad. Sci., 250/1, 156-158.
ROY S. (1997): Genetic diversity of manganese deposition in the terrestrial geological record. In. Niholson K., Hein J.R., Bühn B. and Dasgupta S. (eds), Manganese mineralization: geochemistry and mineralogy of terrestrial and marine deposits, Geol. Soc. Spec. Publ., 119, 5-27.

RUBATTO D., GEBAUER D. and COMPAGNONI R. (1999): Dating of eclogite-facies zircons: the age of Alpine metamorphism in the Sezia-Lanzo Zone (Western Alps). Earth planet. Sci. Lett., 167/3-4, 141-158.
SARTORI (1990): L'unité du Barrhorn (zone Pennique, Valais, Suisse). Mém. Géol. Lausanne, 6, 156p.
SCHAEDLI N. (2000): Géologie, minéralogie et géochimie isotopique et microthermométrie des inclusions fluides des cristaux de quartz des fissures alpines. Région du Griessee (Nufenen, Suisse). Diplôme Univ. Lausannne, Unpubl., 237p.
SCHARDT H. (1893): Sur l'origine des Préalpes romandes. Arch. Sci. Phys. Nat., Genève 30, 570-583.
SCHARDT H. (1903): Note sur le profil géologique et la tectonique du massif du Simplon suivi d'un rapport supplémentaire sur les venues d'eau rencontrées dans le Tunnel du Simplon du côté d'Iselle. Corbaz & Cie, Lausanne, 119p.
SCHARDT H. (1906): Die modernen Anschauungen über den Bau und die Entstehung des Alpengebirges. Mit Karte und Profiltafel. Verh. schweiz. nart. Ges., 1906.
SCHMIDT C. (1907): Uber die Geologie des Simplongebietes und der Tektonik der Schweizeralpen. Eclogae geol. Helv., 9/4, 484-584.
SCHMIDT C. and PREISWERK H. (1908): Geologische Karte der Simplon-Gruppe, 1:50'000. Geologische Spezialkarte Nr. 48, mit Erläurerung. Schweiz. geol. Komm.
SELVERSTONE J., SPEAR F.S., FRANZ G. and MORTEANI G. (1984): High-pressure metamorphism in the SW Tauern Window, Austria; P-T paths from hornblende-kyanite-staurolite schists. J. Petrol., 25/2, 501-531.
SMITH R.C., ROSE A.W. and LANNING R.M. (1975): Geology and geochemistry of Triassic diabase in Pennsylvania. Geol. Soc. Am. Bull., 86, 943-955.
SPEAR F.S. (1993): Metamorphic phase equilibria and pressure-temperature-time paths. Mineral. Soc. Am. Washington D.C, 799p.
SPEAR F.S., SELVERSTONE J., HICKMOTT D., CROWLEY P. and HODGES K.V. (1984): P-T paths from garnet zoning; a new technique for deciphering tectonic processes in crystalline terranes. Geology (Boulder), 12/2, 87-90.
SPICHER A. (1980): Tektonische karte der Schweiz, 1:500'000. Schweiz. Geol. Komm., Basel.
SPRING L., REYMOND B., MASSON H. and STECK A. (1992): La nappe du Lebendun entre Alte Kaserne et le Val Cairasca (massif du Simplon): nouvelles observations et interprétations. Eclogae geol. Helv., 85/1, 85-104.
STAMPFLI G.M. (1993): Le Briançonnais, terrain exotique dans les Alpes? Eclogae geol. Helv., 86/1, 1-45.
STAMPFLI G.M. and MARCHANT R.H. (1997): Geodynamic evolution of the Tethyan margins of the Western Alps. In: Pfiffner O.A., Lehner P., Heitzman P.Z., Mueller S. and Steck A. (Eds.), Deep Structure of the swiss Alps. Deutike, Vienna, 223-239.
STAMPFLI G.M., MOSAR J., MARQUER D., MARCHANT R., BAUDIN T. and BOREL G. (1998): Subduction and obduction processes in the Swiss Alps. Tectonophysics, 296, 159-204.
STAMPFLI G.M., BOREL G., CAVAZZA W., MOSAR J. and ZIEGLER P.A. (2001): The paleotectonic Atlas of the PeriThethyan Domain. European Geoph. Soc., Compact Disc.
STAUB R. (1924): Der Bau der Alpen. Beitr. Geol. Karte Schweiz (N.F.), 52, 272p.
STAUB R. (1958): Klippendecke und Zentralalpenbau. Beitr. Geol. Karte Schweiz (N.F.), 103, 184p.
STECK A. (1984): Structures de déformations tertiaires dans les Alpes centrales (transversale Aar-Simplon-Ossola). Eclogae geol. Helv., 77, 55-100.
STECK A. (1987): Le massif du Simplon-Réflexions sur la cinématique des nappes de gneiss. Schweiz. mineral. petrogr. Mitt., 67, 27-45.
STECK A. (1990): une carte des zones de cisaillement ductile des Alpes Centrales. Eclogae geol. Helv., 83, 603-627.

STECK A. and HUNZIKER J.C. (1994): The tertiary structural and thermal evolution of the Central Alps – compressional and extensional structures in an orogenic belt. Tectonophysics, 238, 229-254.
STECK A., BIGIOGGERO B., DAL PIAZ G.V., ESCHER A., MARTINOTTI G. and MASSON H. (1999): Carte tectonique des Alpes de Suisse occidentale et des régions avoisinantes, 1:100'000. Serv. Hydrol. Géol. Natl. Suisse, Carte géol. spéc. 123.
STECK A., EPARD J.-L., ESCHER A., GOUFFON Y. and MASSON H. (2001): Carte tectonique des Alpes de Suisse occidentale et des régions avoisinantes, 1:100'000. Carte géol. spéc. 123, notice explicative. OFEG, 73p.
STEFFEN D., JAQUES C., NYDEGGER T., PETROONS D. and WILDY W. (1993): La Brèche du Chablais à son extrémité occidentale (Hte-Savoie, France): Sédimentologie, éléments stratigraphiques et interprétation paléogéographique. Eclogae geol. Helv., 86/2, 543-568.
STELLA (1904): Sulla geologia della regione ossolana contigua al Sempione. Boll. Soc. Geol. Italiana, XXIII/1, 84-88.
STELLA (1905): Il problema geo-tettonico dell'Ossola e del Sempione. Boll. R. Com. Geol. Ital., 1, 39p.
STRECKEISEN A., AMSTUTZ G.Ch. and DESMONS J. (1998): Les métabasites du col de Saflisch, couverture du Monte-Leone, Pennique inérieur (valais): des basaltes andésitiques d'arc insulaire?. Schweiz. mineral. petrogr. Mitt., 78/1, 147-155.
STUDER B. (1851): Geologie der Schweiz. Bd1, Mittelzone und südliche Nebenzone der Alpen. Stämpflisch Verlagshandlung, Zürich, 485p.
SUN S.S. and NESBITT R.W. (1977): Chemical heterogeneity of the Archean mantle, composition of the earth and mantle evolution. Earth Planet. Sci. Lett., 35, 429-448.
SUN S.S. and SHARASKIN A.Y. (1979): geochemical characteristics of mid-ocean ridge basalts. Earth Planet. Sci. Lett., 44, 119-138.
SUN S.S. and MCDONOUGH W.F. (1989): Chemical and isotopic systematics of oceanic basalts: implications for mantle composition and processes. In: Saunders A.D. anf Norry M.J. (eds), Magmatism in the Ocean basins, Geol. Soc. Spec. Publ., 42, 313-345.
TAYLOR S.M. and MCLENNAN S.M. (1981): Evidence from rare-earth elements for the chemical composition of the Archaean crust. Geol. Soc. Australia, Spec. Publ., 7, 255-261.
TODD C.S. and ENGI M. (1997): Metamorphic field gradients in the Central Alps. J. metamorphic Geol., 15, 513-530.
TRÜMPY R. (1955): Remarques sur la correlation des unites externs entre la Savoie et le Valais et sur l'origine des nappes préalpines. Bull. Soc. geol. Fr., 6/5, 217-231.
VANCE D. and O'NIONS R.K. (1992): Prograde and retrograde thermal histories from the central Swiss Alps. Earth Planet. Sci. Lett., 114, 113-129.
VENTURINI G., MARTINOTTI G., ARMANDO G., BARBERO M. and HUNZIKER J.C. (1994): New field observations and lithostratigraphic subdivisions. Schweiz. mineral. petrogr. Mitt., 74/1, 115-125.
WENK E. (1955): Eine Strukturkarte der Tessineralpen. Schweiz. mineral. petrogr. Mitt., 35, 311-319.
WINCHESTER J.A. and FLOYD P.A. (+976): Geochemical magma type discrimination; application to altered and metamorphosed basic igneous rocks. Earth planet. Sci. Lett., 28, 459-469.
WYSS R. (1986): Die Urseren-Zone – Lithostratigraphie und Tektonik. Eclogae geol. Helv., 79/3, 731-767.

Atlas of Switzerland (2000), Compact Disc, Federal Office of Topography, Wabern.
National map of Switzerland, Sheet 265: Nufenenpass, 1:50'000, Federal Office of Topography, Wabern.
National map of Switzerland "Sheet 1270: Binntal, 1:25'000, Federal Office of Topography, Wabern.
National map of Switzerland "Sheet 1271: Basodino, 1:25'000, Federal Office of Topography, Wabern.

# ANNEXES

The first number of each annexe refers directly to the appropriate chapter

Annexe 2A Location of the green rocks (green) and the Sabbione metasandstone (pink) relatively to the Monte Leone basement (red) and the associated dolomitic marble (orange).

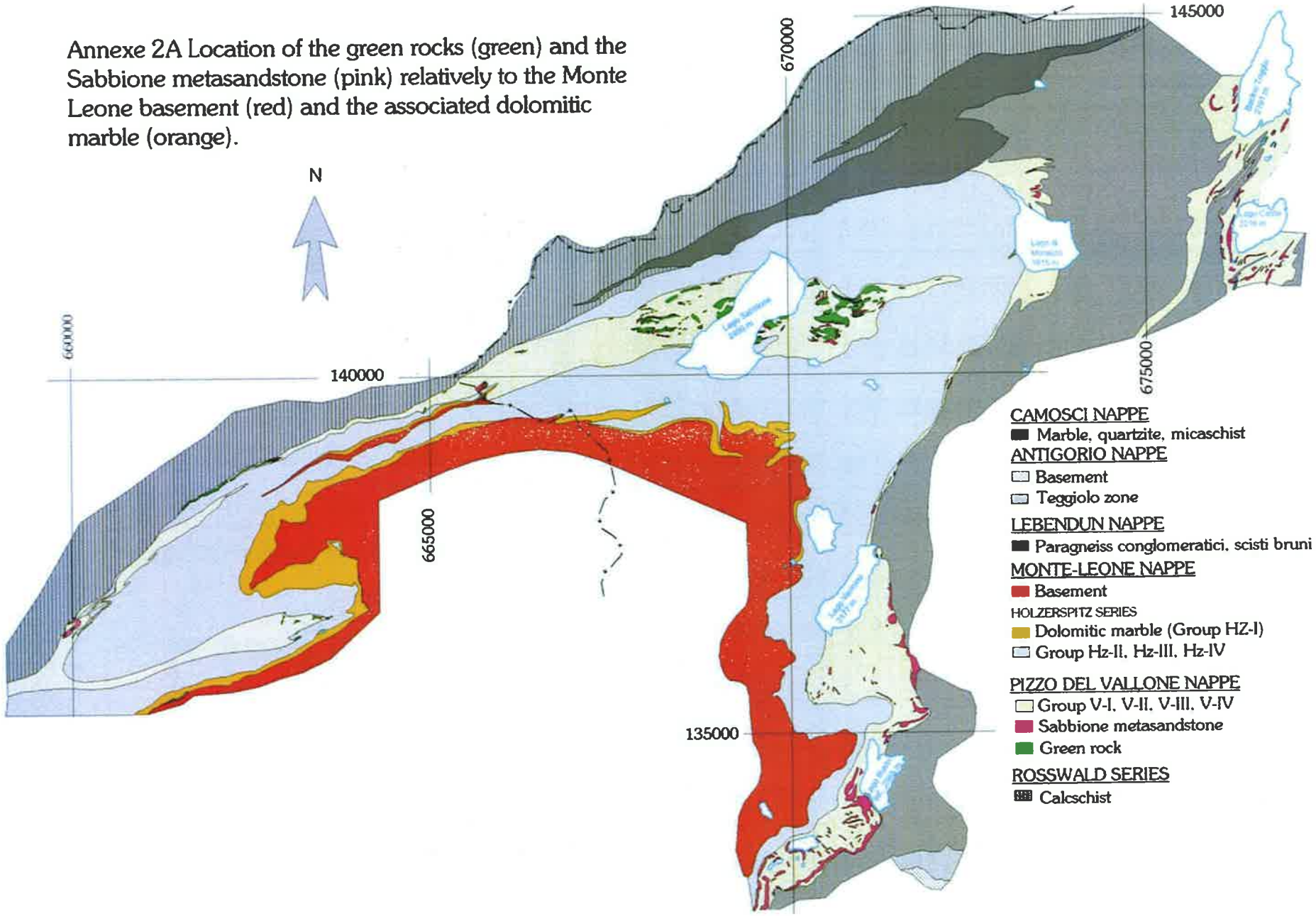

Annexe 4A Microprobe analysises (activities calculated by Thermocalc)

| BIOTITE | ECB16 | StDev ECB16 | EC97 | StDev EC97 | EC31 | StDev EC31 | EC137 | StDev EC137 | EC27 | StDev EC27 | EC179 | StDev EC179 | EC204 | StDev EC204 |
|---|---|---|---|---|---|---|---|---|---|---|---|---|---|---|
| SiO2 | 37.77 | 0.44 | 37.25 | 0.40 | 37.12 | 0.49 | 36.57 | 2.06 | 37.10 | 0.76 | 35.50 | 0.35 | 37.08 | 0.65 |
| TiO2 | 1.51 | 0.12 | 1.49 | 0.24 | 1.13 | 0.17 | 0.80 | 0.42 | 1.52 | 0.16 | 1.56 | 0.05 | 1.29 | 0.28 |
| Al2O3 | 18.90 | 0.32 | 19.15 | 0.77 | 19.51 | 0.64 | 20.25 | 3.22 | 19.11 | 1.18 | 19.05 | 0.32 | 19.45 | 1.22 |
| Cr2O3 | 0.05 | 0.02 | 0.06 | 0.02 | 0.04 | 0.01 | 0.05 | 0.02 | 0.04 | 0.01 | 0.06 | 0.03 | 0.05 | 0.03 |
| FeO | 15.10 | 0.54 | 15.82 | 0.60 | 15.87 | 0.55 | 17.68 | 3.38 | 15.96 | 1.72 | 19.22 | 0.43 | 15.31 | 0.82 |
| MnO | 0.09 | 0.02 | 0.01 | 0.01 | 0.04 | 0.02 | 0.03 | 0.02 | 0.05 | 0.03 | 0.03 | 0.02 | 0.02 | 0.03 |
| MgO | 12.86 | 0.48 | 12.42 | 0.59 | 12.45 | 0.34 | 10.25 | 2.02 | 12.24 | 0.98 | 10.20 | 0.27 | 13.13 | 0.69 |
| Na2O | 0.17 | 0.06 | 0.39 | 0.11 | 0.35 | 0.06 | 0.10 | 0.07 | 0.20 | 0.09 | 0.46 | 0.10 | 0.37 | 0.37 |
| K2O | 9.03 | 0.26 | 8.82 | 0.16 | 8.71 | 0.19 | 11.31 | 0.59 | 9.00 | 0.33 | 9.01 | 0.29 | 8.87 | 0.74 |
| Nbs analysis | 43 | | 23 | | 25 | | 69 | | 19 | | 34 | | 19 | |
| a(phl) | 0.092 | 0.0166 | 0.083 | 0.0159 | 0.088 | 0.0163 | 0.072 | 0.0147 | 0.082 | 0.0158 | 0.050 | 0.0120 | 0.097 | 0.0170 |
| a(ann) | 0.023 | 0.0070 | 0.026 | 0.0078 | 0.027 | 0.0079 | 0.048 | 0.0117 | 0.028 | 0.0081 | 0.051 | 0.0121 | 0.023 | 0.0072 |
| a(east) | 0.069 | 0.0143 | 0.066 | 0.0141 | 0.068 | 0.0143 | 0.061 | 0.0134 | 0.065 | 0.0139 | 0.049 | 0.0119 | 0.074 | 0.0150 |

| MUSCOVITE | ECB16 | StDev ECB16 | EC97 | StDev EC97 | EC31 | StDev EC31 | EC137 | StDev EC137 | EC27 | StDev EC27 | EC179 | StDev EC179 | EC204 | StDev EC204 |
|---|---|---|---|---|---|---|---|---|---|---|---|---|---|---|
| SiO2 | 47.81 | 1.38 | 46.91 | 0.55 | 47.20 | 0.79 | 46.64 | 0.39 | 46.78 | 1.86 | 47.19 | 0.26 | 46.59 | 1.55 |
| TiO2 | 0.36 | 0.10 | 0.39 | 0.08 | 0.36 | 0.07 | 0.50 | 0.08 | 0.45 | 0.19 | 0.31 | 0.05 | 0.25 | 0.13 |
| Al2O3 | 33.24 | 1.68 | 33.83 | 1.03 | 33.60 | 0.99 | 34.33 | 0.57 | 33.53 | 2.15 | 34.58 | 0.46 | 38.03 | 1.90 |
| FeO | 1.28 | 0.19 | 1.25 | 0.23 | 1.09 | 0.16 | 1.43 | 0.25 | 0.94 | 0.21 | 1.43 | 0.13 | 0.63 | 0.29 |
| MnO | 0.01 | 0.01 | 0.00 | 0.01 | 0.01 | 0.01 | 0.01 | 0.01 | 0.01 | 0.01 | 0.01 | 0.01 | 0.01 | 0.02 |
| MgO | 1.52 | 0.49 | 1.38 | 0.30 | 1.41 | 0.28 | 1.18 | 0.15 | 0.74 | 0.35 | 1.08 | 0.17 | 0.32 | 0.28 |
| CaO | 0.03 | 0.06 | 0.01 | 0.01 | 0.02 | 0.01 | 0.01 | 0.04 | 0.07 | 0.12 | 0.01 | 0.01 | 0.36 | 0.25 |
| Na2O | 0.76 | 0.20 | 1.36 | 0.17 | 1.33 | 0.14 | 0.46 | 0.05 | 0.94 | 0.18 | 1.03 | 0.06 | 4.64 | 1.93 |
| K2O | 10.08 | 0.24 | 9.16 | 0.16 | 9.12 | 0.16 | 10.78 | 0.22 | 10.73 | 0.73 | 9.52 | 0.24 | 4.02 | 3.06 |
| Nbs analysis | 40 | | 10 | | 19 | | 80 | | 13 | | 10 | | 29 | |
| a (mu) | 0.66 | 0.066 | 0.65 | 0.065 | 0.65 | 0.065 | 0.72 | 0.072 | 0.75 | 0.075 | 0.68 | 0.068 | 0.69 | 0.0694 |
| a(pa) | 0.751 | 0.0751 | 1.10 | 0.1103 | 1.06 | 0.1056 | 0.603 | 0.0603 | 0.967 | 0.0967 | 1.07 | 0.1073 | 0.80 | 0.080 |
| a(cel) | 0.045 | 0.0112 | 0.037 | 0.0096 | 0.039 | 0.0100 | 0.032 | 0.0087 | 0.023 | 0.0067 | 0.028 | 0.0078 | - | - |
| | | | | | | | | | | | | | 0.0349 | 0.00924 |

| GARNET | ECB16 | StDev ECB16 | EC97 | StDev EC97 | EC31 | StDev EC31 | EC137 | StDev EC137 | EC27 | StDev EC27 | EC179 | StDev EC179 | EC204 | StDev EC204 |
|---|---|---|---|---|---|---|---|---|---|---|---|---|---|---|
| SiO2 | 37.88 | 0.16 | 37.52 | 0.22 | 37.58 | 0.15 | 37.74 | 0.15 | 37.72 | 0.21 | 36.99 | 0.33 | 37.67 | 0.23 |
| TiO2 | 0.10 | 0.12 | 0.08 | 0.07 | 0.07 | 0.02 | 0.09 | 0.04 | 0.09 | 0.02 | 0.06 | 0.03 | 0.08 | 0.03 |
| Al2O3 | 21.04 | 0.11 | 20.71 | 0.20 | 20.82 | 0.19 | 20.99 | 0.10 | 20.94 | 0.17 | 20.55 | 0.09 | 20.82 | 0.07 |
| Cr2O3 | 0.04 | 0.02 | 0.04 | 0.02 | 0.04 | 0.02 | 0.04 | 0.02 | 0.04 | 0.02 | 0.05 | 0.03 | 0.04 | 0.02 |
| FeO | 30.59 | 0.48 | 32.00 | 0.42 | 32.21 | 0.51 | 31.03 | 0.29 | 30.55 | 5.47 | 34.49 | 0.84 | 32.45 | 0.35 |
| MnO | 1.03 | 0.14 | 0.39 | 0.06 | 0.26 | 0.11 | 0.37 | 0.05 | 0.59 | 0.41 | 1.92 | 0.10 | 0.15 | 0.09 |
| MgO | 2.40 | 0.21 | 2.64 | 0.33 | 2.82 | 0.42 | 3.31 | 0.08 | 3.68 | 0.40 | 2.36 | 0.10 | 3.43 | 0.24 |
| CaO | 8.00 | 0.60 | 7.11 | 0.78 | 6.94 | 0.76 | 7.24 | 0.27 | 6.10 | 0.56 | 3.67 | 0.78 | 5.87 | 0.55 |
| Nbs analysis | 50 | | 48 | | 43 | | 29 | | 28 | | 24 | | 23 | |
| a(py) | 0.00257 | 0.001148 | 0.0031 | 0.00134 | 0.0035 | 0.00153 | 0.0056 | 0.00229 | 0.0070 | 0.00274 | 0.00163 | 0.000762 | 0.0053 | 0.00218 |
| a(gr) | 0.013 | 0.00469 | 0.0093 | 0.00347 | 0.0089 | 0.00334 | 0.0108 | 0.00393 | 0.0078 | 0.00301 | 0.0014 | 0.00066 | 0.0059 | 0.00237 |
| a(alm) | 0.26 | 0.039 | 0.29 | 0.043 | 0.29 | 0.043 | 0.25 | 0.037 | 0.27 | 0.040 | 0.40 | 0.060 | 0.30 | 0.045 |
| a(sps) | 0.000011 | 0.0000061 | - | - | - | - | - | - | 0.0000020 | 0.00000118 | 0.000076 | 0.000042 | - | - |

| STAUROTIDE | | | EC97 | StDev EC97 | EC31 | StDev EC31 | | | EC27 | StDev EC27 | EC179 | StDev EC179 | EC204 | StDev EC204 | EC278 | StDev EC278 |
|---|---|---|---|---|---|---|---|---|---|---|---|---|---|---|---|---|
| SiO2 | | | 27.19 | 0.23 | 27.46 | 0.24 | | | 27.81 | 0.16 | 27.71 | 0.32 | 27.95 | 0.22 | 27.95 | 0.28 |
| TiO2 | | | 0.47 | 0.21 | 0.55 | 0.08 | | | 0.68 | 0.08 | 0.58 | 0.15 | 0.57 | 0.08 | 0.60 | 0.03 |
| Al2O3 | | | 54.47 | 0.38 | 53.99 | 0.40 | | | 53.47 | 0.24 | 53.62 | 0.53 | 53.78 | 0.35 | 54.46 | 0.21 |
| FeO | | | 10.86 | 0.47 | 12.24 | 0.14 | | | 12.18 | 0.28 | 14.13 | 0.14 | 12.60 | 0.25 | 10.58 | 0.23 |
| MnO | | | 0.03 | 0.02 | 0.12 | 0.03 | | | 0.20 | 0.02 | 0.09 | 0.03 | 0.03 | 0.02 | 0.02 | 0.02 |
| MgO | | | 1.60 | 0.11 | 1.72 | 0.16 | | | 1.85 | 0.17 | 1.56 | 0.10 | 2.04 | 0.11 | 1.37 | 0.08 |
| ZnO | | | 2.87 | 0.15 | 1.17 | 0.06 | | | 0.99 | 0.09 | 0.72 | 0.09 | 0.89 | 0.10 | 2.62 | 0.20 |
| Nbs analysis | | | 12 | | 12 | | | | 11 | | 19 | | 28 | | 15 | |
| a(mst) | | | 0.0019 | 0.00096 | 0.0018 | 0.00091 | | | 0.0025 | 0.00119 | 0.00082 | 0.00045 | 0.0026 | 0.00124 | 0.0013 | 0.00067 |
| a(fst) | | | 0.39 | 0.078 | 0.40 | 0.079 | | | 0.36 | 0.073 | 0.48 | 0.095 | 0.36 | 0.072 | 0.43 | 0.087 |

| FELDSPATH | ECB16 | StDev ECB16 | EC97 | StDev EC97 | EC31 | StDev EC31 | EC137 | StDev EC137 | EC27 | StDev EC27 | | | EC204 | StDev EC204 | EC278 | StDev EC278 |
|---|---|---|---|---|---|---|---|---|---|---|---|---|---|---|---|---|
| SiO2 | 59.37 | 1.00 | 60.38 | 0.44 | 60.43 | 0.52 | 62.52 | 2.37 | 47.52 | 1.58 | | | 62.49 | 0.91 | 61.00 | 0.56 |
| Al2O3 | 25.51 | 0.65 | 24.52 | 0.26 | 24.59 | 0.24 | 23.38 | 1.55 | 33.54 | 1.17 | | | 23.38 | 0.67 | 23.88 | 0.40 |
| FeO | 0.04 | 0.05 | 0.09 | 0.05 | 0.05 | 0.04 | 0.07 | 0.08 | 0.03 | 0.03 | | | 0.06 | 0.07 | 0.14 | 0.18 |
| CaO | 7.10 | 0.66 | 6.08 | 0.24 | 6.05 | 0.33 | 5.06 | 0.93 | 16.84 | 1.24 | | | 4.42 | 0.41 | 5.53 | 0.30 |
| Na2O | 7.45 | 0.38 | 8.12 | 0.20 | 8.16 | 0.23 | 8.45 | 0.69 | 1.98 | 0.75 | | | 8.86 | 0.37 | 8.50 | 0.18 |
| K2O | 0.14 | 0.13 | 0.06 | 0.02 | 0.05 | 0.02 | 0.24 | 0.07 | 0.03 | 0.02 | | | 0.13 | 0.20 | 0.07 | 0.03 |
| Nbs analysis | 27 | | 20 | | 21 | | 44 | | 18 | | | | 43 | | 30 | |
| a(an) | 0.55 | 0.0273 | 0.46 | 0.0267 | 0.45 | 0.0271 | 0.38 | 0.0292 | 0.86 | 0.0430 | | | 0.33 | 0.0296 | 0.44 | 0.0277 |
| a(ab) | 0.66 | 0.0330 | 0.71 | 0.0357 | 0.72 | 0.0358 | 0.75 | 0.0374 | 0.35 | 0.0296 | | | 0.78 | 0.0391 | 0.74 | 0.0370 |

| EPIDOTE | ECB16 | StDev B16 | EC179 | StDev EC179 |
|---|---|---|---|---|
| SiO2 | 38.35 | 0.56 | 37.53 | 0.34 |
| TiO2 | 0.19 | 0.03 | 0.14 | 0.01 |
| Al2O3 | 28.96 | 0.38 | 26.80 | 0.50 |
| Cr2O3 | 0.01 | 0.01 | 0.01 | 0.01 |
| FeO | 5.54 | 0.34 | 6.79 | 1.61 |
| MnO | 0.05 | 0.04 | 0.22 | 0.11 |
| MgO | 0.05 | 0.02 | 0.18 | 0.13 |
| CaO | 23.44 | 0.19 | 20.94 | 0.15 |
| Nbs analysis | 22 | | 18 | |
| a(cz) | 0.62 | 0.062 | 0.46 | 0.046 |
| a(ep) | 0.33 | 0.033 | 0.37 | 0.037 |
| a(fep) | 0.0075 | 0.00251 | 0.0102 | 0.00329 |

| AMPHIBOLE | EC137 | StDev EC137 | ECB16 | StDev ECB16 |
|---|---|---|---|---|
| SiO2 | 42.11 | 0.47 | 25.91 | 0.27 |
| TiO2 | 0.48 | 0.09 | 0.10 | 0.03 |
| Al2O3 | 17.12 | 0.50 | 22.99 | 0.30 |
| FeO | 16.31 | 0.31 | 0.03 | 0.02 |
| MnO | 0.05 | 0.03 | 21.65 | 0.44 |
| MgO | 8.36 | 0.18 | 0.17 | 0.02 |
| CaO | 10.62 | 0.34 | 17.58 | 0.49 |
| Na2O | 1.48 | 0.15 | 0.01 | 0.01 |
| K2O | 0.48 | 0.07 | 0.02 | 0.01 |
| Nbs analysis | 28 | | 19 | |
| a(tr) | 0.03931 | 0.009828 | 0.056 | 0.0119 |
| a(fact) | 0.00083 | 0.000478 | 0.0097 | 0.00366 |
| a(ts) | 0.013 | 0.0045 | 0.056 | 0.0118 |
| a(parg) | 0.1910 | 0.0477 | | |
| a(gl) | 0.01789 | 0.005467 | | |

| ILMENITE | EC179 | StDev EC179 | ECB16 | StDev ECB16 |
|---|---|---|---|---|
| SiO2 | 0.06 | 0.03 | 0.03 | 0.0185 |
| TiO2 | 52.88 | 0.71 | 53.51 | 1.3724 |
| Al2O3 | 0.01 | 0.01 | 0.01 | 0.0087 |
| Cr2O3 | 0.04 | 0.03 | 0.06 | 0.0470 |
| FeO | 46.68 | 0.44 | 45.92 | 0.7061 |
| MnO | 0.40 | 0.04 | 0.25 | 0.0150 |
| MgO | 0.07 | 0.02 | 0.53 | 0.1315 |
| CaO | 0.02 | 0.02 | 0.06 | 0.0241 |
| Nbs analysis | 10 | | 12 | |
| a(ilm) | 0.98 | 0.098 | 0.96 | 0.096 |
| a(hem) | - | - | - | - |
| a(pnt) | 0.0086 | 0.0028 | 0.0052 | 0.0018 |
| a(gelk) | 0.0025 | 0.0019 | 0.020 | 0.0058 |

a(-) = activity of the pure pôle
StDev = Standard Deviation
Nbs = Number of

## Annexe 4B Personal adaptation and abbreviations

I chose XH2O = 0.8 because the proximity of calcschist, marble,... certainly induced a probable presence of XCO2 in the metamorphi fluids, and because the presence of non-negligible quantities of graphite in the micaschist proves that C is present in the rock.

alm: almandine, amph: green amphibole, an: anorthite, ann: annite, as: aluminosilicate, bt: biotite, cd: cordierite, chl: chlorite, cld: chloritoide, ep: epidote, fcd: ferrocordierite, FP: alkaline feldspath, fst: ferrostaurolite, gph: graphite, gt: garnet, ilm: ilménite, ky: kyanite, lws: lawsonite, marg: margarite, ms: muscovite, phl: phlogopite, q: quartz, ru: rutile, st: staurolite, zo: zoisite.

## Annexe 4C Gibb's modelling

**Sample EC97**
**Minerals**: Quartz, Water, Garnet, Biotite, Plagioclase, Muscovite, Staurotide, Epidote, Chlorite
**System**: Si, Al, Mn, Fe, Mg, K, Ca, Na, H
**Phases:**
50 Garnet: Xpyrope = 0.1096; Xalmandin = 0,7216; Xspessartin = 0.0132; Xgrossular = 0.1753
51 Biotite: Xphlogopite = 0.6021; Xannite = 0.3975; XMnBiotite = 0.0003
48 Plagioclase: Xalbite = 0.7068; Xanorthite = 0.2932
45 Muscovite: Xmuscovite = 0.8188; Xparagonite = 0.1812
12 Staurotide: XMgStaurotide = 0.2070; XFeStaurotide = 0.7904; XMnStaurotide = 0.0026
30 Epidote: Xclinozoisite = 0.6200; Xepidote = 0.3800
14 Chlorite: XMgChlorite = 0.5816; XFeChlorite = 0.4167; XMnChlorite = 0.0017
**T°** initial: 510°C
**P** initial: 7750kbar

| Steps | Dgrossular | Dalmandin | Dspessartin | 510°C | 7750kbar | Xanorhtite |
|---|---|---|---|---|---|---|
| 1 | 0.0209 | -0.0011 | -0.0010 | 496.4 | 8272.8 | 23% |
| | Staurotie out, chlorite in | | | | | |
| 2 | 0.0209 | -0.0131 | 0.0007 | 484.2 | 9009.2 | 17% |
| 3 | 0.0145 | -0.0038 | -0.0049 | 475.3 | 9500.5 | 14% |
| 4 | -0.0075 | 0.0059 | 0.0015 | 478.3 | 9128.4 | 16% |
| 5 | 0.0114 | -0.0076 | 0.0028 | 469 | 9358.8 | 14% |
| 6 | 0.0040 | -0.0044 | 0.0060 | 462.8 | 9204.9 | 14% |
| 7 | -0.0014 | 0.0001 | 0.0031 | 461.8 | 9008.4 | 14% |
| 8 | 0.0125 | -0.0128 | 0.0061 | 451.5 | 9239.4 | 12% |
| 9 | -0.0196 | 0.0156 | 0.0024 | 461.2 | 8350.2 | 16% |
| 10 | 0.0161 | -0.0146 | 0.0051 | 448.7 | 8739.3 | 13% |
| 11 | -0.0176 | 0.0069 | 0.0087 | 457.7 | 7900 | 16% |
| 12 | 0.0079 | -0.0057 | -0.0001 | 452.6 | 8171.9 | 15% |
| 13 | -0.0092 | 0.0056 | 0.0026 | 457.2 | 7740.5 | 17% |
| 14 | 0.0054 | -0.0164 | 0.0129 | 452.6 | 7802.8 | 16% |
| 15 | 0.0021 | -0.0082 | 0.0105 | 447 | 7514 | 16% |
| 16 | -0.0078 | -0.0017 | 0.0098 | 449.3 | 7009 | 18% |
| 17 | -0.0088 | -0.0115 | 0.0217 | 449.8 | 6285 | 21% |
| 18 | 0.0008 | -0.0129 | 0.0064 | 455.6 | 6749 | 20% |
| 19 | 0.0005 | -0.0020 | 0.0123 | 443.6 | 5863 | 22% |
| 20 | -0.0144 | -0.0060 | 0.0225 | 443.9 | 4756.5 | 28% |
| 21 | -0.0015 | -0.0081 | 0.0103 | 440.1 | 4465.4 | 29% |
| 22 | -0.0074 | -0.0340 | 0.0444 | 433.2 | 3397.8 | 40% |
| 23 | -0.0063 | -0.0373 | 0.0491 | 417.7 | 1932.1 | 57% |

**Sample EC31**
**Minerals**: Quartz, Water, Garnet, Biotite, Plagioclase, Muscovite, Staurotide, Epidote, Chlorite
**System**: Si, Al, Mn, Fe, Mg, K, Ca, Na, H
**Phases:**
50 Garnet: Xpyrope = 0.1282; Xalmandin = 0.7249; Xspessartin = 0.0091; Xgrossular = 0.1549
51 Biotite: Xphlogopite = 0.6033; Xannite = 0.3959; XMnBiotite = 0.0008
48 Plagioclase: Xalbite = 0.7072; Xanorthite = 0.2938
45 Muscovite: Xmuscovite = 0.8144; Xparagonite = 0.1856
12 Staurotide: XMgStaurotide = 0.2063; XFeStaurotide = 0.7801; XMnStaurotide = 0.0136
30 Epidote: Xclinozoisite = 0.8; Xepidote = 0.2
14 Chlorite: XFeChlorite = 0.4167; XMgChlorite = 0.5816; XMnChlorite = 0.0017
**T°** initial: 550°C
**P** initial: 8000kbar

| Steps | Dgrossular | Dalmandin | Dspessartin | 550°C | 8000kbar | Xanorhtite |
|---|---|---|---|---|---|---|
| 1 | 0.0234 | 0.0029 | -0.0032 | 492.6 | 8206.4 | 20% |
| 2 | 0.0294 | -0.0080 | -0.0001 | 468.9 | 9389.7 | 27% |
| 3 | 0.0080 | -0.0005 | 0.0019 | 459.1 | 9534.5 | 11% |
| 4 | -0.0039 | 0.0101 | 0.0029 | 455.7 | 8749.2 | 12% |
| 5 | 0.0015 | -0.0068 | 0.0138 | 448.7 | 8254.5 | 13% |
| 6 | -0.0236 | -0.0403 | 0.0711 | 453.5 | 5410.9 | 24% |
| 7 | -0.0069 | -0.0876 | 0.1204 | 418.3 | 1749 | 58% |

Annexe 4C Gibb's modelling

**Sample ECB16**
**Minerals**: Quartz, Water, Garnet, Biotite, Plagioclase, Muscovite, Staurotide, Epidote, Chlorite
**System**: Si, Al, Mn, Fe, Mg, K, Ca, Na, H
**Phases:**
50 Garnet: Xpyrope = 0.0.0997; Xalmandin = 0.6816; Xspessartin = 0.0216; Xgrossular = 0.2007
51 Biotite: Xphlogopite = 0.6179; Xannite = 0.3798; XMnBiotite = 0.0022
48 Plagioclase: Xalbite = 0.6497; Xanorthite = 0.3503
45 Muscovite: Xmuscovite = 0.9868; Xparagonite = 0.0132
30 Epidote: Xclinozoisite = 0.6900; Xepidote = 0.3100
14 Chlorite: XFeChlorite = 0.4072; XMgChlorite = 0.5895; XMnChlorite = 0.0033

**T°** initial: 480°C
**P** initial: 6900kbar

| **Steps** | Dgrossular | Dalmandin | Dspessartin | 480°C | 6900kbar | Xanorhtite |
|---|---|---|---|---|---|---|
| 1 | 0.0328 | -0.0189 | 0.0018 | 464.6 | 8104 | 15% |
| 2 | 0.0011 | 0.0012 | 0.0003 | 463.7 | 8027 | 15% |
| 3 | -0.0080 | 0.0111 | 0.0021 | 466.4 | 7292 | 18% |
| 4 | -0.0019 | 0.0073 | 0.0048 | 464.9 | 6624 | 20% |
| 5 | 0.0201 | -0.0291 | 0.0168 | 453.7 | 7100 | 17% |
| 6 | 0.0043 | -0.0086 | 0.0168 | 447.7 | 6369 | 18% |
| 7 | -0.0084 | -0.0264 | 0.0375 | 447 | 5538 | 22% |
| 8 | -0.0015 | -0.0267 | 0.0335 | 442.6 | 4846 | 24% |
| 9 | -0.0089 | -0.0172 | 0.0321 | 439.3 | 3777 | 31% |
| 10 | -0.0044 | -0.0111 | 0.0149 | 439 | 3520 | 34% |
| 11 | -0.0030 | -0.0036 | 0.0086 | 437.6 | 3168 | 38% |
| 12 | 0.0084 | -0.0085 | -0.0040 | 438.9 | 3088 | 36% |

Annexe 4D P-T recalculated by Thermocalc by varying X(H2O)

BGR2, Gotthard Massif

| XH2O | sigfit | fit | P | T | DT | corr. | React. |
|---|---|---|---|---|---|---|---|
| 1 | 1.37 | 0.93 | 7 | 544 | 33 | 0.915 | 11 |
| 0.8 | 1.37 | 0.94 | 6.9 | 534 | 32 | 0.913 | 11 |
| 0.6 | 1.37 | 0.95 | 6.8 | 526 | 32 | 0.912 | 11 |

"corr." = the correlation c
"React." = the number of reactions found by The

Kambers obtained P=5kbar and T=530°C

BGR17, Nufenen Zone

| XH2O | sigfit | fit | P | T | DT | corr. | React. |
|---|---|---|---|---|---|---|---|
| 1 | 1.54 | 1.33 | 8 | 579 | 62 | 0.939 | 6 |
| 0.8 | 1.54 | 1.34 | 7.9 | 570 | 61 | 0.939 | 6 |
| 0.6 | 1.54 | 1.35 | 7.8 | 562 | 60 | 0.939 | 6 |

"corr." = the correlation c
"React." = the number of reactions found by The

Kambers obtained P=4,8kbar and T=480°C

BGR36, Corno Schuppe

| XH2O | sigfit | fit | P | T | DT | corr. | React. |
|---|---|---|---|---|---|---|---|
| 1 | 1.45 | 0.58 | 9.4 | 627 | 80 | 0.988 | 8 |
| 0.8 | 1.45 | 0.61 | 9.6 | 625 | 80 | 0.988 | 8 |
| 0.6 | 1.45 | 0.63 | 9.7 | 622 | 80 | 0.988 | 8 |

"corr." = the correlation c
"React." = the number of reactions found by The

Kambers obtained P=6kbar and T=520°C

BGR39, Bedretto Zone

| XH2O | sigfit | fit | P | T | DT | corr. | React. |
|---|---|---|---|---|---|---|---|
| 1 | 1.54 | 0.68 | 9.4 | 583 | 82 | 0.949 | 6 |
| 0.8 | 1.54 | 0.68 | 9.6 | 580 | 81 | 0.95 | 6 |
| 0.6 | 1.54 | 0.68 | 9.7 | 577 | 80 | 0.952 | 6 |

"corr." = the correlation c
"React." = the number of reactions found by The

Kambers obtained P=6kbar and T=525°C

M36 (X:685'920/Y:148'105), Maggia Nappe

| XH2O | sigfit | fit | P | T | DT | corr. | React. |
|---|---|---|---|---|---|---|---|
| 1 | 1.61 | 0.37 | 9.2 | 615 | 21 | 0.242 | 5 |
| 0.8 | 1.61 | 0.45 | 8.8 | 595 | 20 | 0.224 | 5 |
| 0.6 | 1.61 | 0.54 | 8.5 | 578 | 18 | 0.219 | 5 |

"corr." = the correlation c
"React." = the number of reactions found by The

Délèze obtained P=10±2kbar and T=580±60°C.

Ma9464 (X:682'980/Y:145'000), Maggia Nappe

| XH2O | sigfit | fit | P | T | DT | corr. | React. |
|---|---|---|---|---|---|---|---|
| 1 | 1.54 | 1.36 | 8.8 | 608 | 60 | 0.76 | 6 |
| 0.8 | 1.54 | 1.38 | 8.7 | 600 | 59 | 0.759 | 6 |
| 0.6 | 1.54 | 1.4 | 8.7 | 592 | 58 | 0.757 | 6 |

"corr." = the correlation c
"React." = the number of reactions found by The

Todd & Engi obtained P=5,67±0,5kbar and T=502±22°C

Annexe 5A Metabasalts: chemical analysises

| | | EC43 | EC74 | EC49 | EC45 | EC103 | EC40 | EC197 | EC87 | EC42 | EC55 | EC71 | EC41 | EC44* | EC57* | EC200 | EC185 | EC199 | EC167 | EC188 |
|---|---|---|---|---|---|---|---|---|---|---|---|---|---|---|---|---|---|---|---|---|
| **SiO2** | wt-% | 48.99 | 48.73 | 48.69 | 48.65 | 48.37 | 48.01 | 47.47 | 47.24 | 46.41 | 46.22 | 46.08 | 44.13 | 47.13 | 40.40 | 45.76 | 45.42 | 42.28 | 54.40 | 42.48 |
| **TiO2** | wt-% | 1.52 | 1.18 | 1.51 | 1.52 | 1.45 | 1.32 | 1.29 | 1.34 | 1.38 | 1.56 | 1.22 | 1.56 | 1.40 | 0.67 | 0.55 | 0.88 | 0.40 | 0.71 | 1.97 |
| **Al2O3** | wt-% | 14.49 | 16.09 | 15.81 | 15.65 | 16.22 | 13.96 | 12.76 | 15.57 | 15.21 | 15.56 | 12.27 | 14.79 | 18.66 | 7.13 | 7.11 | 11.68 | 13.48 | 15.67 | 20.95 |
| **Fe2O3*** | wt-% | 10.37 | 8.28 | 9.70 | 10.72 | 9.49 | 9.44 | 11.68 | 10.29 | 8.51 | 11.46 | 10.31 | 11.49 | 8.92 | 13.14 | 10.25 | 11.36 | 11.05 | 5.78 | 8.80 |
| **Fe2O3** | wt-% | 4.10 | 4.57 | | 5.11 | | 4.78 | 2.37 | | 3.08 | 3.73 | 3.39 | 4.61 | 5.27 | 4.02 | 2.88 | 3.82 | 2.45 | | |
| **FeO** | wt-% | 6.68 | 4.17 | | 6.12 | | 5.14 | 8.38 | | 5.73 | 8.10 | 7.26 | 7.34 | 4.17 | 8.21 | 6.63 | 6.78 | 7.74 | | |
| **MnO** | wt-% | 0.19 | 0.11 | 0.19 | 0.17 | 0.18 | 0.18 | 0.17 | 0.22 | 0.19 | 0.15 | 0.23 | 0.17 | 0.26 | 0.36 | 0.27 | 0.17 | 0.13 | 0.15 | 0.05 |
| **MgO** | wt-% | 8.57 | 8.83 | 7.94 | 6.57 | 8.29 | 6.46 | 11.92 | 6.17 | 6.81 | 9.65 | 14.56 | 8.88 | 4.07 | 24.18 | 15.28 | 16.31 | 19.01 | 6.47 | 0.37 |
| **CaO** | wt-% | 8.85 | 10.93 | 9.99 | 9.95 | 11.02 | 13.17 | 8.47 | 8.81 | 13.29 | 9.35 | 9.85 | 12.09 | 13.42 | 13.31 | 12.45 | 8.04 | 5.67 | 5.78 | 14.05 |
| **Na2O** | wt-% | 3.73 | 3.12 | 3.63 | 3.59 | 2.69 | 2.32 | 1.94 | 2.96 | 2.84 | 2.88 | 2.11 | 2.15 | 2.61 | 0.29 | 1.24 | 0.98 | 0.68 | 3.60 | 3.11 |
| **K2O** | wt-% | 0.18 | 0.16 | 0.24 | 0.23 | 0.29 | 0.16 | 0.79 | 2.23 | 0.17 | 0.28 | 0.16 | 0.24 | 0.08 | 0.01 | 0.29 | 0.92 | 1.06 | 3.42 | 0.34 |
| **P2O5** | wt-% | 0.15 | 0.10 | 0.14 | 0.13 | 0.12 | 0.16 | 0.14 | 0.17 | 0.15 | 0.10 | 0.13 | 0.15 | 0.17 | 0.07 | 0.07 | 0.10 | 0.05 | 0.10 | 0.33 |
| **H20** | wt-% | 1.56 | 1.63 | 0.76 | 1.27 | 0.90 | 1.40 | 3.08 | 1.81 | 1.40 | 2.01 | 2.76 | 1.76 | 1.80 | 0.00 | 2.55 | 3.99 | 6.28 | 1.54 | 3.57 |
| **CO2** | wt-% | 0.13 | 0.04 | 0.00 | 0.12 | 0.00 | 2.45 | 0.00 | 2.13 | 2.47 | 0.19 | 0.07 | 1.14 | 0.00 | 0.00 | 4.11 | 0.00 | 0.00 | 1.29 | 2.32 |
| **Cr2O3** | wt-% | 0.02 | 0.03 | 0.05 | 0.02 | 0.06 | 0.03 | 0.07 | 0.06 | 0.02 | 0.07 | 0.04 | 0.03 | 0.03 | 0.21 | 0.13 | 0.13 | 0.11 | 0.01 | 0.04 |
| **NiO** | wt-% | 0.02 | 0.02 | 0.01 | 0.02 | 0.02 | 0.03 | 0.04 | 0.02 | 0.02 | 0.04 | 0.06 | 0.04 | 0.01 | 0.15 | 0.09 | 0.07 | 0.09 | 0.01 | 0.02 |
| **Sum** | wt-% | 99.18 | 99.71 | 99.73 | 99.12 | 100.16 | 99.59 | 98.88 | 99.04 | 99.18 | 99.71 | ### | 99.08 | 99.09 | 99.01 | 99.42 | 99.28 | 99.44 | 98.92 | 98.39 |

Annexe 5A (continued)

| | | ECB3 | ECB1 | ECB2 | ECB42 | ECB19 | EC154 | EC153 | EC152 | EC132 | EC226 | EC56 | EC192 | EC196 | EC58 | EC85 | R15 | R14 | R12 |
|---|---|---|---|---|---|---|---|---|---|---|---|---|---|---|---|---|---|---|---|
| **SiO2** | wt-% | 50.17 | 50.15 | 50.03 | 48.05 | 48.02 | 52.57 | 51.39 | 50.15 | 48.18 | 44.94 | 54.89 | 54.86 | 53.43 | 49.92 | 49.24 | 48.48 | 53.63 | 44.00 |
| **TiO2** | wt-% | 1.05 | 0.93 | 0.95 | 1.26 | 1.42 | 0.84 | 2.90 | 2.09 | 0.58 | 3.79 | 0.62 | 0.70 | 1.13 | 1.14 | 1.64 | 1.17 | 0.92 | 0.88 |
| **Al2O3** | wt-% | 14.95 | 14.63 | 14.56 | 15.27 | 14.87 | 16.07 | 15.48 | 15.17 | 11.50 | 14.39 | 15.05 | 17.33 | 13.37 | 15.12 | 15.54 | 14.65 | 12.25 | 7.88 |
| **Fe2O3*** | wt-% | 7.67 | 7.62 | 7.66 | 10.16 | 9.89 | 8.66 | 10.65 | 13.72 | 4.71 | 18.23 | 5.39 | 6.37 | 7.64 | 8.41 | 9.96 | 9.07 | 8.52 | 13.84 |
| **Fe2O3** | wt-% | 2.30 | 2.39 | 2.54 | | | | 3.17 | 4.76 | | 6.78 | 3.50 | | 3.64 | | 3.53 | | | 5.31 |
| **FeO** | wt-% | 5.60 | 5.47 | 5.37 | | | | 6.73 | 8.06 | | 10.30 | 1.70 | | 3.60 | | 6.77 | | | 7.67 |
| **MnO** | wt-% | 0.15 | 0.16 | 0.16 | 0.15 | 0.10 | 0.10 | 0.11 | 0.25 | 0.06 | 0.34 | 0.17 | 0.21 | 0.16 | 0.17 | 0.20 | 0.16 | 0.20 | 0.13 |
| **MgO** | wt-% | 8.93 | 9.48 | 9.70 | 7.16 | 8.30 | 6.58 | 6.23 | 6.33 | 12.95 | 4.56 | 5.27 | 5.90 | 8.29 | 7.72 | 7.59 | 9.05 | 7.64 | 23.02 |
| **CaO** | wt-% | 11.76 | 10.68 | 10.90 | 10.72 | 6.63 | 6.43 | 7.92 | 8.26 | 12.00 | 9.77 | 13.42 | 7.30 | 10.69 | 11.08 | 9.85 | 8.82 | 10.42 | 3.17 |
| **Na2O** | wt-% | 2.67 | 2.57 | 2.75 | 3.38 | 3.74 | 2.79 | 2.39 | 2.51 | 0.51 | 2.42 | 1.60 | 4.90 | 3.35 | 3.79 | 3.56 | 3.40 | 4.21 | 0.21 |
| **K2O** | wt-% | 0.44 | 0.67 | 0.61 | 0.28 | 0.48 | 2.54 | 0.72 | 0.49 | 2.46 | 0.27 | 0.10 | 0.17 | 0.23 | 0.23 | 0.34 | 0.76 | 0.11 | 0.02 |
| **P2O5** | wt-% | 0.11 | 0.09 | 0.10 | 0.11 | 0.13 | 0.11 | 0.34 | 0.29 | 0.07 | 1.30 | 0.13 | 0.22 | 0.09 | 0.12 | 0.13 | 0.12 | 0.25 | 0.11 |
| **H20** | wt-% | 1.66 | 1.72 | 1.78 | 1.48 | 3.42 | 1.44 | 2.12 | 1.47 | 2.53 | 0.65 | 1.92 | 1.49 | 1.52 | 0.47 | 1.42 | 2.42 | 1.01 | 6.42 |
| **CO2** | wt-% | 0.13 | 0.08 | 0.11 | 1.25 | 1.57 | 0.79 | 0.00 | 0.00 | 3.10 | 0.28 | 1.03 | 0.15 | 0.00 | 0.28 | 0.00 | 1.52 | 0.65 | 1.01 |
| **Cr2O3** | wt-% | 0.03 | 0.03 | 0.04 | 0.05 | 0.04 | 0.05 | 0.03 | 0.03 | 0.01 | 0.01 | 0.01 | 0.01 | 0.04 | 0.04 | 0.05 | 0.06 | 0.01 | 0.05 |
| **NiO** | wt-% | 0.01 | 0.02 | 0.02 | 0.02 | 0.02 | 0.00 | 0.00 | 0.00 | 0.00 | 0.00 | 0.00 | 0.01 | 0.02 | 0.01 | 0.01 | 0.03 | 0.01 | 0.13 |
| **Sum** | wt-% | 99.96 | 99.07 | 99.62 | 99.34 | 98.64 | 98.96 | 99.53 | 99.86 | 98.66 | 99.80 | 99.40 | 99.61 | 99.55 | 99.43 | 99.86 | 99.70 | 99.83 | 100.02 |

Annexe 5A (continued)

| | | EC43 | EC74 | EC49 | EC45 | EC103 | EC40 | EC197 | EC87 | EC42 | EC55 | EC71 | EC41 | EC44* | EC57* | EC200 | EC185 | EC199 | EC167 | EC188 |
|---|---|---|---|---|---|---|---|---|---|---|---|---|---|---|---|---|---|---|---|---|
| **Nb** | ppm | 2 | 3.5 | 5.4 | 5 | 4.8 | 6.1 | 4 | 5 | 4.2 | 5.8 | 2 | 6 | 0 | 1.7 | 3.7 | 4.3 | 1.5 | 19.2 | 17.3 |
| **Zr** | ppm | 95 | 88 | 107 | 90 | 90 | 85 | 86 | 99 | 99 | 86 | 64 | 85 | 124 | 43 | 43 | 59 | 31 | 109 | 189 |
| **Y** | ppm | 34 | 24.9 | 31.3 | 32 | 28.4 | 26.3 | 24.5 | 23.8 | 28.4 | 24.3 | 26 | 24 | 34 | 12.5 | 10.2 | 17.1 | 10.6 | 30.5 | 79.8 |
| **Sr** | ppm | 63 | 190 | 168 | 145 | 133 | 231 | 135 | 135 | 224 | 158 | 102 | 147 | 373 | 133 | 38 | 33 | 28 | 246 | 2313 |
| **U** | ppm | 0 | <2< | <2< | 1 | <2< | <2< | <2< | <2< | <2< | <2< | 0 | 1 | 3 | <2< | 2 | 2 | <2< | 2 | <2< |
| **Rb** | ppm | 12 | <1.0< | <1.0< | 10 | 2.6 | <1.0< | 26.4 | 36.5 | <1.0< | 8.7 | 13 | 11 | 12 | <1.0< | 7.1 | 33.3 | 30.6 | 91.4 | 10.6 |
| **Th** | ppm | 0 | 3 | 3 | 0 | 2 | 3 | 2 | <2< | 3 | 2 | 0 | 0 | 0 | 3 | 2 | <2< | <2< | 15 | 5 |
| **Pb** | ppm | 11 | 3 | 7 | 5 | 8 | <2< | 12 | <2< | 2 | 5 | 25 | 8 | 10 | 4 | 4 | 5 | 4 | 6 | 75 |
| **Ga** | ppm | 17 | 15 | 19 | 15 | 18 | 18 | 17 | 17 | 19 | 20 | 15 | 18 | 22 | 10 | 12 | 13 | 13 | 20 | 32 |
| **Zn** | ppm | 83 | 74 | 84 | 100 | 76 | 69 | 115 | 110 | 67 | 102 | 106 | 112 | 57 | 88 | 108 | 104 | 77 | 61 | 11 |
| **Cu** | ppm | 44 | 32 | 37 | 47 | 29 | 71 | 59 | 30 | 48 | 60 | 3 | 74 | 94 | 23 | 44 | 19 | <2< | 10 | 25 |
| **Ni** | ppm | 181 | 231 | 107 | 180 | 129 | 262 | 408 | 145 | 167 | 325 | 478 | 309 | 115 | 1103 | 970 | 707 | 869 | 51 | 123 |
| **Co** | ppm | 68 | 63 | 57 | 46 | 59 | 61 | 60 | 42 | 55 | 79 | 78 | 58 | 51 | 78 | 95 | 75 | 77 | 23 | 47 |
| **Cr** | ppm | 318 | 420 | 311 | 494 | 375 | 372 | 540 | 457 | 322 | 470 | 655 | 559 | 490 | 1403 | 1080 | 1023 | 946 | 87 | 295 |
| **V** | ppm | 294 | 198 | 249 | 277 | 235 | 182 | 188 | 238 | 231 | 180 | 197 | 231 | 302 | 88 | 92 | 146 | 77 | 103 | 234 |
| **Ce** | ppm | 14 | 10.5 | 4 | 13.5 | 4 | 10.5 | 10.70 | <3< | 11 | <3< | 10.5 | 13 | 14.00 | 3.00 | 4.40 | <3< | <3< | 63.00 | 20 |
| **Nd** | ppm | 10 | 10 | 15 | 11 | 9 | 9 | 13 | 9 | 11.5 | 14 | 9 | 10 | 20 | 4 | <4< | 12 | <4< | 37 | 21 |
| **Ba** | ppm | 1 | 11 | 16 | 6 | 17 | <9< | 69 | 69 | 25 | 30 | 11 | 9 | 0 | <9< | 41 | 60 | 83 | 331 | 42 |
| **La** | ppm | 6 | 4 | <4< | 5.5 | <4< | 4.5 | 3.8 | <4< | 4 | <4< | 4 | 5.5 | 6 | 1.1 | 1.7 | 6 | <4< | 30 | 10 |
| **S** | ppm | 0 | 0 | <3< | <0< | <3< | 332 | 1079 | <3< | 521 | <3< | 0 | 187 | 343 | <3< | 1217 | 90 | <3< | 71 | 47987 |
| **Hf** | ppm | 6 | 6 | 5 | 4 | 5 | 4 | 5 | 3 | 5 | 5 | 8 | 3 | 2 | 17 | 6 | 9 | 12 | 6 | 3 |
| **Sc** | ppm | 43 | 35 | 39 | 45 | 43 | 33 | 46 | 48 | 31 | 36 | 32 | 38 | 28 | 21 | 33 | 57 | 43 | 19 | 40 |
| **As** | ppm | 1 | 4 | <3< | 4 | <3< | 2 | 3 | 7 | 1 | <3< | 5 | 3 | 2 | 14 | 5 | 5 | 33 | 5 | 7 |
| **L.O.I.** | | 0.75 | 0.67 | 0.95 | 1.21 | 0.76 | 0.71 | 0.90 | 5.42 | 3.28 | 1.64 | 3.23 | 5.89 | 8.37 | 12.84 | 1.11 | 2.02 | 3.24 | 2.83 | 2.08 |

Annexe 5A (continued)

| | | ECB3 | ECB1 | ECB2 | ECB42 | ECB19 | EC154 | EC153 | EC152 | EC132 | EC226 | EC56 | EC192 | EC196 | EC58 | EC85 | R15 | R14 | R12 |
|---|---|---|---|---|---|---|---|---|---|---|---|---|---|---|---|---|---|---|---|
| **Nb** | ppm | 1 | 1 | 2 | 3.2 | 6.1 | 5.1 | 12.5 | 13.6 | 13.9 | 31 | 16.1 | 17.4 | 13.8 | 1 | 5.9 | 7 | 23 | 10 |
| **Zr** | ppm | 69 | 82 | 79 | 101 | 121 | 69 | 78 | 137 | 170 | 276 | 182 | 169 | 108 | 90 | 113 | 83 | 146 | 46 |
| **Y** | ppm | 29 | 28 | 28 | 29.3 | 26.9 | 19.7 | 37.1 | 47.7 | 20.6 | 59 | 29.8 | 30.4 | 27.1 | 31 | 33.7 | 27 | 33 | 18 |
| **Sr** | ppm | 317 | 201 | 207 | 215 | 216 | 204 | 230 | 192 | 598 | 143 | 853 | 961 | 274 | 232 | 174 | 397 | 420 | 16 |
| **U** | ppm | 0 | 0 | 0 | <2< | <2< | <2< | <2< | <2< | <2< | 2 | <2< | <2< | <2< | <2< | <2< | <2< | 4 | <2< |
| **Rb** | ppm | 20 | 28 | 25 | 3 | 20 | 83.3 | 13.6 | 9 | 81.7 | 3 | <1.0< | <1.0< | 1.5 | 15 | 4.8 | 41 | 3 | 7 |
| **Th** | ppm | 0 | 1 | 1 | 2 | 4 | 2 | 3 | 3 | 8 | <2< | 14 | 15 | 8 | 4 | 3 | 3 | 20 | 4 |
| **Pb** | ppm | 17 | 17 | 15 | 5 | 10 | 19 | 22 | 16 | 24 | 12 | 43 | 48 | 18 | 15 | 11 | 25 | 36 | 27 |
| **Ga** | ppm | 15 | 15 | 14 | 16 | 17 | 21 | 19 | 22 | 18 | 22 | 21 | 22 | 18 | 16 | 18 | 15 | 16 | 11 |
| **Zn** | ppm | 66 | 64 | 64 | 79 | 90 | 117 | 134 | 172 | 183 | 167 | 98 | 204 | 68 | 66 | 97 | 59 | 56 | 86 |
| **Cu** | ppm | 57 | 16 | 8 | 23 | 41 | 5 | 14 | 6 | 5 | 30 | 8 | 22 | 19 | 13 | 16 | 7 | 7 | 12 |
| **Ni** | ppm | 93 | 152 | 155 | 200 | 150 | 32 | 36 | 15 | 40 | 9 | 54 | 51 | 212 | 67 | 102 | 213 | 59 | 868 |
| **Co** | ppm | 54 | 57 | 56 | 49 | 43 | 35 | 41 | 45 | 18 | 60 | 39 | 32 | 42 | 62 | 63 | 55 | 42 | 122 |
| **Cr** | ppm | 409 | 545 | 583 | 384 | 316 | 354 | 243 | 199 | 59 | 26 | 70 | 80 | 308 | 256 | 328 | 364 | 92 | 170 |
| **V** | ppm | 241 | 208 | 218 | 215 | 242 | 240 | 342 | 259 | 92 | 187 | 89 | 112 | 161 | 263 | 270 | 197 | 112 | 165 |
| **Ce** | ppm | 13.5 | 15 | 14 | <3< | 8.00 | 18.60 | 26.00 | 48.00 | 61.00 | 88.00 | 77.80 | 63.00 | 42.60 | 15.00 | <3< | 20.00 | 63.00 | 3.00 |
| **Nd** | ppm | 9 | 11 | 10 | 12 | 20 | 16 | 26 | 32 | 38 | 44 | 26 | 33 | 14 | 10 | 10 | 9 | 22 | <4< |
| **Ba** | ppm | 32 | 41 | 42 | 25 | 53 | 619 | 134 | 67 | 424 | 15 | 22 | 66 | 29 | 16 | 39 | 101 | 25 | 20 |
| **La** | ppm | 5.5 | 7.5 | 6 | <4< | 5 | 8.4 | 13 | 25 | 29.4 | <4< | 36.9 | 34 | 18 | <4< | <4< | <4< | 21 | 7 |
| **S** | ppm | 15 | 0 | 0 | 113 | 468 | <3< | 235 | 8 | 499 | <3< | 10 | 162 | 121 | <3< | <3< | 30 | <3< | <3< |
| **Hf** | ppm | 6 | 6 | 6 | 5 | 6 | 4 | 5 | 5 | 5 | 7 | 6 | 6 | 6 | 6 | 5 | 4 | 6 | 11 |
| **Sc** | ppm | 38 | 34 | 35 | 55 | 71 | 51 | 89 | 77 | 22 | 51 | 23 | 25 | 38 | 46 | 40 | 51 | 19 | 108 |
| **As** | ppm | 7 | 5 | 4 | 4 | 4 | 5 | 4 | 4 | 6 | 6 | 11 | 6 | 4 | <3< | <3< | 6 | 3 | 5 |
| **L.O.I.** | | 2.73 | 1.37 | 5.63 | 0.57 | 2.23 | 4.99 | 1.17 | 1.19 | 1.29 | | 2.76 | 3.94 | 2.15 | 5.92 | 1.12 | | | |

Annexe 5B Metabasalts: REE content

| | | ECB3 | ECB1 | ECB2 | EC154 | EC132 | EC56 | EC196 | EC43 | EC74 | EC45 | EC40 | EC197 | EC42 | EC71 | EC41 | EC57 | EC200 |
|---|---|---|---|---|---|---|---|---|---|---|---|---|---|---|---|---|---|---|
| **La** | ppm | 5.5 | 7.5 | 6 | 8.4 | 29.4 | 36.9 | 18 | 6 | 4 | 5.5 | 4.5 | 3.8 | 4 | 4 | 5.5 | 1.1 | 1.7 |
| **Ce** | ppm | 13.5 | 15 | 14 | 18.60 | 61.00 | 77.80 | 42.60 | 14 | 10.5 | 13.5 | 10.5 | 10.70 | 11 | 10.5 | 13 | 3.00 | 4.40 |
| **Pr** | ppm | 2 | 2.3 | 1.9 | 2.40 | 6.90 | 8.40 | 4.90 | 2 | 1.8 | 2.2 | 1.8 | 1.70 | 1.8 | 1.6 | 2 | 0.50 | 0.60 |
| **Nd** | ppm | 9 | 11 | 10 | 11.40 | 27.40 | 33.40 | 21.10 | 10 | 10 | 11 | 9 | 9.10 | 11.5 | 9 | 10 | 2.60 | 3.60 |
| **Sm** | ppm | 2.8 | 3.2 | 2.8 | 2.80 | 5.40 | 6.50 | 4.90 | 3.2 | 3.3 | 3.6 | 3 | 3.30 | 2.9 | 2.7 | 2.9 | 1.10 | 1.20 |
| **Eu** | ppm | 1.2 | 0.9 | 1 | 0.79 | 1.06 | 1.31 | 1.01 | 1.4 | 1.2 | 1.3 | 1.1 | 1.13 | 1.2 | 1.5 | 1.2 | 0.30 | 0.44 |
| **Gd** | ppm | 4.3 | 3.9 | 3.8 | 3.70 | 5.10 | 6.20 | 5.40 | 4.9 | 4.7 | 4.6 | 3.6 | 4.10 | 4.2 | 3.8 | 4.5 | 1.70 | 1.70 |
| **Tb** | ppm | 0.7 | 0.8 | 0.6 | 0.50 | 0.70 | 0.90 | 0.80 | 0.9 | 0.7 | 1 | 0.7 | 0.70 | 0.7 | 0.6 | 0.7 | 0.30 | 0.30 |
| **Dy** | ppm | 4.7 | 4.4 | 4.8 | 3.70 | 4.5 | 5.40 | 5 | 5.9 | 4.1 | 5.8 | 4.6 | 4.40 | 5 | 4 | 4.5 | 2.10 | 1.90 |
| **Ho** | ppm | 1 | 1 | 1 | 0.73 | 0.81 | 1.08 | 0.96 | 1.2 | 1.1 | 1.3 | 1 | 0.90 | 1 | 0.8 | 1 | 0.44 | 0.36 |
| **Er** | ppm | 3.2 | 2.9 | 2.9 | 2.30 | 2.40 | 3.20 | 3.00 | 3.5 | 2.9 | 3.6 | 2.8 | 2.80 | 3.1 | 2.1 | 2.8 | 1.40 | 1.10 |
| **Tm** | ppm | 0.5 | 0.4 | 0.4 | 0.30 | 0.30 | 0.40 | 0.40 | 0.5 | 0.5 | 0.5 | 0.4 | 0.40 | 0.4 | 0.3 | 0.4 | 0.20 | 0.10 |
| **Yb** | ppm | 2.7 | 2.3 | 2.6 | 1.90 | 2.10 | 2.80 | 2.70 | 3.5 | 2.7 | 3.7 | 2.5 | 2.50 | 2.7 | 2.4 | 2.4 | 1.30 | 1.00 |
| **Lu** | ppm | 0.5 | 0.4 | 0.4 | 0.28 | 0.29 | 0.42 | 0.39 | 0.5 | 0.3 | 0.5 | 0.4 | 0.35 | 0.4 | 0.3 | 0.4 | 0.19 | 0.13 |
| **Th** | ppm | 0 | 1 | 1 | 1.30 | 10.10 | 13.30 | 6.50 | 0 | 0 | 0 | 0 | 0.40 | 0 | 0 | 0 | 0.00 | 0.20 |
| **U** | ppm | 0 | 0 | 0 | 0.60 | 3.10 | 3.90 | 1.40 | 0 | 0 | 0 | 0 | 0.20 | 0.5 | 0 | 0 | 0.20 | 0.20 |

Annexe 5C Intercorrelations among analysed major and minor elements of the metabasalts

| | Th | Rb | U | Sr | Y | Zr | Nb | P2O5 | K2O | Na2O | CaO | MgO | MnO | Fe2O3* | Al2O3 | TiO2 | SiO2 |
|---|---|---|---|---|---|---|---|---|---|---|---|---|---|---|---|---|---|
| **SiO2** | | | | | | | | | | | | | | | | | 1.00000 |
| **TiO2** | | | | | | | | | | | | | | | | 1.00000 | -0.13081 |
| **Al2O3** | | | | | | | | | | | | | | | 1.00000 | 0.35692 | 0.30924 |
| **Fe2O3*** | | | | | | | | | | | | | | 1.00000 | -0.28945 | 0.59159 | -0.60329 |
| **MnO** | | | | | | | | | | | | | 1.00000 | 0.51604 | -0.34954 | 0.19866 | -0.21982 |
| **MgO** | | | | | | | | | | | | 1.00000 | 0.18994 | 0.28564 | -0.85181 | -0.46884 | -0.50652 |
| **CaO** | | | | | | | | | | | 1.00000 | -0.27599 | 0.21305 | -0.24087 | 0.12702 | 0.03546 | -0.13355 |
| **Na2O** | | | | | | | | | | 1.00000 | -0.02064 | -0.72656 | -0.10716 | -0.29102 | 0.65224 | 0.21622 | 0.57596 |
| **K2O** | | | | | | | | | 1.00000 | -0.07245 | -0.37451 | -0.05345 | -0.32684 | -0.31379 | 0.06484 | -0.22565 | 0.23233 |
| **P2O5** | | | | | | | | 1.00000 | -0.12164 | 0.08469 | 0.00390 | -0.33254 | 0.38343 | 0.56739 | 0.15571 | 0.80064 | -0.10280 |
| **Nb** | | | | | | | 1.00000 | 0.66165 | 0.13343 | 0.15857 | -0.11437 | -0.34044 | 0.04610 | 0.08601 | 0.10288 | 0.39016 | 0.30276 |
| **Zr** | | | | | | 1.00000 | 0.78367 | 0.70965 | -0.01914 | 0.30907 | 0.21584 | -0.61195 | 0.08219 | -0.00117 | 0.42169 | 0.49469 | 0.24355 |
| **Y** | | | | | 1.00000 | 0.71773 | 0.53861 | 0.61497 | -0.16094 | 0.40922 | 0.22038 | -0.68889 | -0.05941 | 0.13698 | 0.62742 | 0.68712 | 0.05210 |
| **Sr** | | | | 1.00000 | 0.65995 | 0.52918 | 0.40260 | 0.10949 | -0.03731 | 0.20082 | 0.34172 | -0.45161 | -0.35180 | -0.36054 | 0.49400 | 0.04542 | 0.05463 |
| **U** | | | 1.00000 | 0.44961 | 0.11860 | 0.39889 | 0.51502 | 0.21750 | 0.04926 | 0.09986 | 0.07282 | -0.27052 | 0.40410 | 0.10484 | -0.03120 | 0.04860 | 0.11154 |
| **Rb** | | 1.00000 | -0.04689 | 0.02001 | -0.27113 | -0.06346 | 0.04521 | -0.23429 | 0.93647 | -0.15479 | -0.30752 | 0.04520 | -0.41108 | -0.50479 | 0.01671 | -0.41696 | 0.29353 |
| **Th** | 1.00000 | 0.27447 | 0.64143 | 0.35292 | 0.09291 | 0.60023 | 0.85583 | 0.19415 | 0.23786 | 0.24607 | -0.13206 | -0.16690 | -0.08193 | -0.50726 | -0.00542 | -0.37272 | 0.58841 |
| **Pb** | 0.46806 | -0.03128 | 0.11170 | 0.86562 | 0.55395 | 0.47603 | 0.49361 | 0.14195 | -0.07126 | 0.15342 | 0.10825 | -0.32087 | -0.30592 | -0.29519 | 0.29764 | 0.01468 | 0.20857 |
| **Ga** | 0.22419 | 0.04307 | 0.37731 | 0.72173 | 0.79504 | 0.70005 | 0.50121 | 0.38867 | 0.09523 | 0.39763 | 0.20489 | -0.78221 | -0.21561 | -0.14305 | 0.76414 | 0.45375 | 0.21020 |
| **Zn** | 0.12125 | 0.15515 | -0.05603 | -0.16155 | -0.08025 | 0.31503 | 0.33244 | 0.33106 | 0.16261 | -0.14061 | -0.27179 | 0.05670 | 0.21997 | 0.22793 | -0.16240 | 0.21021 | 0.13403 |
| **Cu** | -0.41684 | -0.31253 | 0.15757 | -0.11796 | -0.04864 | -0.10311 | -0.34118 | -0.00611 | -0.30732 | 0.02308 | 0.34910 | -0.15532 | 0.16609 | 0.17094 | 0.17890 | 0.15087 | -0.33839 |
| **Ni** | -0.24781 | -0.15745 | -0.01113 | -0.30087 | -0.56752 | -0.60980 | -0.35739 | -0.27875 | -0.18777 | -0.69332 | -0.11405 | 0.88201 | 0.28990 | 0.38024 | -0.75625 | -0.39552 | -0.66094 |
| **Co** | -0.44898 | -0.48141 | -0.23810 | -0.37200 | -0.32199 | -0.51397 | -0.37860 | -0.07216 | -0.48152 | -0.48363 | -0.13391 | 0.67752 | 0.28690 | 0.55507 | -0.56640 | -0.07104 | -0.62581 |
| **Cr** | -0.51353 | -0.11461 | -0.18715 | -0.30951 | -0.51377 | -0.65950 | -0.61044 | -0.34345 | -0.13435 | -0.50369 | 0.15394 | 0.63987 | 0.34962 | 0.25673 | -0.48475 | -0.33552 | -0.60279 |
| **V** | -0.62710 | -0.32556 | -0.38017 | -0.06901 | 0.39990 | -0.02731 | -0.30050 | 0.11564 | -0.18190 | 0.41640 | 0.03549 | -0.49121 | -0.11298 | 0.17328 | 0.53789 | 0.58413 | 0.03731 |
| **Ce** | 0.84371 | 0.24873 | 0.50703 | 0.27169 | 0.34407 | 0.79222 | 0.86303 | 0.51490 | 0.28472 | 0.14355 | -0.07762 | -0.36488 | 0.08961 | -0.12143 | 0.13145 | 0.17380 | 0.50378 |
| **Nd** | 0.64401 | 0.31271 | 0.54031 | 0.29822 | 0.43376 | 0.78450 | 0.82693 | 0.55988 | 0.33978 | 0.02164 | -0.26340 | -0.36336 | -0.01108 | -0.00922 | 0.16643 | 0.30641 | 0.32751 |
| **Ba** | 0.18149 | 0.87906 | 0.12739 | 0.03915 | -0.18187 | -0.00809 | 0.14641 | -0.11855 | 0.83007 | -0.14112 | -0.29962 | -0.01338 | -0.41367 | -0.31788 | -0.00477 | -0.23740 | 0.28537 |
| **La** | 0.80069 | 0.46304 | 0.43605 | 0.36489 | 0.20920 | 0.73193 | 0.81166 | 0.22010 | 0.34867 | 0.21275 | -0.14104 | -0.32879 | -0.17272 | -0.55233 | 0.21328 | -0.18887 | 0.68200 |
| **S** | 0.03676 | -0.13584 | 0.49897 | 0.87295 | 0.82856 | 0.45128 | 0.33618 | 0.51671 | -0.07008 | 0.08891 | 0.33132 | -0.47160 | -0.44422 | -0.01255 | 0.50457 | 0.28968 | -0.42993 |
| **Hf** | 0.07891 | -0.04956 | -0.20658 | -0.27058 | -0.40733 | -0.33506 | -0.08466 | -0.06454 | -0.13964 | -0.55599 | -0.22647 | 0.83187 | 0.33623 | 0.31808 | -0.67771 | -0.29970 | -0.39563 |
| **Sc** | -0.32223 | -0.23621 | -0.32014 | -0.21771 | 0.08189 | -0.17256 | -0.00465 | 0.16090 | -0.08275 | -0.16771 | -0.58790 | 0.15639 | -0.19196 | 0.52734 | -0.10345 | 0.39113 | -0.16757 |

Annexe 5C (continued)

| | Sc | Hf | S | La | Ba | Nd | Ce | V | Cr | Co | Ni | Cu | Zn | Ga | Pb |
|---|---|---|---|---|---|---|---|---|---|---|---|---|---|---|---|
| **SiO2** | | | | | | | | | | | | | | | |
| **TiO2** | | | | | | | | | | | | | | | |
| **Al2O3** | | | | | | | | | | | | | | | |
| **Fe2O3*** | | | | | | | | | | | | | | | |
| **MnO** | | | | | | | | | | | | | | | |
| **MgO** | | | | | | | | | | | | | | | |
| **CaO** | | | | | | | | | | | | | | | |
| **Na2O** | | | | | | | | | | | | | | | |
| **K2O** | | | | | | | | | | | | | | | |
| **P2O5** | | | | | | | | | | | | | | | |
| **Nb** | | | | | | | | | | | | | | | |
| **Zr** | | | | | | | | | | | | | | | |
| **Y** | | | | | | | | | | | | | | | |
| **Sr** | | | | | | | | | | | | | | | |
| **U** | | | | | | | | | | | | | | | |
| **Rb** | | | | | | | | | | | | | | | |
| **Th** | | | | | | | | | | | | | | | |
| **Pb** | | | | | | | | | | | | | | | 1.00000 |
| **Ga** | | | | | | | | | | | | | | 1.00000 | 0.56187 |
| **Zn** | | | | | | | | | | | | | 1.00000 | 0.06568 | -0.01949 |
| **Cu** | | | | | | | | | | | | 1.00000 | -0.15583 | 0.08839 | -0.35712 |
| **Ni** | | | | | | | | | | | 1.00000 | 0.08329 | -0.09254 | -0.63911 | -0.27341 |
| **Co** | | | | | | | | | | 1.00000 | 0.77133 | 0.16591 | -0.19018 | -0.53668 | -0.26395 |
| **Cr** | | | | | | | | | 1.00000 | 0.51834 | 0.80380 | 0.21234 | -0.17785 | -0.56398 | -0.41949 |
| **V** | | | | | | | | 1.00000 | -0.21681 | -0.09401 | -0.47581 | 0.28123 | -0.13311 | 0.26636 | -0.11211 |
| **Ce** | | | | | | | 1.00000 | -0.44329 | -0.62167 | -0.55869 | -0.47440 | -0.38971 | 0.45476 | 0.41259 | 0.36342 |
| **Nd** | | | | | | 1.00000 | 0.85328 | -0.29165 | -0.65118 | -0.62912 | -0.49547 | -0.25896 | 0.55116 | 0.54404 | 0.32539 |
| **Ba** | | | | | 1.00000 | 0.35279 | 0.21983 | -0.18090 | -0.18967 | -0.45994 | -0.20061 | -0.36406 | 0.26923 | 0.15998 | 0.04994 |
| **La** | | | | 1.00000 | 0.29258 | 0.86157 | 0.97468 | -0.42546 | -0.65287 | -0.62524 | -0.49609 | -0.48908 | 0.43138 | 0.42253 | 0.46731 |
| **S** | | | 1.00000 | -0.04998 | -0.05814 | 0.08050 | -0.06887 | 0.10202 | -0.07891 | -0.06319 | -0.07843 | -0.03887 | -0.39305 | 0.72632 | 0.71781 |
| **Hf** | | 1.00000 | -0.35232 | -0.14155 | -0.11355 | -0.11595 | -0.07325 | -0.52469 | 0.53031 | 0.51289 | 0.73662 | -0.31264 | 0.02522 | -0.58610 | -0.18364 |
| **Sc** | 1.00000 | 0.06078 | -0.01780 | -0.20287 | -0.05454 | 0.03415 | -0.22431 | 0.41657 | -0.12998 | 0.32603 | 0.10226 | -0.15247 | 0.16088 | -0.10676 | -0.03466 |

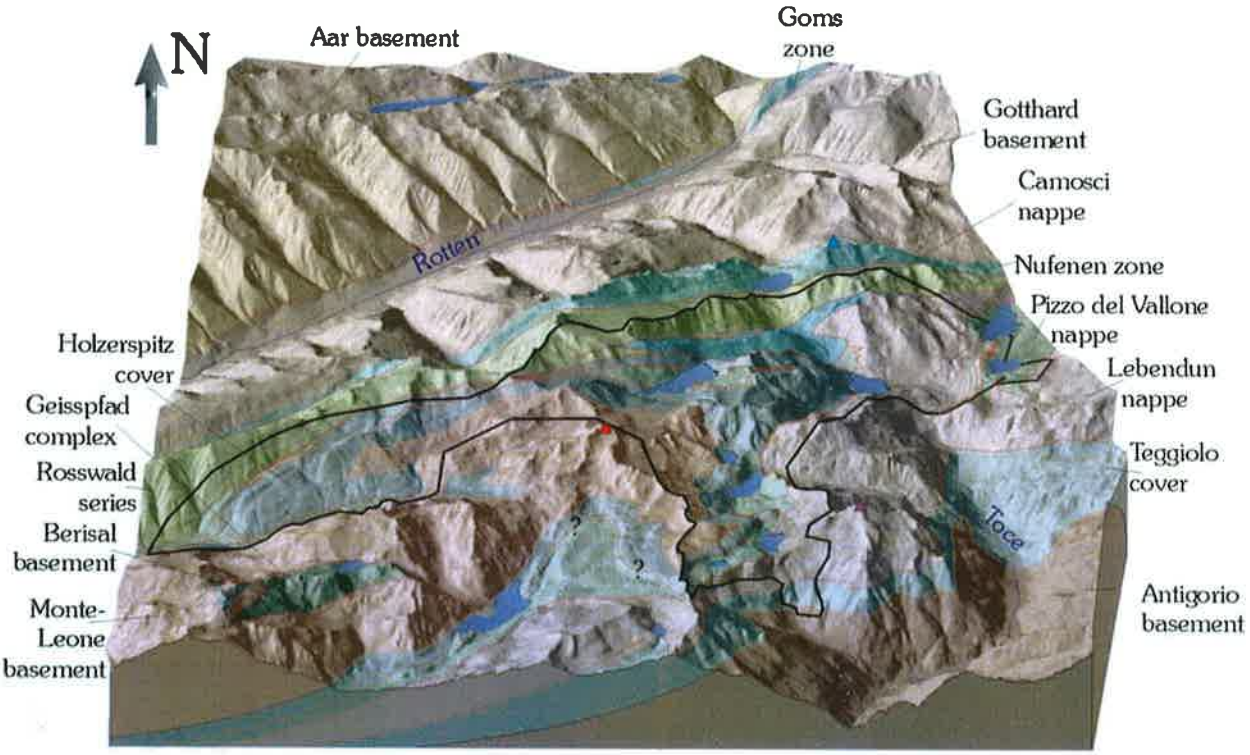


Annexe 6.A 1) Block diagram with the tectonic limits. The mapped area is delimited in black (modified after SPICHER 1980, STECK et al. 1999, and this work).
(▲: Blinnenhorn, ▲: Ofenhorn (Pta Arbola), ▲: Nufenenstock, ▲: Monte Giove)

Annexe 6.A 2) Relief map of the area with:
- some lineaments ——
- some axes ⇨
- some dips-dips directions of the stratification
(▲: Blinnenhorn, ▲: Ofenhorn (Pta Arbola)
▲: Monte Giove).

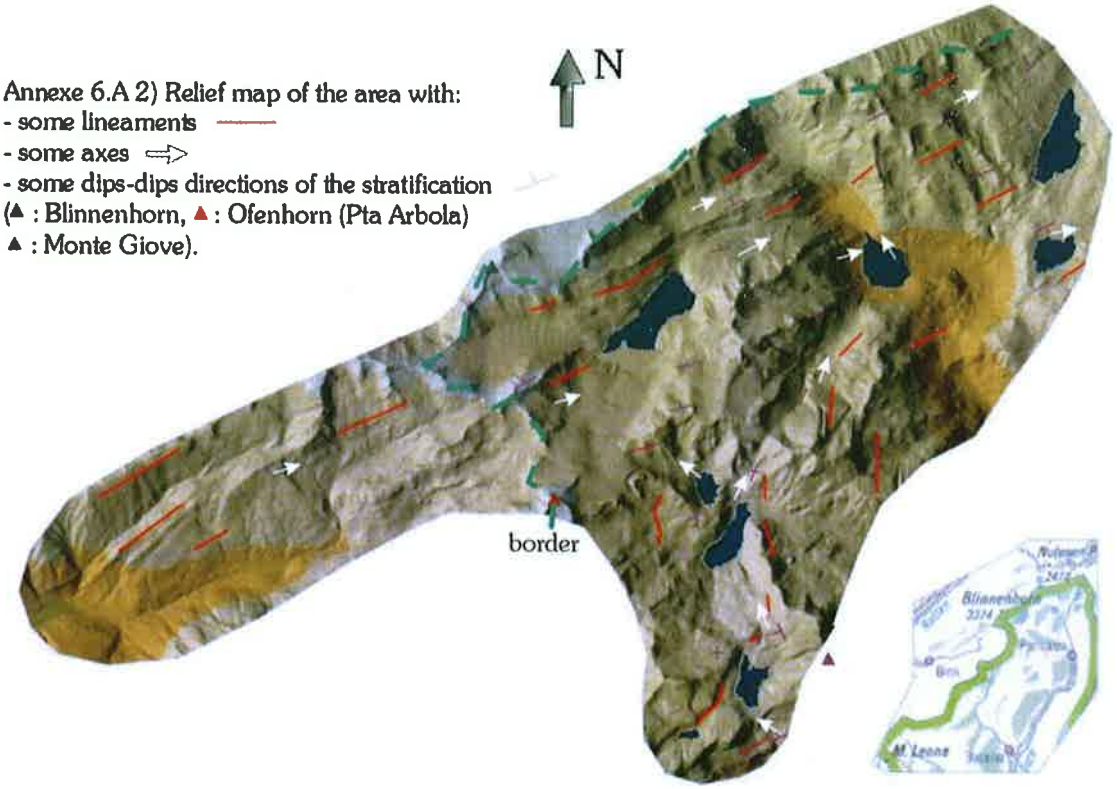

# Tectonic sketch of the Val Formazza - Binntal area

Annexe 6B

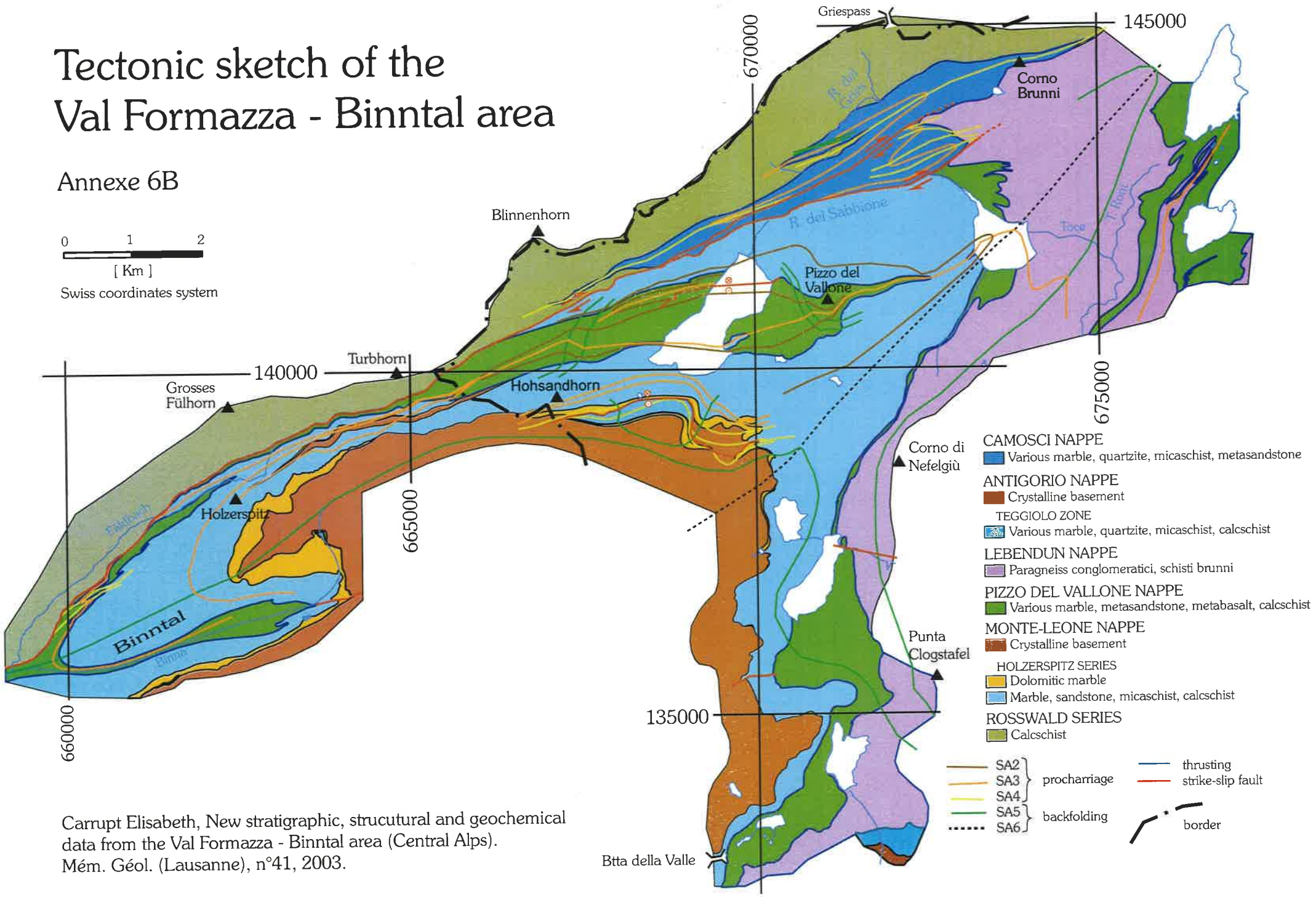


Carrupt Elisabeth, New stratigraphic, strucutural and geochemical data from the Val Formazza - Binntal area (Central Alps). Mém. Géol. (Lausanne), n°41, 2003.

No. 28 HÜRLIMANN A., BESSON-HURLIMANN A and MASSON H. 1995. Stratigraphie et tectonique de la partie orientale de l'écaille de la Gummfluh (Domaine Briançonnais des Préalpes). 132 pp. 62 text-figs., 39 pl.., 6 maps.

No. 29 DOBMEIER C. 1996. Die variskische Entwicklung des südwestlichen Aiguilles Rouges Massives (Westalpen, Frankreich). 191 pp. 70 text-figs., 18 tables., 1 map.

No. 30 BAUD A., POPOVA I., DICKINS J.M., LUCAS S. and ZAKHAROV Y. 1997. Late Paleozoic and early Mesozoic circum-Pacific events : biostratigraphy, tectonic and ore deposits of Primoryie (far East Russia). IGCP Project 272. 202 pp., 71 text-figs., 48 pls.

No. 31 ARMANDO G. 1999. Intracontinental alkaline magmatism : geology, petrography, mineralogy and geochemistry of the Jebel Hayim Massif (Central High Atlas, Morocco). 106 pp. 51 text-figs., 23 tab., 1 map.

No. 32 DEZES P. 1999. Tectonic and metamorphic evolution of the Central Himalayan Domain in Southeast Zanskar (Kashimr, India). 145 pp., 89 text-figs., 1 map.

No. 33 AMODEO F. 1999. Il Triassico terminale- Giurassico del Bacino Lagonegrese. Studi stratigrafici sugli Scisti Silicei della Basilicata (Italia meridionale). 160 pp., 50 text-figs., 10 pl.

No. 34 SAVARY J. and GUEX J. 1999. Discrete biochronological scales and Unitary Associations: Description of the BioGraph computer program. 282 pp. 21 text-figs.

No. 35 GIRARD M. 2001. Metamorphism and tectonics of the transition between non metamorphic Tethyan Himalaya sediments and the North Himalayan Crystalline Zone (Rupshu area, Ladakh, NW India). 96 pp., 7 pl.

No. 36 STAMPFLI G. M. 2001. Geology of the western Swiss Alps, a guide-book. 195 pp., 67 text-figs., 7 pl.

No. 37 REY D. 2002. Shear2F, un logiciel de modélisation tectonique. 52 pp., 122 text-figs.

No. 38 TEMGOUA E. 2002. Cuirassement ferrugineux actuel de bas de versant en zone forestière humide du Sud-Cameroun. 134 pp., 83 text-figs., 4 pl.

No. 39 RAKUS M. and GUEX J. 2002. Les ammonites du Jurassique Inférieur et Moyen de la dorsale Tunisienne. 217 pp., 109 text-figs., 33 pl.

No. 40 ROBYR M. 2002. Thrusting, extension and doming in the high Himalaya of Lahul-Zanskar area (NW India): structural and pressure-temperature constraints. 127 pp., 62 text-figs., 1 pl.

No. 41 CARRUPT E. 2003. New stratigraphic, geochemical and structural data from the Val Formazza – Binntal area (Central Alps). 116 pp., 46 text-figs, 3 pl.

# Mémoires de Géologie (Lausanne)

No. 1* BAUD A. 1987. Stratigraphie et sédimentologie des calcaires de Saint-Triphon (Trias, Préalpes, Suisse et France). 202 pp., 53 text-figs., 29 pls.

No. 2 ESCHER A., MASSON H. and STECK A. 1988. Coupes géologiques des Alpes occidentales suisses. 11 pp., 1 text-figs., 1 map.

No. 3* STUTZ E. 1988. Géologie de la chaîne Nyimaling aux confins du Ladakh et du Rupshu (NW-Himalaya, Inde). Evolution paléogéographique et tectonique d'un segment de la marge nord-indienne. 149 pp., 42 text-figs., 11 pls. 1 map.

No. 4 COLOMBI A. 1989. Métamorphisme et géochimie des roches mafiques des Alpes ouest-centrales (géoprofil Viège-Domodossola-Locarno). 216 pp., 147 text-figs., 2 pls.

No. 5 STECK A., EPARD J.-L., ESCHER A., MARCHANT R., MASSON H. and SPRING L. 1989 Coupe tectonique horizontale des Alpes centrales. 8 pp., 1 map.

No. 6 SARTORI M. 1990. L'unité du Barrhorn (Zone pennique, Valais, Suisse). 140 pp., 56 text-figs., 3 pls.

No. 7 BUSSY F. 1990. Pétrogenèse des enclaves microgrenues associées aux granitoïdes calco-alcalins: exemple des massifs varisque du Mont-Blanc (Alpes occidentales) et miocène du Monte Capanne (Ile d'Elbe, Italie). 309 pp., 177 text-figs.

No. 8* EPARD J.-L. 1990. La nappe de Morcles au sud-ouest du Mont-Blanc. 165 pp., 59 text-figs.

No. 9 PILLOUD C. 1991. Structures de déformation alpines dans le synclinal de Permo-Carbonifère de Salvan-Dorénaz (massif des Aiguilles Rouges, Valais). 98 pp., 59 text-figs.

No. 10* BAUD A., THELIN P. and STAMPFLI G. 1991. (Eds.). Paleozoic geodynamic domains and their alpidic evolution in the Tethys. IGCP Project No. 276. Newsletter No. 2. 155 pp.

No. 11 CARTER E.S. 1993 Biochronology and Paleontology of uppermost Triassic (Rhaetian) radiolarians, Queen Charlotte Islands, British Columbia, Canada. 132 pp., 15 text-figs., 21 pls.

No. 12* GOUFFON Y. 1993. Géologie de la "nappe" du Grand St-Bernard entre la Doire Baltée et la frontière suisse (Vallée d'Aoste - Italie). 147 pp., 71 text-figs., 2 pls.

No. 13 HUNZIKER J.C., DESMONS J., and HURFORD AJ. 1992. Thirty-two years of geochronological work in the Central and Western Alps: a review on seven maps. 59 pp., 18 text-figs., 7 maps.

No. 14 SPRING L. 1993. Structures gondwaniennes et himalayennes dans la zone tibétaine du Haut Lahul-Zanskar oriental (Himalaya indien). 148 pp., 66 text-figs, 1 map.

No. 15 MARCHANT R. 1993. The Underground of the Western Alps. 137 pp., 104 text-figs.

No. 16 VANNAY J.-C. 1993. Géologie des chaînes du Haut-Himalaya et du Pir Panjal au Haut-Lahul (NW-Himalaya, Inde). Paléogéographie et tectonique. 148 pp., 44 text-figs., 6 pls.

No. 17* PILLEVUIT A. 1993. Les blocs exotiques du Sultanat d'Oman. Evolution paléogéographique d'une marge passive flexurale. 249 pp., 138 text-figs., 7 pls.

No. 18 GORICAN S. 1994. Jurassic and Cretaceous radiolarian biostratigraphy and sedimentary evolution of the Budva Zone (Dinarides, Montenegro). 120 pp., 20 text-figs., 28 pls.

No. 19 JUD R. 1994. Biochronology and systematics of Early Cretaceous Radiolaria of the Western Tethys. 147 pp., 29 text-figs., 24 pls.

No. 20 DI MARCO G. 1994. Les terrains accrétés du sud du Costa Rica. Evolution tectonostratigraphique de la marge occidentale de la plaque Caraïbe. 166 pp., 89 text-figs., 6 pls.

No. 21* O'DOGHERTY L. 1994. Biochronology and paleontology of Mid-Cretaceous radiolarians from Northern Apennines (Italy) and Betic Cordillera (Spain). 415 pp., 35 text-figs., 73 pls.

No. 22 GUEX J. and BAUD A. (Eds.). 1994. Recent Developments on Triassic Stratigraphy. 184 pp.

No. 23 BAUMGARTNER P.O., O'DOGHERTY L., GORICAN S., URQUHART E., PILLEVUIT A. and DE WEVER P. (Eds.). 1995. Middle Jurassic to Lower Cretaceous Radiolaria of Tethys: Occurrences, Systematics, Biochronolgy. 1162 p.

No. 24 REYMOND B. 1994. Three-dimensional sequence stratigraphy offshore Louisiana, Gulf of Mexico (West Cameron 3D seismic data). 215 pp., 169 text-figs., 49 pls.

No. 25 VENTURINI G. 1995. Geology, Geochronology and Geochemistry of the Inner Central Sezia Zone. (Western Alps - Italy). 183 pp. 57 text-figs, 12 pls.

No. 26 SEPTFONTAINE M., BERGER J.P., GEYER M., HEUMANN C., PERRET-GENTIL G. and SAVARY, J. 1995. Catalogue des types paléontologiques déposés au Musée Cantonal de Géologie, Lausanne. 76 pp.

No. 27 GUEX, J. 1995. Ammonites hettangiennes de la Gabbs Valley Range (Nevada, USA). 130 pp., 22 figs., 32 pl.

*: out of print

(continued inside)

Order from **Institut de Géologie et Paléontologie,**
**Université de Lausanne. BFSH-2. CH-1015, SWITZERLAND.**
http://www-sst.unil.ch/publications/memoires.htm Fax: (41) 21-692.43.05
Bank Transfer: Banque Cantonale Vaudoise 1002 Lausanne
Account Number: **C.323.52.56** Institut de Géologie, rubrique: Mémoires
Price CHF 30 per volume except volume 23 (CHF 100). The price doesn't include postage and handling.
- Please do not send check -